# Zanclean and Piacenzian otolith-based fish faunas of Estepona (Málaga, Spain)

**Victor W.M. van Hinsbergh [1,3] & Kristiaan Hoedemakers [2]**

[1] *Naturalis Biodiversity Center, Marine Biodiversity, Darwinweg 2, 2333 CR Leiden, The Netherlands. Email: victor.vanhinsbergh@naturalis.nl*
[2] *Royal Belgian Institute of Natural Sciences, OD Nature, Vautierstraat 29, 1000 Brussels, Belgium. Email: khoedemakers@naturalsciences.be*
[3] *Corresponding author*

Received 15 March 2022, revised version accepted 6 October 2022.

Sediments of Zanclean and Piacenzian age are exposed along hill slopes near the community of Estepona (prov. Málaga, Spain) on the shores of the NW Alborán Sea (Mediterranean). Molluscs from these sediments are well known and here we present data on teleost fish otoliths. Our study reveals the presence of 209 taxa, including 17 new to science, all from the Piacenzian and 4 of them also from the Zanclean: *Pythonichthys gibbosus* nov. sp., *Saurenchelys silex* nov. sp., *Paraconger pinguis* nov. sp., *Gnathophis henkmulderi* nov. sp., *Diaphus mermuysi* nov. sp., *Diaphus postcavallonis* nov. sp., *Kryptophanaron nolfi* nov. sp., *Bidenichhys mediterraneus* nov. sp., *Fowleria velerinensis* nov. sp., *Buenia pulvinus* nov. sp., *Gobius alboranensis* nov. sp., *Gobius lombartei* nov. sp., *Thorogobius mirbachae* nov. sp., *'Gobius' pterois* nov. sp., *Snyderina stillaformis* nov. sp., *Prionotus arenarius* nov. sp. and *Pristigenys adrianae* nov. sp. An additional 23 are recorded for the first time as fossil species and several are left in open nomenclature. The most frequent taxa (myctophids, macrourids, *Gadiculus argenteus* Guichenot, 1850, *Micromesistius poutassou* (Risso, 1827), *Verilus mutinensis* (Bassoli, 1906) and *Deltentosteus quadrimaculatus* (Valenciennes, 1837) point to a habitat at an estimated depth of 200 to 400 m. Further bathymetric comparisons of four major sites (one Zanclean and three Piacenzian) based on a distribution model of the extant taxa in our samples indicate marked differences in their depositional environments, with habitats ranging from bathyal to mixed bathyal/ neritic. Comparison of the palaeobiogeography of the nominal species with known Neogene assemblages from the Mediterranean and the adjacent NE Atlantic adds 25 nominal otolith-based teleost species for the Zanclean and 95 for the Piacenzian of the Mediterranean, and to the conclusion, that during the Zanclean the Mediterranean ichthyofauna probably was replenished from the Lusitania Province. Furthermore, the possibility of a refugium in the western Alborán Sea is discussed for some extinct teleost species. The scarce elasmobranch remains are also presented.

Key words: otoliths; Estepona; Piacenzian; Zanclean; present-day; bathymetry; Lusitania Province; tropical eastern Atlantic.

## Introduction

The coastal area between Estepona and Málaga lines the northern side of the western Alborán Sea, the westernmost part of the Mediterranean Sea. It harbours remnants of Pliocene deposits with a rich marine fauna. In particular, outcrops close to Estepona town (El Lobillo and Río del Padrón), various outcrops near Velerín / Velerín Antena Hill, and a temporary outcrop at Parque Antena have provided a wealth of mollusc species, including taxodont bivalves (Lozano Francisco *et al*., 1993), gastropods (Vera-Peláez *et al*., 1999; Landau & Micali, 2021 and references therein), scaphopods (Vera-Peláez *et al*., 2004) and polyplacophorans (Dell'Angelo *et al*., 2004), as well as other invertebrates, such as brachiopods (Bitner & Martinell, 2001), hard corals (Sceleractinia) (Spadini, 2019), and foraminifers (Guerra-Merchán *et al*., 2002; Aguirre *et al*. 2005; Santos & Mayoral, 2006). However, no information has been published on marine vertebrates. Although the sediments are unlikely to yield articulated fish skeletons and elasmobranch remains are very scarce, isolated otoliths and teeth of teleost fish are common.

Of the three pairs of otoliths in each fish, which play a role in receiving and transmitting sounds and positional change signals (Schulz-Mirbach *et al*., 2019), the larger pair called saccular otoliths or sagittas displays family- and species-characteristic features. Families, genera and even species can be recognised based on specific morphological features of these otoliths (usually 0.6 – 20 mm long). Saccular otoliths are therefore a useful tool in reconstructing teleost fish faunas from the past (Koken, 1891; Nolf, 2013; Schwarzhans & Aguilera, 2013; Schwarzhans, 2019a). Statements about phylogeny should be made with care and preferentially in combi-

nation with studies on present-day fishes (Nelson *et al*., 2016).

A number of studies have reported on Pliocene Mediterranean fish otoliths. Most of these studies focused on lower Pliocene Zanclean deposits in the western Mediterranean, *i.e*., from Côte d'Azur (France) (Schwarzhans, 1986; Nolf & Cappetta, 1989), near Barcelona (Spain) (Chaine & Duvergier, 1931; Nolf & Martinell, 1980; Nolf *et al*., 1998), northern Italy (Koken, 1891; Bassoli, 1906; Nolf & Cavallo, 1994; Nolf & Girone, 2006; Schwarzhans *et al*., 2020b) and Sicily (Weiler, 1971; Schwarzhans, 1978). In recent years, otolith assemblages from the eastern Mediterranean Sea (Greece and its islands; Müller, 1994; Agiadi *et al*., 2013a, 2013b; Schwarzhans *et al*., 2020b) have also been studied. Although a few studies dealt with Piacenzian deposits (Nolf & Cappetta, 1989 (in part); Girone, 2006), little is known of the most western part of the Mediterranean Sea, close to the open connection with the Atlantic Ocean. The western Alborán Sea may be of particular interest as its connection with the remainder of the Mediterranean Sea was influenced by volcanic activity and the accompanying formation of a Pliocene archipelago between southeast Spain and the eastern Rif area of North Africa (Booth-Rea *et al*., 2018). Outside the Mediterranean, several Pliocene deposits have been discovered on the Iberian Peninsula, but their otolith associations are rather poor in comparison to those of the Mediterranean: Huelva in Spain (Zanclean, see Ruiz *et al*., 2004) and Vale de Freixo in Portugal (Piacenzian, see Nolf & Marques da Silva, 1997). A more promising locality of Zanclean age is Dar Bel Hamri (NW Morocco) from which four new species have been described (Schwarzhans, 1981, 1993, 1999) and an extensive preliminary list has been provided (Schwarzhans, 1986), although a comprehensive study is not yet available.

## Geological and geographical setting

Between Gibraltar and Málaga a number of Pliocene marine deposits have been preserved. Within the community of Estepona rich outcrops exist that cover both the Zanclean and Piacenzian, and yield a highly diverse marine invertebrate fauna (Fig. 1). They comprise two localities near Estepona town, five near Velerín (a village 6 km east of the centre of Estepona), and the locality Parque Antena (8.7 km east of Estepona). All localities are within the community of Estepona, province of Málaga, Andalusia, Spain.

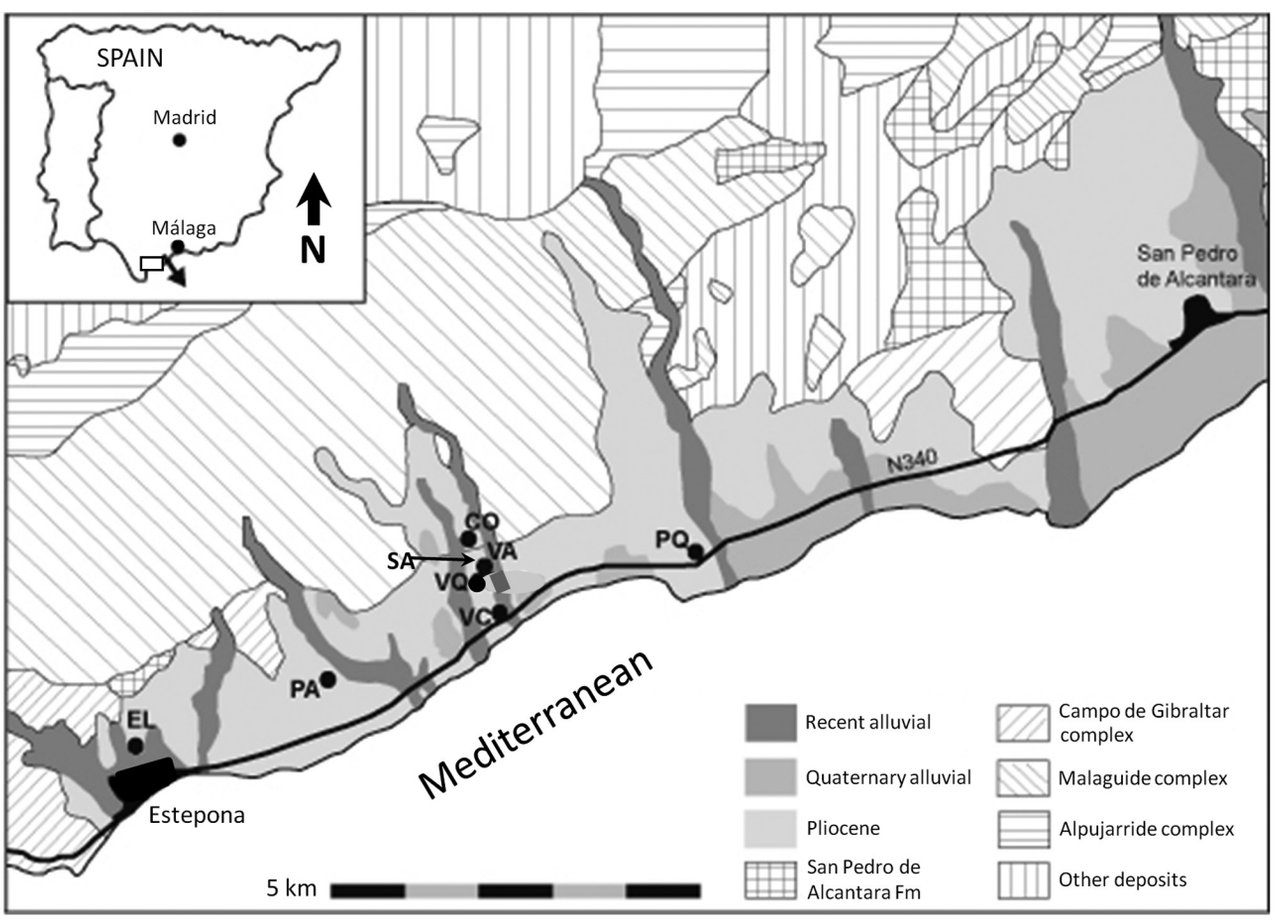


**Figure 1.** Geological context and map of the Pliocene localities near Estepona, modifed after Vera-Peláez *et al*. (1995). Abbreviations: CO = Velerín Conglomerates; EL = El Lobillo; PA = Río del Padrón; PQ = Parque Antena; SA = Velerín Sandy Lens; VA = Velerín Antena Hilltop/Slope; VC = Velerín Carretera; VQ = Velerín Quarry.

***Near Estepona town***

***Río del Padrón*** (36°26'23" N, 5°06'59" W) two km east of Estepona on the western bank of the Río del Padrón is a section of over 15 m of Pliocene sediments. A large part of the section consists of indurated clayey sands that contain solitary corals. About 4-5 metres below the top of the cliff the sediment is intercalated with yellowish fine sands with several levels that contain dispersed and usually eroded molluscs, mainly bivalves, and locally small rounded black pebbles. The presence of Polyplacophora (Dell'Angelo *et al*., 2004) and other molluscs (Lozano-Francisco *et al*., 1993; Landau *et al*., 2003) point to the presence of a solid substrate in the vicinity and a shallow near-coast marine environment. On the basis of Foraminifera from an adjacent Río del Padrón section Guerra-Merchán *et al*. (2002, 2014) dated the sediments to the Early Zanclean, Pliocene unit 2. Additional data on magnetic polarity zones support coincidence with the MPL2 bio-zone as defined by Cita (1975) (Guerra-Merchán *et al*., 2014).

***El Lobillo*** (36°43'91" N, 5°14'47" W; altitude ~76 m). The El Lobillo outcrop is located one km north of the historical centre of Estepona. Pliocene material is exposed on the surface of a small, ploughed field and adjacent to it. The sediment consists of fine sand intermingled with very fine split or rounded gravel particles that have been eroded from the adjacent mountains. It is likely that the sands at El Lobillo have been deposited in the vicinity of a rocky environment, as this outcrop is located close to a site where the Pliocene sediment meets the rocks of the Bejame Mountains. This was also concluded from mollusc data, which further point to a rather shallow marine environment (Landau *et al*., 2003). The mollusc fossils closely resemble the material of Río del Padrón, making it likely that it is of similar Zanclean origin.

***Near El Velerín (6 km east of the centre of Estepona)***

The village El Velerín (community of Estepona) lies about 6 km east of Estepona town and harbours a series of outcrops between the old coastal highway (N340) and the top of the Velerín Antena Hill. Their deposits contain a rich marine association of molluscs, remains of crustaceans, and microfossils. Deposits at Velerín Quarry, Velerín Conglomerates and Velerín Carretera represent different marine environments but are considered to be deposited during a single transgressive phase (Guerra-Merchán *et al*., 2002; Aguirre *et al*., 2005). On the basis of planktonic foraminiferal assemblages, Guerra-Merchán *et al*. (2002, 2014) identified the deposits of these three localities as being of Piacenzian age, unit PL-4 (MPL4b according to Cita, 1975). A subsequent integrated study by Aguirre *et al*. (2005) included molluscs as well as foraminifer and nannoplankton analyses. The analysis of the mollusc fauna placed the Velerín and Velerín Antena outcrops in the upper part of Mediterranean Pliocene Mollusc Unit 1 of Rafii & Monegatti (1993) (MPMU1), which corresponds to a Zanclean or Piacenzian age. On the basis of foraminifers and nannoplankton the Velerín Carretera and Parque Antena outcrops were placed in the Late Zanclean (uppermost part), while the Velerín Antena area was interpreted as lowermost Piacenzian. However, Guerra-Merchán *et al*. (2014) interpreted the foraminifer data of the 20-30 m thick sediment at the Velerín Antena Hill as being Middle Piacenzian age (MPl4b).

***Velerín Conglomerates*** (36°45'38" N, 5°09'77" W, altitude ~32-38 m) is encountered close to Velerín Quarry. This locality has also been indicated as Velerín Pared (Vera-Pelaez *et al*., 2006) or Velerín (Aguirre *et al*., 2005). We studied slumping material from a steep 6 to 8 m-high section located about 150 m NNW of Velerín Quarry. The specific location of this outcrop makes it unlikely that the slumping material was contaminated. According to Guerra-Merchán *et al*. (2002), Velerín Conglomerates represents the end of a marine fan-delta slope. The original sediment consists of a dense package of rounded pebbles of various sizes, with blueish or brown-black colour depending on being dry or wet. Fist-sized and larger stones are intermingled with smaller pebbles, fossils molluscs and brownish fine sand, which all are glued together by calcium carbonate derived from local decalcification and calcareous (re)deposition into a very compact sediment. Locally, the border of the thick conglomerate deposit intertwines with layers of yellow fine sands, which also contains fossil molluscs. Earlier studies on molluscs reported a species-rich gastropod and bivalve fauna (Landau & Micali, 2021; Vera-Peláez *et al*., 2006, and references in both).

***Velerín Antena Quarry*** (36°27'08" N, 5°05'50" W, altitude ~40-45 m) is an abandoned sand quarry located east along the Camino Nicola of Velerín and close to the Velerín Antena plant, for which construction it was excavated. This locality will be referred to as Velerín Quarry in the further text. It has also been indicated as Velerín Antena together with the higher sands on the Velerín Antena Hill (Aguirre *et al.,* 2005). The sediment consists of layers of fossiliferous medium- to fine-grained yellow sands ('bizcornil' facies) and fine grey clayey sand with layers of concentrated fossils. The section displays layers with sparse fossils and local bands with accumulations of molluscs and occasional large barnacles. Upon visual inspection, fish otoliths were found scattered across the floor of the quarry. Freshly obtained sediment was dried and sieved (mostly at 1 or 2 mm, and 15 kg at 0.6 mm).

***Velerín Antena Sandy Lens*** (36°27'11" N, 5°05'51" W): about 60 m north of the Quarry entrance close to the Conglomerates outcrop but E of the Camino Nicola there has been a temporary exposure of a mollusc-rich layer in sandy sediment that was very similar to and at level with that in Velerín Quarry.

***Velerín Antena Slope*** above Velerín Quarry (36°27'09" N, 5°05'49" W, altitude ~45-50 m). From the open area that runs eastward above Velerín Quarry two samples were obtained. The first concerns slumping material that was collected from the sloping ground and is indicated as ***Velerín Antena Slope***. The second, indicated as ***Velerín Antena Hilltop*** is a 50 kg sample collected from the slope area close to the top of Velerín Antena Hill and sieved on mesh size 0.5 mm.

***Velerín Carretera*** (36°44'71" N, 5°09'28" W; altitude ~18 m). At the base of the Velerín Hill, on the slip road close to the N-340 motorway, lies a small roadside outcrop of several metres high. The Pliocene sediment consists of grey clayey fine sand that contains many small molluscs and otoliths. Based on Foraminifera, the deposits at Velerín Quarry, Velerín Conglomerates and Velerín Carretera were considered of a coeval period (Guerra-Merchán *et al*., 2002; Aguirre *et al*., 2005). More detailed studies on the sediments and their connection with other Pliocene deposits in the Estepona-Málaga region revealed that the sands and conglomerates of the Velerín area were deposited during the same transgression period in the Piacenzian (Guerra-Merchán *et al*., 2002, 2014).

***Parque Antena*** (36°27'17" N, 05°03'53" W) is located at about 9 km east of the centre of Estepona. A temporary outcrop at Parque Antena (community of Estepona) was located several km east of Velerín at about 100 m north of the N311 coastal highway. A profile of the outcrop is provided by Guerra-Merchán *et al*., 1996. It consists of layers of fine yellow sand and grey clay. The sediments are contemporaneous with those of Velerín Quarry and Velerín Carretera (Guerra-Merchán *et al*., 2002; Aguirre *et al*., 2005). The material used in our studies consists of two samples. The first a sample consists of sieved sandy material (1.0 and 1.5 mm mesh). The second sample contains the 0.5-1.5 mm fraction from washed clayey sediment.

It is important to note, that to this date no formal names have been proposed for lithostratigraphic units for the Pliocene in this area or any of the outcrops described above.

## Material and methods

In the present study, we use over 30,000 saccular otoliths (sagittas) to identify teleost taxa and recognise 209 taxa that were present in the western Alborán Sea during the Pliocene. Of these, 171 can be identified to species level (including 17 new to science) and 38 are kept in open nomenclature. We compare the marine fish assemblages in the various Pliocene outcrops around Estepona with special emphasis on the differences in geological age, bathymetry and environment.
Sediment samples were taken between 1999 and 2018 at different localities and wet-sieved on different mesh-sizes of 1 mm or larger by various collectors, and for a minor part on a 0.5 mm mesh. The sieved residue was sorted under a stereo microscope.
Due to decalcification and subsequent re-calcification, a part of the specimens showed chemical erosion (often on one side only) or calcareous or sediment precipitation on the otolith. The latter precipitate was (partially) removed from individual otoliths with a blunt needle after immersion in warm water. An attempt to clean the specimens with an ultrasonic device was abandoned after a test because of damage to the otolith surface.
Specimens were photographed with a Leica M165C motorised microscope system using automated Z-stack photography. The photos were subsequently treated using Adobe Photoshop CS ver. 6 and assembled to plates. For each figured otolith the inner surface with the sulcus is shown. When appropriate, the outer surface or one or more lateral views are also included (ventral, dorsal, anterior, posterior, rostral, or caudal views). For several *Diaphus* species, measurements on otolith dimensions were made at a magnification of ≥20x or obtained from photomicrographs.

All type and figured material is stored at Naturalis Biodiversity Center (Leiden, The Netherlands) and given registration numbers of the geology section, RGM numbers (Rijksmuseum van Geologie en Mineralogie). Supplementary Online Table 2 provides these numbers linked to plate and figure number.

### *Abbreviations*

| | |
|---|---|
| a | anterior view |
| b | outer face view |
| c | caudal view |
| CaCL | caudal colliculum length |
| CaL | cauda length |
| d | dorsal view |
| OL | otolith length |
| OH | otolith height |
| OsCL | ostial colliculum length |
| OsL | ostium length |
| OT | otolith thickness |
| p | posterior view |
| PSuL | post-sulcus length |
| r | rostral view |
| SuL | sulcus length |
| SD | standard deviation |
| v | ventral view |

### *Captions plates*

For all plates: inner faces are indicated by numbers.
b = outer view, c = caudal view, d = dorsal view, p = posterior view, r = rostral view, v = ventral view.
Scale bars = 1 mm.

## Systematic part

Table 1 summarises all teleost species based on otoliths (sagittas) from the sediments of the entire Estepona area,

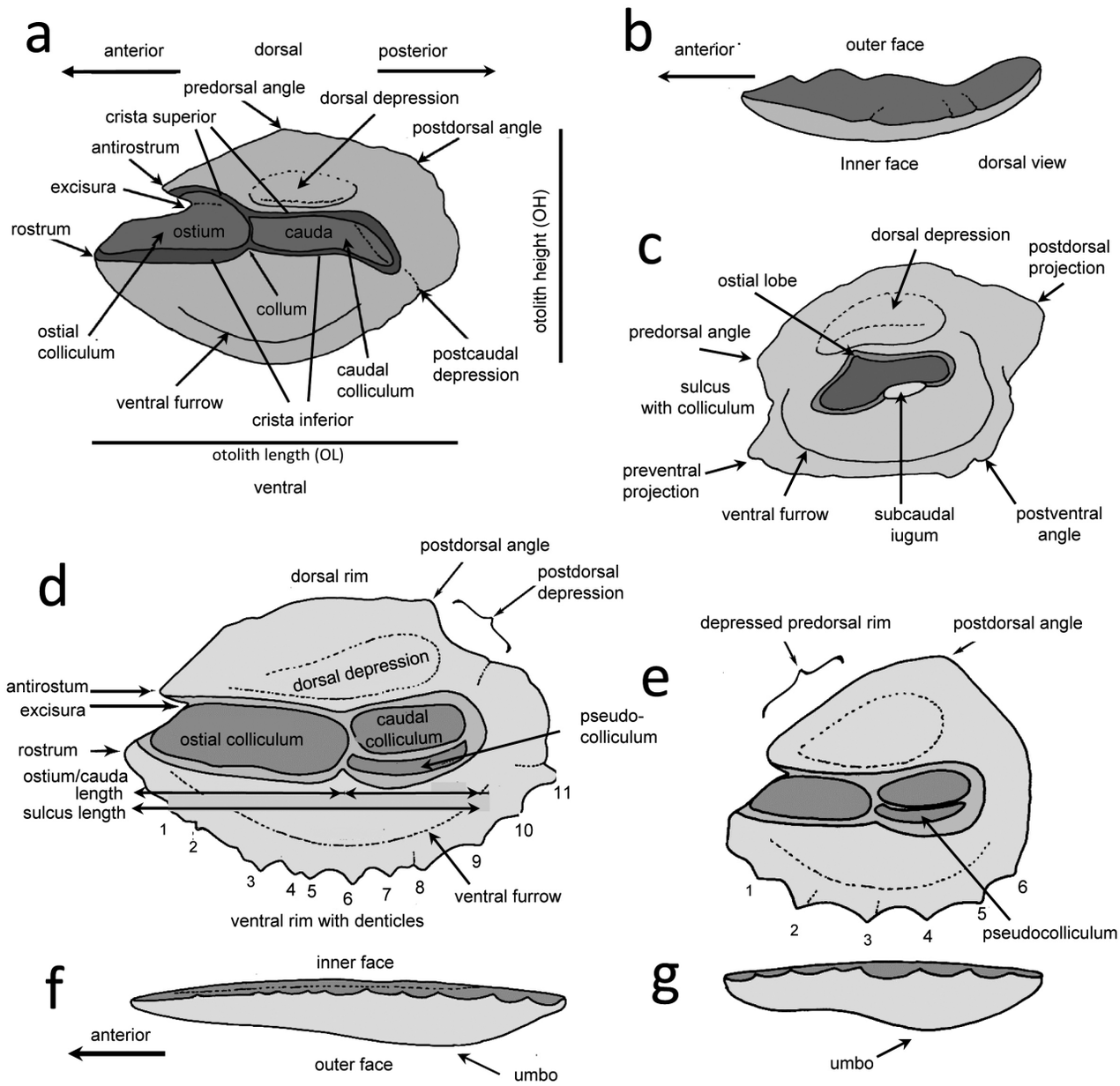


**Figure 2.** Terminology of fish otoliths. **a**. Perciform otolith (inner face) showing general features. **b, c**. Specific features of gobiid otoliths. b: Dorsal view; c: Inner face. **d-g**. Features of Myctophid (*Diaphus*) otoliths. D, E: inner face; F, G: ventral view. Figure after Schwarzhans *et al*. (2013b, 2014) (with permission).

with reference to their iconography on Plates 1-37. An iconography of all encountered species is given in Table 1, last column. The systematic part gives descriptions and discussions of newly described species, as well as of specific species on which comments were made. They are indicated in Table 1, 2nd column by a single black dot (●). However, well-known species are only indicated in Table 1 by name, occurrence, and reference to the plate and figures but without any comment in the Systematic Part. The number of otoliths per species is given for each individual outcrop in Supplementary Online Table 1.

The text of the systematic part contains the descriptions of 17 newly identified species (bold in Table 1). Twenty-three species are recorded for the first time as fossil and are indicated with # in Table 1.

We used Van der Laan *et al*. (2014) for the authorship of family-group names and the online version of *Eschmeyer's Catalog of Fishes* (Fricke *et al*., 2021) for genus names. Systematics follow Nelson *et al*. (2016) and terminology follows Koken (1884), Smale *et al*. (1995) and Schwarzhans (2013b, 2014).

**Table 1.** Distribution of all taxa encountered at Estepona for the Zanclean and Piacenzian outcrops, the Pliocene and Pleistocene in the Mediterranean and the Miocene and present-day inside and outside the Mediterranean. For the present-day records, we consulted Paxton (1979, for *Diaphus* aff. *arabicus*), Whitehead *et al*. (1984), Quéro *et al.* (1990), Ordines *et al.* (2019), Psomadakis *et al.* (2012) as well as Fishbase.org in the case of multiple references (for *Zenion* cf. *hololepis* and *Brotula* cf. *multibarbata*). New species are marked in **bold**.

**Abbreviations:** ? = occurrence not ascertained; ● = refers to a description or comment in the main text of the systematic part; # = first occurrence as fossil; M = Miocene occurrence in the Mediterranean; P = Piacenzian occurrence in the Mediterranean; Plei = Pleistocene occurrence in the Mediterranean; R = present-day occurrence in the Mediterranean; Z = Zanclean occurrence in the Mediterranean; () = occurrence outside the Mediterranean.

**References:** 1 = Agiadi *et al.* (2011); 2 = Agiadi *et al*. (2013a); 3 = Agiadi *et al.* (2016); 4 = Agiadi *et al.* (2018); 5 = Agiadi *et al*. (2019); 6 = Agiadi *et al.* (2020); 7 = Brzobohatý & Nolf (1996); 8 = Brzobohatý & Nolf (2000); 9 = Girone (2000); 10 = Girone (2003); 11 = Girone (2005); 12 = Girone (2006); 13 = Girone & Varola (2001); 14 = Girone *et al.* (2006); 15 = Girone *et al.* (2010); 16 = Hoedemakers & Batllori (2005); 17 = Huyghebaert & Nolf (1979); 18 = Lanckneus & Nolf (1979); 19 = Landini & Sorbini (2005); 20 = Lin *et al.* (2015); 21 = Lin *et al.* (2017b); 22 = Nolf (1978); 23 = Nolf (2013); 24 = Nolf & Brzobohatý (2002); 25 = Nolf & Brzobohatý (2004); 26 = Nolf & Cappetta (1980); 27 = Nolf & Cappetta (1989); 28 = Nolf & Cavallo (1995); 29 = Nolf & Girone (2000); 30 = Nolf & Girone (2006); 31 = Nolf & Marques da Silva (1997); 32 = Nolf & Martinell (1980); 33 = Nolf & Steurbaut (1983); 34 = Nolf *et al.* (1997); 35 = Ordines *et al*. (2019); 36 = Reichenbacher & Cappetta (1999); 37 = Schwarzhans (1978); 38 = Schwarzhans (1981); 39 = Schwarzhans (1986); 40 = Schwarzhans (1999); 41 = Schwarzhans (2010a); 42 = Schwarzhans *et al.* (2020b); 43 = Steurbaut (1983); 44 = Steurbaut (1984); Steurbaut & Jonet (1982); 46 = Hoedemakers (1997); 47 = Gaemers (1976); 48 = Carnevale & Schwarzhans (2022).

| Species | Description/ Remarks in Systematic Part | Number of otoliths | | Species identified in other studies | | | | | References | Iconography |
|---|---|---|---|---|---|---|---|---|---|---|
| | | Zanclean | Piacenzian | Miocene | Zanclean | Piacenzian | Pleistocene | present-day | | |
| *Pterothrissus compactus* Schwarzhans, 1981 | ● | 4 | – | – | Z | – | – | – | 6, 19, 27, 28, 30, 38, 39 | Pl. 1, fig. 2 |
| *Pterothrissus darbelhamriensis* Schwarzhans, 1981 | ● | – | 4 | – | () | () | – | – | 31, 39 | Pl. 1, fig. 1 |
| *Panturichthys subglaber* (Schubert, 1906) | ● | – | 1 | M() | Z | P | – | – | 19, 20, 26, 27, 30, 32, 34, 39, 44, 45 | Pl. 1, fig. 3 |
| ***Pythonichthys gibbosus* nov. sp.** | | – | 1 | – | – | – | – | – | | Pl. 1, fig. 4 |
| *Echelus myrus* (Linnaeus, 1758) | | 1 | 1 | () | Z | – | – | R | 19, 27, 44 | Pl. 1, fig. 5 |
| *Hoplunnis* sp. | ● | – | 2 | – | – | – | – | – | | Pl. 1, fig. 6 |
| ***Saurenchelys silex* nov. sp.** | ● | – | 2 | – | – | – | – | – | | Pl. 1, figs 7-8 |
| ***Paraconger pinguis* nov. sp.** | ● | 2 | 35 | – | Z | – | – | – | 30 | Pl. 2, figs 1-9 |
| *Conger conger* (Linnaeus, 1758) | | 7 | 20 | M() | Z() | () | Plei | R | 4, 5, 6, 9, 13, 14, 18, 19, 21, 29, 30, 31, 34, 44 | Pl. 2, figs 10-11 |
| *Gnathophis mystax* (Delaroche, 1809) | ● | 1 | 16 | M | Z | – | Plei | R | 4, 5, 6, 19, 21, 30 | Pl. 3, figs 1-2 |
| ***Gnathophis henkmulderi* nov. sp.** | | – | 28 | – | – | – | – | – | | Pl. 3, figs 3-10 |
| *Pseudophichthys escaravatierensis* Nolf & Cappetta, 1989 | ● | – | – | – | Z | – | – | – | 2, 19, 27, 30 | Pl. 3, fig. 11 |
| *Japonoconger africanus* (Poll, 1953) | ● | 1 | 20 | – | Z | P | Plei | () | 19, 27, 34, 39 | Pl. 3, figs 12-14 |
| *Rhynchoconger pantanelli* (Bassoli, 1906) | | 1 | 31 | M() | Z | P | Plei | – | 3, 16, 20, 21, 24, 25, 33, 44 | Pl. 3, figs 15-16 |
| *Etrumeus* sp. | ● | – | 1 | – | – | – | – | – | | Pl. 4, fig. 1 |
| *Sardinella* sp. | | – | 2 | – | – | – | – | – | | Pl. 4, fig. 2 |
| *Xenodermichthys copei* (Gill, 1884) | | – | 3 | M | – | – | – | () | 20, 25 | Pl. 4, figs 3-4 |
| *Argentina sphyraena* Linnaeus, 1758 | | – | 28 | M() | Z | P | Plei | R | 4, 9, 12, 13, 14, 15, 19, 24, 27, 30, 39 | Pl. 4, figs 5-7 |
| *Dolichopteryx* sp. | ● | – | 1 | – | – | – | – | – | | Pl. 4, fig. 9 |
| *Microstoma* cf. *microstoma* (Risso, 1810) | # | – | 1 | – | – | – | – | R | | Pl. 4, fig. 8 |
| *Gonostoma* sp. | | – | 2 | M | – | – | – | – | 25 | Pl. 4, figs 11-12 |
| 'Gonostomatoidei' inc. sedis | ● | – | 1 | – | – | – | – | – | | Pl. 4, fig. 13 |
| *Maurolicus muelleri* (Gmelin, 1789) | | – | 10 | M() | Z | P | Plei | R | 1, 2, 4, 9, 10, 11, 12, 13, 14, 15, 19, 21, 24, 25, 27, 30, 33, 39, 44 | Pl. 5, figs 2-4 |

| | | | | | | | | | | |
|---|---|---|---|---|---|---|---|---|---|---|
| *Polyipnus* sp. | | – | 18 | – | – | – | – | – | | Pl. 4, figs 15-17 |
| *Vinciguerria poweriae* (Cocco, 1838) | | – | 1 | M() | Z | P | Plei | R | 1, 2, 4, 9, 10, 11, 12, 14, 19, 24, 25, 27, 30 | Pl. 5, fig. 5 |
| *Phosichthys* cf. *argenteus* Hutton, 1872 | | – | 1 | M | Z | P | – | () | 19, 25, 27, 30 | Pl. 4, fig. 18 |
| *Synodus saurus* (Linnaeus, 1758) | | 1 | – | – | Z | P | Plei | R | 19, 30 | Pl. 4, fig. 10 |
| *Chlorophthalmus agassizi* Bonaparte, 1840 | | – | 1 | – | Z | – | Plei | R | 1, 2, 4 | Pl. 4, fig. 14 |
| *Scopelosaurus* sp. | ● | 1 | – | – | – | – | – | – | | Pl. 5, fig. 1 |
| *Scopelarchus analis* (Brauer, 1902) | | – | 1 | M | Z | – | Plei | () | 1, 4, 14, 19, 20, 21, 27, 30 | Pl. 5, fig. 6 |
| *Notoscopelus elongatus* (Costa, 1844) | ● | 25 | 8 | M() | – | – | Plei | R | 1, 3, 4, 7, 9, 10, 11, 13, 14, 19, 20, 21, 43 | Pl. 5, fig. 13 |
| *Notoscopelus resplendens* (Richardson, 1845) | ● | 1 | 1000 | M | Z | P | Plei | () | 2, 6, 7, 12, 19, 20, 21, 27, 30, 37, 39 | Pl. 5, figs 7-12 |
| *Scopelopsis pliocenicus* (Anfossi & Mosna, 1976) | | 16 | 429 | M | Z | P | Plei | – | 1, 2, 3, 4, 7, 10, 11, 12, 14, 19, 20, 21, 27, 30, 33, 34, 39 | Pl. 5, figs 14-16 |
| *Bolinichthys* cf. *kreffti* Schwarzhans, 1986 | | 2 | 3 | – | Z | P | – | – | 7, 19, 27, 39 | Pl. 6, figs 1-2 |
| *Bolinichthys* sp. | | – | 1 | – | – | – | – | – | | Pl. 6, fig. 3 |
| *Ceratoscopelus maderensis* (Lowe, 1839) | | 2 | 627 | M | Z | P | Plei | R | 1, 2, 3, 4, 5, 6, 7, 9, 10, 11, 12, 13, 14, 19, 27, 29, 30, 32, 34, 37, 39 | Pl. 6, figs 4-7 |
| *Lampadena dea* Fraser-Brunner, 1949 | | – | 15 | M | Z | – | Plei | () | 3, 7, 19, 20, 21, 27, 34, 39 | Pl. 6, figs 8-10 |
| *Lampanyctus crocodilus* (Risso, 1810) | | – | 9 | – | – | P | Plei | R | 1, 4, 7, 10, 11, 13, 14, 19 | Pl. 6, figs 11-12 |
| *Lampanyctus photonotus* Parr, 1928 | | 13 | 94 | – | Z | P | – | () | 7, 19, 27, 29 | Pl. 6, figs 13-15 |
| *Diaphus anderseni* Tåning, 1932 | ● # | 1 | – | – | – | – | – | () | | Pl. 7, fig. 1 |
| *Diaphus* aff. *arabicus* Nafpaktitis, 1978 | ● # | 2 | – | – | – | – | – | () | | Pl. 7, figs 2-3 |
| *Diaphus befralai* Brzobohatý & Nolf, 2000 | | 8 | – | M | – | – | – | – | 3, 8, 15, 20, 21 | Pl. 7, figs 13-15 |
| *Diaphus holti* Tåning, 1918 | | 3 | 78 | M | Z | P | Plei | R | 8, 20, 21 | Pl. 7, figs 7-10 |
| ***Diaphus mermuysi* nov. sp.** | ● | – | 4 | – | – | – | – | – | | Pl. 7, figs 4-6 |
| *Diaphus rafinesquii* (Cocco, 1838) | | 1 | 19 | M | Z | P | Plei | R | 1, 2, 3, 4, 6, 8, 10, 11, 12, 14, 15, 19, 20, 21, 27, 30, | Pl. 7, figs 11-12 |
| *Diaphus taaningi* Norman, 1930 | | 4 | 10 | M() | Z | P | Plei | () | 1, 2, 4, 8, 10, 11, 13, 14, 15, 19, 20, 24 | Pl. 8, figs 1-5 |
| *Diaphus termophilus* Tåning, 1928 | ● # | – | 1 | – | – | – | – | () | | Pl. 8, fig. 6 |
| *Diaphus cavallonis* Brzobohatý & Nolf, 2000 | ● | 1246 | – | M | Z | P | – | – | 2, 3, 8, 12, 15, 19, 20, 21, 30 | Pl. 8, figs 7-18 |
| ***Diaphus postcavallonis* nov. sp.** | ● | – | 3864 | – | – | – | – | – | | Pl. 9, figs 1-15 |
| *Diaphus pedemontanus* (Robba, 1970) | ● | 1 | – | M | Z | – | – | – | 8, 15, 19, 20, 21, 25, 33, 43 | Pl. 10, fig. 1 |
| *Diaphus* sp. 1 | ● | – | 1 | – | – | – | – | – | | Pl. 10, fig. 2 |
| *Diaphus splendidus* (Brauer, 1904) | ● | 8 | 611 | M | Z | P | Plei | () | 2, 3, 6, 8, 15, 19, 20, 21, 30, 34, 37 | Pl. 10, figs 3-13 |
| *Diaphus* sp. 2 | ● | 4 | – | – | – | – | – | – | | Pl. 11, figs 1-3 |
| *Diaphus dirknolfi* Schwarzhans, 1986 | ● | 18 | 413 | – | Z | – | – | – | 39 | Pl. 11, figs 4-8 |
| *Diaphus adenomus* Gilbert, 1905 | ● | – | 4 | – | Z | – | – | () | 2, 30 | Pl. 11, figs 9-11 |
| *Lobianchia dofleini* (Zugmayer, 1911) | ● | 2 | 1 | M() | Z | P | Plei | R | 2, 3, 7, 15, 19, 20, 21, 24, 25, 27, 30, 33, 34 | Pl. 11, fig 12-13 |
| *Lobianchia* cf. *gemellarii* (Cocco, 1838) | ● | 3 | 18 | M | – | – | Plei | R | 14, 20, 21 | Pl. 11, figs 14-17 |
| *Benthosema* aff. *glaciale* (Reinhardt, 1837) | | 17 | 26 | M | Z | P | Plei | R | 1, 4, 7, 9, 10, 11, 12, 13, 14, 19, 21, 33 | Pl. 12, figs 1-4 |
| *Electrona rissoi* (Cocco, 1829) | | 24 | 82 | – | Z | P | Plei | R | 6, 7, 19, 27, 30, 32, 34, 37, 39 | Pl. 12, figs 5-8 |
| *Hygophum* aff. *benoiti* (Cocco, 1838) | ● | – | 5 | – | Z | P | Plei | R | 1, 2, 4, 9, 10, 11, 12, 13, 14, 19 | Pl. 12, figs 13-17 |

| Species | Description/ Remarks in Systematic Part | Number of otoliths | | Species identified in other studies | | | | | References | Iconography |
|---|---|---|---|---|---|---|---|---|---|---|
| | | Zanclean | Piacenzian | Miocene | Zanclean | Piacenzian | Pleistocene | present-day | | |
| *Hygophum hygomi* (Lütken, 1892) | | 273 | 1051 | M() | Z | P | Plei | R | 2, 3, 6, 7, 15, 19, 20, 21, 24, 25, 30, 34, 37, 39 | Pl. 12, figs 9-12 |
| *Myctophum fitchi* (Schwarzhans, 1979) | • | 835 | 369 | M | Z | P | Plei | – | 2, 3, 7, 19, 20, 21, 27, 30, 34, 37, 39 | Pl. 12, figs 19-25 |
| *Myctophum punctatum* Rafinesque, 1810 | | – | 2 | M | Z | P | Plei | R | 1, 3, 4, 7, 9, 10, 11, 12, 13, 14, 20, 21, 32, 33, 43 | Pl. 11, fig. 28 |
| *Polymixia* cf. *lowei* Günther, 1859 | • | – | 1 | () | – | – | – | () | 24 | Pl. 13, fig. 1 |
| *Zenion* cf. *hololepis* Goode & Bean, 1896 | | 1 | 2 | M | Z | – | – | () | 19, 20, 27, 30 | Pl. 13, fig. 2 |
| *Bathygadus novus* (Bassoli, 1906) | | 1 | 5 | M() | Z | – | – | – | 3, 19, 20, 21, 23, 27, 30, 33, 34, 37, 39 | Pl. 13, figs 3-4 |
| *Coelorinchus arthaberoides* (Bassoli, 1906) | • | 2 | 136 | – | Z | P | Plei | – | 19, 34, 27, 39, 41 | Pl. 13, figs 5-7 |
| *Coelorinchus caelorhincus* (Risso, 1810) | • | 41 | 244 | M(?) | Z | P | Plei | R | 9, 10, 11, 14, 19, 20, 21, 23, 25, 27, 30, 33, 37, 41 | Pl. 13, figs 8-10 |
| *Coelorinchus mediterraneus* Iwamoto & Ungaro, 2002 | • # | 1 | 43 | – | – | – | – | R | | Pl. 13, figs 11-16 |
| *Coryphaenoides sicilianus* Schwarzhans, 1986 | | – | 5 | – | Z | P | Plei | – | 11, 12, 14, 19, 27, 30, 39 | Pl. 14, figs 1-2 |
| ? *Coryphaenoides* sp. 1 | • | – | 1 | – | – | – | Plei | – | 10, 14, 19 | Pl. 14, fig. 3 |
| ? *Coryphaenoides* sp. 2 | • | – | 1 | – | – | – | – | – | | Pl. 14, fig. 4 |
| *Coryphaenoides* sp. 3 | • | – | 1 | – | – | – | – | – | | Pl. 14, fig. 10 |
| *Nezumia ornata* Bassoli, 1906 | | 101 | 859 | M() | Z | P | Plei | – | 19, 20, 21, 24, 25, 27, 30, 33, 34, 37, 39 | Pl. 14, figs 5-6 |
| *Nezumia* aff. *sclerorhynchus* (Risso, 1810) | | – | 25 | M | Z | – | Plei | R | 11, 14, 19, 21, 27, 30, 37 | Pl. 14, figs 7-8 |
| *Trachyrincus scabrus* (Rafinesque, 1910) | | 2 | 5 | M | Z | P | Plei | R | 3, 12, 14, 19, 20, 21, 27, 30, 33, 37 | Pl. 14, fig. 9 |
| *Physiculus huloti* Poll, 1953 | • | 6 | 79 | M() | Z() | P | Plei | () | 7, 21, 15, 16, 18, 19, 24, 27, 30, 32, 34, 39, 45 | Pl. 14, figs 11-12 |
| *Laemonema* sp. | • | – | 2 | – | – | – | – | – | | Pl. 14, figs 13-14 |
| *Merluccius merluccius* (Linnaeus, 1758) | | – | 4 | – | – | – | – | – | | Pl. 15, fig. 4 |
| *Bregmaceros albyi* (Sauvage, 1880) | | – | 5 | – | – | – | – | – | | Pl. 15, figs 2-3 |
| *Phycis blennoides* (Brünnich, 1768) | • | 8 | 98 | () | Z | () | Plei | R | 4, 5, 9, 10, 11, 13, 14, 17, 19, 31, 39, 41 | Pl. 15, figs 9-10 |
| *Phycis phycis* (Linnaeus, 1766) | • # | 1 | 8 | – | – | – | – | R | | Pl. 15, fig. 7-8 |
| *Gaidropsarus mediterraneus* (Linnaeus, 1758) | | 1 | – | – | Z | – | – | R | 30 | Pl. 14, fig. 15 |
| Gaidropsarinae sp. | | – | 3 | – | – | – | – | – | | Pl. 15, fig. 1 |
| *Gadiculus argenteus* Guichenot, 1850 | • | 4 | 4324 | M() | Z | P | Plei | R | 1, 4, 9, 10, 11, 12, 13, 14, 15, 19, 20, 21, 24, 27, 30, 33, 34, 37, 39, 44 | Pl. 15, figs 11-13 |
| *Paratrisopterus glaber* Schwarzhans, 2010 | • | 3 | 77 | () | – | – | – | – | 41 | Pl. 15, figs 14-15 |
| *Paratrisopterus labiatus* (Schubert, 1915) | | 3 | – | M() | Z | P | Plei | – | 1, 2, 3, 4, 14, 15, 19, 20, 21, 24, 27, 30, 32, 33, 34, 43, 45 | Pl. 15, figs 16-18 |
| *Micromesistius poutassou* (Risso, 1826) | | 137 | 2557 | (?) | Z | P | Plei | R | 4, 9, 10, 11, 12, 13, 14, 19, 27, 30, 32, 34, 37, 41 | Pl. 15, fig. 5 |
| *Trisopterus minutus* (Linnaeus, 1758) | | 1 | – | () | () | – | – | R | 22, 23, 47 | Pl. 15, fig. 6 |
| ***Kryptophanaron nolfi* nov. sp.** | • | – | 3 | – | – | – | – | – | | Pl. 16, figs 1-3 |
| *Hoplostethus pisanus* Koken, 1891 | | – | 2 | – | Z | – | – | – | 27, 30, 37 | Pl. 16, fig. 4 |

| | | | | | | | | | | |
|---|---|---|---|---|---|---|---|---|---|---|
| *Hoplostethus lawleyi* Koken, 1891 | | – | 4 | M | Z | – | – | – | 21, 23, 33, 37 | Pl. 16, figs 5-7 |
| *Hoplosthetus praemediterraneus* Schubert, 1905 | | 2 | 12 | M | – | – | – | – | 20, 21 | Pl. 17, figs 1-6 |
| *Gephyroberyx darwinii* (Johnson, 1866) | ● | – | 39 | () | – | – | – | R | 24, 44, 47 | Pl. 17, figs 7-10 |
| *Melamphaes typhlops* Lowe, 1843 | | – | 2 | – | Z | – | – | () | 19, 27 | Pl. 17, fig. 11 |
| *Scopelogadus beanii* (Günther, 1887) | ● | 3 | 11 | – | – | – | Plei | () | 14 | Pl. 17, figs 12-16 |
| *Echiodon dentatus* (Cuvier, 1829) | | 3 | 325 | – | Z | P | Plei | R | 2, 4, 13, 14, 19, 27, 30, 39 | Pl. 17, figs 17-18 |
| *Ophidion barbatum* Linnaeus, 1758 | | – | 26 | – | Z | P | Plei | R | 4, 5, 6, 13, 14, 19, 27, 30, | Pl. 18, figs 2-3 |
| *Ophidion rochei* Müller, 1845 | | 13 | 136 | – | Z() | () | Plei | R | 9, 13, 14, 18, 22, 27, 30, 31, 37, 39 | Pl. 18, figs 6-7 |
| *Ophidion* cf. *saldanhai* Matallanas & Brito, 1999 | ● # | – | 6 | – | – | – | – | () | | Pl. 18, figs 4-5 |
| *Brotula* cf. *multibarbata* Temminck & Schlegel, 1846 | ● | – | 2 | – | Z | – | – | () | 19, 30, 34 | Pl. 18, figs 8-9 |
| ? *Benthocometes* sp. | | – | 1 | – | – | – | – | – | | Pl. 18, fig. 1 |
| *Bellotia* aff. *obliqua* (Weiler, 1942) | ● | 1 | – | () | Z | – | Plei | – | 19, 41 | Pl. 19, fig. 3 |
| *Bellottia verecunda* Carnevale & Schwarzhans, 2022 | ● | 1 | 1 | M | – | – | – | – | 48 | Pl. 19, figs 1-2 |
| ***Bidenichthys mediterraneus* nov. sp.** | ● | – | 24 | – | Z() | – | – | – | 18, 19, 34 | Pl. 18, figs 10-15 |
| *Cataetyx alleni* (Byrne, 1906) | ● # | 1 | 4 | – | – | – | – | R | | Pl. 19, fig. 4 |
| *Cataetyx* sp. | ● | – | 1 | – | – | – | – | – | | Pl. 19, fig. 5 |
| *Grammonus ater* (Risso, 1810) | ● | – | 1 | – | Z | – | Plei | R | 2, 4, 5, 9, 13, 14, 19 | Pl. 18, fig. 18 |
| *Grammomus* aff. *bassoli* (Nolf, 1980) | ● | – | 3 | M | Z | – | – | – | 3, 6, 20, 21, 39 | Pl. 18, figs 16-17 |
| '*Bythites*' *pauper* (Schwarzhans, 1986) | ● | – | 1 | – | Z | – | Plei | – | 19, 37 | Pl. 19, fig. 6 |
| *Apogon imberbis* (Linnaeus, 1758) | ● | – | 1 | M() | – | – | – | R | 25, 45 | Pl. 19, fig. 7 |
| *Apogon lozanoi* Bauza, 1957 | ● | 5 | 16 | – | Z | P | Plei | – | 14, 19, 27, 30, 32 | Pl. 19, figs 8-13 |
| ***Fowleria velerinensis* nov. sp.** | ● | – | 23 | – | – | – | – | – | | Pl. 19, figs 14-18 |
| *Buenia massutii* Kovačić, Ordines & Schliewen, 2017 | ● # | 1 | 11 | – | – | – | – | R | 35 | Pl. 20, figs 1-5 |
| ***Buenia pulvinus* nov. sp.** | ● | 4 | 135 | – | – | – | – | – | | Pl. 20, figs 6-13 |
| *Pomatoschistus* sp. | ● | – | 5 | – | – | – | – | – | | Pl. 20, figs 14-16 |
| *Pseudaphya* sp. | ● | 1 | 16 | – | – | – | – | – | | Pl. 20, figs 17-22 |
| *Deltentosteus quadrimaculatus* Valenciennes, 1837 | ● | 169 | 6012 | M | Z | P | Plei | R | 1, 2, 3, 4, 5, 6, 11, 13, 14, 19, 20, 21, 30, 42 | Pl. 20, figs 23-26 |
| *Hoeseichthys brioche* (Lin, Girone & Nolf, 2015) | ● | – | 25 | M | Z | – | – | – | 3, 20, 21, 42 | Pl. 21, figs 1-2 |
| *Lesueurigobius suerii* (Risso, 1810) | | 1 | 51 | M | Z | P | Plei | R | 2, 4, 5, 6, 13, 14, 19, 20, 21, 30, 42 | Pl. 21, figs 3-6 |
| *Lesueurigobius stazzanensis* Schwarzhans *et al.*, 2020 | ● | – | 24 | M | Z | – | – | – | 42 | Pl. 21, figs 7-9 |
| *Gobius bucchichi* Steindachner, 1870 | ● # | – | 2 | – | Z | – | – | R | 6 | Pl. 21, fig. 11 |
| *Gobius* cf. *fallax* Sarrato, 1889 | ● | 1 | – | M | Z | – | – | R | 42 | Pl. 21, fig. 12 |
| *Gobius geniporus* Valenciennes, 1837 | ● | 11 | 9 | () | Z | – | – | R | 5, 6, 24, 42, 44 | Pl. 22, figs 1-2 |
| *Gobius cobitis* Pallas, 1814 | ● | 1 | 1 | – | Z | – | Plei | R | 5, 6 | Pl. 22, figs 3-4 |
| *Gobius kolombatovici* Kovačić & Miller, 2000 | ● # | 7 | 46 | – | – | – | – | R | | Pl. 22, figs 3-4 |
| ***Gobius alboranensis* nov. sp.** | ● | – | 6 | – | – | – | – | – | | Pl. 23, figs 1-3 |
| *Gobius roulei* de Buen, 1928 | ● # | 15 | 3 | – | – | – | – | R | | Pl. 23, figs 4-8 |
| *Gobius* aff. *niger* Linnaeus, 1758 | ● | – | 1 | – | Z | P | Plei | R | 2, 4, 14, 19, 30, 42 | Pl. 23, fig. 9 |
| ***Gobius lombartei* nov. sp.** | ● | 3 | 24 | – | – | – | – | – | | Pl. 24, figs 1-5 |
| *Gobius vittatus* Vinciguerra, 1883 | ● | – | 2 | – | – | – | Plei | R | 5 | Pl. 21, fig. 10 |
| **'*Gobius*' *pterois* nov. sp.** | ● | 6 | 13 | – | – | – | – | – | | Pl. 25, figs 4-7 |
| ***Thorogobius mirbachae* nov. sp.** | ● | – | 1 | – | – | – | – | – | | Pl. 24, fig. 6 |
| *Thorogobius truncatus* Schwarzhans, 1978 | ● | 7 | 38 | – | Z | – | Plei | – | 19, 27, 30, 34, 37, 39 | Pl. 24, figs 5-7 |

| Species | Description/ Remarks in Systematic Part | Number of otoliths | | Species identified in other studies | | | | | References | Iconography |
|---|---|---|---|---|---|---|---|---|---|---|
| | | Zanclean | Piacenzian | Miocene | Zanclean | Piacenzian | Pleistocene | present-day | | |
| *Chromogobius britoi* Van Tassell, 2001 | ● # | 4 | – | – | – | – | – | () | | Pl. 25, figs 9-10 |
| *Chromogobius* cf. *zebratus* (Kolombatović, 1891) | ● | 3 | 3 | – | Z | – | Plei | R | 4, 5, 6 | pl 25, fig 8 |
| *Callogobius weileri* (Bauza, 1955) | | 1 | – | M | Z | P | Plei | – | 14, 21, 27, 30, 39, 42 | Pl. 25, fig. 11 |
| Gobiidae sp. | | 1 | – | – | – | – | – | – | | Pl. 23, fig 10 |
| *Chromis* cf. *chromis* (Linnaeus, 1758) | ● | 23 | 1 | – | – | – | Plei | R | 4, 5, 19 | Pl. 26, figs 1-6 |
| Mugilidae indet. 1 | ● | – | 1 | – | – | – | – | – | | Pl. 26, fig. 7 |
| Mugilidae indet. 2 | ● | – | 1 | – | – | – | – | – | | Pl. 26, fig. 8 |
| *Atherina presbyter* Cuvier, 1829 | ● | 20 | 23 | – | Z | P | Plei | R | 19, 27 | Pl. 26, figs 9-14 |
| *Exocoetus volitans* Linnaeus, 1758 | # | – | 1 | – | – | – | – | R | | Pl. 26, fig. 15 |
| *Tylosurus* cf. *acus* (Lacepède, 1803) | | 4 | 3 | – | Z | – | – | R | 30 | Pl. 26, figs 16-17 |
| *Trachurus* sp. | | 3 | 32 | – | – | – | – | – | | Pl. 26, figs 18-21 |
| *Citharus* cf. *linguatula* (Linnaeus, 1758) | | – | 1 | M() | Z() | – | – | R | 2, 16, 19, 20, 24, 27, 30, 37, 34, 40, 45 | Pl. 27, fig. 12 |
| *Lepidorhombus boscii* (Risso, 1810) | | – | 1 | – | () | – | – | R | 22, 40 | Pl. 27, fig. 3 |
| *Lepidorhombus whiffiagonis* (Walbaum, 1792) | | – | 4 | – | Z() | – | – | R | 19, 30, 40 | Pl. 27, figs 1-2 |
| *Arnoglossus kokeni* (Bassoli, 1906) | | – | 12 | M | Z() | P | Plei | – | 2, 4, 6, 14, 16, 19, 20, 21, 27, 30, 33, 40 | Pl. 27, figs 7-8 |
| *Arnoglossus laterna* (Walbaum, 1792) | | – | 1 | () | Z() | P | Plei | R | 5, 6, 19, 22, 37, 41 | Pl. 27, fig. 9 |
| *Arnoglossus quadratus* Schwarzhans, 1999 | ● | 1 | 3 | – | () | – | – | – | 40 | Pl. 27, figs 4-6 |
| *Buglossidium luteum* (Risso, 1810) | | 1 | 10 | – | Z() | P() | Plei | R | 6, 14, 16, 19, 20, 21, 22, 30, 31, 33 | Pl. 27, figs 10-11 |
| *Microchirus variegatus* (Donovan, 1802) | | 2 | 4 | M | Z() | P | Plei | R | 6, 14, 19, 20, 21, 22, 27, 30, 40 | Pl. 27, figs 13-15 |
| *Solea* sp. | | 1 | – | – | – | – | – | – | | Pl. 27, fig. 16 |
| *Promethichthys prometheus* (Cuvier, 1832) | | – | 5 | M | Z | – | – | () | 19, 20, 27, 30 | Pl. 28, fig. 1 |
| *Benthodesmus elongatus* Clarke, 1879 | ● | – | 2 | – | Z | – | – | () | 19 | Pl. 28, figs 4-5 |
| *Ammodytes* sp. | | – | 1 | – | – | – | – | – | | Pl. 28, fig. 2 |
| *Gymnammodytes cicerelus* (Rafinesque, 1810) | ● # | – | 1 | – | – | – | – | R | | Pl. 28, fig. 3 |
| *Trachinus draco* Linnaeus, 1758 | | – | 32 | M() | Z | () | Plei | R | 5, 14, 20, 24, 30, 31, 33, 44, 45 | Pl. 28, fig. 6 |
| *Trachinus radiatus* Cuvier, 1829 | | – | 2 | () | Z | – | Plei | R | 19, 32, 41 | Pl. 28, fig. 9 |
| *Trachinus* sp. | ● | – | 5 | – | – | – | – | – | | Pl. 28, figs 7-8 |
| *Uranoscopus scaber* Linnaeus, 1758 | ● | – | 2 | M | Z | – | – | R | 16, 30 | Pl. 28, fig. 10 |
| *Uranoscopus* sp. | ● | – | 1 | – | – | – | – | – | | Pl. 28, fig. 11 |
| *Bodianus scrofa* (Valenciennes, 1839) | ● # | – | 1 | – | – | – | – | () | | Pl. 28, fig. 12 |
| Labridae indet. | | 1 | – | – | – | – | – | – | | Pl. 28, fig. 13 |
| *Verilus mutinensis* (Bassoli, 1906) | ● | 344 | 5668 | M() | Z | P | Plei | – | 1, 2, 4, 6, 12, 14, 15, 19, 20, 21, 24, 25, 27, 30, 32, 33, 34, 37, 39 | Pl. 29, figs 1-4 |
| *Epigonus constanciae* (Giglioli, 1880) | | 11 | 35 | M | Z | – | Plei | R | 14, 19, 20, 21, 27, 30, 33 | Pl. 29, figs 5-9 |
| *Polynemus raffii* Nolf & Girone, 2006 | ● | – | 5 | – | Z | – | – | – | 30 | Pl. 29, figs 10-12 |
| *Bathyclupea* sp. | ● | 1 | – | – | – | – | – | – | | Pl. 29, fig. 13 |
| *Anthias anthias* (Linnaeus, 1758) | | 21 | 4 | – | Z | – | – | R | 30 | Pl. 29, figs 14-15 |
| *Chelidoperca* sp. | | 1 | – | – | – | – | – | – | | Pl. 30, fig. 1 |
| Serranidae sp. | | 1 | 1 | – | – | – | – | – | | Pl. 30, fig. 2 |

| | | | | | | | | | | |
|---|---|---|---|---|---|---|---|---|---|---|
| *Scombrops* cf. *boops* (Houttuyn, 1782) | • # | 1 | 16 | – | – | – | – | () | | Pl. 30, figs 6-9 |
| ***Pristigenys adrianae* nov. sp.** | • | – | 2 | – | – | – | – | – | | Pl.30, figs 10-11 |
| *Pomadasys incisus* (Bowdich, 1825) | | – | 6 | M() | Z | P() | Plei | R | 6, 15, 19, 20, 24, 27, 30, 31, 33, 34, 44, 45 | Pl. 31, fig. 1 |
| Haemulinae sp. | • | – | 1 | – | – | – | – | – | | Pl. 31, fig. 2 |
| *Cepola macrophthalma* (Linnaeus, 1766) | • | 3 | 26 | M() | Z | P | Plei | R | 2, 4, 5, 9, 11, 12, 13, 14, 15, 16, 19, 20, 21, 24, 25, 27, 30, 32, 34, 36, 39, 44, 45 | Pl. 30, figs 3-5 |
| *Scorpaena loppei* Cadenat, 1943 | • # | 1 | 2 | – | – | – | – | R | | Pl. 31, fig. 6 |
| *Scorpaena* cf. *notata* Rafinesque, 1810 | • | 1 | 2 | () | – | P | Plei | R | 19, 41 | Pl. 31, figs 7-9 |
| *Pontinus* sp. | • | 1 | – | – | – | – | – | – | | Pl. 31, fig. 10 |
| ***Snyderina stillaformis* nov. sp.** | • | – | 3 | – | – | – | – | – | | Pl. 31, figs 3-5 |
| Scorpaenidae sp. | • | – | 1 | – | – | – | – | – | | Pl. 31, fig. 11 |
| ***Prionotus arenarius* nov. sp.** | • | – | 26 | – | – | – | – | – | | Pl. 32, figs 1-6 |
| *Chelidonichthys cuculus* (Linnaeus, 1758) | | – | 3 | () | – | – | – | R | 17 | Pl. 32, figs 7-8 |
| *Chelidonichthys lastoviza* (Bonnaterre, 1788) | | – | 1 | () | – | – | – | R | 41 | Pl. 32, fig. 9 |
| Platycephalidae sp. | • | 1 | 1 | – | – | – | – | – | | Pl. 32, figs 10-11 |
| *Morone* sp. | | 1 | 2 | – | – | – | – | – | | Pl. 32, figs 12-13 |
| *Umbrina canariensis* Valenciennes, 1843 | # | – | 1 | – | – | – | – | R | | Pl. 31, fig 12 |
| *Boops boops* (Linnaeus, 1758) | | 10 | 34 | – | Z | P() | Plei | R | 5, 6, 19, 30, 31 | Pl. 33, figs 1-4 |
| *Diplodus annularis* (Linnaeus, 1758) | | 5 | 7 | – | Z | () | Plei | R | 4, 6, 19, 30, 31 | Pl. 33, figs 6-7 |
| *Diplodus vulgaris* (Geoffroy St Hilaire, 1817) | # | – | 5 | M | – | – | – | R | 15 | Pl. 33, fig. 5 |
| *Diplodus* cf. *puntazzo* (Walbaum, 1792) | | 5 | 2 | – | – | – | Plei | R | 14, 19, 30 | Pl. 33, figs 8-11 |
| *Lithognathus mormyrus* (Linnaeus, 1758) | | 5 | 40 | () | Z | – | Plei | R | 14, 19, 30 | Pl. 34, figs 1-2 |
| *Oblada melanura* (Linnaeus, 1758) | | – | 2 | – | Z | – | Plei | R | 2, 4, 6, 30 | Pl. 33, figs 12-13 |
| *Pagellus acarne* (Risso, 1827) | | 20 | 13 | M() | Z | P | Plei | R | 3, 6, 19, 20, 30, 32, 33, 44, 45 | Pl. 34, figs 3-8 |
| *Pagellus bogaraveo* (Brünnich, 1768) | | 24 | 93 | – | Z() | – | Plei | R | 4, 5, 6, 18, 30 | Pl. 34, figs 9-13 |
| *Rhabdosargus sarba* (Gmelin, 1789) | • # | – | 1 | – | – | – | – | () | | Pl. 35, fig. 1 |
| *Sarpa salpa* (Linnaeus, 1758) | • # | – | 1 | – | – | – | – | R | | Pl. 35, fig. 2 |
| Sparidae sp. | • | – | 2 | – | – | – | – | – | | Pl. 35, figs 12-13 |
| *Spicara* cf. *maena* (Linnaeus, 1758) | • | 7 | 12 | – | Z | – | – | R | 6, 30 | Pl. 35, figs 7-11 |
| *Spicara smaris* (Linnaeus, 1758) | | 80 | 34 | () | Z | P() | Plei | R | 4, 5, 9, 13, 14, 19, 27, 30, 31, 44 | Pl. 35, figs 3-6 |
| *Dentex macrophthalmus* (Bloch, 1791) | | 6 | 17 | M() | Z | P() | Plei | R | 5, 6, 15, 16, 19, 20, 27, 30, 31, 33, 34, 44, 45 | Pl. 36, figs 1-2 |
| *Dentex maroccanus* Valenciennes 1830 | | – | 4 | M() | Z | P | Plei | R | 5, 6, 13, 14, 15, 16, 19, 20, 21, 24, 25, 27, 30, 32, 33, 36, 44, 45 | Pl. 36, fig. 3 |
| *Pagellus* cf. *bellottii* Steindachner, 1882 | • | – | 1 | () | – | () | – | R | 24, 31 | Pl. 36, fig. 7 |
| *Pagellus erythrinus* (Linnaeus, 1758) | | 7 | 21 | – | Z() | P() | Plei | R | 2, 6, 18, 19, 27, 30, 31, 32 | Pl. 36, figs 4-6 |
| *Spicara alta* (Osório, 1917) | • # | – | 5 | – | – | – | – | () | | Pl. 36, figs 8-9 |
| *Capros aper* (Linnaeus, 1758) | | 1 | – | () | – | P | Plei | R | 19, 41 | Pl. 37, fig. 1 |
| *Chaunax pictus* Lowe, 1846 | | – | 4 | M | – | – | – | R | 20 | Pl. 37, figs 2-5 |
| *Chaunax pugetensis* (Schwarzhans, 1986) | | – | 33 | – | Z | – | – | – | 19, 39 | Pl. 37, figs 6-10 |
| Lapilli Ariidae sp. | | – | 1 | – | – | – | – | – | | Pl. 37, figs 11 |
| Lapillus *inc. sedis* | | – | 10 | – | – | – | – | – | | Pl. 37, figs 12-13 |
| **Total number of otoliths** | | **3720** | **30832** | | | | | | | |
| **Total number of species identified** | | | | **63 (41+?2)** | **107 (16)** | **58 (13)** | **81** | **90 (27)** | | |

Family Albulidae Bleeker, 1849
Subfamily Pterothrissinae Gill, 1893
Genus *Pterothrissus* Hilgendorf, 1877

Two species of *Pterothrissus* are known from Zanclean deposits in the study area: *P. compactus* Schwarzhans, 1981 from the Mediterranean (type area: Le-Puget-sur-Argens, SE France) (Schwarzhans, 1981; Nolf & Cappetta, 1989) and *P. darbelhamriensis* Schwarzhans, 1981 from the NE Atlantic (type area: Dar Bel Hamri, Morocco) (Schwarzhans, 1981, 1986), the latter also known from the Piacenzian of Portugal (Nolf & Marques da Silva, 1997). The extant eastern Atlantic *P. belloci* Cadenat, 1937 was transferred to the genus *Nemoossis* Hidaka *et al*., 2017 based on morphological characters of the entire fish, while the extant Pacific *Pterothrissus gisu* Hilgendorf, 1877 remained in the genus (Hidaka *et al*., 2017). The otoliths of both extant species are figured in Nolf (2013). The morphology of the Pliocene otoliths has a higher resemblance to those of *Nemoossis belloci* than to *Pterothrissus gisu* due to opening of the ostium towards the dorsal *vs.* anterior rim; presence or absence of a notch on the dorsal rim; relatively straight *vs.* curved post ventral rim. Such relationship is supported by the biogeographic occurrence of these species, but skeletal remains to confirm it are not available.

***Pterothrissus darbelhamriensis* Schwarzhans, 1981**
Plate 1, fig. 1

1981 *Pterothrissus darbelhamriensis* – Schwarzhans, figs 6-8.
1997 *Pterothrissus darbelhamriensis* – Nolf & Marques da Silva, p. 11 figs 1-3.
2013 *Pterothrissus darbelhamriensis* – Nolf, pl. 15

*Material* – 4 sagittas. Velerín Carretera 1, Velerín Conglomerates 1, Velerín Quarry 2.

*Remarks* – The two adult specimens from Velerín Quarry represent *Pterothrissus darbelhamriensis* as evidenced by their smooth outer surface, the deep notch anteriorly on the dorsal rim and less convex outer face in ventral view as opposed to *P. compactus* (Pl. 1, fig. 1). The other two specimens of the same species are juveniles.

***Pterothrissus compactus* Schwarzhans, 1981**
Plate 1, fig. 2

1981 *Pterothrissus compactus* – Schwarzhans, figs 9-12.
1989 *Pterothrissus compactus* – Nolf & Cappetta, pl. 1 figs 1-4.
1998 *Pterothrissus compactus* – Nolf, Mané & Lopez, pl. 1 figs 1a, b.

*Material* – 4 sagittas. Río del Padrón 2, El Lobillo 2.

*Remarks* – One of the juvenile specimens from Río del Padrón (Pl. 1, fig. 2) fits in the growth series of the species as illustrated by Schwarzhans (1981) and Nolf & Cappetta 1989 (pl. 1, figs 1-4) and is characterised by ornamented inner and outer faces, a more convex outer face in ventral view and the absence of a notch on the dorsal rim as opposed to *P. darbelhamriensis*.

Family Heterenchelyidae Regan, 1912
Genus *Panturichthys* Pellegrin, 1913

***Panturichthys subglaber* (Schubert, 1906)**
Plate 1, fig. 3

1906 *Otolithus* (*Solea*) *subglaber* – Schubert, p 672; pl. VI, figs 19-26.
1980 *Panturichthys subglaber* – Nolf & Martinell, pl. 1 figs 3, 4, 6, not 5.
1998 *Panturichthys subglaber* – Nolf, Mané & Lopez, pl. 1, figs 4a, b.

*Material* – 1 sagitta. Velerín Carretera 1.

*Remarks* – A small otolith (Pl. 1, fig. 3) fully matches specimens of *Panturichthys subglaber* known from the Zanclean of southern France, Catalunya and northern Italy (Nolf & Cappetta, 1989; Nolf & Cavallo, 1995; Nolf *et al*., 1998). It has also been reported from the undifferentiated Pliocene of Figueras (Catalunya, Nolf & Martinell, 1980, pl. 1, figs 3-6); however, the specimen on their pl. 1, fig. 5 doesn't seem to fit the growth series because of its wide sulcus, the prominent rostrum and the overall shape.

Genus *Pythonichthys* Poey, 1868

***Pythonichthys gibbosus* nov. sp.**
Plate 1, fig. 4

*Holotype* – RGM.1390304, Velerín Antena Hilltop.

*Locus typicus* – Velerín Antena Hilltop, Velerín, Estepona, province of Málaga, Spain.

*Stratum typicum* – Middle Pliocene, Piacenzian, fossiliferous medium- to fine-grained sands.

**Plate 1**
Figure 1. ***Pterothrissus darbelhamriensis*** Schwarzhans, 1981, Velerín Quarry.
Figure 2. ***Pterothrissus compactus*** Schwarzhans, 1981, Río del Padrón.
Figure 3. ***Panturichthys subglaber*** (Schubert, 1906), Velerín Carretera.
Figure 4. ***Pythonichthys gibbosus* nov. sp.,** holotype, Velerín Antena Hilltop.
Figure 5. ***Echelus myrus*** (Linnaeus, 1758), Velerín Conglomerates.
Figure 6. ***Hoplunnis* sp.**, Velerín Antena Slope.
Figure 7. ***Saurenchelys silex* nov. sp.**, holotype, Velerín Quarry.
Figure 8. ***Saurenchelys silex* nov. sp.**, paratype, Velerín Conglomerates.

*Etymology* – The species is named after the very gibbose antero-dorsal angle, giving the otolith a humped appearance.

*Diagnosis* – The otolith is characterised by a small, pointed rostrum, a prominent antero-dorsal angle (predorsal lobe), and a convex posterior rim with straight upper part (Pl. 1, fig. 4). The middorsal rim has 3 small lobes, while the ventral rim is regularly convex and smooth. The sul-

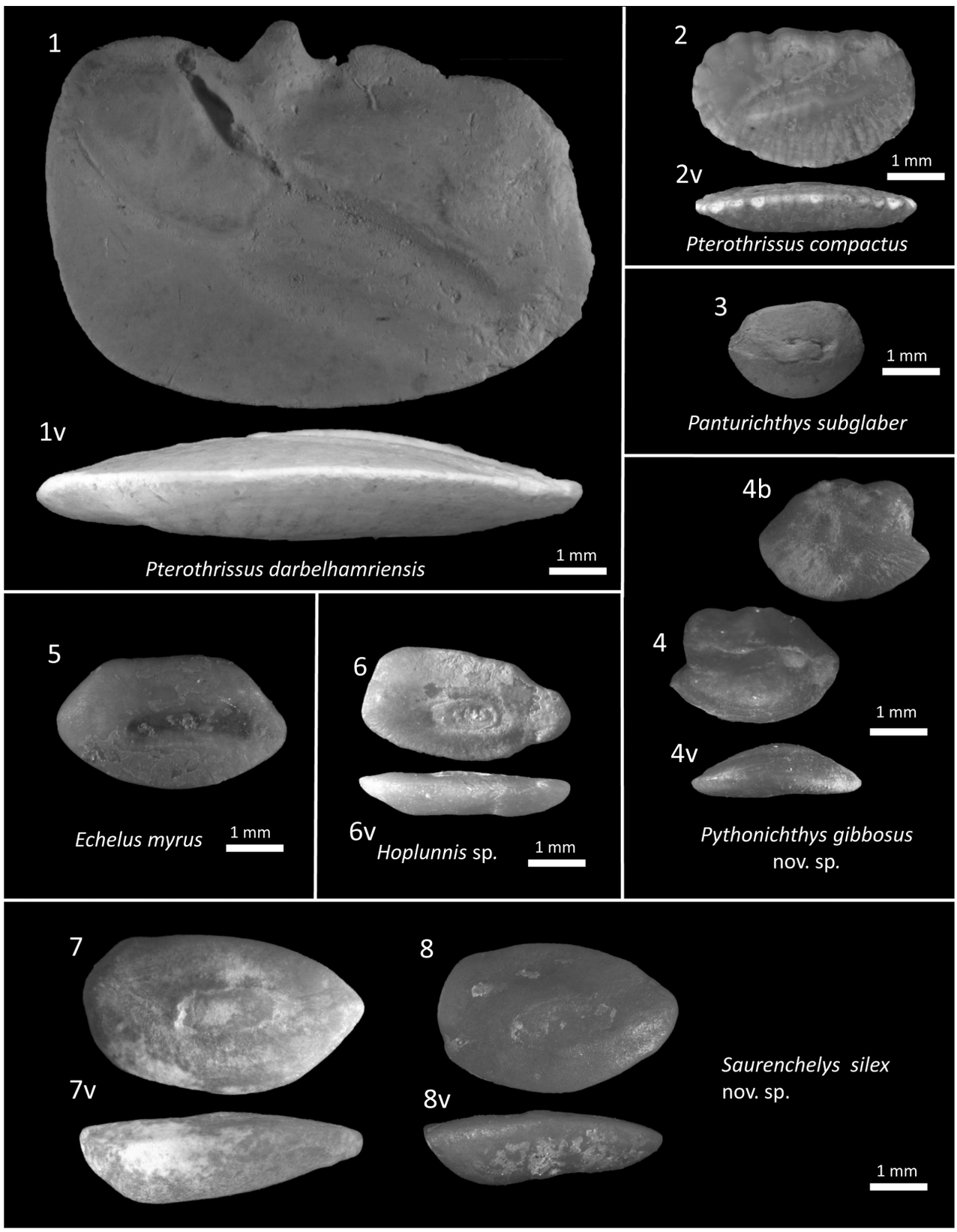


**Plate 1**

cus is sigmoid and of constant width, slightly widening at its anterior end. A faint ventral furrow is present from the rostrum to the postero-ventral angle. The very convex inner face in ventral view is typical of Heterenchelyidae. The outer face is slightly convex along its antero-posterior axis, almost straight.

*Differential diagnosis* – Two extant species of *Pythonichthys* occur in the Gulf of Guinea, NE Atlantic (*P. macrurus* (Regan, 1912) and *P. microphthalmus* (Regan, 1912), see Quéro *et al*., 1990, 154-155), but none in the Mediterranean. Otoliths of both species have been illustrated by Schwarzhans (2013a, pl. 2, figs 5-6; 2019b, pl. 1, fig. 14) and our analysis is based on these figures. The figured otolith of *P. macrurus* resembles that of the new species in several aspects, but differs substantially in others. Both have a distinct rostrum, but in *P. macrurus* its upper rim runs straight upward and relates to the straight anterior rim at an angle of *ca* 90°, whereas in *P. gibbosus* nov. sp. the upper rostral rim declines obliquely making an angle of *ca* 135° to the straight rostral rim. The predorsal lobe in *P. macrurus* is at an angle of *ca* 90° with the dorsal rim, only slightly convex and followed by an almost straight dorsal rim, whereas that in *P. gibbosus* nov. sp. is much more convex and followed by a concavity. The upper part of the posterior rim in *P. macrurus* is much less than 45° as in *P. gibbosus* nov. sp. The cauda of *P. macrurus* is short and ends well before the posterior rim, whereas in *P. gibbosus* nov. sp. it is much longer and ends much closer to the posterior rim. Moreover, the cauda in *P. macrurus* widens towards the dorsal rim, whereas it widens towards the ventral rim in *P. gibbosus* nov. sp. The ratio OL/OT is 3.3 in *P. macrurus*, whereas it is 3.0 in *P. gibbosus* nov. sp., making the latter otolith slightly more thickset.

*Remarks* – This species differs from *Panturichthys subglaber* by the strong predorsal angle, the lobed dorsal rim, the more convex posterior rim that is equally divided by a blunt angle in an obliquely running upper part and a curved lower part, and the presence of a ventral furrow. *Panturichthys subglaber* can also develop a rostrum as known from Pliocene specimens from northern Italy (Nolf & Cavallo, 1994) and Catalunya (Nolf *et al*., 1998), but these don't show the very straight anterior rim of our specimen. The latter is a feature of *Pythonichthys macrurus* (Schwarzhans, 2013a, pl. 2, fig. 5), which also shows the sigmoid sulcus, but has a more angular rather than prominently bulged predorsal angle. The straight anterior rim is also shown in a specimen from Figueras (Nolf & Martinell, 1980, pl. 1, fig. 5), but that specimen lacks the prominent predorsal angle and the sigmoid sulcus.

Family Nettastomatidae Kaup, 1859
Genus *Hoplunnis* Kaup, 1859

***Hoplunnis* sp.**
Plate 1, fig. 6

1994 *Pseudophichtys* sp. – Nolf & Cavallo, pl. 1, fig. 9

*Material* – 2 sagittas. Velerín Carretera 1, Velerín Antena Slope 1.

*Remarks* – The otolith (Pl. 1, fig. 7) shows the characteristics of *Hoplunnis* sp. (see iconography in Schwarzhans, 2013b, pl. 2, fig. 7; 2019b, pl. 9, figs 5-6), a taxon also known from the Early Pliocene of northern Italy (Nolf & Cavallo, 1994, pl. 1, fig. 9 as *Pseudophichthys* sp.). Nolf & Cappetta (1989, pl. 1, fig. 5) illustrated a specimen of *Hoplunnis* sp. from the Zanclean of SE France, which differs from our specimen in the more elongated shape, the more rounded posterior rim, the more prominent rostrum, the narrower sulcus and the larger distance between sulcus and posterior rim.

Genus *Saurenchelys* Peters, 1864

***Saurenchelys silex* nov. sp.**
Plate 1, figs 7, 8

*Holotype* – RGM.1390307, Velerín Quarry

*Paratype* – 1 sagitta: RGM.1390308, Velerín Conglomerates

*Locus typicus* – Velerín Quarry, close to Velerín Antena, along Camina Nicolas, Velerín, Estepona, province of Málaga, Spain.

*Stratum typicum* – Middle Pliocene, Piacenzian, fossiliferous medium- to fine-grained sands.

*Etymology* – *silex* (Latin for hard stone) based on the gravel stone shape of the otolith.

*Diagnosis* – Elliptical and thickset shaped otoliths with a bluntly pointed anterior part. A median sulcus covered by a small and slightly oblique oval colliculum (anterior part upward). The anterior end of the sulcus tapers into a thin and straight ostial channel, running straight forward to just dorsal of the anterior-most point. Outer face very thick posteriorly, in ventral view tapering toward a 2- to 3-fold thinner anterior side.

*Description* – The holotype (Pl. 1, fig. 7) is 5.0 mm long, 2.3 mm high and 0.61-1.46 mm thick (range between anterior and posterior thickness). The dorsal rim curves smoothly and merges after a minor shallow concavity in a blunt postdorsal angle connecting to the posterior rim. The posterior rim is largely rounded and slightly thickened, with a continuous (holotype) or slightly concave (paratype, Pl. 1, fig. 8) connection to the ventral rim.
The median sulcus covers 40% of the otolith length. The sulcus is covered by an oval colliculum except for its anterior part which tapers into a faint and straight ostial channel that connects the sulcus with the dorso-anterior rim.
The outer face is humpy at the posterior part (OT:OH=0.63) and tapers to the anterior rim (till OT:OH=0.27 in the

holotype). In ventral view, the thickest part of the otolith lies close to the posterior end (at 75-80% of the OL), from where the thickness decreases gradually in anterior direction, becoming 2- to 3-times less thickset anteriorly. The inner surface is slightly concave in the length direction. In the holotype this is due to a blunt angle of 170° between equally long and flat anterior and posterior parts (see ventral view).

*Remarks* – The medially positioned sulcus connected to the anterior rim and the very convex outer face place our specimens in the family Nettastomatidae (see iconography in Schwarzhans, 2019b, pl. 9). The thickness of the otoliths, the shape of the inner face in ventral view, the tapering connection between sulcus and anterior rim, the orientation and size of the oval colliculum, and the angular projection of the postdorsal area with a rounded posterior rim resemble otoliths of representatives of the extant genus *Saurenchelys* Peters, 1864. Several *Saurenchelys* species (*S. fierasfer* (Jordan & Snyder, 1901) and *S. finitima* (Whitley, 1935)) have more elongated otoliths with a longer sulcus. The sulcus size and posterior rim are similar to the otoliths of extant West Pacific *S. taiwanensis* Karmovskaya, 2004 known from the Philippines, while otoliths of the extant *S. cancrivora* Peters, 1864 also have a comparable sulcus and colliculum. *Saurenchelys cancrivora* has been reported in the Atlantic off the Congo River, but apparently is absent from the Mediterranean (see Klausewitz & Zajonz, 2000). Schwarzhans (2019b, pl. 9, fig. 11) figured one right otolith, which is roughly the same size as our specimens, but differs from them by a constant thickness, being less thickset in the posterior part, and having a more concave posterior rim. These differences suggest that our specimens belong to a different species.
Part of the specimens earlier reported as *Pseudophichthys* sp. (Nolf *et al*., 1998, pl. 1, fig 5 and 8, but not fig. 6) probably belong to the Nettastomidae and possibly the genus *Saurenchelys*. None of them display the bulky posterior part that tapers so markedly in anterior direction as in *Saurenchelys silex*.

Family Congridae Kaup, 1856
Genus *Paraconger* Kanazawa, 1961

***Paraconger pinguis* nov. sp.**
Plate 2 , figs 1-9

| | |
|---|---|
| 1980 | *Ariosoma coheni* – Nolf & Martinell, pl. 1, figs 11-12. |
| 1989 | *Paraconger caudilimbatus* – Nolf & Cappetta, pl. 2, fig. 6. |
| ?2006 | *Paraconger notialis* – Nolf & Girone, p. 83, remark 2; p. 11, figs 1-2. |

*Holotype* – RGM.1390309, Velerín Conglomerates.

*Paratypes* – 7 sagittas: RGM.1390310-RGM.1390316, Velerín Conglomerates. (Figs 1, 3-8).

*Additional material* – Río del Padrón 2 juv.; Velerín Conglomerates 20, Velerín Carretera 1; Velerín Quarry 1; Velerín Slope 1.

*Locus typicus* – Velerín Conglomerates, west side of the Camino Nicola, Velerín, community of Estepona.

*Stratum typicum* – Early to Middle Piacenzian, massive conglomerate deposit.

*Etymology – pinguis* (Latin for thick, fat) underlining the thick shape of this species.

*Diagnosis* – Compact *Paraconger*–type otoliths (material between 1.5 and 7.8 mm OL), which are characterised by: (1) A relatively short sulcus, which is accompanied by a marked distance between the posterior end of the cauda and the posterior rim (indicated as post-sulcus length; PSuL/OL=0.23±0.02). (2) A relatively narrow sulcus. (3) The posterior ⅓ of the edge of the ventral rim is bent outward causing a concavity at the posterior outer face.

*Description*: Oval otoliths with a markedly convex inner side. The dorsal rim displays a prominent predorsal extension and a concave dorsal part posteriorly that connects to the posterior rim by a distinct angle. The ventral rim is slightly V-shaped with a blunt angle that separates the rim in a shorter anterior part and a two times larger posterior part. The latter curves at its posterior end and joins the posterior rim. The straight horizontal sulcus is narrow and opens upward anteriorly via an S-shaped ostial channel; it is separated from the anterior and posterior rims by a short and a relatively longer distance amounting to 5-10% and 21-27% of the otolith length, respectively. The narrow colliculum is more pronounced in the holotype than in several other specimens, in particular that of Pl. 2, fig. 5. It should be noted that the caudal end of the sulcus of the holotype displays a faintly visible 0.26 mm zone between the caudal colliculum and crista, which has eroded in other specimens. The ventral view of the holotype shows that the edge of the ventral rim forms a 20° outward angle, halfway between the deepest part of the ventral rim and the posterior end. One large specimen (Pl. 2, fig. 3) is available with OL=7.8 mm. It displays the relatively short sulcus and the accompanying large post-sulcus part. Although damaged at its crista inferior, the sulcus is similarly narrow as in the smaller specimens.
The outer face of the holotype displays an elevated convex middle part connected by concavities to the outward bending posterior part, the thickened predorsal extension and the anterior rim. In ventral view this results in a convexity of the outer contour that is less outspoken than that of the inner contour.

*Comparison* – The otoliths of *Paraconger pinguis* from Velerín Conglomerates have the general morphology of those of extant *Paraconger* (Nolf & Cappetta, 1989, pl. 2, figs 7-10; Veen & Hoedemakers 2005, pl. 1, fig. 4;

Lombarte *et al*., 2006; Schwarzhans, 2019b, pl. 3, figs 9-13) and *Chiloconger* Myers & Wade, 1941 otoliths (Schwarzhans, 2019b, pl. 3, figs 7, 8), but are specific in several aspects. The sulcus length/otolith length ratio of *P. pinguis* (n=14, 0.69±0.01, mean ± SD) is less than that of otoliths of present-day *P. notialis* Kanazawa, 1961 (n=9, 0.79±0.15) or *P. caudilimbatus* (Poey, 1867) (n=2, both 0.72), and markedly higher than that of single specimens of *Chiloconger philippinensis* Smith & Karmovskaya, 2003 (0.57) and *C. dentatus* Garman, 1899 (0.58). The post-sulcus length/OL ratio shows comparable differences, but in an opposite way. Quantification of PSuL/OL gives an average ratio of 0.23± 0.02 which is higher than in otoliths known from extant *Paraconger notialis* (0.11±0.02), but lower than in the *Chiloconger* otoliths (both 0.33). The 7 largest specimens of *P. pinguis* (6.0-7.8 mm) showed the same mean values for these ratios as the smaller 7 specimens (2.1-5.9 mm). The ratio sulcus height/OL was higher in the specimens of *P. notialis* (0.27±0.03) and *P. caudilimbatus* (0.23-0.25) than in those of *P. pinguis* (0.20±0.02), while those of *Chiloconger philippinensis* and *C. dentatus* (0.16 and 0.18) were lower than or bordered at the minimal values of *P. pinguis.* In addition, the edge of the ventral rim of *P. pinguis* is not straight as in *Chiloconger* (Schwarzhans, 2019b), but makes a slight angle by which its one-third posterior part bends outward tapering towards the posterior rim (see Pl. 2, fig. 2v). Overall, this data supports the identification of *P. pinguis* as a member of the genus *Paraconger*, rather than *Chiloconger*. This conclusion matches with biogeographic data showing the extant *Paraconger* as essentially (sub)tropical eastern and western Atlantic as well as eastern Pacific of the Americas, while *Chiloconger* is confined to tropical Pacific waters. The genus is also known from the Pliocene of the Mediterranean (Nolf & Cappetta, 1989; Nolf & Cavallo, 1994; Nolf & Girone, 2006).

*Paraconger pinguis* otoliths are similar to otoliths from the upper Zanclean of Biot (Côte d'Azur, France) (Nolf & Cappetta, 1989) and Zanclean of northern Italy (Nolf & Girone, 2006). The specimens of Biot were published as *Paraconger caudilimbatus*, a subtropical species of the Central Western Atlantic. While later re-identified as *P. notialis* (Nolf & Girone *et al*., 2006, p. 83, remark 2), we consider the sulcus and dimensions of the Biot specimens as being comparable to those of *P. pinguis*. The identification of the *P. notialis* specimens from northern Italy (Nolf & Girone, 2006) is less clear. It is likely that they represent the same species, but it should be mentioned that the sulcus length of the specimens published by Girone *et al*. (2006, pl. 1, figs 1-2) is intermediate between *P. notialis* and *P. pinguis*. The specimen from the Zanclean of Río del Padrón (Pl. 2, fig. 9; OL=3.8 mm) is congruent with *P. pinguis*, but juvenile.

*Occurrence* – Piacenzian and Late Zanclean of Velerín Conglomerates and Biot (Côte d'Azur, France). The juvenile specimen from Río del Padrón confirms its presence during the late Early Zanclean.

Genus *Gnathophis* Kaup, 1859

Two species of *Gnathophis* have been reported from the Mediterranean Pliocene: *G. mystax* (Delaroche, 1809), an extant species, and *G. kanazawai* Nolf & Martinell, 1980 from Pliocene deposits in SE Spain (Nolf & Martinell, 1980). The specimens figured in Nolf & Martinell (1980, pl. 1, figs 7-8) are the same size as those of *G. mystax* on their pl. 2 (fig. 2) and don't fit into the ontogenetic series of the latter (Tuset *et al.,* 2008, fig. 14 D1-D2; Lin *et al*., 2018, pl. 2, figs J-S). The Piacenzian deposits of Estepona yielded specimens of *Gnathophis* which cannot be assigned to either of these species. They are herein described as a new species, as they also differ from the nominal *G. kanazawai*, which we consider as a doubtful species (see below).

***Gnathophis mystax* (Delaroche, 1809)**
Plate 3, figs 1-2

| | |
|---|---|
| 2008 | *Gnatophis mystax* – Tuset, Lombarte & Assis, figs 14D1-D2 (present-day otoliths). |
| 2018 | *Gnatophis mystax* – Lin *et al*., pl. 2, figs J-S. |
| 2019b | *Gnatophis mystax* – Schwarzhans, pl. 4, figs 12-13 (present-day otoliths). |

*Material* – 17 sagittas. El Lobillo 1, Velerín Carretera 8, Velerín Conglomerates 5, Velerín Quarry 1, Velerín Antena Slope 2.

*Remarks* – The Pliocene otoliths of *Gnathophis mystax* have a rhomboidal-rounded structure with a deep mid-ventral angle and a regularly curved dorsal rim with insignificant predorsal and dorsal angles. The inner face is convex along the length axis. The posterior part of the otoliths is bluntly pointed and displays a specific fold separating the convex inner side of the otolith body and the thinner posterior tip. In part of the specimens a dorsal notch accompanies this fold. The median sulcus position is slightly oblique compared to the length axis; the ostium opens broadly towards a wide excisura at the anterior rim. The outer face is flat in the centre to slightly convex in the marginal areas.

***Gnathophis henkmulderi* nov. sp.**
Plate 3, figs 3-10

*Holotype* – RGM.1390321, Velerín Carretera.

*Paratypes* – 6 specimens: RGM.1390322, RGM.1390323, RGM.1390325-RGM.1390328, Velerín Carretera.

*Other material* – 21 sagittas. Velerín Carretera 19; Velerín Quarry 1, Parque Antena 1.

*Locus typicus* – Velerín Carretera, Velerín, Estepona, province of Málaga, Spain.

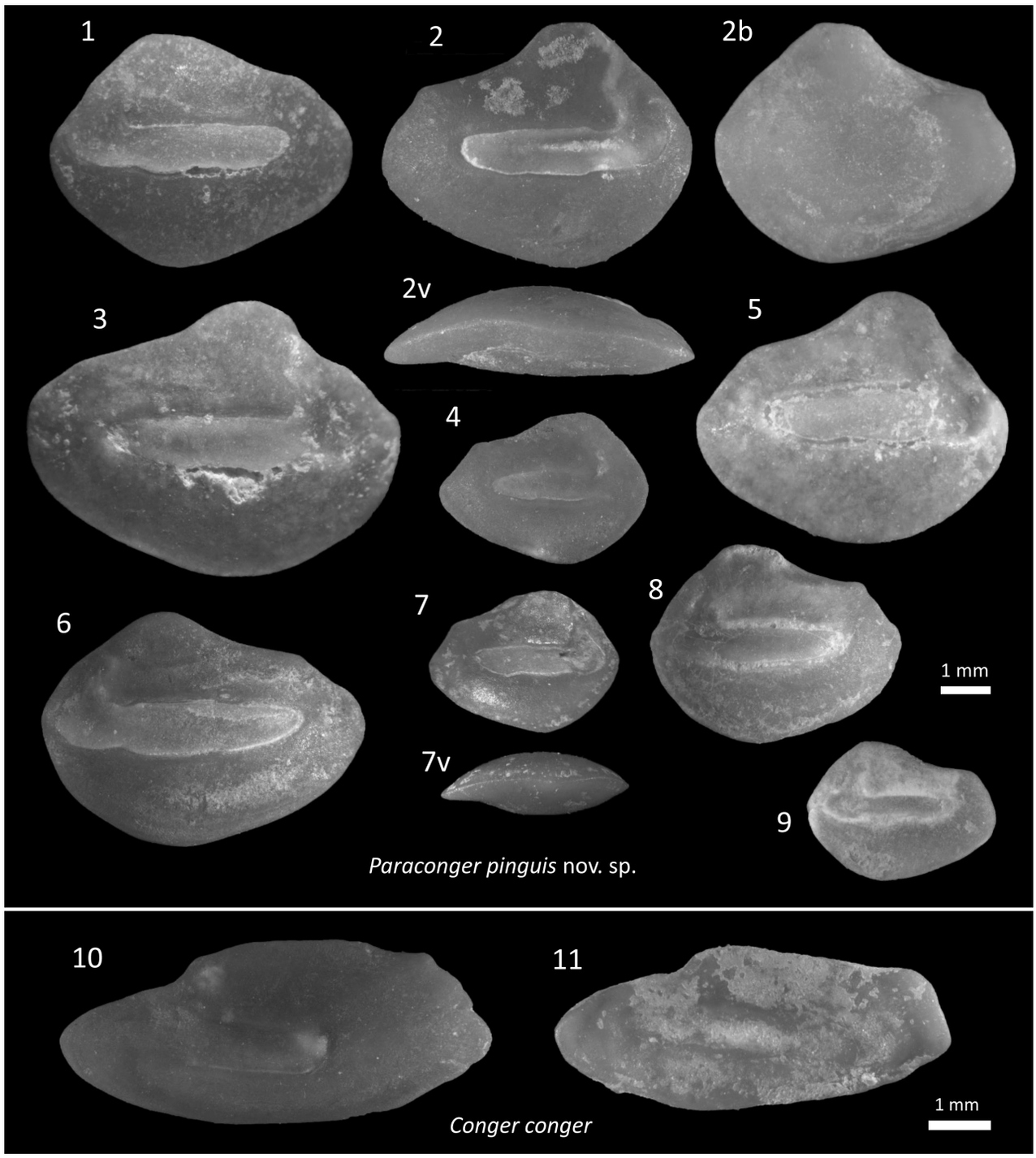


**Plate 2**

Figure 2. ***Paraconger pinguis* nov. sp.,** holotype, Velerín Conglomerates.
Figures 1, 3-8. ***Paraconger pinguis* nov. sp.,** paratypes, Velerín Conglomerates.
Figure 9. ***Paraconger pinguis* nov. sp.**, Río del Padrón.
Figures 10-11. ***Conger conger*** (Linnaeus, 1758), Velerín Conglomerates.

*Stratum typicum* – Middle Pliocene, Piacenzian, fossiliferous medium- to fine-grained sands.

*Etymology* – Named after Mr Henk Mulder, who collected the holotype and donated his collection of otoliths from Estepona to the authors.

*Differential diagnosis* – The sulcus of the otoliths of *G. henkmulderi* is similar to that of *G. mystax* and typical of *Gnathophis*. The main differences can be found in their shape. The main characteristic of otoliths of *G. mystax* is the distinct angle on the ventral rim anterior to the middle (Nolf *et al*., 2009; Lin *et al*., 2018), which

gives them an elongated appearance. Otoliths of *G. henkmulderi* nov. sp. have a regularly rounded ventral rim without a conspicuous angle, the deepest part of the otoliths is about halfway, which gives them a more compact appearance. The dorsal rim is regularly rounded in the anterior part, but straight in the posterior part in *G. henkmulderi* nov. sp., whereas it is regularly rounded to almost straight in *G. mystax* (Nolf *et al*., 2009; Lin *et al*., 2018, pl. 2, figs J-S; Schwarzhans, 2019b, pl. 3, figs 12-13).

*Description* – Otoliths of *G. henkmulderi* nov. sp. are characterised by a rounded pentagonal shape with a striking dorso-posterior extension which is bordered by an almost straight rim that runs obliquely from the prominent postdorsal angle to the posterior tip. The anterior part of the dorsal rim is regularly rounded, forming an obtuse predorsal angle at its highest point. Between pre- and postdorsal angles the straight dorsal rim slightly declines. The ventral rim is regularly rounded with the lowest part about halfway. The anterior rim is straight or slightly convex and passes in a round angle to the ventral rim.

The inner face is regularly convex in ventral view, the outer face becomes more robust in its posterior portion in the holotype, but this is not the case in all specimens. The shallow and short sulcus opens to the anterior rim in a broad channel, it is entirely covered by colliculum. The anterior rim is straight and regularly rounded in all specimens. There is a small but distinct dorsal area. A shallow ventral furrow runs from the crista inferior of the ostium to along the posterior rim.

The posterior rim of the otoliths of *G. henkmulderi* nov. sp. is straight with distinct pre- and postdorsal angles *vs.* a more rounded postdorsal angle and posterior rim in *G. mystax* (compare Lin *et al*., 2018, pl. 2, figs j-s), although this feature seems to be variable (see Nolf *et al*., 2009; Schwarzhans, 2019b, pl. 3, fig. 12). Overall, however, the posterior portion in otoliths of *G. mystax* is more extended than in that of *G. henkmulderi*. Another difference is the absence of a typical shallow fold in the posterior portion, which is markedly present in otoliths of *G. mystax*. Otoliths of juveniles are much harder to assign to any of the species, since they do not yet show all characters of the adult otoliths; moreover, they have more crenulated rims (Pl. 3, fig. 6). Our juvenile specimens were found at Velerín Carretera where both species occur. Based on the distinct postdorsal angle, they may belong to *G. henkmulderi* nov. sp.

*Remarks* – Upon studying the type material of *G. kanazawai*, we observed that the holotype has a sulcus with only an upward ostial channel, no broad opening on the anterior rim. Its size (OL=6.1 mm) is larger than suggested in the original paper, as the magnification of holo- and paratype is different and only the size bar of the small specimen was depicted. The holotype of *G. kanazawai* may represent another species (within *Rhynchoconger* Jordan & Hubbs 1925) with an erosion-inflicted reduced predorsal part. The specimen seems unsuitable for species identification. The 2.0 mm paratype is indeed *Gnathophis*, but probably *G. mystax*, whose otoliths show a marked variability (Nolf *et al*., 2009). Altogether, the specimens of *G. henkmulderi* cannot be attributed to *G. kanazawai*, which we consider a doubtful species.

*Distribution* – *Gnathophis henkmulderi* nov. sp. is only known from the Piacenzian deposits of Velerín and Parque Antena and are encountered largely (89% of all specimens) in Velerín Carretera.

Genus *Pseudophichthys* Roule, 1915

***Pseudophichthys escaravatierensis* Nolf & Cappetta, 1989**
Plate 3, fig. 11

1989 *Pseudophichthys escaravatierensis* – Nolf & Cappetta, pl. 2, figs 12-15.
1998 *Pseudophichthys* sp. – Nolf, Mané & Lopez, pl. 1, fig. 6.

*Material* – 1 sagitta. El Lobillo 1.

*Remarks* – The species is based on a large number of otoliths from the Zanclean of Le Puget (France) (Nolf & Cappetta, 1989). *Pseudophichthys* sp. from Catalunya (Nolf *et al.,* 1998, pl. 1, fig. 6) represents the same species.

Genus *Japonoconger* Asano, 1958

***Japonoconger africanus* (Poll, 1953)**
Plate 3, figs 12-14

1986 *Japonoconger caribbeus* – Schwarzhans, pl. 1, figs 4-5.
1989 *Japonoconger carribeus* [sic] – Nolf & Cappetta, pl. 1, figs 11-12.

**Plate 3**

Figures 1-2. ***Gnathophis mystax*** (Delaroche, 1809), Velerín Antena Slope (1), Velerín Conglomerates (2).
Figure 4. ***Gnathophis henkmulderi* nov. sp.,** holotype, Velerín Carretera.
Figures 3, 5, 7-10. ***Gnathophis henkmulderi* nov. sp.,** paratypes, Velerín Carretera.
Figure 6. ***Gnathophis henkmulderi* nov. sp.**, juvenile, Velerín Carretera.
Figure 11. ***Pseudophichthys escaravatierensis*** Nolf & Cappetta, 1989, El Lobillo.
Figures 12-14. ***Japonoconger africanus*** (Poll, 1953), Velerín Carretera.
Figures 15-16. ***Rhynchoconger pantanelli*** Bassoli, 1906, Velerín Antena Slope (15), Velerín Carretera (16).

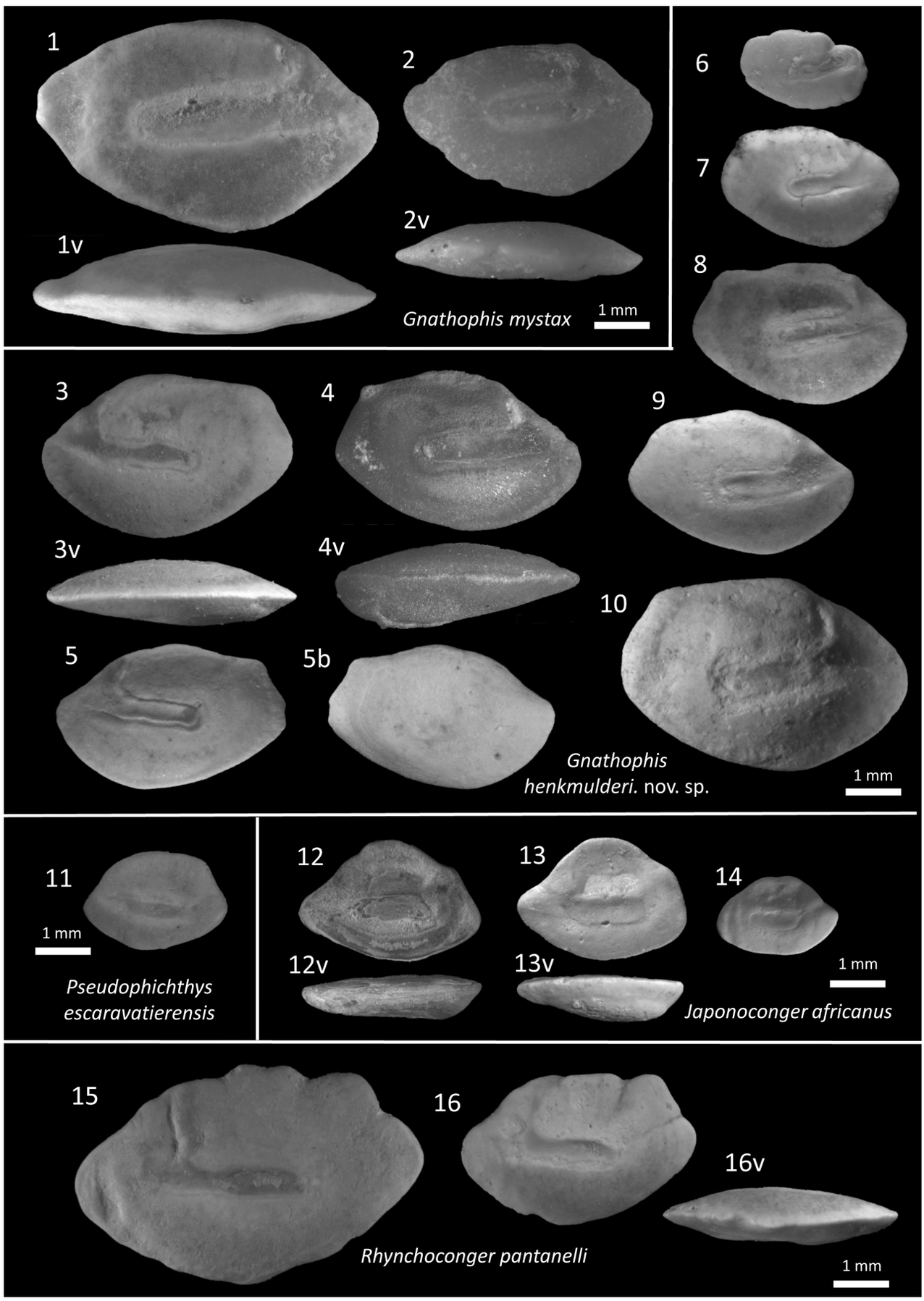
1
2
1v
2v
Gnathophis mystax
1 mm
6
7
8
3
4
9
3v
4v
10
5
5b
Gnathophis
henkmulderi. nov. sp.
1 mm
11
1 mm
Pseudophichthys
escaravatierensis
12
13
14
12v
13v
1 mm
Japonoconger africanus
15
16
16v
Rhynchoconger pantanelli
1 mm

**Plate 3**

2006 *Pseudophichthys splendens* – Girone, pl. 1, figs 2a-b.
2019b *Japanoconger africanus* – Schwarzhans, pl. 6, figs 11-12 (present-day otoliths).

*Material* – 21 sagittas. El Lobillo 1, Velerín Carretera 19; Velerín Quarry 1.

*Remarks* – These otoliths have a good resemblance with those of *Japonoconger africanus* from Gabon and Congo (see Schwarzhans, 2019b, pl. 6, fig. 12). In previous studies, they have been reported as *Japonoconger caribbeus* Smith & Kanazawa, 1977 from the Zanclean of France (Schwarzhans, 1986; Nolf & Cappetta, 1989) and Italy (Nolf & Cavallo, 1994) or erroneously as *Pseudophichthys splendens* (Lea, 1913) (Nolf, 2013).

Family Clupeidae Cuvier, 1816
Genus *Etrumeus* Bleeker, 1853

***Etrumeus* sp.**
Plate 4, fig. 1

1989 *Spratelloides* sp. – Nolf & Cappetta, pl. 3, figs 3-4.

*Material* – 1 sagitta. Velerín Conglomerates 1.

*Remarks* – One intact specimen of *Etrumeus* (Pl. 4, fig. 1) matches the characters of the extant *E. teres* (DeKay, 1842) closely, but here it is reported as *Etrumeus* sp.. *Etrumeus teres* was reported as occurring worldwide, but molecular research proved it to comprise several undescribed cryptic species (DiBattista *et al*., 2012), some of them occurring in the Mediterranean and off southern Africa. Since the otoliths of these new species are as yet unknown, we have left our specimen in open nomenclature. Otoliths of '*Etrumeus teres*' have been illustrated by, *e.g*., Steurbaut (1982: pl. 1, fig. 25), Tuset *et al*. (2012) and Lin & Chang (2012), and they show some morphological variability, making a positive species identification of our specimen doubtful.

Family Ophisthoproctidae Schmidt, 1918
Genus *Dolichopteryx* Brauer, 1901

***Dolichopteryx*? sp**.
Plate 4, fig. 9

2004 *Rhynchohyalus* aff. *natalensis* – Nolf & Steurbaut, pl. 2, fig. 5.

*Material* – 1 sagitta. Velerín Carretera 1.

*Remarks* – The specimen from Velerín Carretera exhibits the characters of an ophistoproctid otolith reported as *Rhynchohyalus natalensis* (Gilchrist & von Bonde, 1924), from the Rupelian of Italy and based on a single present-day Atlantic otolith (Nolf & Steurbaut, 2004, pl. 2, figs 4-5). However, these otoliths differ markedly from those of *R. natalensis* known from the Pacific (Rivaton & Bourret, 1999, pl. 88), while the reported identification of the extant Atlantic specimen seems doubtful. This suggests that our specimen belongs to a different species, probably within or close to the genus *Dolichopteryx* (compare extant specimens in Nolf, 2013 and Schwarzhans, 2013a).

Family Gonostomatidae Cocco, 1838

**'Gonostomatoidei' *inc. sedis***
Plate 4, fig. 13

*Material* – 1 sagitta. Velerín Antena Hilltop 1.

*Description* – A single, well-preserved otolith probably represents an unknown group or species within the order Stomiiformes / suborder Gonostomatoidei. It is disc-shaped, with a straight to slightly concave posterior rim and very convex ventral and dorsal rims, which end at the anterior side in a blunt but massive rostrum and anti-rostrum, respectively. The excisura is prominently V-shaped. A broad slightly bent sulcus cleaves the inner side over 85% of the otolith. The sulcus has a long, deepened ostium and a short cauda that is separated from the ostium. Both inner and outer faces are moderately convex. To the best of our knowledge, it pertains to an unknown species.

**Plate 4**
Figure 1. ***Etrumeus* sp**., Velerín Conglomerates.
Figure 2. ***Sardinella* sp**., Velerín Carretera.
Figures 3-4. ***Xenodermichthys copei*** (Gill, 1884), Velerín Carretera.
Figures 5-7. ***Argentina sphyraena*** Linnaeus, 1758, Velerín Quarry (5), Velerín Conglomerates (6), Velerín Antena Slope (7).
Figure 8. ***Microstoma* cf. *microstoma*** (Risso, 1810), Velerín Carretera.
Figure 9. ***Dolichopteryx* sp.**, Velerín Carretera.
Figure 10. ***Synodus saurus*** (Linnaeus, 1758), El Lobillo.
Figures 11-12. ***Gonostoma* sp.**, Velerín Quarry (11), Velerín Carretera (12).
Figure 13. '**Gonostomatoidei**' ***inc. sedis***, Velerín Antena Hilltop.
Figure 14. ***Chlorophthalmus agassizi*** Bonaparte, 1840, El Lobillo.
Figures 15-17. ***Polyipnus* sp**., Velerín Quarry.
Figure 18. ***Photichthys* cf. *argenteus*** Hutton, 1872, Velerín Carretera.

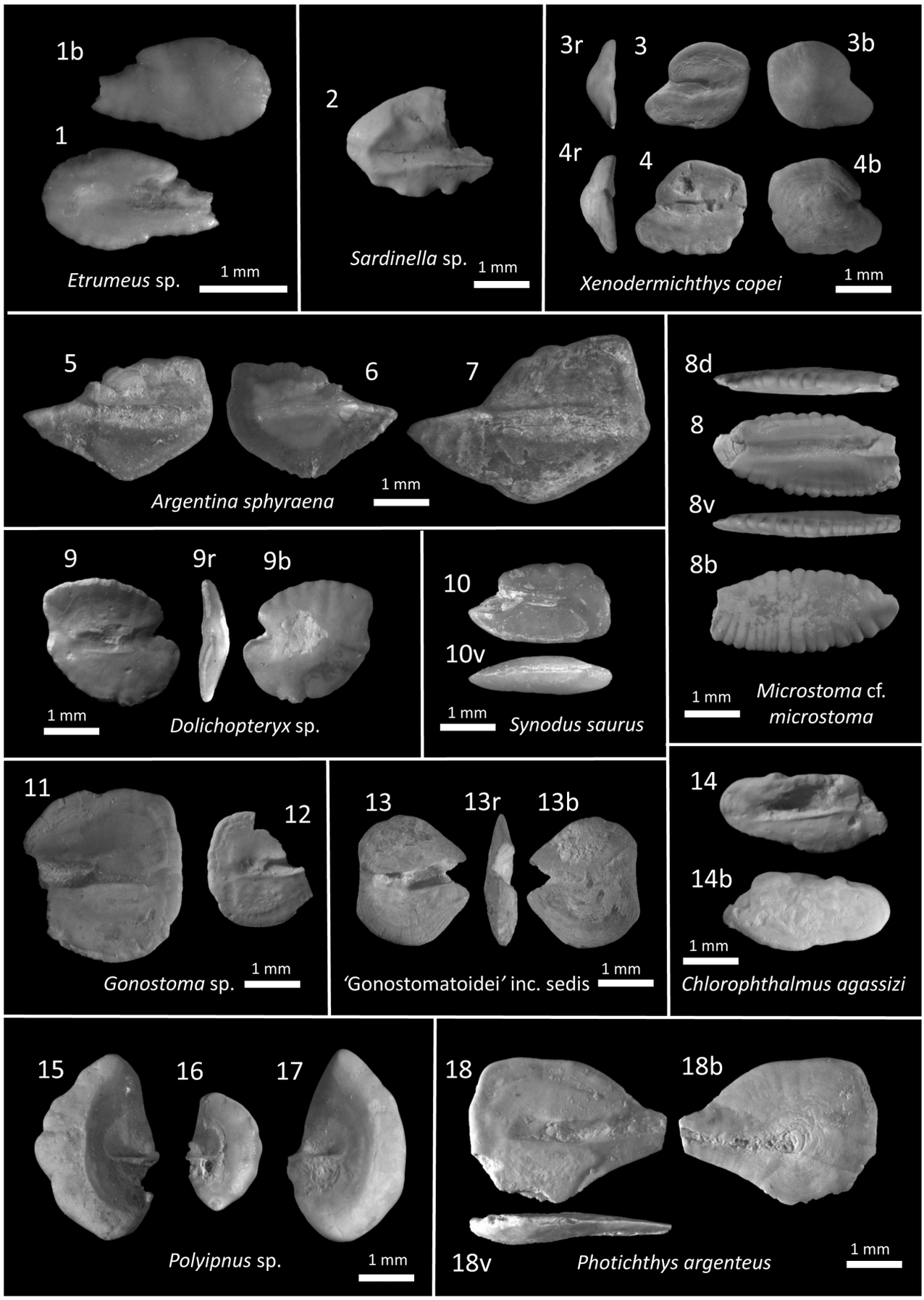
1b
1
Etrumeus sp.
1 mm
2
Sardinella sp.
1 mm
3r
3
3b
4r
4
4b
Xenodermichthys copei
1 mm
5
6
7
Argentina sphyraena
1 mm
8d
8
8v
8b
1 mm
Microstoma cf. microstoma
9
9r
9b
1 mm
Dolichopteryx sp.
10
10v
1 mm
Synodus saurus
11
12
Gonostoma sp.
1 mm
13
13r
13b
'Gonostomatoidei' inc. sedis
1 mm
14
14b
1 mm
Chlorophthalmus agassizi
15
16
17
Polyipnus sp.
1 mm
18
18b
18v
Photichthys argenteus
1 mm

**Plate 4**

Family Notosudidae Parr, 1928
Genus *Scopelosaurus* Bleeker, 1860

***Scopelosaurus* sp.**
Plate 5, fig. 1

*Material* – 1 sagitta. Río del Padrón 1.

*Description* – Thin elongated otolith with broken rostrum and slightly damaged posterior rim. The dorsal rim is convex and crenulated centrally, straight in its posterior part and sloping towards the antirostrum. The ventral rim is crenulated and less convex. The sulcus runs from the ostial excisura to about where the dorsal rim becomes straight and has an ostium and a long cauda. It is demarcated by a prominent crista superior that widens towards the anterior side but terminates and slightly widens where the ostium starts. It also has a prominent but thinner crista inferior of constant thickness and continuing along the ostium. Above the crista superior a large dorsal area is observed.

*Remarks* – The otolith resembles those of extant *Scopelosaurus* or *Saurida* Valenciennes, 1850 (Synodontidae). Given the very thin nature of the otolith and after comparing with otoliths of several species of *Scopelosaurus* and *Saurida* (see Smale *et al*., 1995, pl. 14; Nolf, 2013), we favour an identification as *Scopelosaurus*. However, a more accurate identification must wait due to lack of information on otolith shapes of several extant species of *Scopelosaurus* from the eastern Atlantic Ocean.

Order Myctophiformes Regan, 1911
Family Myctophidae Gill, 1893

In the Zanclean deposits of Río del Padrón and El Lobillo, the Myctophidae are by far the dominant group of fish otoliths encountered. Among the Piacenzian otoliths of Velerín Hill, they represent a substantial part of the encountered specimens. On the basis of structural studies by Paxton (1972, 1979) and subsequent molecular genetic data (Denton, 2018; Martin *et al*., 2018), Martin *et al.* (2018) proposed a subdivision of the Myctophidae into five subfamilies, four of which are represented in our material. For this family only taxa of uncertain assignment or new species will be discussed. Table 1 provides a full record of all species encountered in Estepona and Velerín.

Subfamily Gymnoscopelinae (*sensu* Martin *et al.*, 2018)
Genus *Notoscopelus* Günther, 1864

In the Velerín deposits large and medium-sized specimens of *Notoscopelus resplendens* (Richardson, 1845) are frequently encountered, but they are rare at Río del Padrón and El Lobillo. Several species of this genus occur in the present-day NE Atlantic and Mediterranean, and some of them have been recorded since the Neogene in the Mediterranean (oldest occurrence between brackets): *N. bolini* Nafpaktitis, 1975 (Tortonian of Italy, Lin *et al*., 2015), *N. resplendens* (Tortonian of Italy, Lin *et al*., 2015), *N. elongatus* (Costa, 1844) (Tortonian of Italy, Lin *et al*., 2015), *N. kroyeri* (Malm, 1861) (Pleistocene of the Mediterranean, Agiadi *et al*., 2018). Otoliths of all these species are quite similar and can only be identified based on adult specimens, juveniles are even more difficult to separate unless they fit into a growth series. Otoliths of adult specimens of *N. bolini* (Brzobohatý & Nolf, 1996, pl. 5, figs 1-5; Tuset *et al*. 2008, fig. 23b) seem to differ from those of the other species by a very large posterior portion behind the postdorsal angle. Such specimens have not been recognised in our material; they were reported from the Tortonian of Italy (Lin *et al*., 2015, figs 3.19-3.20) and from the Zanclean of SE France (Brzobohatý & Nolf, 1996, pl. 5, figs 6-11), although none of the specimens figured displays the large posterior portion behind the postdorsal angle.

***Notoscopelus elongatus* (Costa, 1844)**
Plate 5, fig. 13

1983 *Notoscopelus elongatus* – Nolf & Steurbaut, pl. 3, figs 14-16.
2000 *Notoscopelus elongatus* subsp. indet.– Brzobohatý & Nolf, pl. 7, figs 1-7 and 10-11.
2006 *Notoscopelus elongatus* – Girone, Nolf & Cappetta, fig. 4, 1-4(a-c).

*Material* – 33 sagittas. Río del Pádron 9; El Lobillo 16; Velerín Conglomerates 4; Velerín Sandy Lens 2; Velerín Antena Hilltop 1; Parque Antena 1.

*Remarks* – Represented by 22 sagittas that can be differentiated from the other small *Notoscopelus* specimens based on their somewhat elongated shape (OL:OH=1.66-1.71 *vs.* 1.53-1.60 in similar-sized *Notoscopelus resplendens* specimens from Velerín Conglomerates and Velerín Quarry). They display a shallow dorsal rim anteriorly that continues in a straight to slightly concave mid-dorsal part until a prominent postdorsal angle that in height often exceeds the rest of the dorsal rim. The posterior part runs either partly straight and/or curved to the posterior end. The ventral rim is convex and particularly in its middle part finely denticulated.

***Notoscopelus resplendens* (Richardson, 1845)**
Plate 5, figs 7-12

1996 *Notoscopelus resplendens* – Brzobohatý & Nolf, pl. 6 figs 1-11.
1999 *Notoscopelus resplendens* – Rivaton & Bourret, pl. 123 figs 3-8.

*Material* – 1001 sagittas. El Lobillo 1; Velerín Carretera 213; Velerín Conglomerates 135; Velerín Quarry 257; Velerín Sandy Lens 190; Velerín Antena Slope 160; Velerín Antena Hillop 43; Parque Antena 2.

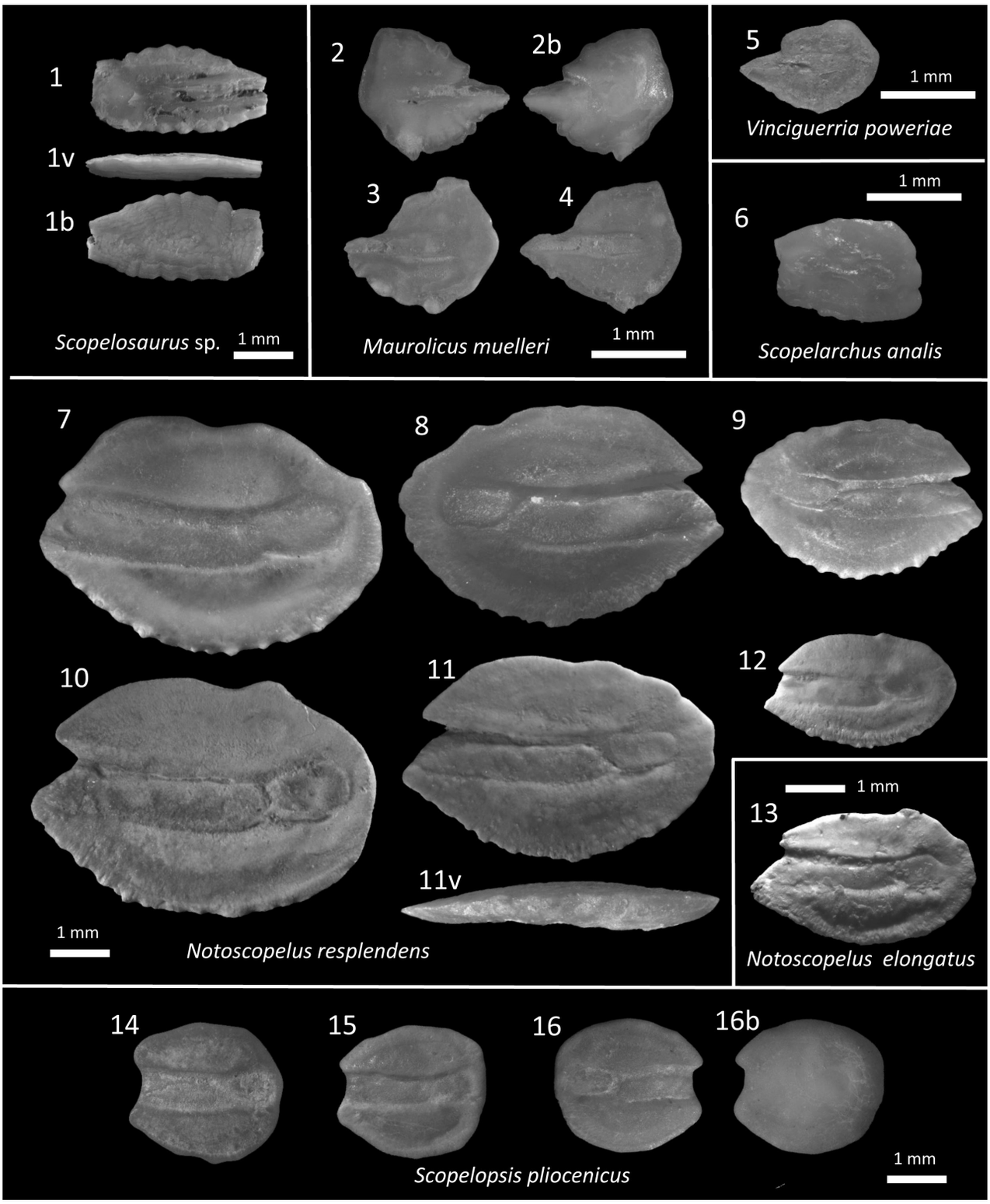


**Plate 5**

Figure 1. ***Scopelosaurus* sp.**, Río del Padrón.

Figures 2-4. ***Maurolicus muelleri*** (Gmelin, 1789), Velerín Conglomerates (2), Velerín Antena Slope (3, 4).

Figure 5. ***Vinciguerria poweriae*** (Cocco, 1838), Parque Antena.

Figure 6. ***Scopelarchus analis*** (Brauer, 1902), Velerín Quarry.

Figures 7-12. ***Notoscopelus resplendens*** (Richardson, 1845), Velerín Carretera (7,10), Velerín Sandy Lens (8), Velerín Quarry (9), Velerín Conglomerates (11), El Lobillo (12).

Figure 13. ***Notoscopelus elongatus*** (Costa, 1844), Río del Padrón.

Figures 14-16. ***Scopelopsis pliocenicus*** (Anfossi & Mosna, 1976), Velerín Quarry.

*Remarks* – In the Velerín deposits (Piacenzian) large and medium-sized specimens of *Notoscopelus resplendens* are frequently encountered but they are rare at Río del Padrón and El Lobillo (Zanclean). Our specimens are quite similar to those figured by Brzobohatý & Nolf (1996, pl. 6, figs 1-11). The species was present in the Mediterranean from the Tortonian to the Pleistocene (Schwarzhans, 1986, pl. 5, fig. 54; Nolf & Cappetta, 1989 pl. 6, figs 21-24; Brzobohatý & Nolf, 1996, pl. 6, figs 1-6, 7-11; Agiadi *et al*., 2013a, fig. 7.16; Girone, 2006, pl. 2, fig. 4; Lin *et al*., 2015, fig. 3.13), but is absent from the present-day Mediterranean (Whitehead *et al*., 1984).

Subfamily Diaphinae (*sensu* Martin *et al*., 2018)

In the Estepona and Velerín area two closely related genera of the subfamily Diaphinae are recognised, *Diaphus* Eigenmann & Eigenmann, 1891 and *Lobianchia* Gatti, 1904, which together account for 16 species. Dominant species are *D. cavallonis* Brzobohatý & Nolf at Río del Padrón and El Lobillo, and *D. postcavallonis* nov. sp. and *D.* aff. *splendidus* Brauer, 1904 in the Velerín area, which have a moderate to large size. It can be difficult to separate their often abundantly occurring juveniles from otoliths of other oval *Diaphus* species. Therefore, we had to focus on specimens with a well-preserved state to allow species identification. For the small *Diaphus* otoliths, damage to the sulcus, polishing of the dorsal rim or loss of denticles on the ventral rim resulted in excluding 80% to 90% of these specimens for identification. Notwithstanding, otoliths of many small *Diaphus* species could be identified, including *D. anderseni* Tåning, 1932*, D.* aff. *arabicus* Nafpaktitis, 1978*, D. mermuysi* nov. sp., *D. taaningi* Norman, 1930*, D. thermophilus* Tåning, 1928 and *D. dirknolfi* Schwarzhans, 1986 together with juvenile specimens of *D. holti* Tåning, 1918*, D. cavallonis* and *D. postcavallonis* and the related Diaphinae *Lobianchia dofleini* (Zugmayer, 1911) and *L. gemelarii* Cocco, 1838.
Schwarzhans (2013b) reported on the otoliths of a large number of extant *Diaphus* species and grouped their otoliths on the basis of photophores of the fish and otolith characteristics in several otolith groups and subgroups. We have followed the otolith group division as proposed by Schwarzhans (2013b, p. 80-81) (Table 1).

Genus *Diaphus* Eigenmann & Eigenmann, 1891
**Diaphus theta *otolith group***

***Diaphus anderseni* Tåning, 1932**
Plate 7, fig. 1

1999 *Diaphus anderseni* – Rivaton & Bourret, pl. 111 figs 11-14 (present-day otoliths).
2013b *Diaphus anderseni* – Schwarzhans, pl. 1, figs 11-13 (present-day otoliths).

*Material* – 1 sagitta. El Lobillo 1.

*Description* – Small and round otolith (OL:OH=1.04) with a short solid rostrum that runs in line with the excisura ostia until a distinct but shorter antirostrum. The dorsal rim is round, slightly interrupted by a postdorsal angle. Including the rostral denticles the regularly bent ventral rim has 7 prominent denticles. The connection between dorsal and ventral rims runs nearly vertically. The median sulcus is rather wide, the ostium 1.8 times as long as the cauda. The crista superior is developed along the ostium, but absent along the cauda. Below the sulcus the inner face is slightly thickened, which demarcates an insignificant ventral furrow. Above the sulcus a dorsal field is observed, which is bordered by a fold of the inner face that runs from the postdorsal angle to just behind the middle of the cauda. The outer face is convex reaching its maximal thickness in the middle of the otolith (OH:OT=4.1).

*Discussion* – These characteristics are in line with otoliths of the extant *D. anderseni*, a panglobal (sub)tropical oceanodromic *Diaphus* species (see Schwarzhans, 2013b, pl. 1, figs 11-13). Although there are no records of the extant *D. anderseni* in the Mediterranean and only scarce records in the Indian Ocean and the northern Atlantic Ocean (https://www.gbif.org/species/2406298), the Early Pliocene conditions might have been favourable for this species to reach the Strait of Gibraltar.

***Diaphus* aff. *arabicus* Nafpaktitis, 1978**
Plate 7, figs 2-3

2013b *Diaphus arabicus* – Schwarzhans, pl. 1, figs 1-4 (present-day otoliths).

*Material* – 2 sagittas. El Lobillo 2.

*Description* – Small round to septangular otoliths (OL:OH=1.09-1.10) with a short solid rostrum that runs in line with the excisura ostia until a distinct but shorter antirostrum. The dorsal rim is divided in three parts by a predorsal and postdorsal angle. Including the rostral denticles the regularly bent ventral rim has 5-7 prominent denticles. The connection between ventral and dorsal rims runs up in slightly posterior direction with an almost straight part dorsally. The median sulcus is divided in the ostium and a smaller cauda of similar height; the ostium is 1.7-1.8 times as long as the cauda. The crista superior runs along the entire ostium and about 75% of the cauda. The inner face is nearly flat, but with a shallowly deepened dorsal field. The outside is slightly convex reaching its maximum thickness in the middle of the otolith (OH:OT=3.8-4.0).

*Discussion* – The otoliths have several properties in common with those of *Diaphus anderseni*, but differ by (1) their slightly more elongate and less round appearance; (2) their predorsal angle; and (3) the longer crista superior that also runs along the cauda. Their characteristics match better with *Diaphus arabicus* otoliths

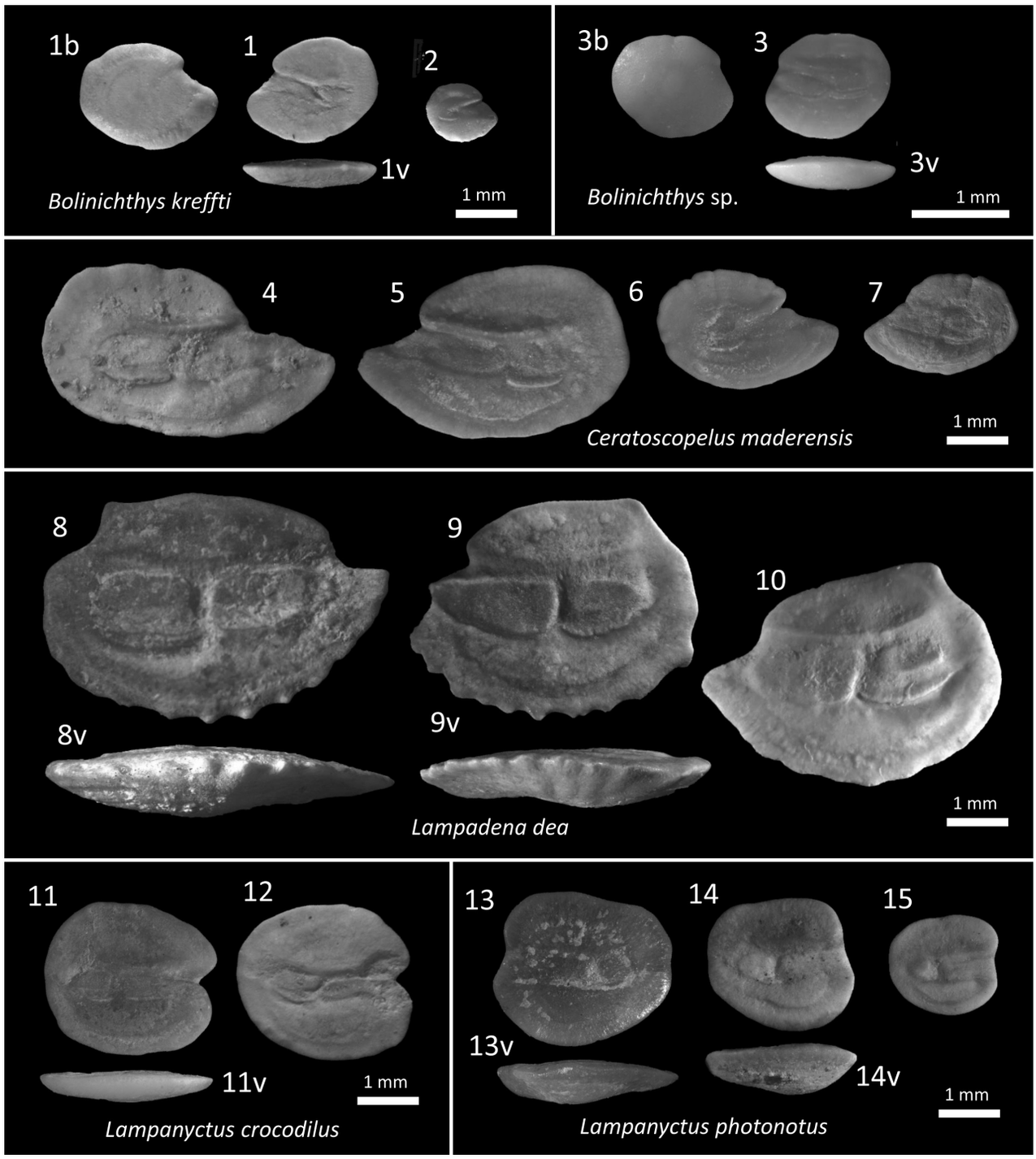


**Plate 6**

Figures 1-2. ***Bolinichthys kreffti*** Schwarzhans, 1986, Río del Padrón (1), Velerín Quarry (2).
Figure 3. ***Bolinichthys* sp.,** Parque Antena.
Figures 4-7. ***Ceratoscopelus maderensis*** (Lowe, 1839), Velerín Carretera (4,5), Velerín Quarry (6,7).
Figures 8-10. ***Lampadena dea*** Fraser-Brunner, 1949, Velerín Carretera.
Figures 11-12. ***Lampanyctus crocodilus*** (Risso, 1810), Velerín Quarry (11), Velerín Carretera (12).
Figures 13-15. ***Lampanyctus photonotus*** Parr, 1928, Velerín Conglomerates (13), Velerín Carretera (14, 15).

(see Schwarzhans, 2013b, pl. 1, figs 1-4), a species that nowadays lives in the Arabian Sea and Indian Ocean, and probably as a recent invader in the Red Sea (Lin *et al*., 2018). They have not been observed in earlier studies on Mediterranean otoliths. Such small myctophid otoliths may have been overlooked in studies on Pliocene fish.

***Diaphus mermuysi* nov. sp.**
Plate 7, figs 4-6

*Holotype* – RGM.1390387, Parque Antena.

*Paratypes* – 2 sagittas: Parque Antena RGM.1390388, RGM.1390389.

*Other material* – 1 sagitta: Parque Antena.

*Locus typicus* – Parque Antena, Estepona, province of Málaga, Spain (see Fig. 1).

*Stratum typicum* –Pliocene, upper Zanclean/ lower Piacenzian, grey clayey sand.

*Etymology* – Named after Stef Mermuys, who provided us with sieved material from Parque Antena.

*Diagnosis* – Small-sized otoliths, with a compact shape, nearly as high as long (OL/OH=1.06-1.09) and moderate thickness (OH/OT=3.6-3.9). They have a prominent rostrum, a half-sized antirostrum, and a distinct excisura. Furthermore, a depressed predorsal rim is followed by a straight or slightly curved and undulating middorsal rim. After the posteriorly positioned inconspicuous postdorsal angle the dorsal rim turns smoothly to the vertical posterior rim. The regularly convex ventral rim has 3-5 strong denticles of which the postventral one is the most prominent and largest.

*Description* – Small-sized otoliths (OL=1.3-1.4 mm) with a distinct, almost vertical posterior rim. The predorsal rim is convex, passing onto the dorsal rim with a predorsal angle. In well-preserved specimens, the dorsal rim is straight, with a distinct middorsal angle, leading to a postdorsal angle. The posterior rim starts with an oblique rim running and then passing onto a straight part with a notch in the middle, after which it connects with the ventral rim via a short oblique rim. The ventral rim is regularly convex, with 3-5 strong denticles of which the postventral one is the most prominent and largest. The otoliths have a prominent, bluntly pointed rostrum and a distinct but short antirostrum, with a clear excisura. The sulcus is divided in a wide ostium and narrower cauda. The ostium is 1.2 times as long as the cauda and becomes wider towards the excisura before it opens on the anterior rim. The crista superior of the ostium reaches the anterior rim in a straight line underneath which it displays a supracollicular furrow anteriorly. The cauda is bordered by a convex crista inferior, above which is a pseudocolliculum. Ostium and cauda are covered by a colliculum. The inner face of the otoliths is nearly flat except for a slightly convex portion at the height of the sulcus; the outer face is convex along the antero-posterior axis, reaching its thickest part at about ⅔ of this axis (*i.e.*, ⅓ from the posterior end), near the point where the cauda is at its widest.

*Remarks* – The sample from Parque Antena also contained juvenile specimens of *Diaphus holti* and *Lobianchia gemellarii*. However, both differ from *D. mermuysi* nov. sp. in the arrangement of the denticles on the ventral rim, lacking the prominent postventral denticle, having more convex posterior and dorsal rims and generally being more elongated. Otoliths of *Diaphus rubus* Girone, Nolf & Cavallo, 2010 from the lower Messinian of Piemonte, Italy (Girone *et al*., 2010) have some resemblance with those of the new species, but differ in the generally wider sulcus, the almost straight crista inferior of the cauda, the more widely spaced denticles on the ventral rim, the parallel running cristae superior and inferior and the more acute postdorsal angle.
Otoliths of *Diaphus barrigonensis* Schwarzhans & Aguilera, 2013 from the western Atlantic Zanclean of Venezuela (OL=1.5-3.0 mm) differ by a slightly more elongate shape (OL/OH=1.1-1.2) from *D. mermuysi* (OL/OH=0.97-1.08) and are thinner (OH/OT=5 *vs.* OH/OT=4.0-4.2. *Diaphus barrigonensis* displays a characteristic pointed postdorsal angle that is emphasised at its posterior side by a concavity and an obliquely cut dorso-posterior rim, while the mid- and post-dorsal rims of *D. mermuysi* display only minor undulations with a rounded and more posteriorly positioned postdorsal angle after which the rim smoothly turns to the vertical posterior rim. The ventral rim of *D. barrigonensis* contains 5 to 7 minor denticles, rather than the prominent few along the post- and mid-ventral rim in *D. mermuysi*. From these differences we consider *D. barrigonensis* and *D. mermuysi* being two different species.
*Diaphus* aff. *rubus* recorded by Carnevale *et al.* (2019, fig. 11i) from Moncucco Torinese ('Lago-mare' deposits), Piedmont Basin was recently reported as *Diaphus* cf. *barrigonensis* (Carnevale & Schwarzhans, 2022). On the basis of these Late Messinian otoliths Carnevale & Schwarzhans (2022) suggested that *Diaphus* cf. *barrigonensis* may have evolved as an eastern Atlantic counterpart of the western Atlantic. The size and dorsal shape of the specimen of *Diaphus* cf. *barrigonensis* (Carnevale & Schwarzhans, 2022, figs 7c-e) show a similarity with those of *D. mermuysi* rath-

**Plate 7**

Figure 1. ***Diaphus anderseni*** Tåning, 1932, El Lobillo.
Figures 2-3. ***Diaphus* aff. *arabicus*** Nafpaktitis, 1978, El Lobillo.
Figure 4. ***Diaphus mermuysi* nov. sp.** holotype, Parque Antena.
Figures 5-6. ***Diaphus mermuysi* nov. sp.** paratypes, Parque Antena.
Figures 7-10. ***Diaphus holti*** Tåning 1918, Velerín Carretera (7), Velerín Quarry (8, 9), Parque Antena (10).
Figures 11-12. ***Diaphus rafinesquii*** (Cocco, 1838), Velerín Quarry (11), Velerín Antena Slope (12).
Figures 13-15. ***Diaphus befralai*** Brzobohatý & Nolf, 2000. Río del Padrón.

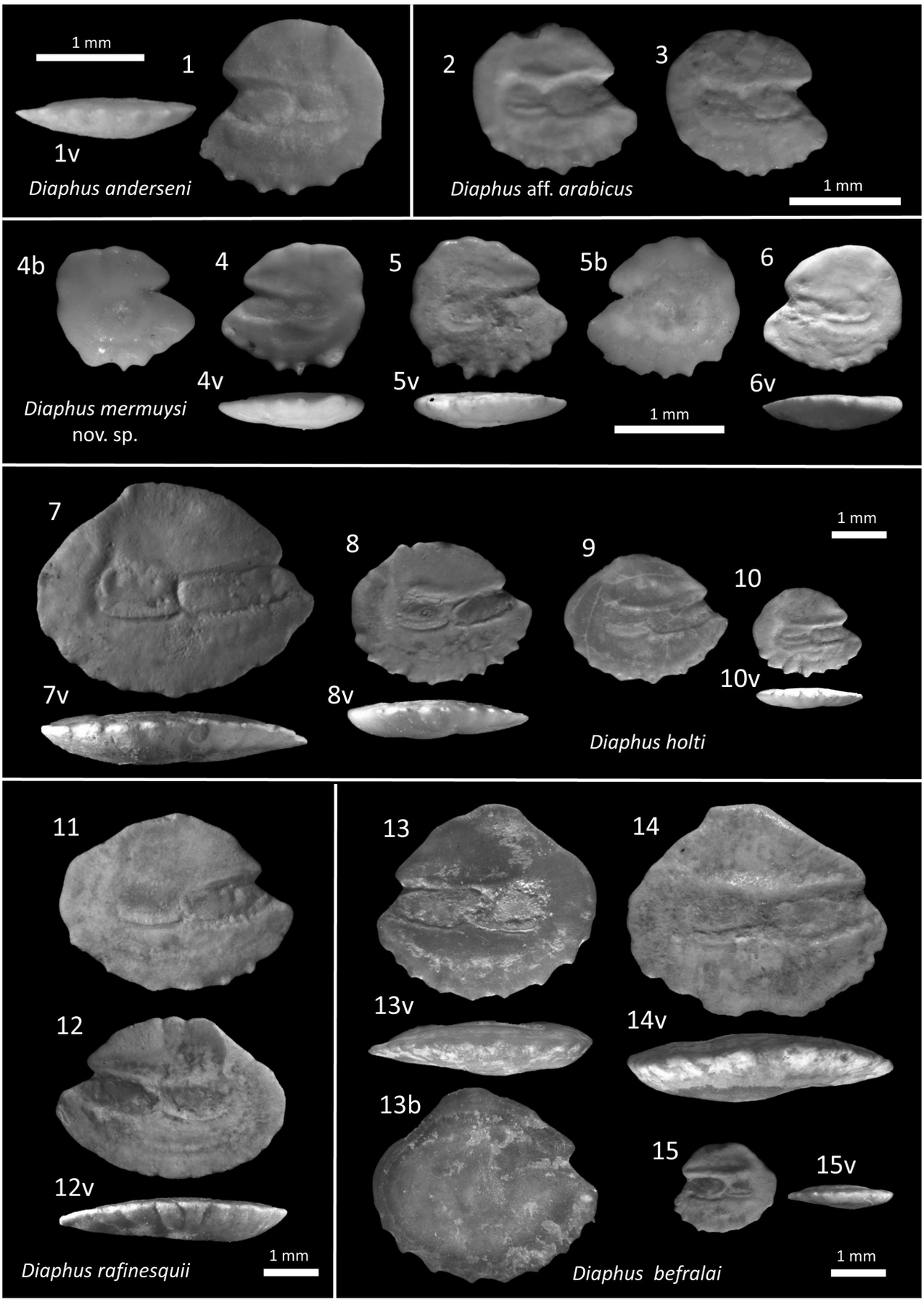
1 mm
1
1v
Diaphus anderseni
2
3
Diaphus aff. arabicus
1 mm
4b
4
4v
5
5v
5b
6
6v
Diaphus mermuysi
nov. sp.
1 mm
7
7v
8
8v
9
10
10v
1 mm
Diaphus holti
11
12
12v
Diaphus rafinesquii
1 mm
13
13v
13b
14
14v
15
15v
Diaphus befralai
1 mm

**Plate 7**

er than *D. barrigonensis* (Schwarzhans & Aguilera, 2013, pl. 7, figs 1-9), but its ventral rim has more and smaller denticles than *D. mermuysi*.

*Distribution* – Piacenzian of the type area only.

**Diaphus termophilus *otolith group***

***Diaphus termophilus* Tåning, 1928**
Plate 8, fig. 6

1999 *Diaphus termophilus* – Rivaton & Bourret, pl. 117, figs 13-17 (present-day otoliths).
2013b *Diaphus termophilus* – Schwarzhans, pl. 6, figs 6-9 (present-day otoliths).

*Material* – 1 sagitta. Velerín Carretera 1.

*Remarks* – Small specimen, highly compressed in antero-posterior direction (OL:OH=1.19), which belongs to the *D. termophilus* group. According to Schwarzhans (2013b, pl. 6, fig. 6), tropical western Atlantic specimens can be more compressed than their Pacific counterparts. Our specimen has a smaller rostrum and antirostrum than the specimens depicted by Schwarzhans (2013b, pl. 6, figs 6-9), which could be due to erosion or to the fact that our specimen is smaller than those depicted by Schwarzhans. Its ventral rim is regularly rounded and crenulated mid-ventrally with no distinct denticles, which probably is a result of the juvenile status.

**Diaphus splendidus *otolith group***

***Diaphus cavallonis* Brzobohatý & Nolf, 2000**
Plate 8, figs 7-18; juveniles figs 14, 15

1986 *Diaphus* aff. *rossiae* (Robba, 1970) – Schwarzhans, pl. 4, fig. 46.
1986 *Diaphus sulcatus* s.l. (Bassoli, 1906) – Schwarzhans, pl. 4, figs 47-49.
2000 *Diaphus cavallonis* – Brzobohatý & Nolf, p.188-189, pl. 5, figs 7-14.
2013 *Diaphus cavallonis* – Schwarzhans & Aguilera, pl. 8, figs 7-9.

*Material* – > 1000 sagittas. Río del Padrón: 502 adult (≥ 3 mm), 215 juvenile (< 3 mm); El Lobillo 348 adult, 181 juvenile.

*Remarks* – Otoliths of this extinct species were described and depicted in Brzobohatý & Nolf (2000). This species is frequently encountered in Zanclean deposits. As we describe a new species, *Diaphus postcavallonis* nov. sp., we also provide an extended description of *Diaphus cavallonis* based on the specimens from Río del Padrón and El Lobillo. Our description and discussion focus on adult specimens. Only well-preserved juvenile otoliths of this species were counted.

*Description* – The otoliths of *D. cavallonis* have a specific compact ellipsoid shape. The ventral rim is regularly bent, flattening anteriorly towards the rostrum, with 8-12 denticles, which become indistinct towards the rostrum. The dorsal rim is salient in its anterior part and convex towards its highest point before the middle of the otolith, after which it becomes straight or slightly concave towards the postdorsal angle. A small but distinct postdorsal angle is situated above the middle of the caudal colliculum. Behind the postdorsal angle is a concave undulation. The posterior rim of the otolith is almost straight to slightly rounded. The ventral rim is regularly convex, but slightly more elongated towards the anterior rim. The rostrum is consistently larger than the short antirostrum, with a distinct excisura showing an angle of about 80°, but a variation ranging from 60 to 90° can be encountered. The ostium is 1.6-1.8 times as long as the cauda, it slightly narrows towards the rostrum and opens on the anterior rim. The posterior part of the ostium and cauda are of similar height. However, while the ostium is fully covered by the colliculum, the cauda is covered by a rather rectangular colliculum that covers the upper 60-80% of the space between the crista superior and the pseudocolliculum. The crista superior aligns along the ostium and cauda and slightly bends upward posteriorly above the cauda. Above the crista superior is a shallow, usually flat dorsal area. A ventral furrow marks a slightly concave area below the sulcus. The inner face is slightly convex in ventral view. The caudal part of the outer face is markedly more convex than the rostral part.
Three large *Diaphus* specimens (Pl. 8, figs 16-18) have an irregular convex dorsal rim, with a salient anterior part and a prominent dorsal angle between shallow concavities. The sulcus is rather wide, tapering slightly anteriorly. Although they have a relatively massive postero-ventral part, we consider them as *Diaphus cavallonis* otoliths from older fish.

*Distribution* – *Diaphus cavallonis* is frequently encountered in Zanclean deposits in southern France and Italy (Nolf & Cappetta, 1989; Nolf & Cavallo, 1994; Nolf & Girone, 2006). It is the dominant species of *Diaphus* in the Zanclean deposits of Río del Padrón and El Lobillo at Estepona, although it uncommonly occurs in upper Miocene strata as well.

***Diaphus postcavallonis* nov. sp.**
Plate 9, figs 1-13 and figs 14-15 (juveniles)

2007 *Diaphus* aff. *cavallonis* – Girone, p. 163, pl. 1, figs 8a, c.

*Holotype* –Velerín Quarry RGM.1390416 (Pl. 9, fig. 4).

*Paratypes* – 11 sagittas: RGM.1390417-RGM.1390427; Velerín Quarry (5); Velerín Sandy Lens (3); Velerín Carretera (3).

*Other material* – 615 sagittas ≥ 3.0 mm. Velerín Carretera 129; Velerín Conglomerates 164, Velerín Quarry 81;

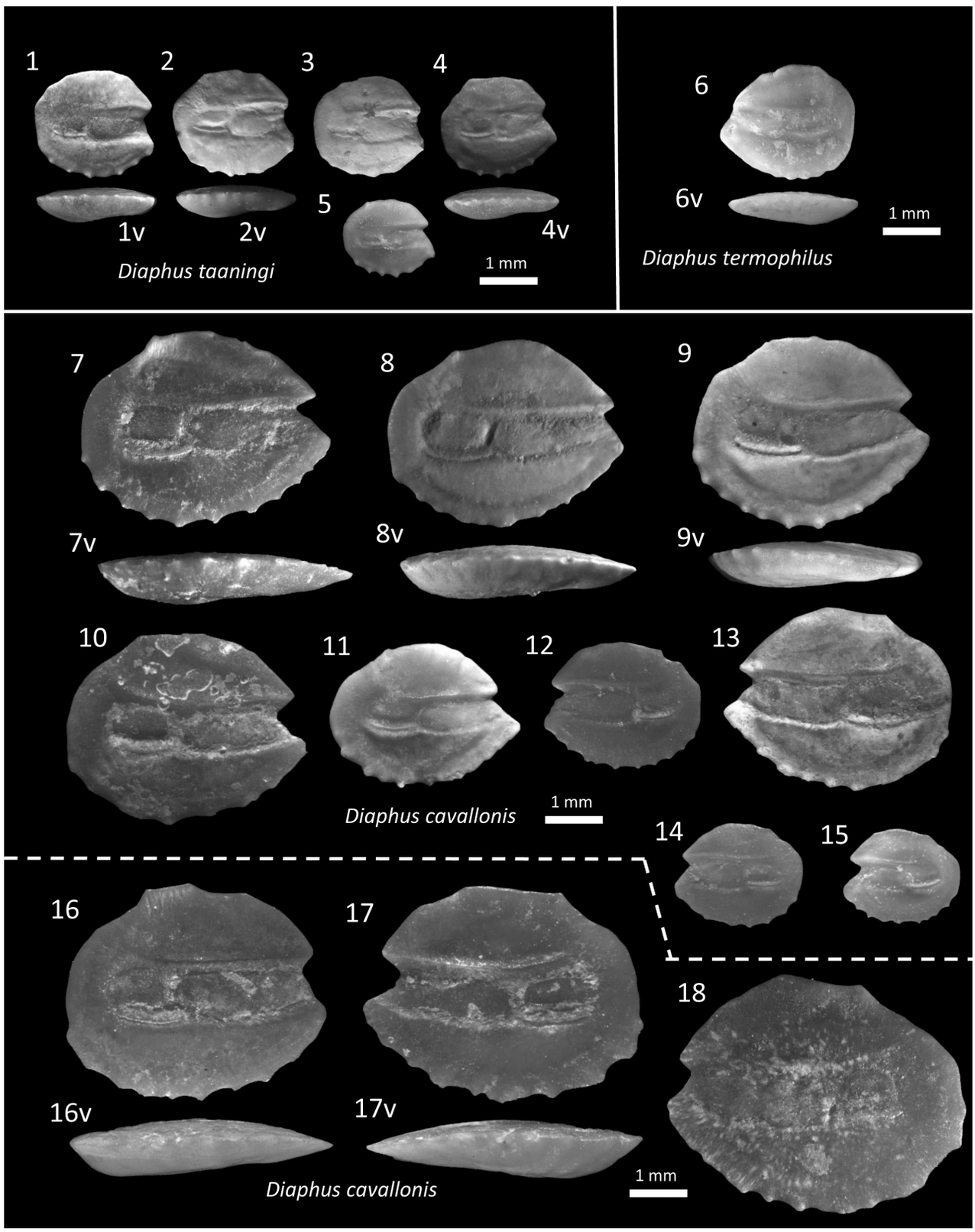


**Plate 8**

Figures 1-5. ***Diaphus taaningi*** Norman, 1930, Velerín Antena Slope (1), El Lobillo (2), Velerín Carretera (3,4), Velerín Quarry (5).
Figure 6. ***Diaphus termophilus*** Tåning, 1928, Velerín Carretera.
Figures 7-15. ***Diaphus cavallonis*** Brzobohatý & Nolf, 2000, El Lobillo (7, 8, 10, 11, 13), Río del Padrón (9, 12, 14, 15).
Figures 16-18. ***Diaphus cavallonis*** Brzobohatý & Nolf, 2000 (large specimens), El Lobillo.

Velerín Sandy Lens 48; Velerín Antena Slope 96; Velerín Hilltop 87; Parque Antena 10; and 3237 juvenile sagittas (≤ 2.9 mm) from the Velerín sites together.

*Locus typicus* – Velerín Quarry, close to Velerín Antena, along Camina Nicolas, Velerín, Estepona, province of Málaga, Spain.

*Stratum typicum* – Pliocene, Piacenzian, fossiliferous medium- to fine-grained sands.

*Etymology* – Named after *D. cavallonis* to which it is similar, but the new species is restricted to the Piacenzian deposits, whereas *D. cavallonis* is abundant in the older Zanclean deposits.

*Diagnosis* – Regular oval otoliths up to a maximum length of 6 mm (average OL:OH=1.30, range 1.21-1.35). In contrast to *D. cavallonis*, no squeezed antero-ventral part on the ventral rim. Dorsal rim curves convexly from antirostrum to a rather horizontal middorsal part and merges after a distinct postdorsal angle concavely with the posterior rim that forms a blunt posterior end. Sulcus with long ostium and shorter cauda (OsL:CaL=1.57-1.72 in adult specimens) with distinct colliculi. Regularly curved ventral rim with 10-11 denticles.

*Description* – Medium- to large-sized otoliths usually 3 to 4.5 mm, but up to a maximum length of 6 mm (average OL:OH=1.30, range 1.21-1.35). The anterior part of the dorsal rim is very salient; the subsequent part is almost straight or bent slightly upwards to a distinct postdorsal angle. The posterior rim displays a wide concavity dorsally after which it becomes straight or slightly convex. It connects with the ventral rim at the last denticle. The ventral rim is regularly convex from the tip of the rostrum to the postventral angle before the posterior rim, roughly at the height of the crista inferior of the cauda. It has 10-11 denticles. In most specimens the postdorsal angle is the highest point of the otolith and is situated above the middle of the caudal colliculum. The median sulcus has a rather long ostium and shorter cauda (OsL:CaL=1.57-1.72 in adult specimens) with clear colliculi. The upper and lower margins of the ostial colliculum as well as the cristae superior and inferior usually run parallel towards the excisura, but in some specimens a slight narrowing is observed at its anterior end. A supracollicular furrow can be observed under the crista superior of the ostium near the anterior rim. A prominent crista superior runs nearly straight or slightly salient along the cauda. The crista inferior of the cauda is only slightly convex. The caudal colliculum parallels only the upper part of the ostial colliculum leaving ample space bordered by a distinct pseudocolliculum. The ventral furrow is shallow, but sometimes absent. The rostrum is larger than the short antirostrum. The distinct but often shallow excisura has an angle of about 80° in most specimens, but some variation ranging from 60° to 90° can be observed. The inner face is slightly convex along its antero-posterior axis, the outer face is more convex, with the thickest part under the cauda.

*Remarks* – The otoliths of this species are reminiscent of those of *Diaphus cavallonis*, but differ from them by a more elongated oval shape due to a straighter middle part of the dorsal rim, a more regularly bent anterior ventral rim, a less consistent narrowing of the ostium and a much larger concavity of the posterior rim behind the postdorsal angle. Fig. 3 shows the length *vs.* height of a range of *D. postcavallonis* otoliths as compared to those dimensions of other common large *Diaphus* species in this study. Otoliths of *D. postcavallonis* are closely related to those of *D. cavallonis* which is abundant in Zanclean deposits and they may reflect a further evolution of

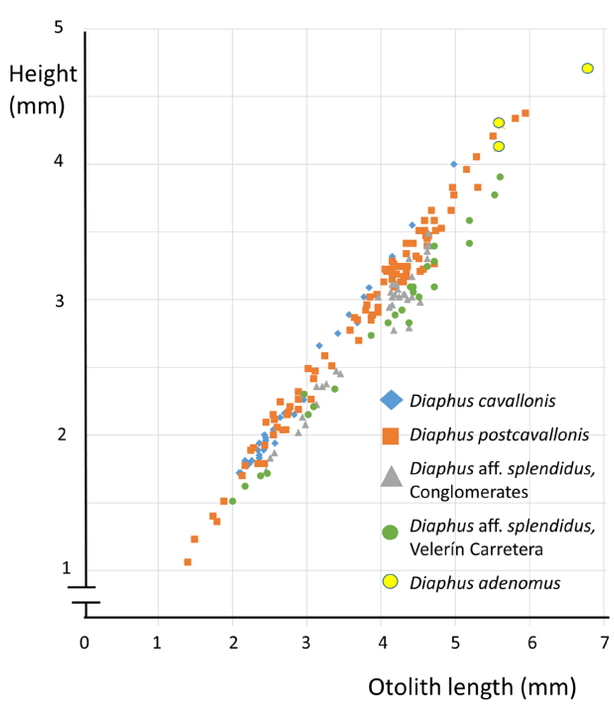


**Figure 3.** Otolith length and height in 4 species of Pliocene *Diaphus* from Estepona. *Diaphus cavallonis* from Río del Padrón and El Lobillo combined; *Diaphus postcavallonis* from Velerín Quarry Velerín Conglomerates and Velerín Carretera; *Diaphus* aff. *splendidus* separately from Velerín Carretera and Velerín Conglomerates showing the same OL:OH ratio; *Diaphus adenomus* from Velerín Carretera.

**Plate 9**

Figures 1-3, 5-13. ***Diaphus postcavallonis* nov. sp.**, paratypes, Velerín Quarry (1, 2, 5, 11-12), Velerín Sandy Lens (6-8), Velerín Carretera (3, 9, 10, 13).

Figure 4. ***Diaphus postcavallonis* nov. sp.,** holotype, Velerín Quarry.

Figures 14-15. ***Diaphus postcavallonis* nov. sp.,** juveniles, Velerín Carretera.

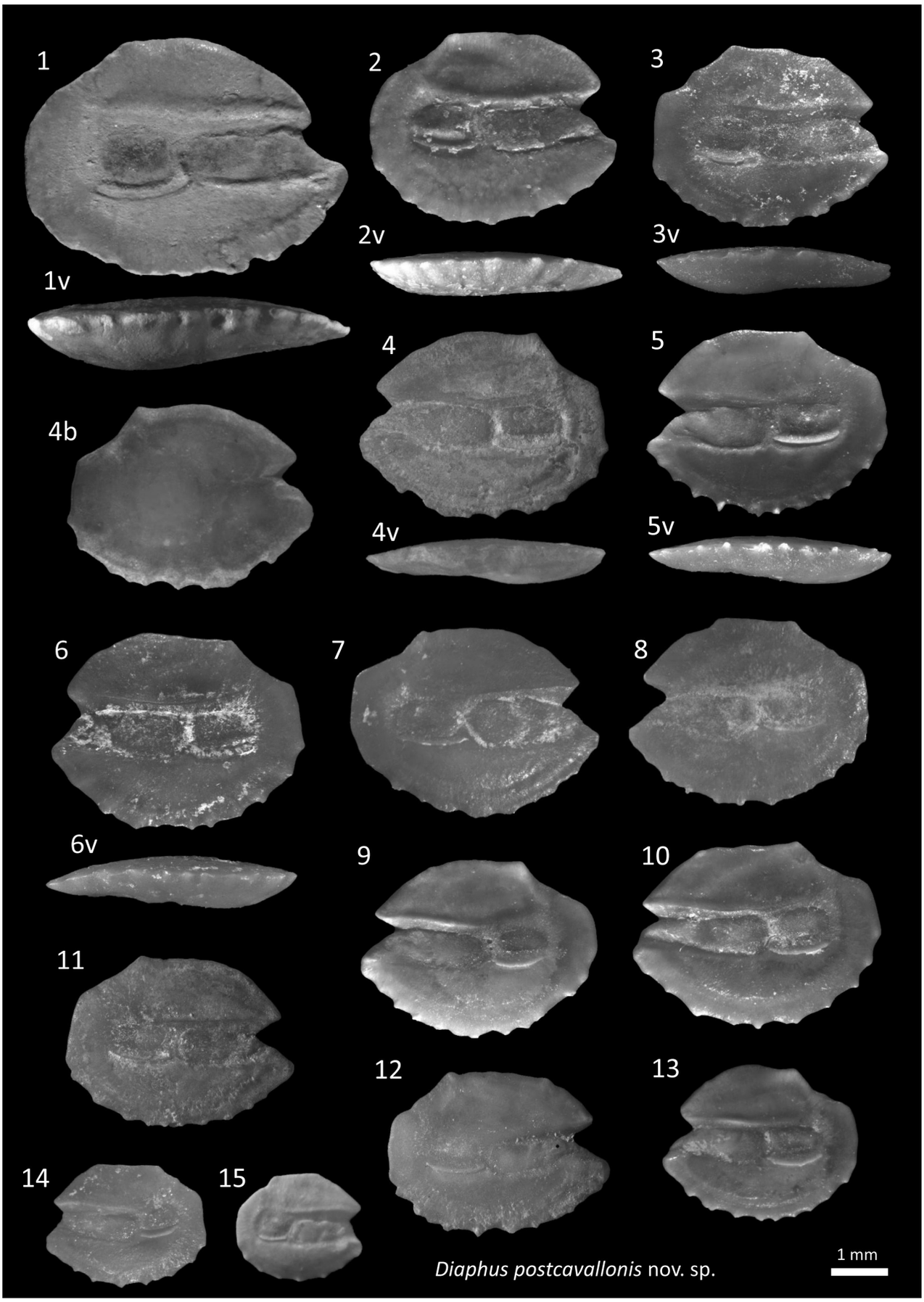
1
2
3
2v
3v
1v
4
5
4b
4v
5v
6
7
8
6v
9
10
11
12
13
14
15
*Diaphus postcavallonis* nov. sp.
1 mm

**Plate 9**

the latter species during the Piacenzian. Girone (2006) also recognised these differences when she reported *D.* aff. *cavallonis* from the Piacenzian deposits of Emilia Romagna in Italy. Otoliths of *D. splendidus* are more elongated, have a shallower concavity after the postdorsal angle and are consistently less thick in ventral view than those of *D. postcavallonis*.

The distinction between juvenile specimens of *D. postcavallonis* and *D. dirknolfi* is not unambiguously delimitated due to intraspecific variation. The narrowing ostium and middle part of the dorsal rim that runs parallel to the sulcus are properties of *D. postcavallonis*, while the *D. dirknolfi* specimens have a wider ostium with a characteristic right angle in the crista inferior, and an obliquely declining dorsal rim after the anteriorly localised highest point of the dorsal rim.

*Distribution* – Known from the Piacenzian of Velerín, Estepona and Rio Merli (Emilia Romagna, Italy).

***Diaphus splendidus* (Brauer, 1904)**
Plate 10, figs 3-13

| | |
|---|---|
| 1994 | *Diaphus* aff. *splendidus* – Nolf & Cavallo, pl. 2, figs 8-11. |
| 2000 | *Diaphus* aff. *splendidus* – Brzobohatý & Nolf, pl. 6, fig. 1 (not 2-5). |
| 2006 | *Diaphus* aff. *adenomus* – Nolf & Girone, pl. 4, figs 2-9. |
| 2013b | *Diaphus splendidus* – Schwarzhans, pl. 8, figs 1-5 (present-day otoliths). |
| 2013 | *Diaphus splendidus* – Schwarzhans & Aguilera, pl. 8, figs 22-25. |

*Material* – 619 sagittas. El Lobillo 8; Velerín Carretera 406; Velerín Conglomerates 188; Velerín Quarry 2; Velerín Antena Sandy Lens 9; Velerín Antena Slope 3; Parque Antena 3.

*Remarks* – The extant *Diaphus splendidus* (Brauer, 1904) is known from the subtropical and tropical Atlantic, Indian and Pacific oceans. Extant otoliths have been depicted in Rivaton & Bourret (1999), Nolf & Cappetta (1989) and Schwarzhans (2013b). In Pliocene deposits of Velerín-Estepona these thin and oval to fusiform otoliths can reach a length of 5.9 mm. They are characterised by a slightly depressed but gently convex predorsal rim; a well-developed postdorsal angle, which is followed by a concavity of the posterior rim. The ventral rim is regularly convex and decorated with 9-13 denticles. In the fossil record, *Diaphus splendidus* is often used to indicate otoliths that are similar and sometimes identical to those of their extant counterparts (Brzobohatý & Nolf, 2000). The material of Velerín Carretera and Velerín Antena displays a considerable variability (compare Pl. 10, figs 3, 5 & 8), which may point to a complex nature of this species. Their OL:OH ratio for the OL sizes 2.0-5.6 mm is consistently higher than that of *D. cavallonis*, *D. postcavallonis* nov. sp. and *D. adenomus* (Gilbert, 1905) (Figure 3). The posterior part of the outer face of the otoliths in ventral view is only slightly thicker than the anterior part. The inner face is slightly convex in antero-posterior direction. OsL:CaL ratio of adult specimens is 1.9-2.2, usually above 2.0. Juvenile specimens of *D. splendidus* (Pl. 10, figs 10-12) can be distinguished from juvenile *Diaphus* spp. By their flat and usually regular lobated outer face, the characteristic regular shape (oval with a characteristic anterior portion, rostrum and tiny excisura), and the poorly developed postdorsal angle (the latter in contrast to adult *D. splendidus*).

Brzobohatý & Nolf (2000) used the *Diaphus* aff. *splendidus* species complex to identify all species of *Diaphus* that show a reasonable similarity to otoliths of the present-day *D. splendidus*. Subsequently, Nolf & Girone (2006) identified thin elongate otoliths of *Diaphus* (up to 4.9 mm) in a sample from Rio Torsero (Ceriale, Italy) as *Diaphus* aff. *adenomus* on the basis of size and comparison of a series of specimens of extant *D. adenomus*. Unfortunately, they only depicted a much larger specimen of an extant *D. adenomus* and the match with extant *D. adenomus* (iconography in Schwarzhans, 2013b) is not convincing. In our view, these Pliocene specimens with an almost straight crista superior are better identified as *Diaphus splendidus* (species complex) rather than as *D. adenomus* which displays a lower OsL:CaL ratio and a less strong upward bending crista superior along the cauda. Therefore, we propose to keep the long and thin otoliths of *Diaphus* in the *D. splendidus* species complex, while *D. postcavallonis* nov. sp. is separated from them as a distinct species (see above).

**Diaphus adenomus *otolith group***

***Diaphus adenomus* Gilbert, 1905**
Plate 11, figs 9-11

| | |
|---|---|
| 1983 | *Diaphus adenomus* – Nolf & Steurbaut, pl. 1, fig. 24 |
| 2013b | *Diaphus adenomus* – Schwarzhans, pl. 12, figs 6-13. |
| *non* 2006 | *Diaphus* aff. *adenomus* – Nolf & Girone, pl. 4, figs 2-9. |

*Material* – 4 sagittas. Velerín Carretera 4.

*Remarks* – Three adult specimens and one juvenile were present in the material from Velerín Carretera. The adult specimens are characterised by a large size

**Plate 10**

Figure 1. ***Diaphus pedemontanus*** (Robba, 1970), El Lobillo.
Figure 2. ***Diaphus* sp. 1**, Velerín Conglomerates.
Figures 3-13. ***Diaphus splendidus*** (Brauer, 1904), Velerín Carretera (3, 5, 6, 8, 10-12), Velerín Conglomerates (4, 7, 9, 13).

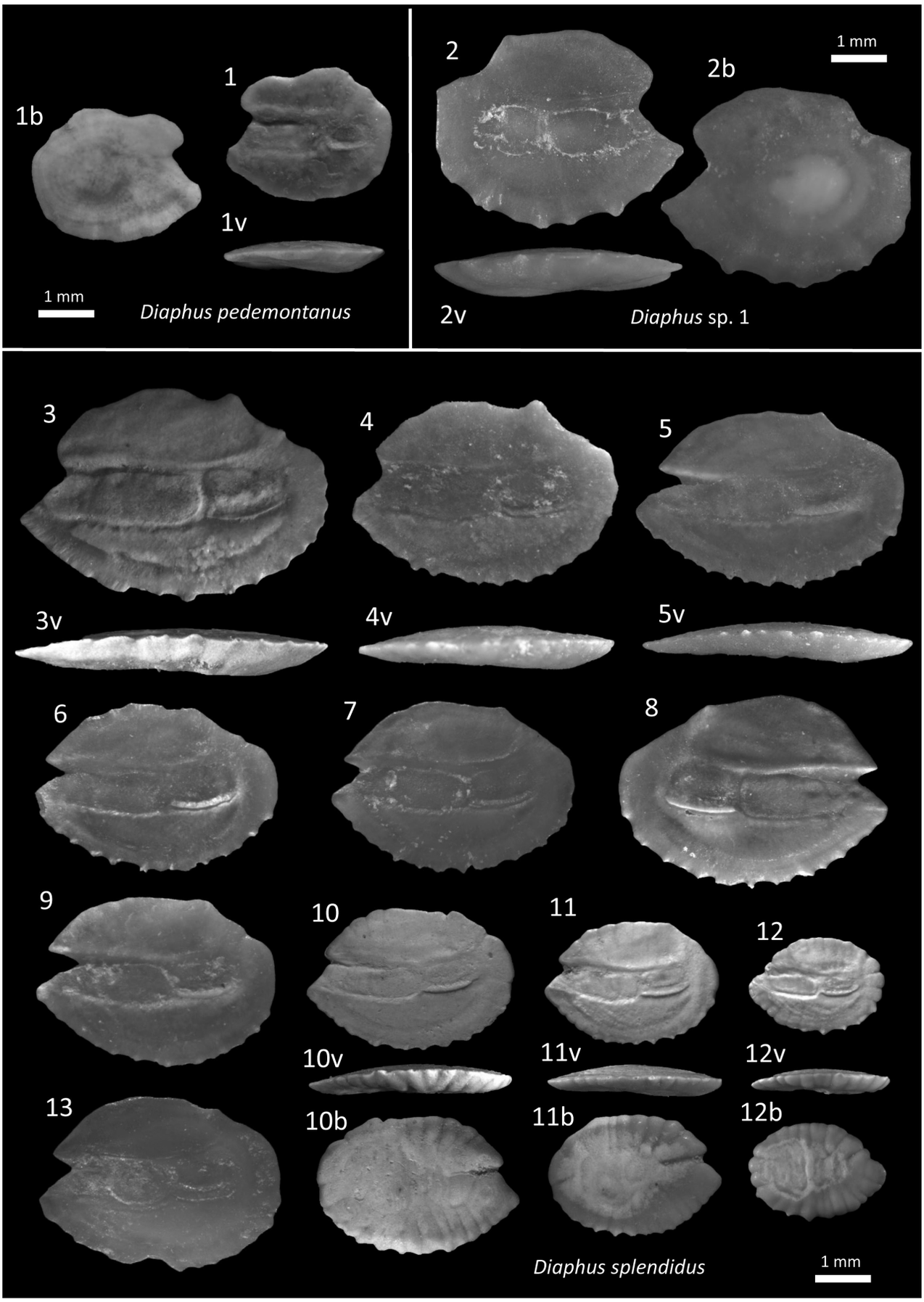
1
1b
1v
1 mm
*Diaphus pedemontanus*
2
2b
1 mm
2v
*Diaphus* sp. 1
3
4
5
3v
4v
5v
6
7
8
9
10
11
12
10v
11v
12v
13
10b
11b
12b
*Diaphus splendidus*
1 mm

**Plate 10**

(OL=5.6, 5.6 and 6.8 mm) and a relatively large cauda (OsL:CaL=1.42-1.45) whose crista superior bends up considerably and fades away at its posterior end. While the general shape of the otoliths is similar to those of *Idiolychnus urolampus* (Gilbert & Cramer, 1897) (illustrated in Schwarzhans 2013b, pl. 15, figs 11-12), it differs markedly by a more rounded anterior rim and a much lower OsL:CaL ration, which is 1.42-1.45 *vs.* 1.9-2.1 in *Idiolychnus urolampus*. Instead, it is reminiscent of middle-sized specimens of the extant *D. adenomus* (see Schwarzhans, 2013b, figs 10-13), but more material is needed for an unambiguous identification. A *Diaphus* aff. *adenomus* has also been reported from the Pliocene of Rio Torsero, Ceriale, northern Italy (Nolf & Girone, 2006). However, as discussed under the *Diaphus splendidus* species group, these otoliths probably pertain to another species than *D. adenomus*, quite close to *Diaphus splendidus* (see above).

***Diaphus pedemontanus*** **(**Robba, 1970)
Plate 10, fig. 1

| | |
|---|---|
| 1970 | *Porichthys pedemontanus* – Robba, pl. 16, fig. 8. |
| 1983 | *Diaphus pedemontanus* – Nolf & Steurbaut, pl. 1, figs 26-37. |
| 2000 | *Diaphus pedemontanus* – Brzobohatý & Nolf, pl. 4, figs 1-6 |
| 2010 | *Diaphus pedemontanus* – Girone, Nolf & Cavallo, figs 7b1-7b6. |
| 2013 | *Diaphus pedemontanus* – Schwarzhans & Aguilera, pl. 9, figs 1-4. |

*Material* – 1 sagitta. El Lobillo 1.

*Description* – Small thin otolith with a prominent rostrum and antirostrum and a wide excisura. The undulating convex dorsal rim has a characteristic mid-dorsal concavity and continues after a blunt postdorsal angle in the posterior rim that has an oblique upper part and a lower part that runs almost perpendicular to the ventral rim. The ventral rim is regularly convex, with 6 to 7 flattened and hardly visible denticles. The sulcus consists of a wide and straight ostium and a two times shorter cauda; the width of the caudal part enclosing the caudal colliculum and pseudocolliculum is of similar height as the ostial colliculum. The outer face is nearly flat, but slightly thickened at its posterior part.

*Remarks* – *Diaphus pedemontanus* was originally described as *Porichthys pedemontanus* by Robba (1970) based on the single and very large holotype from the Tortonian of the Piacenza region in Italy. Nolf & Steurbaut (1983) presented an ontogenetic series of the species as *Diaphus pedemontanus* based on material from the type locality. Zanclean specimens were depicted in a paper on Neogene otoliths of *Diaphus* by Brzobohatý & Nolf (2000). Other studies – Girone *et al*. (2010) on the Messinian of Italy and Schwarzhans & Aguilera (2013) on the Tortonian of Panama – also identified *D. pedemontanus*, albeit that a considerable variability is seen between the various populations: "*Diaphus pedemontanus* is a rather problematical species, because of the strong ontogenetic changes and considerable variability of their otoliths" (Girone *et al*., 2010, p. 413).

**Diaphus garmani *otolith group***

***Diaphus dirknolfi*** **Schwarzhans, 1986*, sensu*** **Carnevale & Schwarzhans, 2022**
Plate 11, figs 4-8

| | |
|---|---|
| 1971 | *Myctophum splendidum* (Prochazka, 1893) – Weiler, pl. 1, fig. 3. |
| 1980 | *Diaphus* sp. 2 – Nolf & Martinell, pl. 3, fig. 13. |
| 1986 | *Diaphus dirknolfi* – Schwarzhans, pl. 3, figs 34-35. |
| 2019 | *Diaphus splendidus* (Brauer, 1904) – Carnevale *et al*., fig. 11f. |
| 2022 | *Diaphus dirknolfi* – Carnevale & Schwarzhans, figs 7J-P. |

*Material* – 444 sagittas. Río del Padrón 11; El Lobillo 7; Velerín Conglomerates 10; Velerín Carretera 280; Velerín Quarry 123; Velerín Antena Slope 13.

*Description* – Within the well-preserved small ellipsoid *Diaphus* otolith assemblages from Velerín Carretera, Velerín Conglomerates and Velerín Quarry many small otoliths (OL=2.3-3.1 mm; OL:OH=1.18-1.35) display the typical shape of *D. garmani*-related otoliths, which in addition to *D. garmani* also include *D. regani* Tåning, 1932*, D. dumerilii* (Bleeker, 1856) and *D. dirknolfi* Schwarzhans, 1986. The dorsal rim is anteriorly expanded with the highest point above the middle of the ostium. Its curvature is continuous until a small postdorsal angle, after which it runs straight or slightly concave to the posterior rim. A distinct rostrum is present (7.5-12% of OL) together with a small pointed antirostrum and notch. The ventral rim is regularly curved and has 7-11 prominent denticles. The posterior rim is usually rounded, but can run straight upward in a minor part of the specimens.
The ostium is wide and 2.0 to 2.4 times as long as the cauda. The ostium has a lobate dorsal rim; its dorsally re-

**Plate 11**
Figures 1-3. ***Diaphus*** **sp. 2**, Río del Padrón.
Figures 4-8. ***Diaphus dirknolfi*** (Schwarzhans, 1986 sensu Carnevale & Schwarzhans, 2022), Velerín Carretera.
Figures 9-11. ***Diaphus adenomus*** Gilbert, 1905, Velerín Carretera.
Figures 12-13. ***Lobianchia dofleini*** (Zugmayer, 1911), Velerín Carretera (12), El Lobillo (13).
Figures 14-17. ***Lobianchia*** **cf.** ***gemellarii*** (Cocco, 1838), Velerín Carretera.

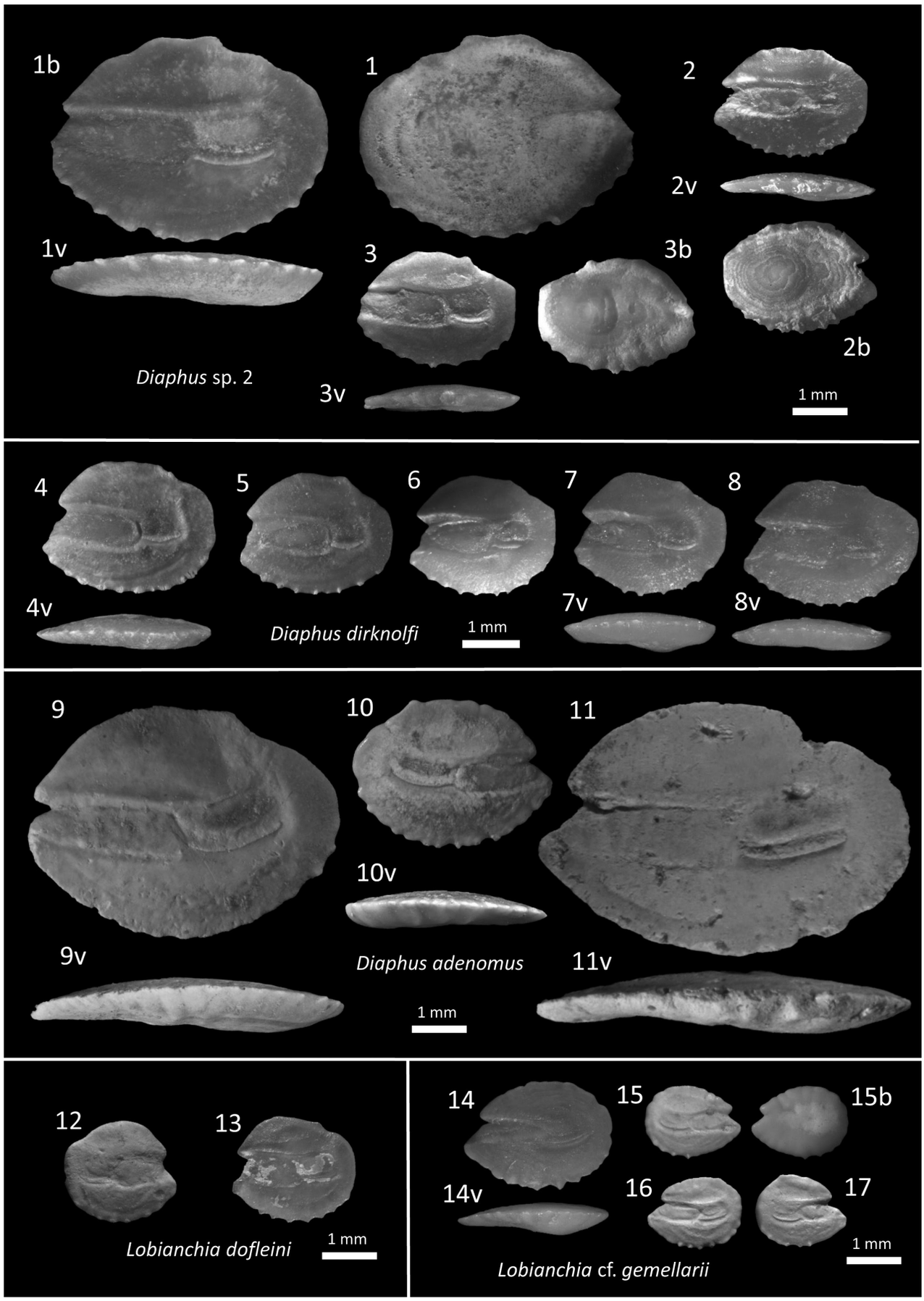
1b
1
2
2v
1v
3
3b
2b
Diaphus sp. 2
3v
1 mm
4
5
6
7
8
4v
7v
8v
Diaphus dirknolfi
1 mm
9
10
11
10v
9v
Diaphus adenomus
11v
1 mm
12
13
Lobianchia dofleini
1 mm
14
15
15b
14v
16
17
1 mm
Lobianchia cf. gemellarii

**Plate 11**

duced ostial colliculum narrows in anterior direction, but sometimes widens again just before reaching the excisura ostia. The inferior ostial lining lies somewhat below the pseudocolliculum (OCH:CCHP=1.25-1.45), thus causing a right angle of the crista inferior at the ostium-cauda junction. OCH:CCHP stands for the ratio between ostial colliculum height and the height spanning both caudal colliculum and pseudocolliculum.
The inner face is convex along the antero-posterior and dorso-ventral axes. The outer face is thin and flat to slightly concave at the anterior side and becomes about twice as thick and convex at the posterior side.

*Remarks* – These Pliocene otoliths share many features with those of the extant *Diaphus garmani* otolith group, in particular *D. garmani* and *D. dumerilii*, such as the wide ostium and the anteriorly expanded dorsal rim. They differ from those of the extant Indo-West Pacific *D. regani* and *D. jenseni* Tåning, 1932, which both have a much higher number of denticles (15-17 and 15 *vs*. 7-11 in *D. garmani* Gilbert, 1906) along their ventral rims.
Very recently, Carnevale & Schwarzhans (2022, figs 7J-P) re-described the properties of *D. dirknolfi* Schwarzhans, 1986 otoliths based on Late Messinian (Lago Mare phase) specimens from Italy and Zanclean material from Morocco. The rostrum is longer (reaches more anteriorly) than the antirostrum, the ostium is 2.0-2.3 times longer than and as wide as the cauda, and the ventral rim has 6 to 8 denticles. Otoliths of *Diaphus dirknolfi* (*sensu* Carnevale & Schwarzhans, 2022) differ from those of *D. dumerilii* by having a longer ostium (OsCL:CaCL=2.0-2.3 *vs*. 1.7-2.0) and fewer denticles along the ventral rim (6-8 *vs*. 9-12) (Carnevale & Schwarzhans, 2022, figs 7J-L). Our specimens probably are Late Zanclean/ Early to Middle Piacenzian representatives of *D. dirknolfi*. They have a similar rostrum and ostium length, and a number of ventral denticles that is comparable to the range of denticles in Zanclean specimens reported earlier from Dar Bel Hamri, Morocco (Schwarzhans, 1986 pl. 3, fig. 34; Carnevale & Schwarzhans, 2022, figs M-P). The shift in the inferior lining of the ostium and cauda is clearer than in the Zanclean and Late Messinian specimens, but less pronounced than in otoliths of present-day *D. garmani* and *D. regani* (compare Schwarzhans, 2013b, pl. 10).

***Diaphus* sp. 1**
Plate 10, fig. 2

*Material* – 1 sagitta. Velerín Conglomerates 1.

*Remarks* – A single well-preserved adult specimen from the Conglomerates has a specific OL/OH ratio=1.23, that does not fit well in any of the known species of *Diaphus*. The low number of ventral denticles (n=7), the blunt posterior side and the bulky predorsal part of the otolith resemble features of *D. pedemontanus*, but the large postdorsal concavity of the rim and thin nature of this Piacenzian otolith differ. There is a resemblance with *Diaphus* sp. 1 in Girone *et al*. (2010, fig. 3e) in the general outline and structure of the sulcus, but our specimen has a different dorsal rim and a much wider excisura. While the general outline is comparable to a compact *D. postcavallonis*, the sulcus is wider and the number of denticles less.

***Diaphus* sp. 2**
Plate 11, figs 1-3

*Material* – 4 sagittas. Río del Padrón 3; El Lobillo 1.

*Diagnosis* – Large-size otolith (OL=5.0 mm; OH=3.7 mm) that belongs to the *Diaphus splendidus* otolith group, but discriminates itself from the other members by its almost perfect oval shape (OL:OH=1.35), the large number (12) of almost equally-sized denticles along the ventral rim. The narrow sulcus has an ostium that is twice as large as the cauda and with a colliculum tapering toward the anterior rim. The outside is flat at two levels, as the thickness of the posterior half is bigger than that of the anterior part (OT=0.83 mm and 0.55 mm, respectively.

*Description* – Four specimens are available, one adult (OL=5.0 mm; OH=3.7 mm; Pl. 11, fig. 1) and three smaller otoliths, of which two (OL=2.7-2.9 mm; OH=2.0-2.1 mm) are depicted on Plate 11, figs 2-3. They are ellipsoid otoliths with an OL/OH ratio of 1.35-1.38. In the larger specimen, the dorsal rim is salient anteriorly and continues regularly rounded with 3 shallow undulations, of which the last one forms a blunt postdorsal angle that projects to the anterior part of the cauda, after which it continues concavely to the posterior rim. The posterior rim is slightly convex and connects with the regularly convex ventral rim that has 12 denticles. The rostrum is blunt with a shallow antirostrum and excisura. In the smaller specimen, the dorsal rim is salient anteriorly, undulates towards the highest point and then continues concavely to the postdorsal angle. The posterior rim is straight. The rostrum, antirostrum and excisura are more prominent.
The median sulcus of all specimens has a long ostium and shorter cauda (OsL:CaL=1.89-2.5) with clear col-

**Plate 12**

Figures 1-4. ***Benthosema* aff. *glaciale*** (Rheinhardt, 1837), Velerín Quarry (1, 3, 4), Río del Padrón (2).
Figures 5-8. ***Electrona rissoi*** (Cocco, 1829), Velerín Conglomerates (5), Velerín Carretera (6-8).
Figures 9-12. ***Hygophum hygomi*** (Lütken, 1892), Velerín Carretera.
Figures 13-17. ***Hygophum* aff. benoiti** (Cocco, 1838), Velerín Carretera.
Figure 18. ***Myctophum punctatum*** Rafinesque, 1810, Velerín Carretera.
Figures 19-25. ***Myctophum fitchi*** Schwarzhans, 1978, Río del Padrón (19,20), Velerín Carretera (21, 23, 25), Velerín Quarry (22), Velerín Conglomerates (24).

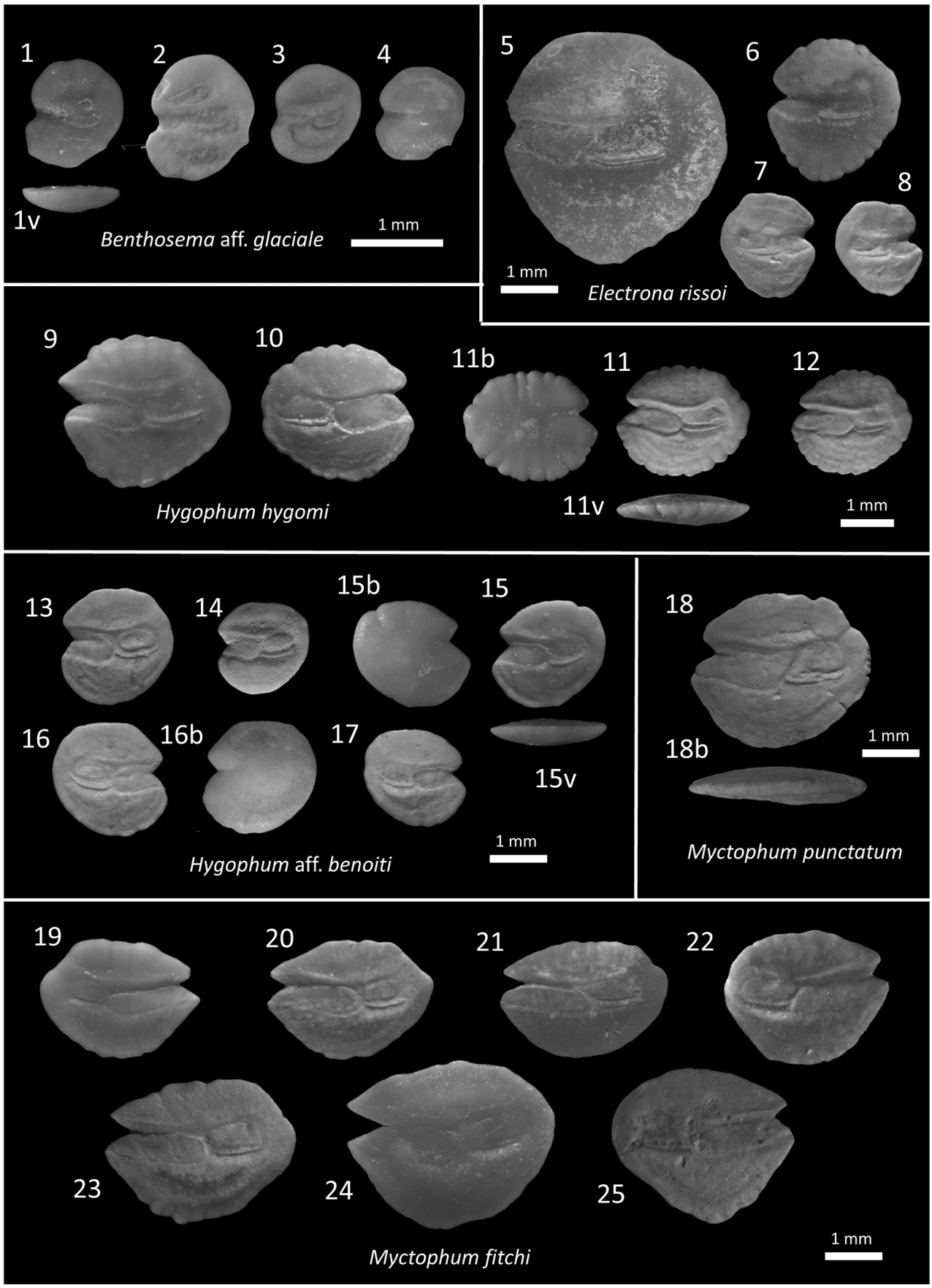
1
2
3
4
1v
Benthosema aff. glaciale
1 mm
5
6
7
8
1 mm
Electrona rissoi
9
10
11b
11
12
Hygophum hygomi
11v
1 mm
13
14
15b
15
16
16b
17
15v
1 mm
Hygophum aff. benoiti
18
1 mm
18b
Myctophum punctatum
19
20
21
22
23
24
25
1 mm
Myctophum fitchi

**Plate 12**

liculi. The ostial colliculum narrows a bit towards the excisura and displays a supracollicular furrow at its anterior end. A prominent crista superior runs nearly straight along the sulcus but slightly bends upward along the cauda. The caudal colliculum fills the upper part of the cauda and shows a distinct collicular crest. The crista inferior and ventral furrow are less prominent. The inner face is slightly convex in antero-posterior direction. The outer face is straight anteriorly flat, but somewhat thicker after the ostium-cauda junction (adult specimen OT=0.55-0.83 mm).

*Remarks* – The specimens here presented were obtained from Zanclean deposits at Río del Padrón and El Lobillo. They differ from *Diaphus cavallonis* by their highly oval shape that has no squeezed trait at its preventral lining. Moreover, they display an ostium/cauda ratio of about 2, compared to 1.6-1.8 in *D. cavallonis*, and have 12 regular denticles along the ventral rim (*vs*. 8-12 in *D. cavallonis*). Finally, most of the *Diaphus* sp. 2 specimens (Pl. 11, figs 1, 3) have a very small excisura and antirostrum as compared to *D. cavallonis*.

Genus *Lobianchia* Gatti, 1904

***Lobianchia dofleini* (Zugmayer, 1911)**
Plate 11, figs 12-13

1983 *Lobianchia dofleini* – Nolf & Steurbaut, pl. 3, figs 26-29.
1995 *Lobianchia dofleini* – Smale, Watson & Hecht, pl. 24, fig. C.
2013b *Lobianchia dofleini* – Schwarzhans, pl. 15, figs 1-5 (present-day otoliths).

*Material* – 3 sagittas. El Lobillo 2; Velerín Carretera 1.

*Remarks* – *Lobianchia dofleini* is a still existing species, whose otoliths are shaped as those of *Diaphus* with a relatively wide ostium and – compared to *Diaphus garmani* group otoliths – a lower OsL:CaL ratio. Only a few otoliths were identified as *L. dofleini*, but we cannot fully exclude to have over- or underestimated their presence because of possible shape overlap with variable specimens of *Diaphus dirknolfi*. *Lobianchia dofleini* is known since the Tortonian of the Mediterranean (Nolf & Steurbaut, 1983, pl. 3, figs 22-25; not Lin *et al.,* 2015, fig. 3.1, which seems to represent a *Diaphus cavallonis* rather than a *Lobianchia*) and was also recognised from the Piacenzian of Jamaica (Schwarzhans & Aguilera, 2013, pl. 14, fig. 6).

***Lobianchia* cf. *gemellarii* (Cocco, 1838)**
Plate 11, figs 14-17

1999 *Lobianchia gemellarii* – Rivaton & Bourrett, pl. 121, figs 16-22 (present-day otoliths).
2013b *Lobianchia gemellarii* – Schwarzhans, pl. 15, figs 6-10 (present-day otoliths).
2017b *Lobianchia gemellarii* – Lin *et al*., figs 5P, Q and 6A-J.

*Material* – 21 sagittas. Río del Padrón 3; Velerín Carretera 14; Velerín Conglomerates 2; Parque Antena 2.

*Remarks* – Mainly juvenile specimens of *Lobianchia* cf. *gemellarii* were found in the studied material, of which Pl. 11, fig. 17 fits best the illustrated extant specimens in Schwarzhans (2013b, pl. 15, figs 6-10) and those in Lin *et al.* (2017b, figs 5p-q (Tortonian), 6a-j (present-day)). The other specimens (Pl. 11, figs 14-16) seem a bit too elongated to fit the description of otoliths of the extant *L. gemellarii*. The latter always show a convex dorsal rim up to the postdorsal angle, which is situated above the mid-cauda (see ontogenetic series in Lin *et al*., 2017b, fig. 6), whereas the specimens depicted on Pl. 11, figs 14-16 have a regularly convex dorsal rim and the postdorsal angle is situated more posteriorly. Moreover, the posterior rim has a wide concavity behind the postdorsal angle in extant adult specimens, whereas it is regularly rounded in the specimens on Pl. 11, figs 14-16.

Subfamily Myctophinae (*sensu* Martin *et al*., 2018)
Genus *Hygophum* Bolin, 1939

***Hygophum* aff. *benoiti* (Cocco, 1838)**
Plate 12, figs 13-17

2013 *Hygophum benoiti* – Schwarzhans & Aguilera, pl 2, fig. 6

*Material* – 5 sagittas. Velerín Carretera 5.

*Description* – Among the small (0.6-1.3 mm) otoliths of *Hygophum* from Velerín Carretera, we encountered not only round to oval specimens with markedly or only dorsally crenulated rims (well known as *Hygophum hygomii* (Lütken, 1892), Pl. 12, figs 9-12), but also several slenderer specimens with a relatively high shape (OL:OH=0.95-0.98), smooth rims with a prominent postdorsal angle and a regularly rounded dorsal rim with a straight anterior part (Pl. 12, figs 13, 14, 16). The ventral side is anteriorly expanded, and the curvature of the rounded ventral rim is

**Plate 13**
Figure 1. ***Polymixia* cf. *lowei*** Günther, 1859, Velerín Antena Slope.
Figure 2. ***Zenion* cf. *hololepis*** (Goode & Bean, 1896), Velerín Sandy lens.
Figures 3-4. ***Bathygadus novus*** (Bassoli, 1906), Velerín Conglomerates (3), El Lobillo (4).
Figures 5-7. ***Coelorinchus arthaberoides*** (Bassoli, 1906), Velerín Carretera.
Figures 8-10. ***Coelorinchus caelorhincus*** (Risso, 1810), Velerín Carretera.
Figures 11-16. ***Coelorinchus mediterraneus*** Iwamoto & Ungaro, 2002, Velerín Carretera (11-14, 16), El Lobillo (15).

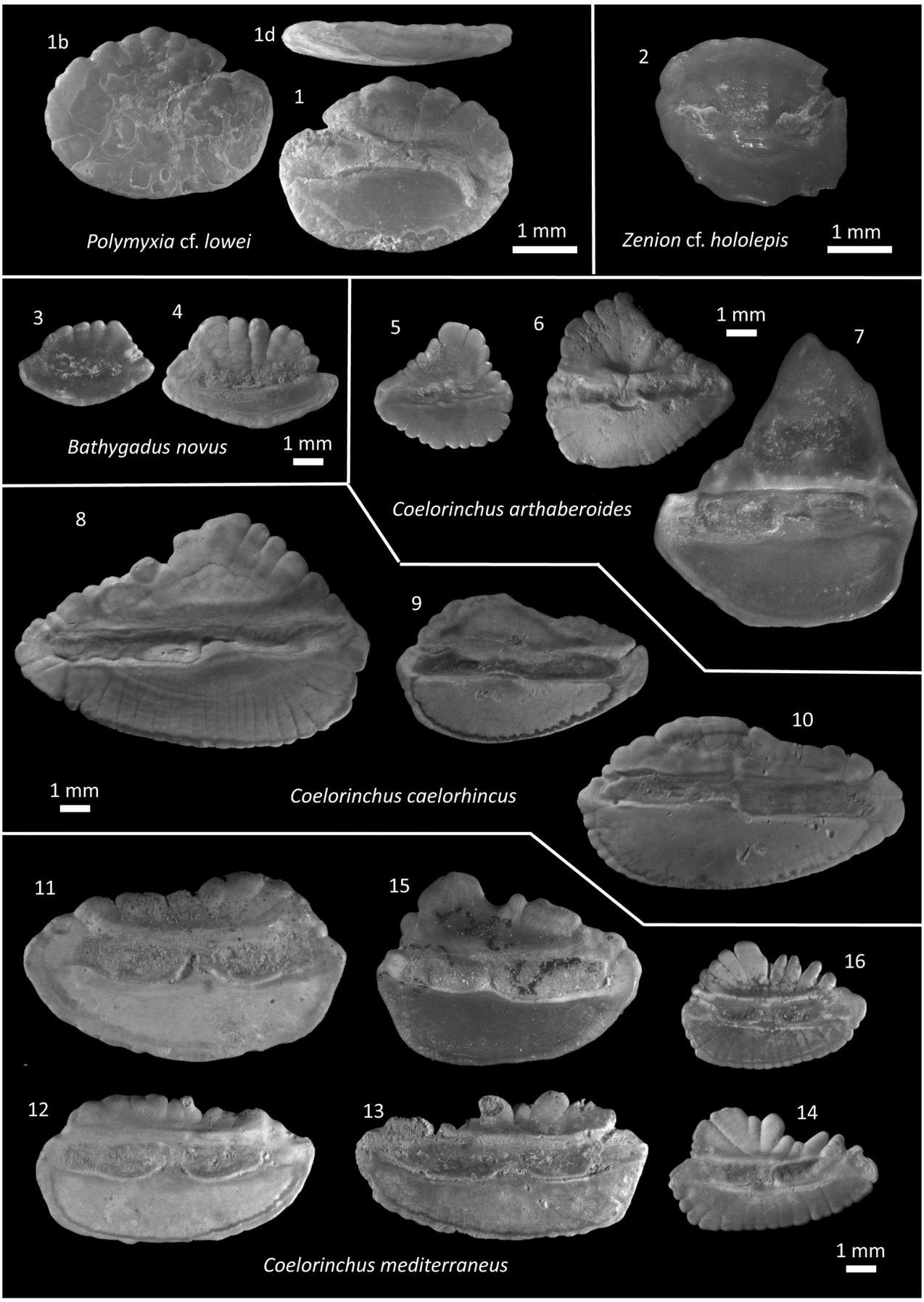
1b
1d
1
Polymyxia cf. lowei
1 mm
2
Zenion cf. hololepis
1 mm
3
4
Bathygadus novus
1 mm
5
6
1 mm
7
Coelorinchus arthaberoides
8
9
1 mm
Coelorinchus caelorhincus
10
11
15
16
12
13
14
Coelorinchus mediterraneus
1 mm

**Plate 13**

strong at the anterior side but much less along the posterior part. Their inner side is flat with an elevated ventral field between sulcus and ventral furrow. The anterior part of the ventral field can display several tiny furrows parallel to the ventral furrow. Two specimens are slightly longer (OL:OH=1.06-1.09) (Pl. 12, figs 15, 17).

*Remarks* – Our specimens resemble otoliths of the present-day N Atlantic and Mediterranean *H. benoiti* (Cocco, 1838) (see Schwarzhans & Aguilera, 2013, pl. 2, fig. 6; Campana, 2004, p. 107), which was relatively abundant in samples taken on the present-day floor of the Mediterranean Sea off southern Italy (Lin *et al*., 2017a, fig. 2). However, the Pliocene specimens lack the extended V-shaped ventral rim of the extant otoliths of *H. benoiti*.

*Distribution* – *Hygophum benoiti* has previously been recorded from the Piacenzian of the Rio Merli section in northern Italy (Girone, 2006, pl. 1, fig. 6d). Otoliths from the Late Miocene of the Dominican Republic were tentatively assigned to *H. benoiti* (Nolf & Stringer, 1992, pl. 10, fig. 32) but later to *Hygophum* sp. (Schwarzhans & Aguilera, 2013), which have a more expanded dorsal rim than those of *H. benoiti* and *H.* aff. *benoiti*.

Genus *Myctophum* Rafinesque, 1810

***Myctophum fitchi* Schwarzhans, 1979**
Plate 12, figs 19-25

1978 *Gymnoscopelus fitchi* – Schwarzhans, figs 30-31, 129.
1986 *Myctophum fitchi* – Schwarzhans, pl. 2, figs 25-27.
2017b *Myctophum fitchi* – Lin, Brzobohatý, Nolf & Girone, fig. 7 D.

*Material* – 1204 sagittas. Río del Padrón 395; El Lobillo 440; Velerín Carretera 131; Velerín Conglomerates 94; Velerín Quarry 2; Velerín Sandy Lens 27; Velerín Slope 5; Velerín Antena Hilltop 92; Parque Antena 18.

*Remarks* – *Myctophum fitchi* is encountered as small otoliths with a constant shape in Zanclean deposits. In the Velerín deposits its average size has markedly increased. Notably, in Velerín Conglomerates (Pl. 12, fig. 24) one finds many aberrant forms with variations (undulations), in particular on the dorsal rim. In specimens from Velerín Quarry (Pl. 12, fig. 22) and Velerín Carretera (Pl. 12, fig. 25) the height of the otoliths tends to increase.

Family Polymixiidae Bleeker, 1859
Genus *Polymixia* Lowe, 1836

***Polymixia lowei* Günther, 1859**
Plate 13, fig. 1

2004 *Polymixia lowei* – Campana, figs on p. 216.
2002 *Polymixia* cf. *lowei* – Nolf & Brzobohatý, pl. 6, fig 2.

*Material* – 1 sagitta. Velerín Antena Slope 1.

*Remarks* – One specimen was obtained from Velerín Antena Slope. It matches the characteristics of the extant *Polymixia lowei* (depicted by Schwarzhans 2010b, p. 67, fig. 154 and Campana, 2004, p. 216). In particular, the well-developed dorsal area and rim discriminate our otolith from those of other extant species of *Polymixia*. Our specimen is a juvenile otolith, whose ventral rim is more rounded and the postdorsal angle is hardly developed, just as in a similar-sized otolith of *Polymixia* cf. *lowei* from the Langhian marls of Saubrigues in France (Nolf & Brzobohatý, 2002, pl. 6, figs 2a-b).

Family Macrouridae Bonaparte, 1831
Genus *Coelorinchus* Giorna, 1809

***Coelorinchus arthaberoides* (Bassoli, 1906)**
Plate 13, figs 5-7

1906 *Ot. (Macrurus) Arthaberoides* – Bassoli, pl., 1 fig. 26.
2010a *Coelorinchus arthaberoides* – Schwarzhans, pl. 49, figs 10, 11.

*Material* – 138 sagittas. El Lobillo 2; Velerín Carretera 70; Velerín Conglomerates 2; Velerín Quarry 48; Velerín Sandy Lens 2; Velerín Antena Slope 5; Velerín Antena Hilltop 9.

*Remarks* – *Coelorinchus arthaberoides* is found in the Estepona region, particularly at Velerín Carretera and Velerín Quarry. *Coelorinchus arthaberoides* has been synonymised with *C. arthaberi* by Nolf (2013), but is recognised from the Pliocene of SE France by Schwarzhans (2010a, pl. 49, figs 10-11). This Pliocene species is similar to the Miocene *C. arthaberi* (Schubert, 1905), but – as pointed out by Schwarzhans (2010a, p. 137-138) – it differs from it in several aspects: a more pronounced and pointed predorsal projection, in particular in the larger specimens; large elongate colliculi; and the absence of an indentation behind the predorsal lobe that is present in most specimens of *C. arthaberi*. Following these criteria, *C. arthaberoides* is also present in the Tortonian of Italy (Nolf & Steurbaut, 1983, pl. 5, fig. 4; Lin *et al*., 2017b, fig. 7Q).

***Coelorinchus caelorhincus* (Risso, 1810)**
Plate 13, figs 8-10

2008 *Coelorinchus caelorhincus* – Tuset *et al*., fig. 24 C1-C3 (present-day otoliths).

*Material* – 285 sagittas. Río del Padrón 19; El Lobillo 22; Velerín Carretera 145; Velerín Conglomerates 54; Velerín Quarry 8; Velerín Sandy Lens 9; Velerín Antena Slope 7; Velerín Antena Hilltop 16; Parque Antena 5.

*Remarks* – *Coelorinchus caelorhincus* otoliths are de-

scribed in the literature, both as a present-day species and from Miocene and Pliocene deposits. It is encountered in the Pliocene material with the elongate shape of large specimens (Pl 13, figs 9-10) as well as a more triangular form in smaller specimens (Pl. 13, fig. 8), similar as observed in otoliths of extant *C. caelorhincus*. It has an elongated narrow sulcus divided in ostium and a longer cauda, each fully covered by a long and narrow colliculum.

***Coelorinchus mediterraneus* Iwamoto & Ungaro, 2002**
Plate 13, figs 11-16

1986 *Coelorinchus* sp. – Schwarzhans, pl. 5 fig. 63.
2008 *Coelorinchus mediterraneus* – Tuset *et al*., figs 25 A1-A3.

*Material* – 44 sagittas. El Lobillo 1; Velerín Carretera 31; Velerín Conglomerates 7; Velerín Sandy Lens 3; Velerín Quarry 1; Velerín Antena Slope 1.

*Remarks* – *Coelorinchus mediterraneus* represents a third species of *Coelorinchus*, in particular at Velerín Carretera. The extant species was identified in 2002 from the western and central part of the Mediterranean Sea (Iwamoto & Ungaro, 2002). Specific information on their sagittal otoliths was provided by Nolf (personal communication), Tuset *et al*. (2008) and Lombarte *et al.* (2006). In comparison with *C. caelorhincus* the Pliocene *C. mediterraneus* displays a wider sulcus, which is divided in an ostium and a cauda of more equal size, covered by oval colliculi. Furthermore, the posterior end of the convex ventral rim bends strongly upward to the rounded posterior rim making it less pointed than that of *C. caelorhinchus*. One specimen from El Lobillo displays a profound predorsal projection followed by a notch that separates the predorsal projection from the posterior part of the dorsal rim, which probably reflects variability within the species (Pl. 13, fig. 15). We are not aware of any earlier recognition of *C. mediterraneus* in the Pliocene fossil record. However, a single specimen indicated as *Coelorinchus* sp. from Le Puget (Schwarzhans, 1986, pl. 5, fig. 63) can be attributed to the same species.

Genus *Coryphaenoides* Gunnerus, 1765

***Coryphaenoides?* sp. 1**
Plate 14, fig. 3

*Material* – 1 sagitta. Velerín Quarry 1.

*Remarks* – One thin and oval shaped gadiform sagitta (Pl. 12, fig. 19) was discovered at Velerín Quarry. The inner surface is flat; the outer surface is flat with lobes, radiating from the central axis. The dorsal and ventral rims are ornamented with small lobes. The ostium and cauda are of equal size, closely opposed, and the most central parts are covered with oval colliculi. It is tentatively identified as a macrourid species, possibly belonging to the genus *Coryphaenoides*.

***Coryphaenoides?* sp. 2**
Plate 14, fig. 4

*Material* – 1 sagitta. Velerín Carretera 1.

*Remarks* – This single macrourid sagitta shows some resemblance with otoliths of *Lyconus brachycolus* Holt & Byrne, 1906 (depicted in Schwarzhans, 2013a, pl. 16 fig. 8), but in our specimen the posterior rim is slightly pointed, the rims are finer lobed and the inner surface appears less flat than in *L. brachycolus*. It probably represents a juvenile species of *Coryphaenoides*, but additional material is needed for further identification.

***Coryphaenoides sp.* 3**
Plate 14, fig. 10

*Material* – 1 sagitta. Velerín Carretera 1.

*Remarks* – The inner face of this single specimen is almost flat, while the outer face is bulging with many lobes. The sulcus has two closely aligned oval colliculi which cover part of the ostium and cauda, respectively. The otolith represents a juvenile macrourid otolith probably of the genus *Coryphaenoides*, but due to the lack of comparative juvenile material, we could not reach a more specific identification.

Family Moridae Moreau, 1881
Genus *Physiculus* Kaup, 1858

***Physiculus huloti* Poll, 1953**
Plate 14, figs 11-12

1979 *Physiculus huloti* – Steurbaut, pl. 6, figs 1-2 (present-day).
1979 *Physiculus* aff. *huloti* – Steurbaut, pl. 6, figs 3-5.
1980 *Physiculus* aff. *huloti* – Nolf & Martinell, pl. 3, figs 16-17.
1986 *Physiculus* aff. *huloti* – Schwarzhans, pl. 5, figs 57-58.
1994 *Physiculus* aff. *huloti* – Nolf & Cavallo, pl. 4, fig. 8.
1998 *Physiculus* aff. *huloti* – Nolf, Mané & Lopez, pl. 4, figs 8-9.
2013a *Physiculus huloti* – Schwarzhans, pl. 7, figs 1-4 (present-day).
2019c *Physiculus huloti* – Schwarzhans, pl. 4, fig. 11 (present-day).

*Material* – 85 sagittas (many broken). Río del Padrón 4; El Lobillo 2; Velerín Carretera 37; Velerín Conglomerates 6; Velerín Quarry 26; Velerín Antena Slope 8; Velerín Antena Hilltop 1; Parque Antena 1.

*Description* – Adult specimens (Pl. 14, figs 7-8) differ from juvenile ones as age affects the shape of morid otoliths. The general shape is a bi-lobed spindle with pointed anterior and posterior rims (OL: 4.8-5.0 mm; OH: 1.6-1.8 mm; OL:OH=2.8-3.0). The inner side is flat. The ostium is small and covered by an oval colliculum. The cauda is 2.3-2.7 times as long as the ostium. The cauda is narrow at the junction with the ostium, but strongly widens so that its thick crista superior runs towards halfway (50-60%) the dorsal rim. The crista inferior runs as a thick crest from the posterior part of the ostium to close to the posterior rim. In some of the otoliths this crest consists of two parallel bars suggesting that it represents a merger of the crista inferior and the original ventral rim that has folded over the lower part of the inner side of the otolith. The caudal colliculum lies as a tiny, curved string in the upper part of the cauda and reaches the postdorsal rim just before or on the pointed posterior end of the otolith. In the lower part of the cauda a similar slightly more wrinkling string runs over the inferior part of the cauda along to the crista inferior. The outer side is inflated (Pl. 14, fig. 11b) and consists in adult specimens of two major lobes of which the first one joins the crista superior at the inner side, while the second one corresponds with the posterior part of the dorsal rim until the postdorsal depression that accentuates the pointed posterior end of the otolith. In dorsal view (Pl. 14, fig. 11d) the otoliths show a smooth bulging anterior part and a similarly smooth shoulder at the posterior half, from which a stretch (lower part in dorsal view) is damaged by a curved cut. Juvenile specimens are more elongate and often display several lobes on the outside with one dominant (corresponding to the large preventral one in adult specimens). The posterior part and inner surface are usually damaged in the juvenile and part of the adult specimens. Notwithstanding, all fit in an ontogenetic series of one species.

*Remarks* – *Physiculus huloti* is an extant tropical species from West African waters (iconography in Schwarzhans, 2013a, pl. 7, figs 1-4). Our data confirm its presence in Mediterranean Pliocene deposits, from where it has been reported earlier as *Physiculus* aff. *huloti* (Nolf & Martinell, 1980; Schwarzhans, 1986; Nolf & Cavallo, 1994).

Genus *Laemonema* Günter, 1962

***Laemonema* sp.**
Plate 14, figs 13-14

2006 *Laemonema* sp. A – Girone, pl. 2, fig 10.

*Material* – 2 sagittas. Velerín Carretera 1; Velerín Conglomerates 1.

*Description* – A second morid species is represented by two specimens of different sizes (OL: 4.42-4.96 mm; OH: 1.44-1.92 mm; OL:OH =2.6-3.1). The ostium is short and oval. The cauda runs in a thin almost straight line from the ostium towards the superior part of the posterior end. The cauda is 3.3-3.5 times as long as the ostium. The inferior part of the cauda is formed by the parallel-running crista inferior, which in turn is flanked by the slightly bent ventral rim. A prominent ridge of large lobes on the outside extends beyond the ventral rim, albeit less prominent in the more adult specimen (Girone, 2006, pl. 2, fig. 10). The crista superior is shorter and runs from the posterior part of the ostium obliquely to just after the middle of the dorsal rim. The dorsal view (Pl. 14, figs 13d, 14d) shows the prominent presence of lobes on the anterior and middle parts of the otoliths and the general shape of *Laemonema* otoliths. The lower posterior part is cut away (in ventral view) by a straight cut.

*Remarks* – There is a high morphological similarity between one of these otoliths (Pl. 14, fig. 13) and otoliths of the extant species *Laemonema yuvto* Parin & Sazonov, 1990, recently depicted by Schwarzhans (2019c). However, *L. yuvto* is a SE Pacific species with no known presence in the Atlantic Ocean or Mediterranean Sea and the similarity may be due to the juvenile nature of our specimen. Three extant species of the genus *Laemonema* are known from the eastern Central and North Atlantic: *L. laureysi* Poll, 1953, *L. robustum* Johnston, 1862 and *L. yarrelli* Lowe, 1841 (Whitehead *et al*., 1984; Quéro *et al*., 1990; Carneiro *et al*., 2014), but their otoliths are different (see Lombarte *et al*., 2006 and Schwarzhans, 2019c for iconography). Furthermore, *Laemonema* sp. A was reported from the Piacenzian of Italy (Girone, 2006) and the Mediterranean Pleistocene (Girone *et al*., 2006). Our specimens are less thickset, but may represent less adult specimens of the same or closely related species (compare Pl. 14, fig. 14). As

**Plate 14**

Figures 1-2. ***Coryphaenoides sicilianus*** Schwarzhans, 1986, Velerín Carretera.
Figure 3. ***Coryphaenoides***? **sp. 1**, Velerín Quarry.
Figure 4. ***Coryphaenoides***? **sp. 2**, Velerín Carretera.
Figures 5-6. ***Nezumia ornata*** Bassoli, 1906, Velerín Quarry.
Figures 7-8. ***Nezumia* aff. *sclerorhynchus*** (Risso, 1810), Velerín Carretera.
Figure 9. ***Trachyrincus scabrus*** (Rafinesque, 1910), Velerín Conglomerates.
Figure 10. ***Coryphaenoides* sp. 3**, Velerín Carretera.
Figures 11-12. ***Physiculus huloti*** Poll, 1953, Velerín Conglomerates.
Figures 13-14. ***Laemonema* sp.,** Velerín Carretera (13), Velerín Conglomerates (14).
Figure 15. ***Gaidropsarus mediterraneus*** (Linnaeus, 1758), Río del Padrón.

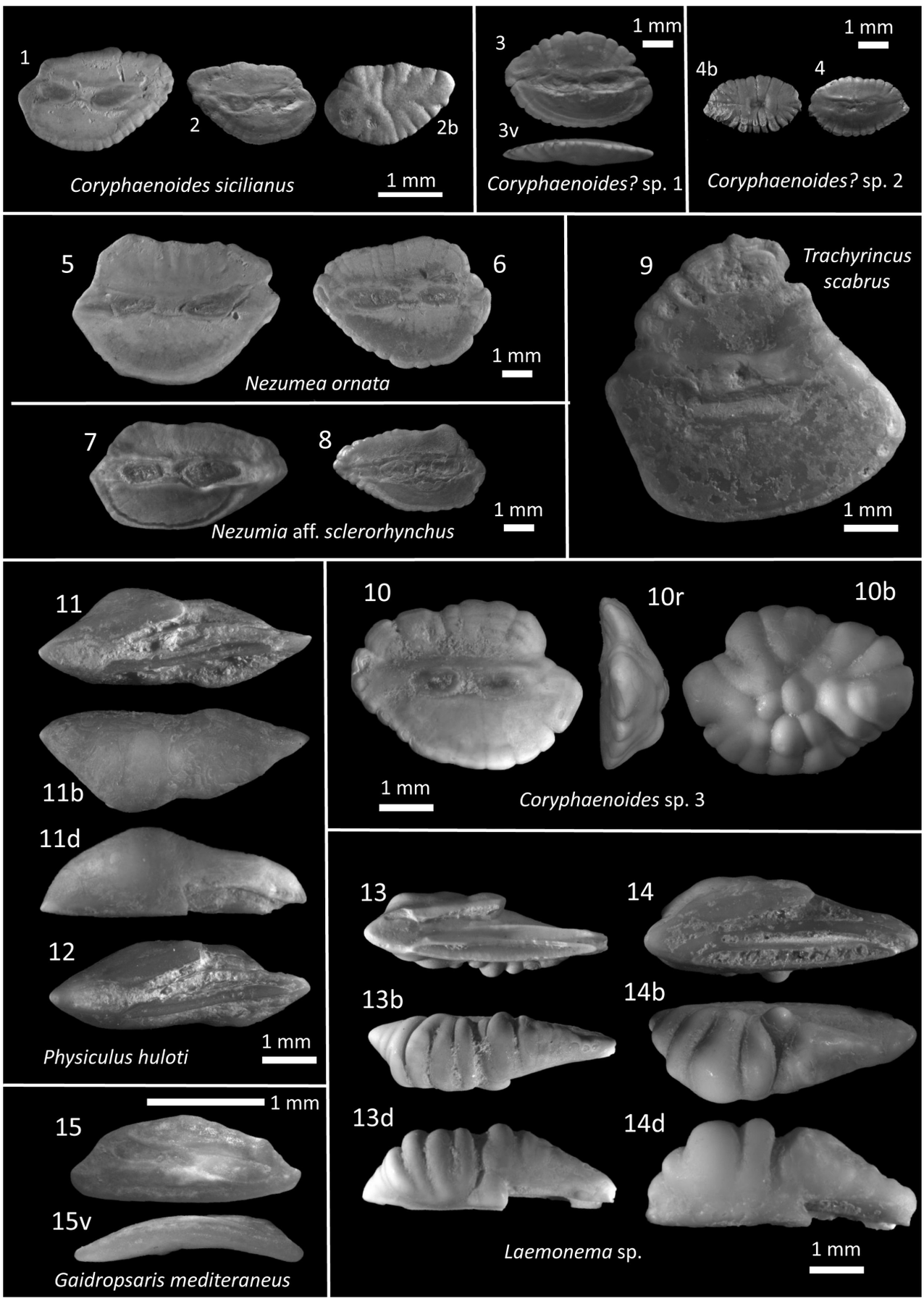
1
2
2b
Coryphaenoides sicilianus
1 mm
3
3v
1 mm
Coryphaenoides? sp. 1
4b
4
1 mm
Coryphaenoides? sp. 2
5
6
1 mm
Nezumea ornata
7
8
1 mm
Nezumia aff. sclerorhynchus
9
Trachyrincus scabrus
1 mm
11
11b
11d
12
1 mm
Physiculus huloti
10
10r
10b
1 mm
Coryphaenoides sp. 3
13
14
13b
14b
13d
14d
Laemonema sp.
1 mm
1 mm
15
15v
Gaidropsaris mediteraneus

**Plate 14**

only 2 specimens are available and uncertainties remain, we have left this species in open nomenclature.

Family Phycidae Swainson, 1838
Genus *Phycis* Walbaum, 1792

***Phycis blennoides* (Brünnich, 1768)**
Plate 15, figs 9-10

2008 *Phycis blennoides* – Tuset *et al*., figs 30 B1-B3 (present-day otoliths).

*Material* – 106 sagittas. Río del Padrón 4; El Lobillo 4; Velerín Carretera 38; Velerín Conglomerates 25; Velerín Quarry 24; Velerín Sandy Lens 2; Velerín Antena Slope 6; Velerín Antena Hilltop 2; Parque Antena 1.

*Remarks* – Many small and medium-sized sagittas match the characteristics of otoliths of the extant *Phycis blennoides* (Brünnich, 1768): slender and elongated, with a crenulated, almost straight ventral rim anteriorly.

***Phycis phycis* (Linnaeus, 1766)**
Plate 15, figs 8,9

2008 *Phycis phycis* (present-day otoliths) – Tuset *et al*., figs 30 C1-C3.

*Material* – 9 sagittas. El Lobillo 1; Velerín Carretera 3; Velerín Conglomerates 2; Velerín Quarry 3.

*Remarks* – Nine large sagittas of this species were found, characterised by a wide convex anteroventral portion as found in the European Miocene *P. musicki* Cohen & Lavenberg, 1984 and the extant *P. phycis* (Linnaeus, 1766). Tuset *et al*. (2008) and Lombarte *et al*. (2006) illustrated otoliths of *P. phycis* with a broad lobation ('dentition') on the anterior part of the ventral rim, which is absent in *P. musicki*. This lobular structure was visbible in two specimens – from El Lobillo and Velerín Carretera –, while it was absent in the other ones (compare Pl. 15, fig. 7v with fig 8v). However, this variation also exists in extant specimens. We observed otoliths of an present-day *P. phycis* from Madeira, in which the lobes were largely fused. Overall, the large Pliocene specimens of *Phycis* cannot be discriminated from the extant *P. phycis* and, therefore, we place them in the same species.

Family Gadidae Rafinesque, 1810
Genus *Gadiculus* Guichenot, 1850

***Gadiculus argenteus* Guichenot, 1850**
Plate 15, figs 11-13

2008 *Gadiculus argenteus* – Tuset *et al*., figs 30 D1-D3 (present-day otoliths).

*Material* – 4327 sagittas. El Lobillo 3; Velerín Carretera 1700; Velerín Conglomerates 237; Velerín Quarry 1250; Velerín Sandy Lens 120; Velerín Antena Slope 606; Velerín Antena Hilltop 406; Parque Antena 5.

*Remarks* – In very adult sagittas (less than 1%) the anterior and posterior rims display an indentation (Pl. 15, fig. 13), as is common in *G. thori* Schmidt, 1913. However, Gaemers & Poulsen (2017) reported that some old specimens of *G. argenteus* can rarely also show this feature. *Gadiculus argenteus* is very common in the Velerín outcrops, but rare at the Estepona sites. Only four specimens were found at El Lobillo and none in the material from Río del Padrón. The relative infrequence in the Zanclean deposits in the study area contrasts with its regular presence in the Zanclean deposits from Le Puget, SE France (Nolf & Cappetta, 1989) and Sicily (Schwarzhans, 1979). This may be due to shallower water conditions and/or the vicinity of a rocky environment in the Estepona basin.

***Paratrisopterus glaber* Schwarzhans, 2010**
Plate 15, figs 14-15

2006 *Gadiculus labiatus* – Girone, pl. 2, fig. 9a-e.
2010a *Paratrisopterus glaber* – Schwarzhans, pl. 30, figs 12-15.

*Material* – 80 sagittas. El Lobillo 3; Velerín Carretera 52; Velerín Conglomerates 2; Velerín Quarry 22; Velerín Antena Slope 1.

*Remarks* – *Paratrisopterus glaber* has an outwardly squeezed preventral rim and a reduced length, distin-

**Plate 15**
Figure 1. **Gaidropsarinae sp.,** Velerín Conglomerates.
Figures 2-3. ***Bregmaceros albyi*** (Sauvage, 1880), Velerín Quarry.
Figure 4. ***Merluccius merluccius*** (Linnaeus, 1758), Velerín Carretera.
Figure 5. ***Micromesistius poutassou*** (Risso, 1826), Velerín Quarry.
Figure 6. ***Trisopterus minutus*** (Linnaeus, 1758), El Lobillo.
Figures 7-8. ***Phycis phycis*** (Linnaeus, 1766), Velerín Quarry (7), El Lobillo (8).
Figures 9-10. ***Phycis blennoides*** (Brünnich, 1768), Velerín Quarry.
Figures 11-13. ***Gadiculus argenteus*** Guichenot, 1850, Velerín Quarry. 13. Large specimen with notches.
Figures 14-15. ***Paratrisopterus glaber*** Schwarzhans, 2010, Velerín Quarry.
Figures 16-18. ***Paratrisopterus labiatus*** (Schubert, 1905 sensu Schwarzhans, 2010), El Lobillo.

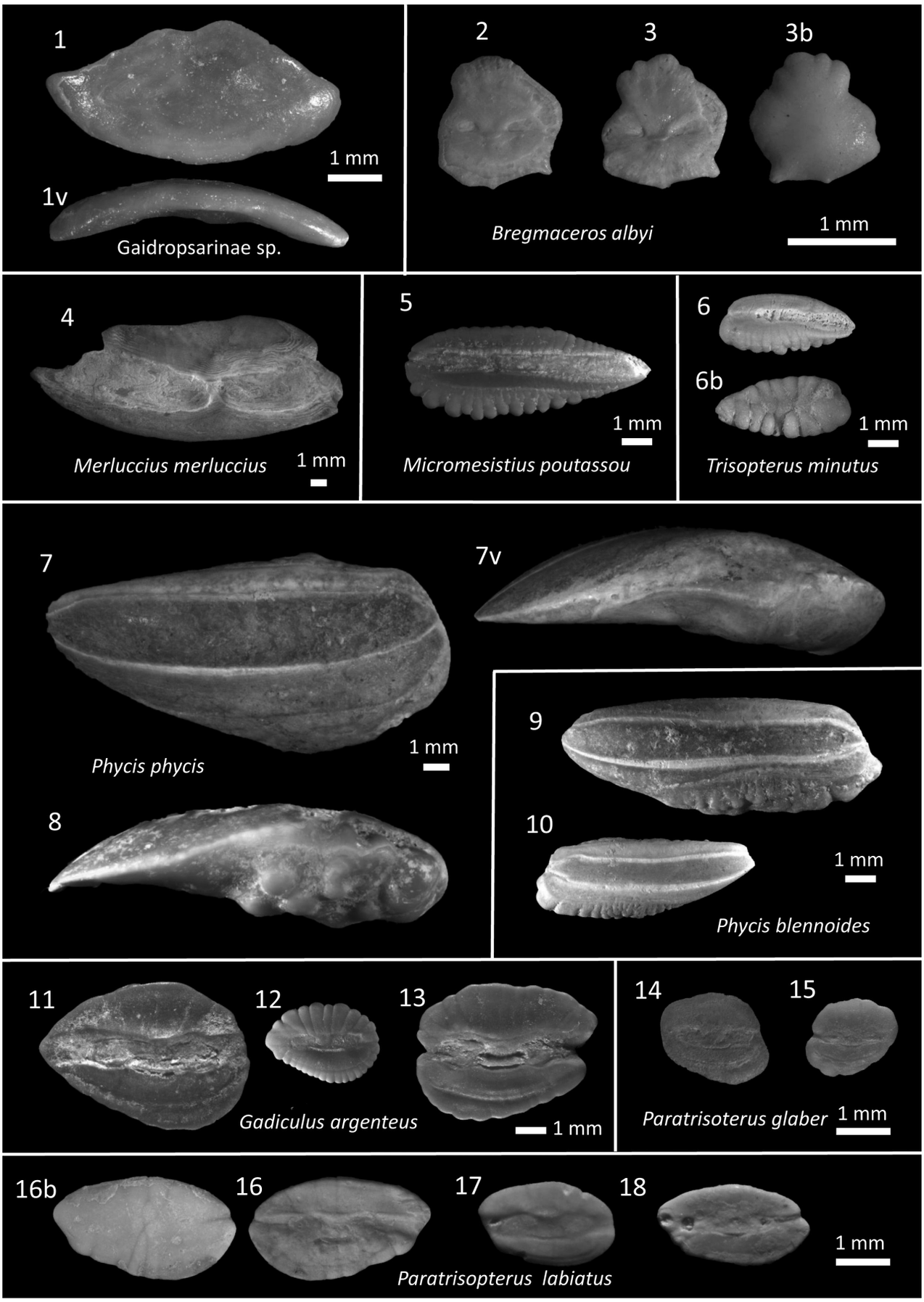
1
1 mm
1v
Gaidropsarinae sp.
2
3
3b
Bregmaceros albyi
1 mm
4
Merluccius merluccius
1 mm
5
1 mm
Micromesistius poutassou
6
6b
1 mm
Trisopterus minutus
7
7v
Phycis phycis
1 mm
8
9
10
1 mm
Phycis blennoides
11
12
13
Gadiculus argenteus
1 mm
14
15
Paratrisoterus glaber
1 mm
16b
16
17
18
1 mm
Paratrisopterus labiatus

**Plate 15**

guishing it from *P. labiatus* (Schubert, 1905). There is a variation in the posterior rim, which can be more convex or somewhat truncated. According to Schwarzhans (2010a) *P. glaber* and *P. labiatus* are two different species that both belong in the genus *Paratrisopterus*, which was considered a synonym of *Gadiculus* by Prokofiev (2004). Later comparison of skeletal remains added additional evidence for a generic difference between *G. argenteus* and *P. labiatus* (Schwarzhans *et al*., 2017). *Paratrisopterus* is common in Late Miocene to Pleistocene deposits of the North Sea Basin and the Mediterranean (see Schwarzhans, 2010a). Nolf (2013) considered *P. glaber* as synonym of *P. labiatus* and it was as such also mentioned from the Plio-Pleistocene of Italy (Girone 2006, pl. 2, fig. 9; Girone *et al.* 2006, fig. 3, 4). However, our finding of *P. labiatus* (Pl. 15, figs 16-18) and *P. glaber* (Pl. 15, figs 14-15) in two different environments at El Lobillo (Zanclean, shallow sea, close to reef) and Velerín Carretera (Piacenzian, large content of deep-sea species) further strengthens the occurrence of two distinct species.

Family Anomalopidae Gill, 1889
Genus *Kryptophanaron* Silvester & Fowler, 1926

***Kryptophanaron nolfi* nov. sp.**
Plate 16, figs 1-3

1983 *Kryptophaneron* sp. – Nolf & Steurbaut: p. 178, pl. 6, fig. 15 (Tortonian).
1989 *Kryptophaneron* sp. – Nolf & Cappetta: p. 221, pl. 14, figs 6 (Tortonian) and 7 (Zanclean).
1995 *Kryptophaneron* sp. – Nolf & Cavallo: table 1, pl. 6, fig. 2.

*Holotype* – RGM.1390535, Velerín Quarry, (Pl. 16, fig. 1).

*Paratypes* – 2 sagittas: RGM.1390536, RGM.1390537. Velerín Quarry (1); Velerín Conglomerates (1).

*Locus typicus* – Velerín Quarry, close to Velerín Antena, along Camino Nicolas, Velerín, Estepona, province of Málaga, Spain.

*Stratum typicum* – Middle Pliocene, Piacenzian, fossiliferous medium- to fine-grained sands.

*Etymology* – Named after Dirk Nolf, who recognised this extinct species as *Kryptophanaron* sp. (Nolf & Steurbaut, 1983; Nolf & Cavallo, 1994).

*Diagnosis* – Rhomboid-shaped outline with blunt but prominent posterior and anterior angles. Mid-ventral and postero-dorsal extensions. Outer face flat, slightly concave at anterior side. Inner face convex and with thickening between the sulcus and ventral furrow. Broad, median sulcus across almost entire length of otolith and divided in very large obliquely oriented ostium and wide cauda (but about half of the width of the ostium), both of equal length.

*Description* – The otoliths resemble a rectangle with rounded angles, turned at 40-45°. The length is slightly larger than the height (OL:OH=1.12-1.18). The dorsal rim displays a middorsal and a postdorsal angle, and connects to the ventral rim at a pointed posterior extension. The dorsal rim of the holotype (Pl. 16, fig. 1) is largely convex with a slight concavity before the middorsal angle and a straight part behind the postdorsal angle. In the two paratypes (Pl. 16, figs 2-3) it consists of straight or slightly concave parts, but it is particularly concave between the postdorsal angle and the posterior end.
The pre- and mid-ventral rims each represent roughly a quarter of the ventral rim, while the straight posterior part forms almost half of it. The anterior and posterior parts of the ventral rim are almost straight and form an angle close to 90°, but are separated by a central part that can develop as a blunt crest-like extension (Pl. 16, figs 1-2).
The median sulcus is divided in a very large ostium and a less large but still wide cauda of comparable length. The ostium is directed upwards in anterior direction and opens onto the anterior rim. The cauda is directed upwards in posterior direction and is connected to the posterior rim, just below the postventral angle. The crista superior makes a single blunt angle of about 30° at the ostium-cauda transition. The crista inferior is only distinct along the anterior part of the cauda, ending mid-way under the crista superior. Above the crista superior is a large dorsal depression. The ventral portion of the inner face is bulged down to a regularly curved, but weak, ventral furrow. This feature renders the inner face convex in ventral view. The outer face is concave but thickens at the anterior tip and the middle part of the otolith, which form a ridge on the outside towards the outward bent posterior point.

*Discussion* – There are differences in the development of the dorsal rim in the specimens, which may reflect a degree of variation, as the otoliths are similar in size. Although it is likely that the otolith of Velerín Conglomerates (Pl. 16, fig. 3) has been polished during diagenesis, the annual rings on the outside suggest that no major changes in overall contour have occurred.
The family of Anomalopidae consists of several genera, each with one or two extant species. Nolf & Steurbaut (1983) reported on *Kryptophaneron* sp. from the Tortonian of Montegibbio, northern Italy, and demonstrated a

**Plate 16**
Figure 1. ***Kryptophanaron nolfi* nov. sp.,** holotype, Velerín Quarry.
Figures 2-3. ***Kryptophanaron nolfi* nov. sp.,** paratypes, Velerín Quarry (2), Velerín Conglomerates (3).
Figures 4. ***Hoplosthetus pisanus*** Koken, 1891, Velerín Carretera.
Figures 5-7. ***Hoplosthetus lawleyi*** Koken, 1891, Velerín Carretera (5,7), El Lobillo (6).

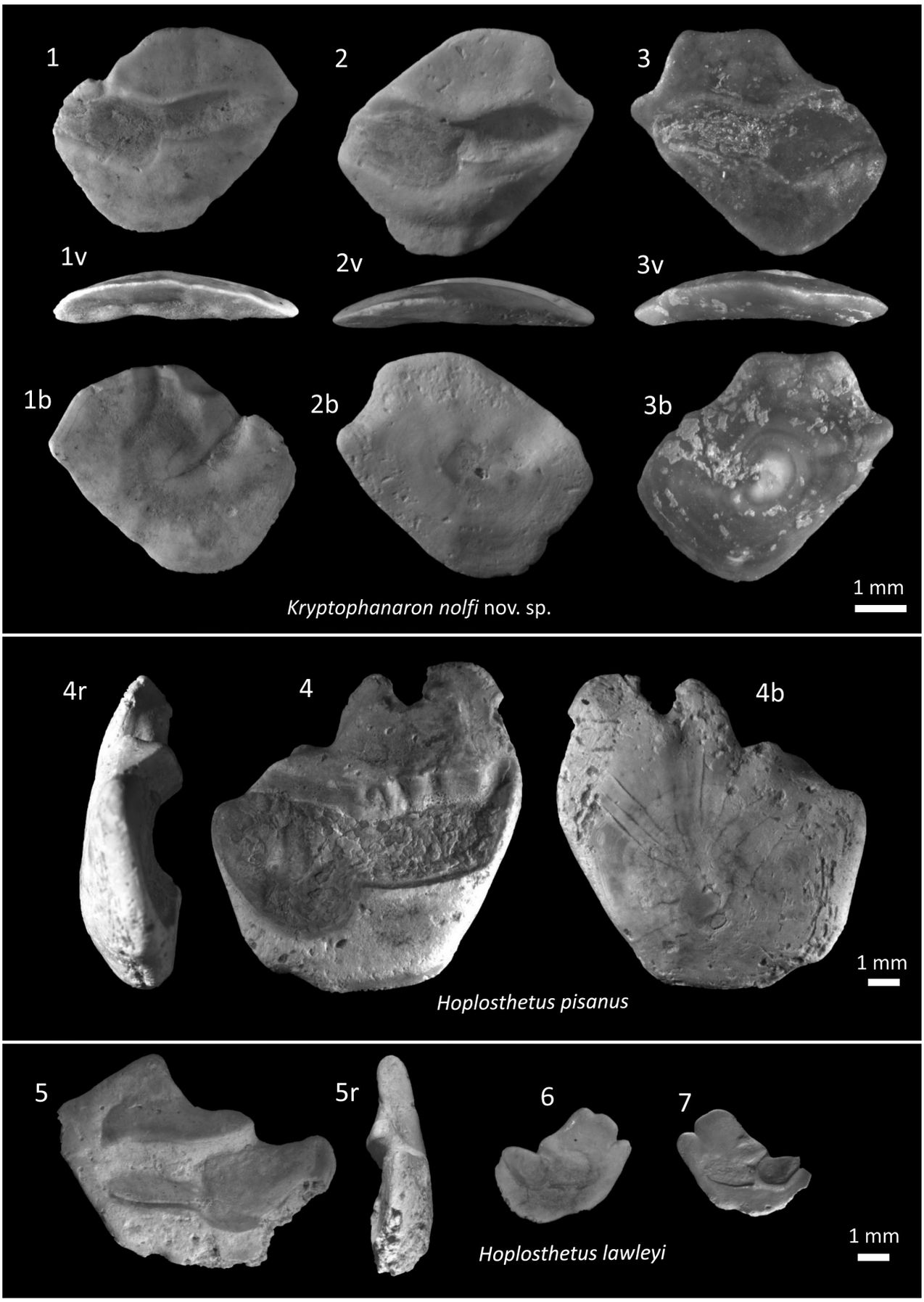
1
2
3
1v
2v
3v
1b
2b
3b
1 mm
*Kryptophanaron nolfi* nov. sp.
4r
4
4b
1 mm
*Hoplosthetus pisanus*
5
5r
6
7
1 mm
*Hoplosthetus lawleyi*

**Plate 16**

resemblance to the Caribbean *Kryptophanaron alfredi* Silvester & Fowler, 1926 (otolith depicted in Nolf, 1985, fig. 54h). Later, Nolf & Cappetta (1989) confirmed the allocation to *Kryptophaneron*, when reporting one specimen from the lower Pliocene (Zanclean) of the French Côte d'Azur. These otoliths have an identical shape as our specimen in Pl. 16, fig. 1. Later, otoliths of several other extant Anomalopidae have been documented: *Anamalops katoptron* Bleeker, 1856 (in Lin & Chang, 2012); *Photoblephaneron steinitzi* Abe & Hanada 1973 (in Schwarzhans, 2010b, fig. 104); *Photoblephaneron palpebratum* Boddaert, 1781 (in Rivaton & Bourret, 1999); *Protoblephaneron mccoskeri* Ho & Johnson 2012 (in Lin & Chang, 2012); *Phthanophaneron harveyi* Rosenblatt & Johnson, 1976 (in López-Fuerte *et al*., 2018).
Of all these, our otoliths match best those of *Kryptophanaron alfredi* Silvester & Fowler, 1926. However, the figured specimen of *Kryptophanaron alfredi* differs from the Pliocene specimens by (1) a more compressed dorsal portion in particular posteriorly, while the dorsal portion is more developed in *K. nolfi*; (2) the absence of the postero-dorsal and mid-ventral extensions; and (3) a smooth ventral part of the otolith without the thickened ventral field and ventral furrow. The three specimens that we encountered in the Piacenzian deposits of the Velerín Hill (Velerín Quarry and Velerín Conglomerates) are very similar to the three earlier western Mediterranean finds of *Kryptophanaron* sp. of Pliocene (Nolf & Cappetta, 1989; Nolf & Cavallo, 1994) and Tortonian age (Nolf & Steurbaut, 1983), which probably belong to the same species. Further anomalopid otoliths, *e.g*., from *Protoblephaneron rosenblatti* Baldwin, Johnson & Paxton, 1997, *Parmops echinatus* Johnson, Seeto & Rosenblatt, 2001 and *Parmops coruscans* Rosenblatt & Johnson, 1991 are not known. They all represent Pacific species, which are unlikely to have occurred in the Mediterranean Pliocene.

Genus *Gephyroberyx* Boulenger, 1902

***Gephyroberyx darwinii* (Johnson, 1866)**
Plate 17, figs 7-10

1979 *Gephyroberyx darwinii* – Steurbaut, pl. 6, figs 17-25.

*Material* – 39 sagittas. Velerín Quarry 39.

*Remarks* – The extant *Gephyroberyx darwinii* is a cosmopolitan species including the subtropical Eastern Atlantic waters from Madeira and Canary Islands to South Africa. There are two records of single individuals from the Mediterranean Sea (Andaloro *et al*., 2012). The present finding demonstrates an earlier invasion into the Mediterranean Sea and points to a relatively high frequency of this species during the deposition of the Velerín Quarry sediment. The species has also been encountered in the Miocene of SW France (Steurbaut, 1979) and the North Sea Basin (Hoedemakers, 1997; Schwarzhans, 2010a).

Family Melamphaidae Gill, 1893
Genus *Scopelogadus* Vaillant, 1888

***Scopelogadus beanii* (Günther, 1887)**
Plate 17, figs 12-16

1980 *Scopelogadus beani* – Schwarzhans, p 101, figs 323-324.
2006 *Scopelogadus* aff. *beanii* – Girone, Nolf & Cappetta, figs 7.12a-12b.

*Material* – 14 sagittas. Río del Padrón 1; El Lobillo 2; Velerín Carretera 10; Velerín Quarry 1.

*Remarks* – Very small otoliths mainly from Velerín Carretera display the features of those of the extant and circumtropical *S. beanii* and *S. mizolepis* (Günther, 1878). However, the otoliths have a reduced (rather simple) shape and the specimens encountered provide a continuum between the 'typical' shapes of the juvenile otoliths of these species. Otoliths of small *S. beanii* and *S. mizolepis* show the same features as our specimens (figured in Schwarzhans, 1980, figs 323-324 and 326-327; Lombarte *et al*., 2006; Rivaton & Bourret, 1999, pl. 141, figs 11-16) with a slight variation in the outline. Otoliths of *S. beanii* have been described from the Pleistocene and other Mediterranean deposits (Girone *et al*., 2006, pl. 7.12) and we therefore tentatively place our otoliths in the same species.

Family Ophidiidae Rafinesque, 1810
Genus *Ophidion* Linnaeus, 1758

Otoliths of *Ophidion* are regularly encountered in Pliocene Mediterranean deposits and commonly reported as *Ophidion* cf. *rochei* or *Ophidion barbatum* (Nolf & Cappetta, 1989; Nolf & Girone, 2006). Four extant species of the genus *Ophidion* are known from the Mediterranean / eastern Atlantic, of which *O. barbatum* (Pl. 18, figs 2-3) and *O. rochei* (Pl. 18, figs 6-7) are

**Plate 17**
Figures 1-6. ***Hoplosthetus praemediterraneus*** Schubert, 1905, Velerín Quarry (1, 4, 6), Río del Padrón (2, 3), Velerín Sandy Lens (5).
Figures 7-10. ***Gephyroberyx darwinii*** (Johnson, 1866), Velerín Quarry.
Figure 11. ***Melamphaes typhlops*** Lowe, 1843, Velerín Quarry.
Figures 12-16. ***Scopelogadus beanii*** (Günther, 1887), Velerín Carretera (12-14,16), El Lobillo (15).
Figures 17-18. ***Echiodon dentatus*** (Cuvier, 1829), Velerín Antena Slope.

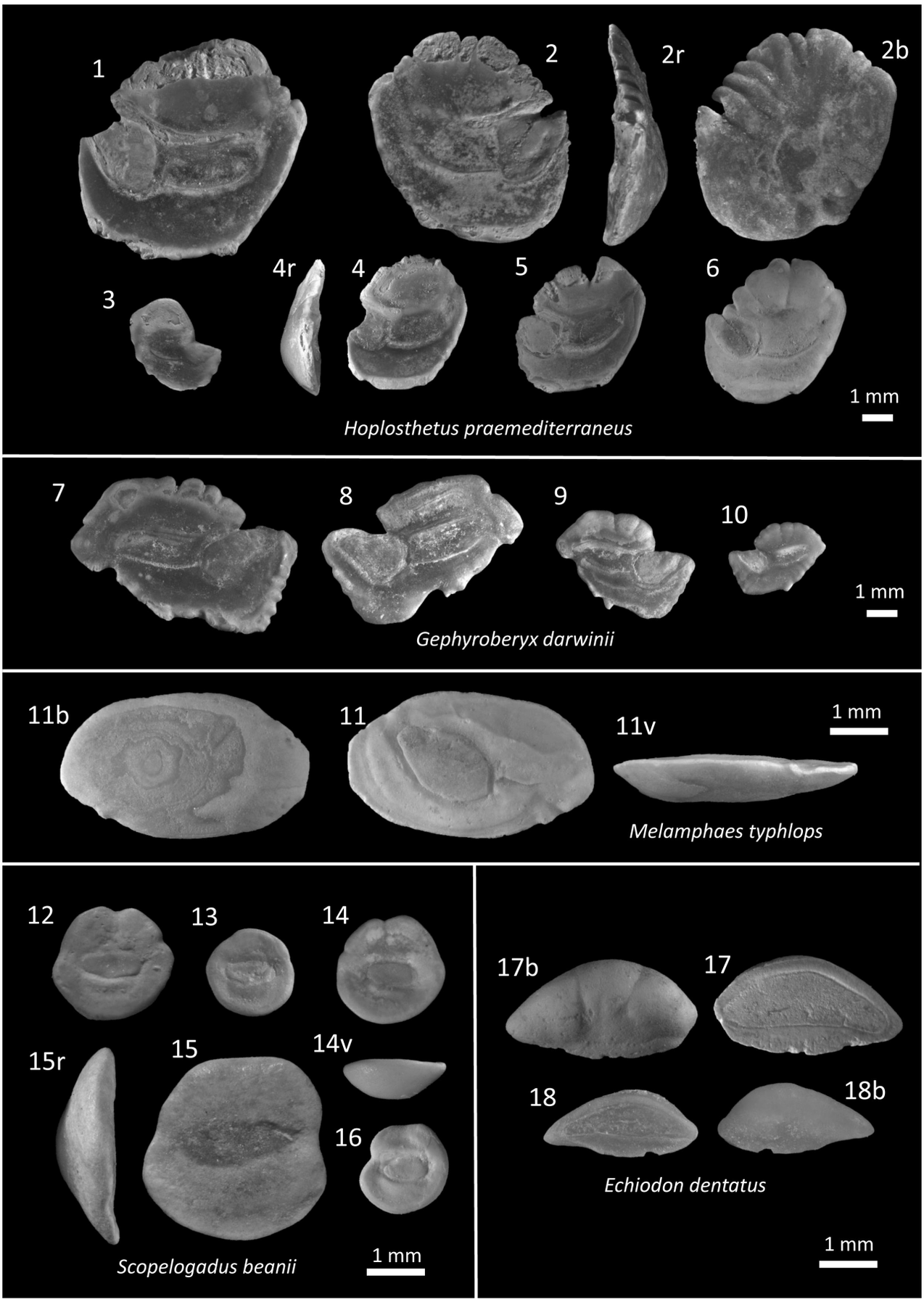
1
2
2r
2b
3
4r
4
5
6
1 mm
Hoplosthetus praemediterraneus
7
8
9
10
1 mm
Gephyroberyx darwinii
11b
11
11v
1 mm
Melamphaes typhlops
12
13
14
15r
15
14v
16
Scopelogadus beanii
1 mm
17b
17
18
18b
Echiodon dentatus
1 mm

**Plate 17**

endemic to the Mediterranean Sea. *Ophidion saldanhai* Matallanas & Brito, 1999 and *O. lozanoi* Matallas, 1990 dwell in tropical and subtropical W African waters. The otoliths of these 4 *Ophidion* species have been illustrated (see Nolf, 1980; Tuset *et al*., 2008; Nolf *et al*., 2009; Schwarzhans, 2013a); however, an identification of individual species remains difficult due to the limited availability of extant comparative material – except for *O. barbatum* – and to the poorly defined variability within the species. Otoliths of extant *O. barbatum* and *O. rochei* cannot be separated with certainty, although both have been reported from various Pliocene deposits. The dorsal and ventral margins display a variation of lobes, but this probably occurs in both species. Large otoliths of *O. barbatum* (Pl. 18, figs 2-3) show a variability of a slightly compressed and oval to a bold triangular outline with a marked predorsal angle that is delineated by a slight outward fold (in Nolf *et al*., 2009, pl. 35). Similar specimens were encountered at Velerín Quarry and Velerín Antena Hilltop and are here considered *O. barbatum*.

***Ophidion* cf. *saldanhai* Matalanas & Brito, 1999**
Plate 18, figs 4-5

2013a *Ophidion saldanhai* – Schwarzhans, pl. 8, figs 15-18.

*Material* – 6 sagittas. Velerín Conglomerates 5, Velerín Quarry 1.

*Remarks* – Otoliths of the extant *O. saldanhai* (OL:OH= 1.34-1.47) differ from those of *O. barbatum* and *O. rochei* by 1) a slenderer shape accompanied by a more anteriorly oriented deepest part of the ventral rim (*vs*. close to the middle in the other species), 2) a straight to slightly concave dorsal rim before the distinct postdorsal angle, and 3) a prominent anterodorsal angle, usually with lobes at its anterior rim, which may show overlapping variation with the other species (see Schwarzhans, 2013a, pl. 8, figs 15-18). These features are present in five of the specimens from Velerín Conglomerates (OL:OH=1.42-1.56), which are therefore assigned to *Ophidion* cf. *saldanhai*. The distribution of the extant *O. saldanhai* is limited to the tropical marine eastern Atlantic waters between the Gulf of Guinea and Cape Verde.

Genus *Brotula* Cuvier, 1829

***Brotula* cf. *multibarbata* Temminck & Schlegel, 1846**
Plate 18, figs 8-9

1999 *Brotula multibarbata* – Rivaton & Bourret, pl 133, figs 15-18 (present-day otoliths).
2006 *Brotula* cf. *multibarbata* – Nolf & Girone, pl 1, fig. 14; pl 4, fig. 18.

*Material* – 2 sagittas. Velerín Conglomerates 2 (of which 1 is broken at its caudal end, Pl. 17, fig. 9).

*Remarks* – Two specimens from Velerín Conglomerates fully match the features of otoliths of *Brotula multibarbata*, an extant species that is found in Indo-Pacific waters, including the Red Sea. They are more compact than the slender otoliths of *Brotula barbata* (Bloch & Schneider, 1801) (see illustrations in Schwarzhans, 2013a, pl. 8, figs 6-10) that is found in the (sub)tropical eastern and western Atlantic waters. It confirms earlier reports from the Pliocene in the Mediterranean by Nolf *et al.* (1998) from NE Spain and Nolf & Girone (2006) from Italy.

Family Bythitidae Gill, 1861
Genus *Bellottia* Giglioli, 1883

***Bellottia* aff. *obliqua* (Weiler, 1942)**
Plate 19, fig. 3

1942 Ot. (Ophidiidarum) *obliquus* – Weiler, pl.5, figs 35-37
1979 *Oligopus obliquus* – Huygebaert & Nolf, pl.3, figs 17-19
2010a *Bellottia obliqua* – Schwarzhans, pl. 54, figs 1-6

*Material* – 1 sagitta. El Lobillo 1.

*Remarks* – One bythitid specimen (Pl. 19, fig. 3) in the collection closely resembles small otoliths of the Miocene *Bellotia obliqua* (Weiler, 1942) (compare Schwarzhans 2010a, pl. 54, figs 3, 5). It has an oval to spindle-like structure (OL:OH=1.9), with a high dorsal rim and a prominent predorsal angle, an almost flat inner face, and a convex outer face. The elongated homotypic sulcus (OL/SuL=2.26) is orientated obliquely to the antero-posterior axis of the otolith. This latter

**Plate 18**
Figure 1. ***Benthocometes*? sp.**, Velerín Carretera.
Figures 2-3. ***Ophidion barbatum*** Linnaeus, 1758, Velerín Quarry.
Figures 4-5. ***Ophidion* cf. *saldanhai*** Matalanas & Brito, 1999, Velerín Conglomerates.
Figures 6-7. ***Ophidion rochei*** Müller, 1845, Velerín Conglomerates.
Figures 8-9. ***Brotula* cf. *multibarbata*** Temminck & Schlegel, 1846, Velerín Conglomerates.
Figure 10. ***Bidenichthys mediterraneus* nov. sp.**, holotype, Velerín Quarry.
Figures 11-15. ***Bidenichthys mediterraneus* nov. sp.**, paratypes, Velerín Quarry.
Figures 16-17. ***Grammonus* aff. *bassoli*** Nolf, 1980, Velerín Quarry.
Figure 18. ***Grammonus ater*** (Risso, 1810), Velerín Conglomerates.

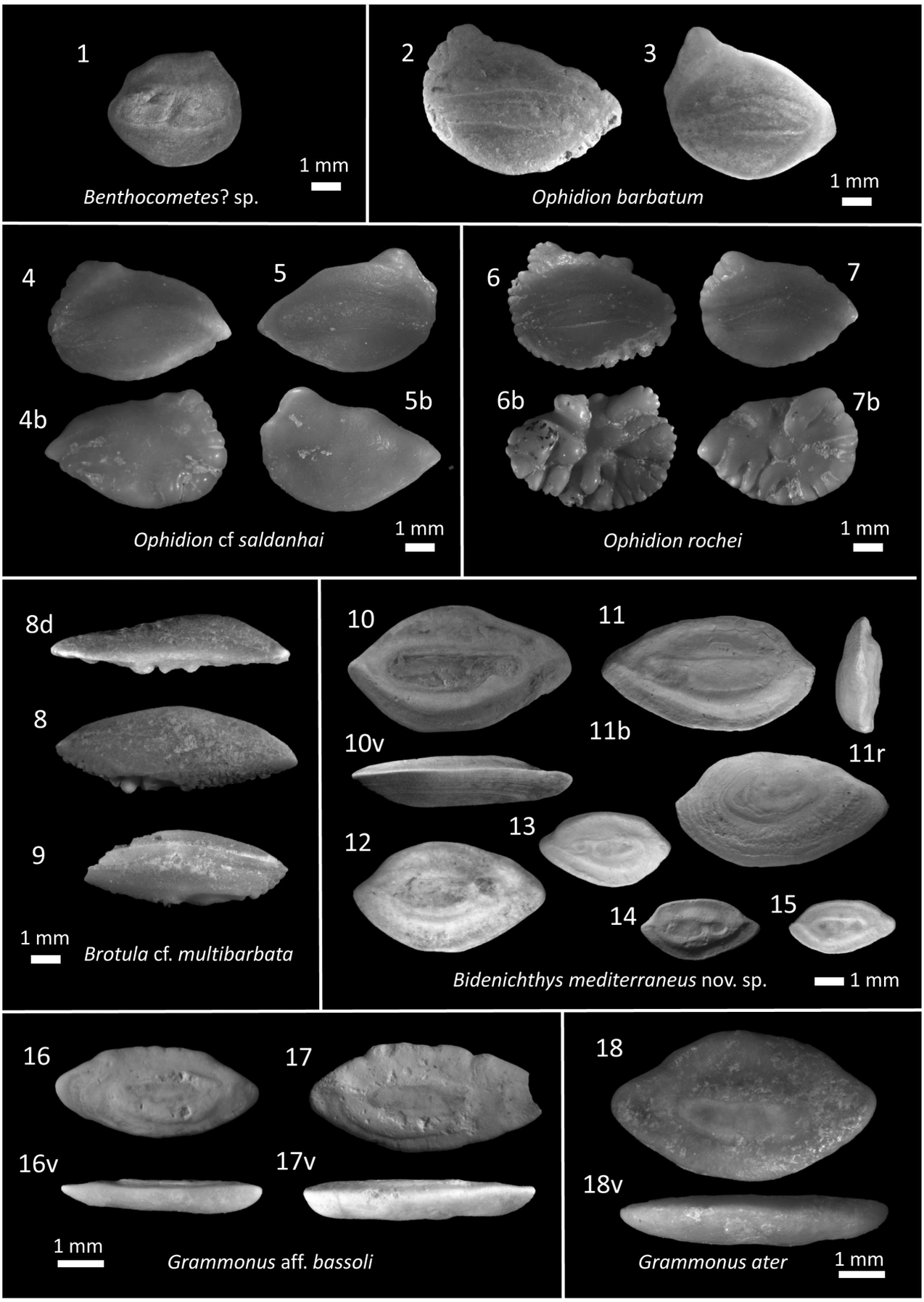
1
1 mm
*Benthocometes*? sp.
2
3
1 mm
*Ophidion barbatum*
4
5
4b
5b
1 mm
*Ophidion* cf *saldanhai*
6
7
6b
7b
1 mm
*Ophidion rochei*
8d
8
9
1 mm
*Brotula* cf. *multibarbata*
10
11
10v
11b
11r
12
13
14
15
*Bidenichthys mediterraneus* nov. sp.
1 mm
16
17
16v
17v
1 mm
*Grammonus* aff. *bassoli*
18
18v
*Grammonus ater*
1 mm

**Plate 18**

character is in common with the otoliths of the extant *Bellotia apoda* (Rheinhardt, 1837), but the latter have a more compressed oval shape and a shorter sulcus and colliculum.

***Bellottia verecunda* Carnevale & Schwarzhans, 2022**
Plate 19, figs 1-2

2022 *Bellotia verecunda* Carnevale & Schwarzhans, p. 308, fig. 9J-N (see also for synynomy).

*Material* – 2 sagittas. El Lobillo 2.

*Remarks* – The specimens regard small oval bythitid otoliths that were recently identified as *Bellotia verecunda* Carnevale & Schwarzhans, 2022. They are slightly shorter than those of *B. obliqua* (OL:OH=1.72-1.84 *vs.* OL:OH=1.92), are more rounded, and have a centrally localised oval sulcus that is obliquely orientated. The sulcus is shorter (OL:SuL=2.8-3.1) than that of *B. obliqua* (OL:SuL=2.3). The extant *Bellotia apoda* has a more compressed and rounded outline and sulcus than *B. verecunda* (see Carnevale & Schwarzhans 2022 for detailed comparisons).

Genus *Bidenichthys* Barnard, 1934

***Bidenichthys mediterraneus* nov. sp.**
Plate 18, figs 10-15

*Holotype* – Velerín Quarry (Pl. 18, fig. 10) RGM.1390569.

*Paratypes* – 5 sagittas: RGM.1390570-RGM.1390574, Velerín Quarry.

*Other material* – 24 sagittas. Velerín Carretera 2; Velerín Conglomerates 2; Velerín Quarry 18; Velerín Antena Hilltop 2.

*Locus typicus* – Velerín Quarry, close to Velerín Antena, along Camina Nicolas, Velerín, Estepona, province of Málaga, Spain.

*Stratum typicum* – Middle Pliocene, Piacenzian, fossiliferous medium- to fine-grained sands.

*Etymology* – Mediterranean refers to the first occurrence of otoliths of this genus and species in Mediterranean deposits.

*Diagnosis* – Fusiform otoliths (OL:OH=1.73-1.86) with the highest part of dorsal and ventral rims at the anterior side (at about 35% counted from the anterior rim); bluntly pointed at both anterior and posterior ends. Ventral and dorsal rims rounded and tapering towards the posterior end, with shallow concavities on the dorsal rim above the anterior and posterior ends. In most specimens the median sulcus is divided in a large and wide ostium and a small and narrower cauda with separated oval colliculi, but in the larger holotype the colliculi of ostium and cauda are connected at the upper half of the sulcus (OsL:CaL=3.3 in holotype). The outer face is smooth, but displays eccentric growth lines.

*Description* – Pear-shaped otoliths with bluntly pointed anterior and posterior rims accentuated by shallow pre- and post-dorsal concavities in the convex dorsal rim. A postdorsal angle is best developed in juvenile specimens (Pl. 18, figs 14-15). The ventral rim is convex; in the holotype convex but slight flattened in its middle part (Pl. 18, fig. 10). The ventral rim has a sharp edge, while the dorsal rim is flat at the inner side and rounded at the outside. The centrally localised sulcus is elongate without connection to the rims, and covers ⅔ of the OL. It consists of a large and wide ostium and a short and narrow cauda (OsL:CaL ratio: 2.0 to 3.3), which are distinctly separated in juvenile specimens and are partly connected in the holotype. The crista superior is straight in the large specimens; in some of the juvenile specimens it follows the ostium-cauda transition. Instead of a crista inferior the ventral field is swollen between the sulcus and a ventral furrow-like structure and– from anterior to posterior tip – depressed along the ventral rim. A shallow dorsal depression exists. The outer face is thick at the dorsal side, while the thickness gradually decreases in ventral direction. The outer face is smooth, but growth lines are distinctly visible (see Pl. 18, fig. 11b) showing that these otoliths have grown faster at their ventral side than dorsally.

*Remarks – Bidenichthys mediterraneus* otoliths are reminiscent of otoliths described as 'genus aff. *Ogilbia' heinzelini* (Lanckneus & Nolf, 1979: 90, pl. II, fig. 17, and redrawn in Nolf 2013, pl. 142) reported from the Pliocene

**Plate 19**

Figure 1-2. ***Bellottia verecunda*** (Carnevale & Schwarzhans, 2022), El Lobillo.
Figure 3. ***Bellottia* aff. *obliqua*** (Weiler, 1942), El Lobillo.
Figure 4. ***Cataetyx alleni*** (Byrne, 1906), Velerín Carretera.
Figure 5. ***Cataetyx* sp.,** Velerín Conglomerates.
Figure 6. ***'Bythites' pauper*** (Schwarzhans, 1978), Velerín Carretera.
Figure 7. ***Apogon imberbis*** (Linnaeus, 1758), Velerín Conglomerates.
Figures 8-9. ***Apogon lozanoi*** Bauzá Rullán, 1957, Río del Padrón.
Figures 10-13. ***Apogon lozanoi*** Bauzá Rullán, 1957, Velerín Conglomerates (10,12,13), Velerín Antena Slope (11).
Figures 14, 16-18. ***Fowleria velerinensis* nov. sp.,** paratypes, Velerín Conglomerates.
Figures 15. ***Fowleria velerinensis* nov. sp.,** holotype, Velerín Conglomerates.

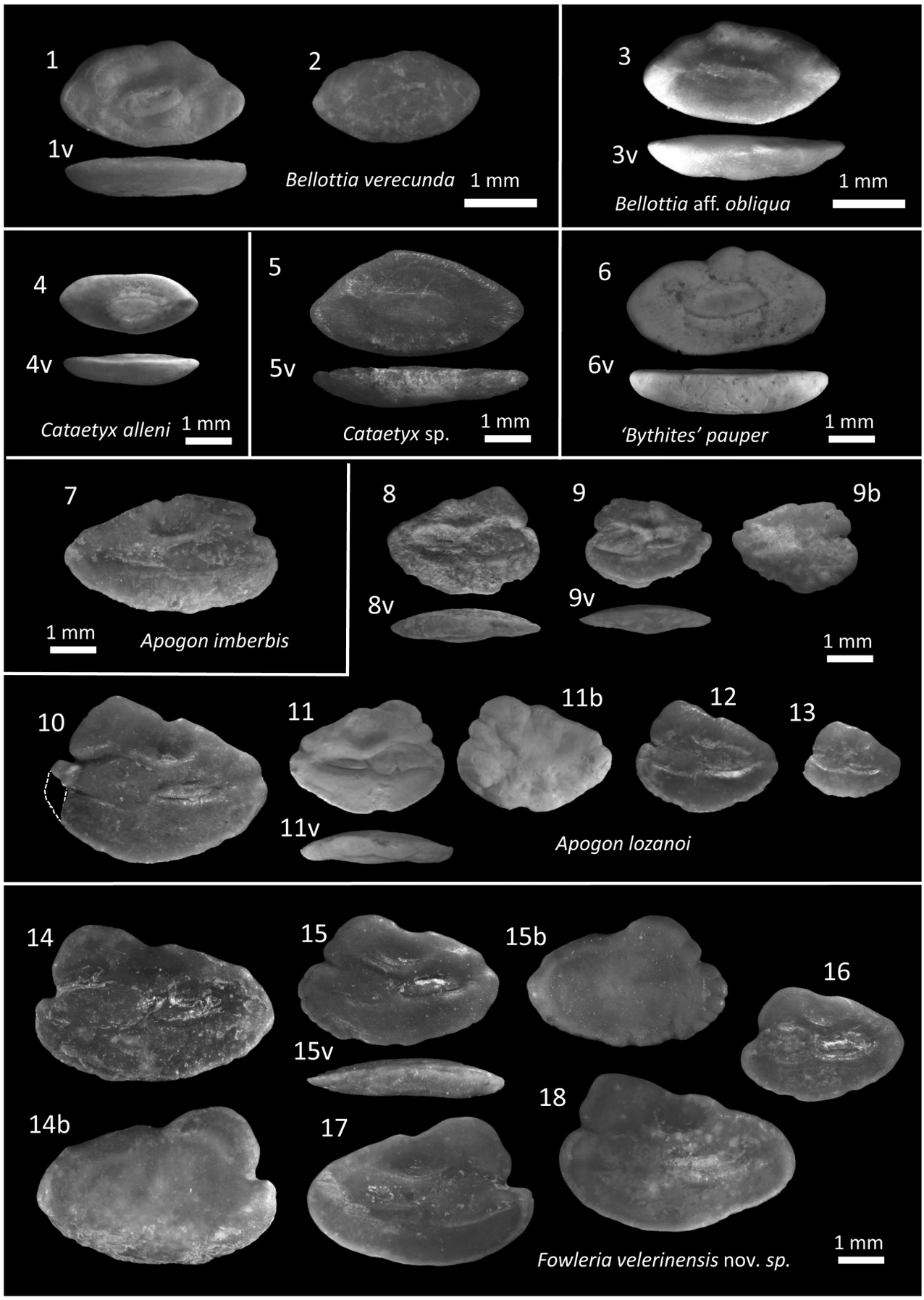
1
1v
2
Bellottia verecunda
1 mm
3
3v
Bellottia aff. obliqua
1 mm
4
4v
Cataetyx alleni
1 mm
5
5v
Cataetyx sp.
1 mm
6
6v
'Bythites' pauper
1 mm
7
1 mm
Apogon imberbis
8
8v
9
9b
9v
1 mm
10
11
11b
12
13
11v
Apogon lozanoi
14
14b
15
15v
15b
16
17
18
Fowleria velerinensis nov. sp.
1 mm

**Plate 19**

interval of the Redonian, Brittany, France. However, this Atlantic species – only known from small otoliths – differs in its less tapered shape and nearly equal size of ostial and caudal collicula. A fused ostium and cauda, as visible in the holotype of *B. mediterraneus*, is also visible in the otolith of *Melodichthys hadrocephalus* (Nielsen & Cohen, 1986, p. 385, fig. 3), but otoliths of this latter species are more compressed and have a very large ostium and a tiny cauda (Møller *et al*., 2021, fig. 3). In contrast, *B. mediterraneus* otoliths combine various features of those of different extant *Bidenichthys* species including the typical fusiform outline with tapered posterior part as in *B. slastibartfasti* (Paulin, 1995), *B. paxtoni* (Nielsen & Cohen, 1986) and *B. okamotoi* Møller *et al*. 2021 (for iconography of extant otoliths see Møller *et al*., 2021, fig. 3). In otoliths of the smaller *B. capensis* Barnhard, 1934 (known from the South African SE Atlantic) this feature is seen as well, but combined with a postdorsal angle, similar as in our small specimens (Pl. 18, figs 14-15). Ostium and cauda are separate in *B. capensis*, while they display a variety of partly to fully joined ostial and caudal parts of the sulcus in *B. okamotoi* specimens (from the northern Pacific near Japan). In contrast, in the other (SW Pacific) species the sulcus is completely fused and with a single colliculum. Overall, the otoliths of *B. mediterraneus* have the highest degree of similarity to those of *B. capensis,* but *B. capensis* is more elongate (OL/OH=2.2-2.45, data from Smale *et al*., 1995, pl. 34, fig. A1 and Møller *et al*., 2021, fig. 3) than *B. mediterraneus* (OL/OH=1.73-1.86), also when comparing otoliths of equal size. Furthermore, the caudal colliculum of *B. capensis* is wider.

*Occurrence* – The find of *Bidenichthys* otoliths in deposits of the western Mediterranean Sea is unexpected and was made only in the Piacenzian deposits of the Velerín Hill, largely from the sands of Velerín Quarry.

Genus *Cataetyx* Günther, 1887

***Cataetyx alleni* (Byrne, 1906)** and ***Cataetyx* sp.**
Plate 19, figs 4 and 5

2008 *Cataetyx alleni* – Tuset *et al*., figs 34.A1-A3.

*Material* – 5 juvenile sagittas. Río del Padrón 1; Velerín Carretera 3; Velerín Quarry 1 and 1 sagitta Velerín Conglomerates.

*Remarks* – Flat inner face; convex outer face; area around the sulcus depressed, thus creating an elevated impression of the colliculum in ventral view; sulcus with a narrow, elevated connection to the anterior rim. Otoliths of extant species of *Cataetyx* usually have a straight dorsal rim (see Nolf, 1980, pl. 12, fig. 8; Smale *et al*., 1995, pl. 34, figs B1-C1; Schwarzhans, 2013a, pl. 9, fig. 4). The smaller specimens from Velerín Carretera (Pl. 19, fig. 4) display the features of extant *Cataetyx* and could represent a juvenile *C. alleni* (Byrne, 1906). A 4.9 mm specimen from Velerín Conglomerates (Pl. 19, fig. 5) distinguishes itself by a convex dorsal rim and may represent a different species of *Cataetyx*, it is thus left in open nomenclature.

Genus *Grammonus* Gill, 1896

***Grammonus ater* (Risso, 1810)**
Plate 18, fig. 18

1980 *Oligopus ater* – Nolf, pl. 12, fig 12.

*Material* – 1 sagitta. Velerín Conglomerates 1.

*Remarks* – Large otolith (6.0 mm). Robust spindle-shaped otolith (OL:OH=1.76). An expansion of the dorsal field is accompanied by a convex dorsal rim. The sulcus lies submedian, its length is about half the length of the otolith. Thickset along, in particular above the sulcus. Inner face rather flat especially along the antero-posterior axis; dorsoventrally becoming convex towards the rims. Outer face convex. The features correspond to those of otoliths of the extant *Grammonus ater*, which still occurs in the Mediterranean Sea and has been reported from the Zanclean (Agiadi *et al*., 2013a) and Pleistocene (Girone & Varola, 2001) (a very slender, elliptical specimen with narrowly convex anterior and posterior rims); Girone *et al*., 2006; Agiadi *et al*., 2018) as well. A specimen reported from the Zanclean of SE France (Nolf & Cappetta, 1989, as *Oligopus* sp.) shows similarities with *G. ater.*

***Grammonus* aff. *bassolii* Nolf, 1980**
Plate 18, figs 16-17

1980 *Oligopus bassolii* – Nolf, p. 121-122; pl 19, figs 1-5.

*Material* – 3 sagittas. Velerín Quarry 3.

*Remarks* – Spindle-shaped elongated otoliths (OL:OH= 2.2-2.3). Dorsal and ventral rims are equally convex. While the ventral rim is smooth, the central part of the dorsal rim is rather straight and with several obtuse lobes. The small oval sulcus is centrally oriented and elongated in anteroposterior direction. The inner face is slightly convex dorsoventrally and shows a distinct and broad circular elevation around the entire sulcus. The outer face is convex along the anteroposterior axis and even more so dorso-ventrally. The specimens come close to *G. bassolii* from the Tortonian (Nolf, 1980), but differ by the lobes present on the dorsal rim, the smaller sulcus and a slightly lower OL:OH ratio.

Genus *inc. sedis*

**‘*Bythites*’ *pauper* (Schwarzhans, 1978)**
Plate 19, fig. 6

1978 *Heptocara pauper* – Schwarzhans, figs 114, 144.
1989 ‘*genus Bythitinorum*’ *pauper* – Nolf & Cappetta, pl. 14, figs 1-2.

*Material* – 1 sagitta. Velerín Carretera 1.

*Remarks* – The otolith is characterised by a flat inner face and a rounded outer face with 3 to 4 big lobes along the dorsal rim. Despite its simple shape and few characteristics, these otoliths are easily recognised. Originally described as *Hepthocara pauper* (Schwarzhans, 1979, p. 36, pl. 13, fig. 144) this species still is in need of a suitable genus. It is also known from the Zanclean of SE France (Nolf & Cappetta, 1989).

Family Apogonidae Günther, 1859
Genus *Apogon* Lacepède, 1801

***Apogon imberbis* (Linnaeus, 1758)**
Plate 19, fig. 7

2013 *Apogon imberbis* – Nolf, pl. 228 (present-day otoliths).

*Material* – 1 sagitta. Velerín Conglomerates 1.

*Description* – Elongate *Apogon* otolith (OL:OH=1.73), which has a round and solid rostrum, a smaller round antirostrum and a flat predorsal extension. After the antirostrum, the dorsal rim continues in two straight parts that make a middorsal angle of 150° downward and are separated by a small round concavity. The ventral rim is curved, strongly at its anterior part and less at the posterior part. The dorsal and ventral rims taper toward the posterior end. The median sulcus covers 77% of the otolith length and consists of a very long and broad ostium and a smaller narrower cauda (OsL:CaL=2.04), which joins with an upward angle of 35°. The cauda displays a collicular crest along its inferior part. The crista superior is markedly thickened along the middle part of the sulcus and bends upward on both sides thus bordering a small deepened dorsal area that is connected to the concavity on the dorsal rim.
Two properties distinguish it from other apogonid otoliths of the same locality: (1) the elongate ostium which covers over 50% of the otolith length, and (2) the broad predorsal extension that exhibits a straight rim from rostrum to middorsal concavity. They come close to some of the otoliths of *A. imberbis* in Nolf (2013, pl. 228), but the specimens of *A. imberbis* depicted in Tuset *et al*. (2008) appear more compact, although their ostium is comparable to that of our specimen.

***Apogon lozanoi* Bauzá Rullán, 1957**
Plate 19, figs 8-13

1957 *Apogon lozanoi* – Bauzá Rullán, 1957

*Material* – 21 sagittas. Río del Padrón 3; El Lobillo 2; Velerín Conglomerates 12; Velerín Quarry 1; Velerín Sandy Lens 2; Velerín Antena Hilltop 1.

*Description* – The otoliths (OL:OH=1.27-1.41) have a massive predorsal extension giving them a triangular shape, with the predorsal angle at 30-35% from the tip of the rostrum. The anterior rim has a massive rostrum, but only a slightly perceptible antirostrum with an excisura in-between. The ventral rim is regularly curved, strongly at its anterior half and less at its posterior part. From the predorsal angle, the dorsal rim descends obliquely to the posterior rim in a straight line that is shifted a bit upward at a middorsal angle behind a notch. The posterior part of the otoliths tapers toward their end. The median sulcus covers 75-80% of the otolith length. It is divided in a wide ostium and a smaller and narrower cauda (OsL:CaL=1.54-1.73) that displays a marked collicular crest at its inferior part. The outer face of the otoliths is decorated with blunt bulges, in particular ventrally and anteriorly.

Genus *Fowleria* Jordan & Evermann, 1903

***Fowleria velerinensis* nov. sp.**
Plate 19, figs 14-18

*Holotype* – RGM.1390591, Velerín Conglomerates.

*Paratype*s – 4 sagittas: RGM.1390592-RGM.1390595, Velerín Conglomerates.

*Other material* – 18 sagittas. Velerín Conglomerates 15; Velerín Antena Hilltop 3.

*Locus typicus* – Velerín Conglomerates, along Camino Nicola, Estepona, Prov. Málaga, Andalusia, Spain.

*Stratum typicum* – Pliocene, Piacenzian, conglomerate sediment.

*Etymology* – Named after the village Velerín and Velerín Antena Hill where the fossil-rich Velerín Conglomerates deposits are exposed.

*Diagnosis* – Elongate and rather thin otoliths (holotype OL=4.4 mm; OL:OH=1.54; OH:OT=3.36); They are characterised by an oval shape with a blunt rounded rostrum and a prominently broadly bulging predorsal rim that starts at a distinct but small excisura. Sulcus with a large and wide ostium and a shorter but still well-developed elongate cauda at some distance to the posterior rim. Smooth outer face, in the holotype with shallow lobation along the anterior part.

*Description* – The specimens (Pl. 19, figs 14-18) are thin, elongated and ellipsoid (OL largest specimen is 5.6 mm; OL:OH=1.49-1.54). Their dorsal rim is characterised by a massive and rounded predorsal angle projected anteriorly, a mid-dorsal concavity above the junction of ostium and cauda, followed by a straight postdorsal part that ends in a postdorsal angle. The posterior rim is mostly convex and connected to the ventral rim without a clear angle, but it can be straight with a clear postventral angle (Pl. 19, fig. 14) or even slightly concave (Pl. 19, fig. 15). The ventral rim has a strongly rounded anterior part that can be smooth or orna-

mented with lobes and furrows (Pl. 19, fig. 15). The median sulcus consists of a wide ostium and a slightly narrower cauda; ostium longer than cauda (OsL:CaL=1.41-1.67).

*Discussion* – Otoliths of *Fowleria velerinensis* resemble those of *F. manei* Hoedemakers & Battlori, 2005 from the Early Miocene of Spain in general shape, but differ in the shape of rostrum and excisura. They differ from those of *A. lozanoi* by the bulging predorsal rim without the triangular shape of *A. lozanoi*. They also differ by the greater length, the prominent rounded rostrum, the higher OL:OH ratio, the smooth outer surface, the non-tapering posterior rim and the rather flat midventral rim in large specimens. Otoliths of *F. velerinensis* and *A. imberbis* differ in several aspects: (1) the predorsal extension is less pronounced in *A. imberbis*, (2) the ostium is twice the size of the cauda in *A. imberbis*, while it ranges from 1.41 to 1.67 in *F. velerinensis*, (3) the distance between the posterior part of the cauda and the dorsal rim is smaller in *A. imberbis*.

*Distribution* – The species is only known from Piacenzian sediments of Velerín Hill near Estepona.

Family Gobiidae Cuvier, 1816

Within the Gobiidae, members of three major clusters are recognised in the Pliocene environment of Estepona, in line with extant Gobiidae known from the western Mediterranean Sea (Agorreta *et al*., 2013; Lombarte *et al.,* 2018). They comprise a *Pomatoschistus* Gill, 1863 related cluster, a cluster comprising *Aphia* Risso, 1827 and *Lesueurigobius* Whitley, 1950, and one that includes gobiid members related to the genus *Gobius* Linnaeus, 1758. Figs 2B, C summarise the structural details and terminology used to describe these rectangular and rhomboid otoliths. Table 1 and Plates 20-25 provide an overview of all gobiid species that have been encountered in Estepona/Velerín outcrops.

**Pamatoschistus *lineage***
Genus *Buenia* Iljin, 1930

***Buenia massutii* Kovačić, Ordines & Schliewen, 2017**
Plate 20, figs 1-3 and 4-5 (juveniles)

2006 *Buenia massutii* – Lombarte *et al*., figs 11263, 11264, 11309.

*Material* – 12 sagittas. Río del Padrón 1; Velerín Carretera 4; Velerín Conglomerates 2; Velerín Quarry 5.

*Description* – The otoliths of *B. massutii* are almost square (OL:OH ratio: 0.91-0.94) with round angles. They have straight linings of the ventral, anterior and posterior rims and a slightly convex curvature of the dorsal rim. The inner and outer faces are convex. *Buenia massutii* displays no or insignificant concavities on the anterior and posterior rims, respectively. The median sulcus is consistently small and divided in ostium and cauda. The cauda is horizontally oriented, while the ostium is slightly inclined (17-20°) in ventral direction.

*Comparison* – *Buenia massutii* is a small gobiid fish (max 3.3 cm) with almost square otoliths that hardly reach a size of 1 mm (iconography of otoliths of extant *B. massutii* and *B. affinis* Iljin, 1930 see Lombarte *et al*. (2006). The orientation of the ostium shows an inclination of 17-20°, while the inclination in otoliths of *B. affinis* is larger (to 44°). In *B. massutii* the dorsal rim is slightly convex with the top mid-dorsally. In *B. affinis* the highest point of the curved dorsal rim is a bit skewed to the posterior side.
The two relatively short specimens given on Pl. 20, figs 4-5 probably represent juvenile *Buenia massutii* specimens.

***Buenia pulvinus* nov. sp.**
Plate 20, figs 6-13

*Holotype* – Velerín Quarry RGM.1390601 (Pl. 19, fig. 6)

*Paratypes* – 6 sagittas: RGM.1390602-RGM.1390607. Velerín Quarry 2; Velerín Antena Slope 1; Velerín Carretera 3.

*Other material* – 132 sagittas. Río del Padrón 4; Velerín Carretera 66; Velerín Conglomerates 4; Velerín Quarry 40; Velerín Antena Slope 16; Velerín Hilltop 1; Parque Antena 1.

*Locus typicus* – Velerín Quarry, close to Velerín Antena, along Camino Nicolas, Velerín, Estepona, province of Málaga, Spain.

*Stratum typicum* – Middle Pliocene, Piacenzian, fossiliferous medium- to fine-grained sands.

*Etymology* – From the Latin '*pulvinus*', meaning 'pillow'

**Plate 20**
Figures 1-3. ***Buenia massutii*** Kovacic, Ordines & Schliewen, 2017, Velerín Quarry (1, 2), Velerín Carretera (3).
Figures 4-5. ***Buenia massutii*** Kovacic, Ordines & Schliewen, 2017, juvenile specimens, Velerín Quarry.
Figure 6. ***Buenia pulvinus* nov. sp.**, holotype, Velerín Quarry.
Figures 7-12. ***Buenia pulvinus* nov. sp.**, paratypes, Velerín Quarry (8, 12), Velerín Antena Slope (7), Velerín Carretera (9-11).
Figure 13. ***Buenia pulvinus* nov. sp.**, non-type, Velerín Carretera.
Figures 14-16. ***Pomatoschistus* sp.,** Velerín Quarry.
Figures 17-22. ***Pseudaphya* sp.,** Velerín Carretera (18), Velerín Quarry (17, 19, 20, 22), Velerín Conglomerates (21).
Figures 23-26. ***Deltentosteus quadrimaculatus*** Valenciennes, 1837. Velerín Antena Slope (23,25), Velerín Carretera (24,26).

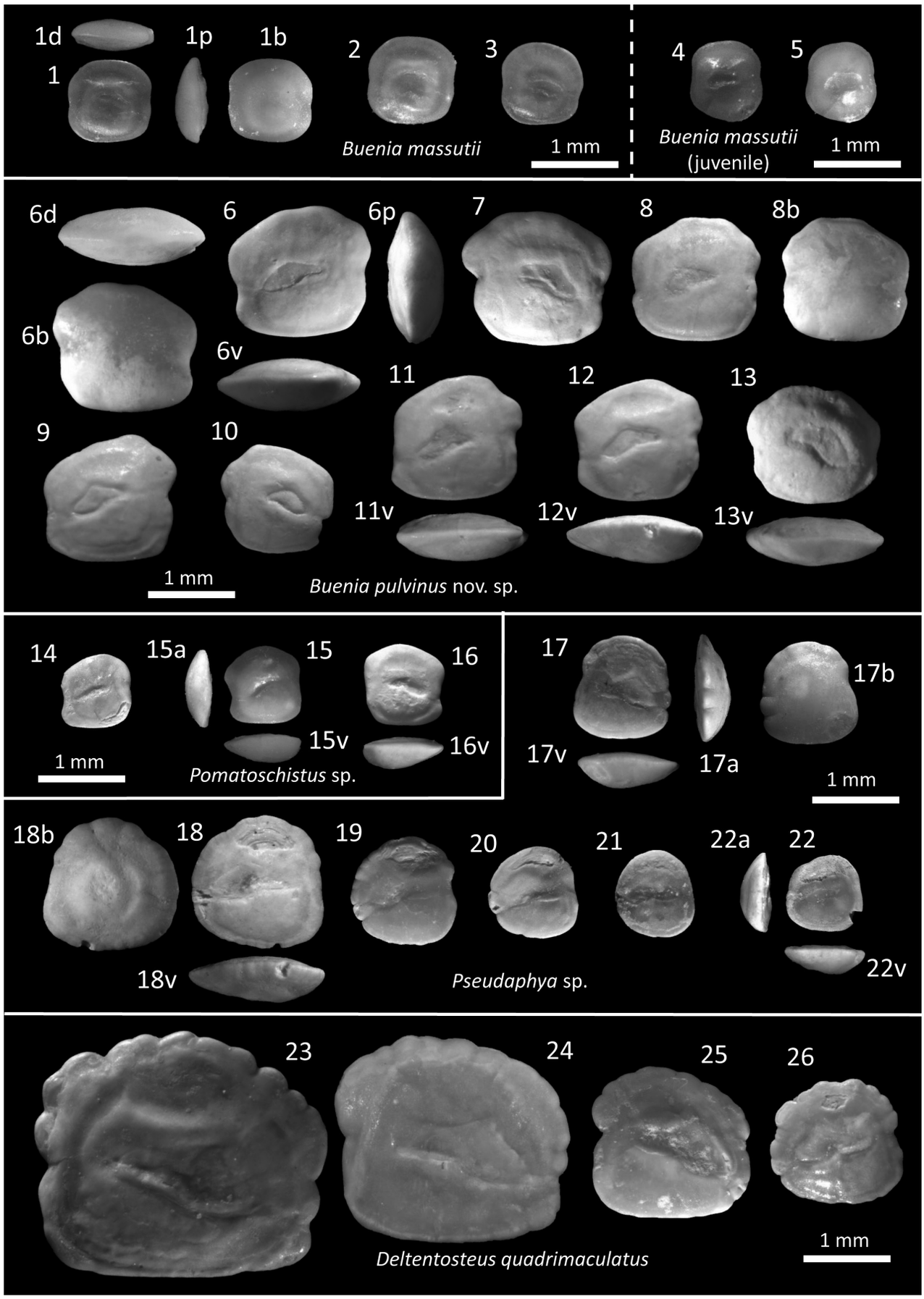
1d
1p
1b
1
2
3
Buenia massutii
1 mm
4
5
Buenia massutii
(juvenile)
1 mm
6d
6
6p
7
8
8b
6b
6v
11
12
13
9
10
11v
12v
13v
1 mm
Buenia pulvinus nov. sp.
14
15a
15
16
15v
16v
1 mm
Pomatoschistus sp.
17
17b
17v
17a
1 mm
18b
18
19
20
21
22a
22
18v
22v
Pseudaphya sp.
23
24
25
26
1 mm
Deltentosteus quadrimaculatus

**Plate 20**

and referring to the pillow-like shape of these small otoliths.

*Diagnosis* – Almost square small otoliths (OL=1.6-1.8 mm; OL:OH=1.11-1.18) with blunt concavities in the low-anterior and middle-posterior rim. The length of the upper part is slightly larger than the lower part. The dorsal rim is curved, but with a minor postdorsal angle and a subsequent concavity that forms the upper lining of a blunt dorsal projection and merges with the posterior rim. Sulcus small (about 40% of OL); ostium with dorsal angle and inclining. Cauda very small and variably thickened at its crista inferior. Convex inner face, strongly convex outer face.

*Description* – Small otoliths reaching 1.6 to 1.8 mm in length (OL/OH=1.11-1.18). Shallow concavities – halfway the otolith at the posterior rim and more ventrally at the anterior rim – mark the transition between upper and lower part. The rim of the upper part is curved along the pre-, mid- and postdorsal angles and the connection to the posterior rim, with three rather straight stretches between them, and has a slightly extended dorso-posterior part. The lower half of the otolith is more rectangular with rounded angles. The sulcus is small with a tiny cauda and a prominent ostium with a 35-45° inclination angle. A thickening on the crista inferior runs along the anterior half of the cauda and the ostium-cauda transition (Pl. 20, figs 6-7), but it is not visible in all specimens. Inner and outer surfaces are convex. A ventral furrow is formed by the peri-sulcular thickening of the inner surface; a slightly depressed dorsal field is visible.

*Discussion* – The otoliths display properties both of *Buenia* and *Pomatoschistus*, but also several differences. The size of the otoliths of extinct species is rather large (OL: 1.5-1.8 mm) compared with that of extant *Buenia* species; the convex inner surface fits with *Buenia*, while in most *Pomatoschistus* species the inner surface is flatter. Moreover, the usually elevated position of the colliculum of the sulcus favours positioning this species in the genus *Buenia*. Furthermore, they discriminate themselves within the genus *Buenia* by the size of their sulcus. The size of the sulcus relative to that of the entire otolith is smaller in *B. pulvinus* than in otoliths of the extant *B. affinis* Iljin, 1930 (see Lombarte *et al*., 2006 and Schwarzhans *et al*., 2020b) and larger than that in *Buenia pisiformis* Schwarzhans, Agiadi & Carnevale, 2020 from the pre-evaporitic Messinian of Greece (Schwarzhans *et al*., 2020b). Finally, otoliths of the extant *B. affinis* generally have a more convex anterior part of the dorsal rim and a smaller postdorsal extension than otoliths of *B. pulvinus* nov. sp.
A recently discovered third Mediterranean *Buenia*, *B. lombartei* Kovačić *et al*., 2018 is related to *B. jeffreysi* (Günther, 1867) from the northern Atlantic and lives on sandy ground in deeper waters along the continental slope of the Mediterranean Sea. Adult size of cold-water *B. jeffreysii* amounts to 6 cm, while the Mediterranean *B. lombartei* amounts to 3 cm, similar to *B. affinis*. Unfortunately, no otolith description is available yet, either of *B. jeffreysii*, or of *B. lombartei*.

*Occurrence* – The otoliths of *B. pulvinus* are frequently encountered in various sandy deposits of the Velerín area and few were found in Río del Padrón. As this species has not yet been reported from other marine deposits of the Mediterranean Zanclean, its distribution may be confined to upper Zanclean and Piacenzian deposits.

Genus *Pomatoschistus* Gill, 1863

***Pomatoschistus* sp.**
Plate 20, figs 14-16

*Material* – 5 sagittas. Velerín Quarry 4; Velerín Conglomerates 1.

*Remarks* – The Pliocene specimens resemble in general the outline otoliths of the freshwater sand goby *Pomatoschistus montenegrensis* Miller & Šanda, 2008 (see Gut *et al*. 2020, figs 6n-p), which display a marked concavity in the anterior rim. However, the sulcus of *P. montenegrensis* is wider and the ostium declines less than in our specimens. Instead, the narrower sulcus and the inclination angle of the ostium are comparable to those in otoliths of the marine Mediterranean *P. quagga* Heckel, 1837 (Gut *et al*., 2020, figs 6r-t). However, in *P. quagga* the ventral and anterior rims are straight and a concavity is consistently observed in the posterior rim (Gierl, 2019, figs 3G-I; Gut *et al*., 2020; Schwarzhans *et al*., 2020b). Our specimens also show a more marked preventral angle than otoliths of *P. quagga* and the outer face is much more convex (compare Schwarzhans *et al*., 2020b, fig. AJ), most strongly at the posterior side, as also seen in species of *Knipowitschia* Iljin, 1927. As in our specimens the differences are consistent, it is likely that the specimens represent another not yet recognised species of the *Pomatoschistus* group.

Genus *Pseudaphya* Iljin, 1930

***Pseudaphya* sp.**
Plate 20, figs 17-22

*Material* – 17 sagittas. Río del Padrón 1; Velerín Carretera 2; Velerín Quarry 7; Velerín Conglomerates 7.

*Description* – These otoliths (Pl. 20, figs 18-22) are characterised by their compressed shape (OL:OH=0.9 and 1.0), the straight posterior rim which runs vertically to slightly obliquely upward, and the rounded anterior rim that lines half of the otolith including the preventral and predorsal parts. The dorsal rim is short; a minor rounded postdorsal extension can be present which joins the posterior rim and occasionally forms a shallow concavity. Furthermore, the median sulcus consists of a short cauda and a wide ostium, which has an angled dorsal lobe. The ostium is deepest near the crista inferior. A straight iugum lines almost the entire cauda. The otoliths have a rather flat inner surface and a convex outer surface. In ventral view, the convexity is skewed to the posterior part. One

specimen (Pl. 20, fig. 17) is narrower (OL:OH=0.83) and may represent variability within the same species. The specimens are close to otoliths reported as *Pseudaphya ferreri* (de Buen & Fage, 1908), from the Zanclean of Agia Triada (Schwarzhans *et al*., 2020b, figs 13AZ, BA). It is uncertain whether our otoliths fit within the characteristics of the only extant *Pseudaphya* Iljin, 1930, *P. ferreri*, or represent a separate extinct species.

*Remarks* –Schwarzhans *et al*. (2020b, figs 13Y-AA) recorded two otoliths of *Knipowitschia stironenesis* (Lin, Brzobohatý, Nolf & Girone, 2017b) from the Late Tortonian of Stazzano (Italy) and suggested that they are juveniles of *Lesueurigobius stironensis* Lin, Brzobohatý, Nolf & Girone, 2017. The larger of the two specimens has a similar general outline as our *Pseudaphya* sp. specimens and may be closely related. However, *Lesueurigobius stironensis* differs in various aspects from our *Pseudaphya* sp., in particular by the pronounced ornamentation of the dorsal rim and the presence of the small preventral extension (see Lin *et al*., 2017b, figs 11F-I).

Genus *Deltentosteus* Gill, 1863

***Deltentosteus quadrimaculatus* (Valenciennes, 1837)**
Plate 20, figs 23-26

2000 *Deltentosteus quadrimaculatus* – Nolf & Girone, pl. 3, figs 1-4.
2000 *Deltentosteus* aff. *quadrimaculatus* – Nolf & Girone, pl. 3, figs 5-12.
2020b *Deltentosteus quadrimaculatus* – Schwarzhans *et al*., figs 12AE-EJ.

*Material* – 6181 sagittas. Present in all outcrops in Estepona and Velerín.

*Discussion* – *Deltentosteus quadrimaculatus* has been amply reported from the present-day fauna and Pliocene and Pleistocene Mediterranean deposits (Nolf & Girone, 2000). In our material it displays a variation in shape (square to rectangular), a degree of convexity of the inner and outer faces. A small group (n=7) regards specimens that are rather flat on the inner face with a considerable decoration around the sulcus and other parts of the inner face (as depicted in Pl. 19, fig. 23). The large size (up to 3.5 mm) of these otoliths makes it unlikely that they represent *D. collonianus* (Risso, 1820), the only other, but small, extant *Deltentosteus* species, known from Portugal (one picture available in Lombarte *et al*., 2006 that in particular elucidates the contour of the otolith).

**Aphia *lineage***

Three members of the *Aphia* lineage were encountered in the Velerín deposits, of which only *Hoeseichthys brioche* (Lin, Girone & Nolf, 2015) was also found at El Lobillo. The other two belong to *Lesueurigobius*. *Lesueurigobius suerii* (Risso, 1810) (Pl. 20, figs 3-6) is an extant species whose present-day and Pliocene otoliths have been illustrated by a.o. Girone & Nolf (2000), Nolf *et al.* (2009) and Schwarzhans *et al*. (2020b), while *L. stazzanensis* Schwarzhans, Agiadi & Carnevale, 2020 is an extinct species from the Tortonian of Stazzano, recently identified by Schwarzhans *et al*. (2020b).

Genus *Hoeseichthys* Schwarzhans, Brzobohatý & Radwanska, 2020

***Hoeseichthys brioche* (Lin, Girone & Nolf, 2015)**
Plate 21, figs 1-2

1986 *Acentrogobius* sp. – Schwarzhans, pl. 6, fig. 73.
1989 '*Gobiidarum'* sp. 2 – Nolf & Cappetta, pl. 17, figs 7-8.
2015 'Gobiida' *brioche* – Lin *et al*., p.259-260, figs 7.16-20.
2017b '*Gobius*' *brioche* – Lin *et al*., p. 44, fig. 11.O.
2020b *Hoeseichthys brioche* – Schwarzhans *et al*., p. 673, figs 6i-n (contains further synonyms).

*Material* – 25 sagittas. Velerín Carretera 6; Velerín Conglomerates 8; Sandy Lens 6; Velerín Quarry 4; Velerín Antena Slope 1.

*Remarks* – *Hoeseichthys brioche* otoliths were described as *Lesueurigobius brioche* from Tortonian deposits in Italy by Lin *et al*. (2015) and reported as *Lesueurigobius* sp. and *Hoeseichthys brioche* from marine Pliocene deposits of Mediterranean France (Nolf & Cappetta, 1989) and northern Italy (Schwarzhans *et al*., 2020b), respectively.

Genus *Lesueurigobius* Whitley, 1950

***Lesueurigobius stazzanensis* Schwarzhans, Agiadi & Carnevale, 2020**
Plate 21, figs 7-9

2020b *Lesueurigobius stazzanensis* – Schwarzhans *et al*., p. 673-674, figs 6ag-ap (see for further synonymy).

*Material* – 24 sagittas. Velerín Carretera 3; Velerín Conglomerates 11; Velerín Quarry 4; Velerín Sandy Lens 5; Velerín Hilltop 1.

*Description*– Slightly elongated otoliths (OL:OH=1.08-1.16) that match the characteristics of *L. stazzanensis* described from the upper Tortonian of Italy (Schwarzhans *et al*., 2020b, figs 6AG-AM). The dorsal rim is convex with a short but massive postdorsal extension, which is more pronounced in larger specimens. The ventral rim is straight with rounded pre- and postventral angles. A ventral furrow runs close to the rim. The sulcus declines slightly anteriorly (18-20°). The sulcus is lined at almost its entire

inferior side by a long iugum, of which the thickest part is at the cauda-ostium transition.

**Gobius *lineage***

The *Gobius* lineage is represented in the Pliocene of the western Mediterranean by several genera including *Gobius*, *Thorogobius* Miller, 1969, *Chromogobius* de Buen, 1930, and *Callogobius* Bleeker, 1874. It comprises many extant species whose number is still rising (e.g., *G. kolombatovici* Kovačić & Miller, 2000; *G. incognitus* Kovačić & Sanda, 2016; *G. xoriguer* Iglésias, Vukić & Šanda, 2021). Within the genus *Gobius* several species can be clustered according to their otolith morphology. They comprise subgroups that are closely related to *G. geniporus* Valenciennes, 1837 / *G. kolombatovici* Kovačić & Miller, 2000, *G. roulei* de Buen, 1928 / *G. niger* Linnaeus, 1758, *G. paganellus* Linnaeus, 1758, and small *Gobius* species, such as *G. bucchichi* Steindachner, 1870 and *G. vittatus* Vinciguerra, 1883.

Genus *Gobius* Linnaeus, 1758

***Gobius bucchichi*** Steindachner, 1870
Plate 21, fig. 11

2020 *Gobius bucchichi* – Gut *et al*., fig. 5a-c (present-day otoliths).

*Material* – 2 sagittas. Velerín Conglomerates 1, Velerín Antena Hilltop 1.

*Remarks* – Plate 21, fig. 11 presents a small square-bodied *Gobius* otolith with a prominent postdorsal projection and a little-extended antero-ventral point. The posterior rim projects perpendicularly to the ventral rim, except for its most ventral part that bends anteriorly as if the postventral right angle part had been cut off obliquely. This latter character is also seen in SEM pictures of *G. fallax* Sarato, 1989 and *G. bucchichi* and is less strong in *G. incognitus* Kovačić & Šanda, 2016 (Gut *et al*., 2020). In addition, the smooth transition of the dorsal rim into the postdorsal projection, the shape and direction of the sulcus and the prominent oval to round iugum fit well with *Gobius fallax* and *Gobius bucchichi*. The preventral point is more strongly developed in *G. fallax* than in *G. bucchichi* (Gut *et al*., 2020), but this character can be variable. Overall, the specimen matches very well with *G. bucchichi*.

***Gobius* cf. *fallax*** Sarato, 1989
Plate 21, fig. 12

2013a *Gobius* sp. 1 – Agiadi *et al.*, fig. 8.13
2020b *Gobius fallax* – Schwarzhans *et al*., p. 676, figs 7D, E
2020 *Gobius fallax* – Gut *et al.*, figs 3g, h (present-day otoliths).

*Material* – 1 sagitta. Río del Padrón 1.

*Remarks* – A specimen from Río del Padrón (Pl. 10, fig. 12) – identified as *Gobius* cf. *fallax* – is more skewed to a rhomboid shape by the more oblique position of the anterior and posterior rims and by a more prominent and pointed preventral projection. Overlap between *G. bucchichi* and *G. fallax* cannot be excluded because of intraspecific variability.

***Gobius geniporus*** Valenciennes, 1837
Plate 22, figs 1-2

?2006 *Gobius* aff. *niger* Linnaeus, 1758 – Nolf & Girone, pl. 10, figs 7-8.
2020 *Gobius* cf. *geniporus* Valenciennes, 1837 – Agiadi *et al*, fig. 3i.
2020 *Gobius geniporus* – Gut *et al*., figs 3d-f (present-day otoliths).

*Material* – 20 sagittas. Río del Padrón 4; El Lobillo 7; Velerín Carretera 2; Velerín Conglomerates 4; Velerín Quarry 1; Velerín Slope 2.

*Description* – The Pliocene specimens are relatively large gobioid otoliths (OL=3.9-4.0 mm; OL:OH=1.47-1.49) with a rhomboid rather than rectangular shape, in which the posterior rim makes a blunt angle of 110° with the slightly convex ventral rim. The regularly curved dorsal rim declines toward the predorsal angle which is localised at 40-60% of the overall height of the otolith. The predorsal angle projects as far as or a bit less than the preventral extension (Pl. 22, figs 1-2). A thick postdorsal extension bends outward in a smooth curve; in inner face view it looks breast-shaped and shows in the middle of its tip a minor protrusion. The sulcus is sole-shaped, with a slender to moderate-sized ostial lobe. The cauda lies nearly horizontally; the larger ostium declines (25-30°) to the ventral side. A clear but thin iugum runs along the cauda. The crista superior is pronounced – distinctly visible in posterior view – and borders a deepened dorsal field.

**Plate 21**

Figures 1-2. ***Hoeseichthys brioche*** (Lin, Girone & Nolf, 2015), Velerín Quarry (1), Velerín Antena Slope (2).
Figures 3-6. ***Lesueurigobius suerii*** (Risso, 1810), Velerín Conglomerates.
Figures 7-9. ***Lesueurigobius stazzanensis*** Schwarzhans, Agiadi & Carnevale, 2020, Velerín Quarry (7), Velerín Carretera (8, 9).
Figure 10. ***Gobius vittatus*** Vinciguerra, 1883, Velerín Antena Slope.
Figure 11. ***Gobius bucchichi*** Steindachner, 1870, Velerín Conglomerates.
Figure 12. ***Gobius* cf. *fallax*** Sarato, 1989, Río del Padrón.

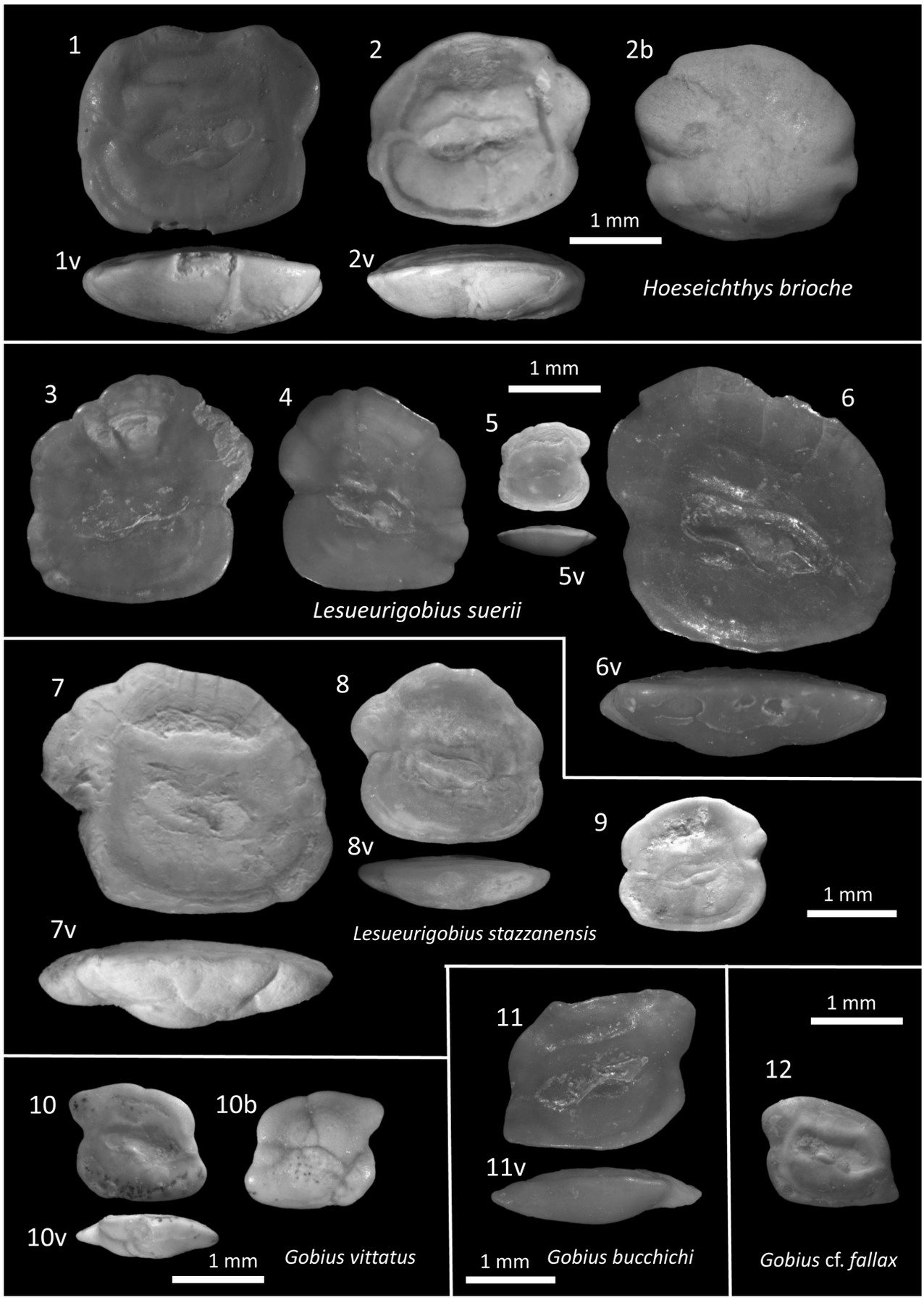
1
2
2b
1 mm
1v
2v
Hoeseichthys brioche
1 mm
3
4
5
6
5v
Lesueurigobius suerii
6v
7
8
9
8v
1 mm
7v
Lesueurigobius stazzanensis
1 mm
11
12
10
10b
11v
10v
1 mm
Gobius vittatus
1 mm
Gobius bucchichi
Gobius cf. fallax

**Plate 21**

*Remarks* – Extant *Gobius geniporus* can grow to a relatively large size for gobies (18 cm); their otoliths can reach 6 mm (Lombarte *et al*., 2006; Gut *et al*., 2020). Prominent features are an elongated rectangular shape (OL:OH=1.46-1.52); a regularly curved dorsal rim that declines toward the predorsal angle which is localised at 40-60% of the overall height of the otolith, and a thin iugum. Except for their rhomboid rather than rectangular shape the Pliocene specimens match those of *G. geniporus*. Various publications show a variability in otoliths of extant *G. geniporus*, such as in the elongate shape, the shape of the iugum and the antero-ventral extension (Schwarzhans, 2020b; Nolf *et al*., 2009).

***Gobius cobitis*** Pallas, 1814
Pl. 22, figs 3-4

2020 *Gobius cobitis* – Gut *et al*., figs 4a-c (present-day otoliths).

*Material* – 2 sagittas. Río del Padrón 1, Velerín Conglomerates 1.

*Remarks* – While extant *Gobius cobitis* ('giant goby') can grow to a large size (19.5 mm) and obtain irregular-shaped otoliths, middle sized specimens (10-12 cm) have otoliths with a rectangular body of OL=3.5-3.7 mm (Lombarte *et al*., 2006), similar to the size of the fossil specimens shown on Pl. 22, figs 3 and 4. *G. cobitis* otoliths from Velerín Conglomerates and Río del Padrón are characterised by a spout-shaped preventral expansion and a prominent postdorsal extension that is thin (in ventral view) and strongly bent outward (Pl. 22, figs 3v, 4v). They have a compressed almost rectangular body with a rounded dorsal rim. Due to the longer spout-shaped antero-ventral projection they have an OL:OH ratio (OL:OH=1.42-1.47) that is similar to that of *G. geniporus*. The dorsal rim is continuously curved and runs from the postdorsal extension to just above the anteroventral extension. The postdorsal extension bends strongly outward and is thin and pointed in ventral view. The otoliths have an oval iugum under the anterior part of the cauda. Their thickness is rather constant along the otolith body.

***Gobius kolombatovici*** **Kovačić & Miller, 2000**
Plate 22, figs 5-7

2020 *Gobius kolombatovici* – Gut *et al*., figs 3 k, l (present-day otoliths).

*Material* – 53 sagittas. Río del Padrón 6; El Lobillo 1; Velerín Carretera 4; Velerín Conglomerates 34; Velerín Quarry 5; Velerín Sandy Lens 2; Velerín Antena Slope 1.

*Description* – The Pliocene otoliths are rectangular (OL= 2.5-2.7; OL:OH=1.20-1.37), but with a curved dorsal rim and a rounded postdorsal extension that is similarly shaped as in *G. geniporus*. The dorsal rim runs upward in posterior direction until about 60% of the rim, after which it declines in a straight or slightly concave way towards the postdorsal extension. The anterior and posterior rims run vertically except for the dorsal and ventral extensions. In inner face, the postventral angle looks like a partly cut right angle between the posterior and ventral rims. A bluntly pointed preventral extension of variable size exists; a ventral furrow is visible. The sole-shaped sulcus declines toward the anterior side, slightly stronger for the ostial part than for the cauda. Cristae superior and inferior are well developed. A clear oval iugum is present below the transition between ostium and cauda. Inner and outer faces are convex. The otoliths are markedly thicker at their ventral side; thickest near the ventral rim, as shown in posterior view (Pl. 22, figs 5p, 7p). In this respect, they differ from *G. geniporus* and *G. cobitis*.

*Remarks* – The inner faces of two otoliths of extant *Gobius kolombatovici* were recently illustrated by Gut *et al*. (2020). The otoliths of these Mediterranean fish (up to 9.2 cm; otoliths OL=3.3-3.6 mm) largely resemble those of *G. geniporus*, to which the species is also genetically related (Iglésias *et al*., 2021). Their OL:OH (1.44-1.49) is comparable. However, *G. kolombatovici* otoliths differ in the less pronounced and round predorsal angle, and the large round to oval-shaped iugum at the anterior part of the cauda. Moreover, the Pliocene otoliths – whose inner faces match those of extant *G. kolombatovici* specimens – also differ from those of *G. geniporus* and *G. cobitis* by their almost angular thickening of the ventral outside. *G. geniporus* also differs by a more oblique orientation of the lower half of the posterior rim.

***Gobius alboranensis*** **nov. sp.**
Plate 23, figs 1-3

*Holotype* – RGM.1390641, Velerín Conglomerates.

*Paratypes* – 2 sagittas: RGM.1390642, RGM.1390643. Velerín Quarry 1; Velerín Conglomerates 1.

*Other material* – 3 otoliths: Velerín Conglomerates 1; Velerín Quarry 1; Velerín Antena Slope 1.

*Locus typicus* – Velerín Conglomerates, community of Estepona, province of Málaga, Spain.

*Stratum typicum* – Velerín Conglomerates, lower-Middle Piacenzian.

**Plate 22**

Figures 1-2. ***Gobius geniporus*** Valenciennes, 1837, Velerín Conglomerates (1), El Lobillo (2).
Figures 3-4. ***Gobius cobitis*** Miller, 1974, Velerín Conglomerates (3), Río del Padrón (4).
Figures 5-7. ***Gobius kolombatovici*** Kovačić & Miller, 2000, Velerín Conglomerates (5, 7), El Lobillo (6).

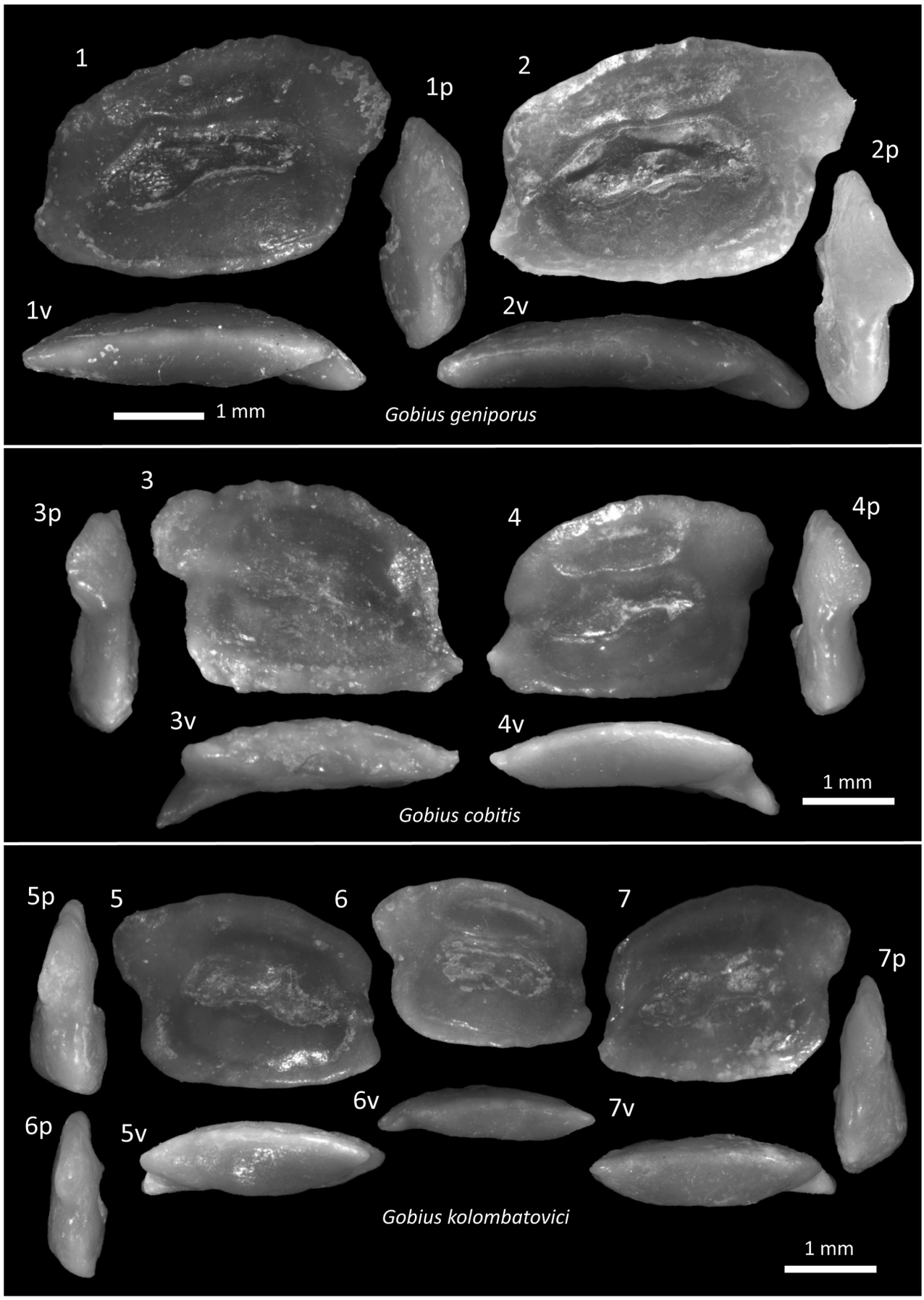
1
1p
2
2p
1v
2v
1 mm
Gobius geniporus
3
3p
4
4p
3v
4v
1 mm
Gobius cobitis
5p
5
6
7
7p
6v
7v
6p
5v
Gobius kolombatovici
1 mm

**Plate 22**

*Etymology – alboranensis*: from the Alborán Sea, referring to the original water in which the fish lived that provided these otoliths.

*Diagnosis* – Small *Gobius*-type otolith (OL=2.4-2.6 mm) with a dorsal rim that is highest at an obtuse angle behind the middle of the rim, and has an outwardly bent postdorsal projection angle. It has a short spout-shaped but cut preventral projection, and a predorsal angle that projects close to the preventral projection. The anterior rim displays a deep concavity of which the deepest point lies below the middle of the otolith height. A prominent oval iugum aligns the anterior part of the cauda.

*Description* – Small rectangular *Gobius* otoliths (OL= 2.4-2.6 mm) (OL:OH=1.30-1.37) that display a dorsal rim that consists of a ⅔ anterior part and a ⅓ dorsal part separated by an obtuse postdorsal angle (140°-145°) at the highest point of the otolith. The predorsal angle is prominent and projects to or slightly behind the preventral projection. This is accompanied by an incised concavity in the middle of the anterior rim, and a preventral projection with a cut tip. The moderate postdorsal projection is rounded at its tip and curves slightly outwards. The ventral rim is flat. The inner face is slightly convex, mainly reflecting a thickened ventral field that is bordered by a disinct ventral furrow that curves upwards close to the anterior and posterior rims. The centrally located sulcus is sole-shaped with a weak ostial lobe; the ostium is moderately declining towards the anterior side. Along the anterior part of the cauda a prominent oval iugum is present. The outer face is convex and smooth.

*Remarks* – At first sight the general contour of the otolith resembles that of the recently described *Gobius peloponnesus* Schwarzhans, Agiadi & Carnevale, 2020 from the Zanclean of Agia Triada (Peloponnesus, Greece) (Schwarzhans *et al*., 2020b), which is slightly smaller (1.7 mm). However, *G. peloponnesus* differs by an angular tip of the postdorsal projection and a narrow iugum. The Miocene *Gobius mustus* Schwarzhans, 2020b differs from our specimens by a slight concavity in the anterior rim and the straight rather than outwards bent postdorsal projection. In contrast to *G. alboranensis*, *G. kolombatovici* has a more rounded dorsal rim and a less prominent preventral angle and anterior concavity (see above and Gut *et al*., 2020).

*Occurrence* – Conglomerates and sand deposits of Velerín Antena Hill and Quarry, Community of Estepona (lower to Middle Piacenzian).

***Gobius roulei* de Buen, 1928**
Plate 23, figs 4-8

2020 *Gobius roulei* – Gut *et al*., figs j-l (present-day otoliths).

*Material* – 18 sagittas. Río del Padrón 8; El Lobillo 7; Velerín Conglomerates 2; Velerín Quarry 1.

*Discussion* – Molecular phylogeny of *Gobius* species indicates a close relationship between the extant *Gobius niger* and *G. roulei* (Iglésias *et al*., 2021). Hence, it is not certain whether the sagittas of these species can be fully discriminated in lower and Middle Pliocene material. *Gobius roulei* displays a thick ventral part, no rostrum; the dorsal rim is curved with an out-swinging lobe in posterior-dorsal direction, or with several shallow lobes along the dorsal rim, most pronounced posterior-dorsally. The crista superior is modest, the crista inferior weak. In the related *G. niger* the highest point of the dorsal rim lies above the ostium-cauda junction, while it is more posterior above the end of the cauda in *G. roulei*.

***Gobius* aff. *niger* Linnaeus, 1758**
Plate 23, fig. 9

2020 *Gobius niger* – Gut *et al*., figs 5g-i (present-day otoliths).

*Material* – 1 sagitta. Velerín Sandy Lens 1.

*Description* – The otolith is recognised by a significantly outward bending postdorsal projection that is ornamented with furrows and folds at the outside of the otolith connected to lobes along the dorsal rim. The posterior rim below the postdorsal extension displays a deep concavity. Moreover, a pointed antero-ventral projection exists. In the presented Pliocene specimen the most anterior point lies above the level of the rather straight ventral rim to which it is obliquely connected. The inner face is convex along the antero-dorsal axis, the outer face is concave and markedly thickened in the centre and close to the ventral rim. Ostium and cauda of the sulcus are of equal length. However, the cauda is narrow and the ostium is very wide with a sharply angled ostial lobe that reaches close to the predorsal rim. The salient crista superior borders a distinct dorsal field. The ventral part is thick with a rather flat lower side. The specimen has the strongly declining dorsal rim of *Gobius geniporus* as well as the wide posterior extension that reaches over half of its height. But *Gobius* aff. *niger* has an obliquely backward running

**Plate 23**

Figures 1, 3. ***Gobius alboranensis* nov. sp.** paratypes, Velerín Quarry (1), Velerín Conglomerates (3).
Figure 2. ***Gobius alboranensis* nov. sp.,** holotype, Velerín Conglomerates.
Figures 4-8. ***Gobius roulei*** de Buen, 1928, El Lobillo (4), Río del Padrón (5-8).
Figure 9. ***Gobius* aff. *niger*** Linnaeus, 1758, Velerín Sandy Lens.
Figure 10. **Gobiidae sp.**, El Lobillo.

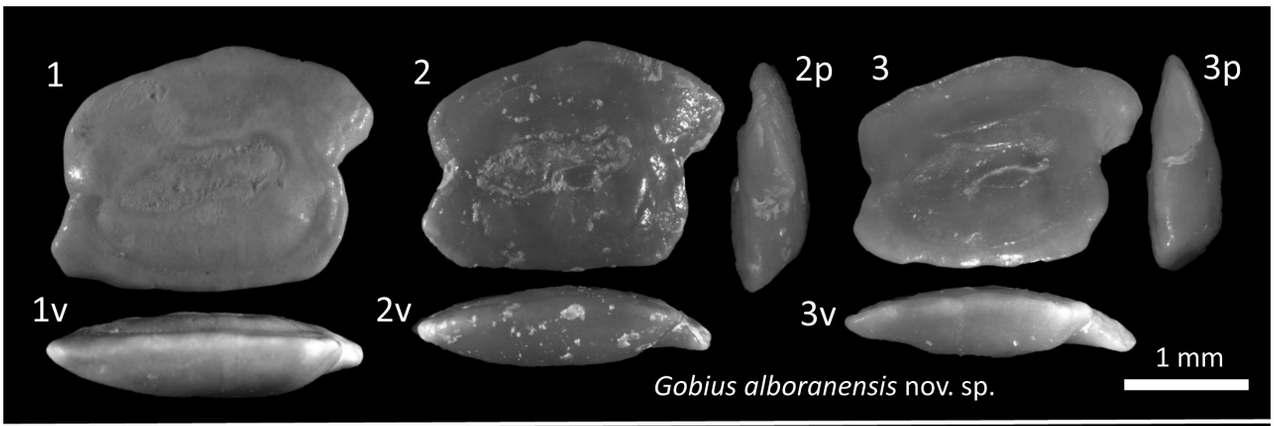
1
2
2p
3
3p
1v
2v
3v
1 mm
*Gobius alboranensis* nov. sp.

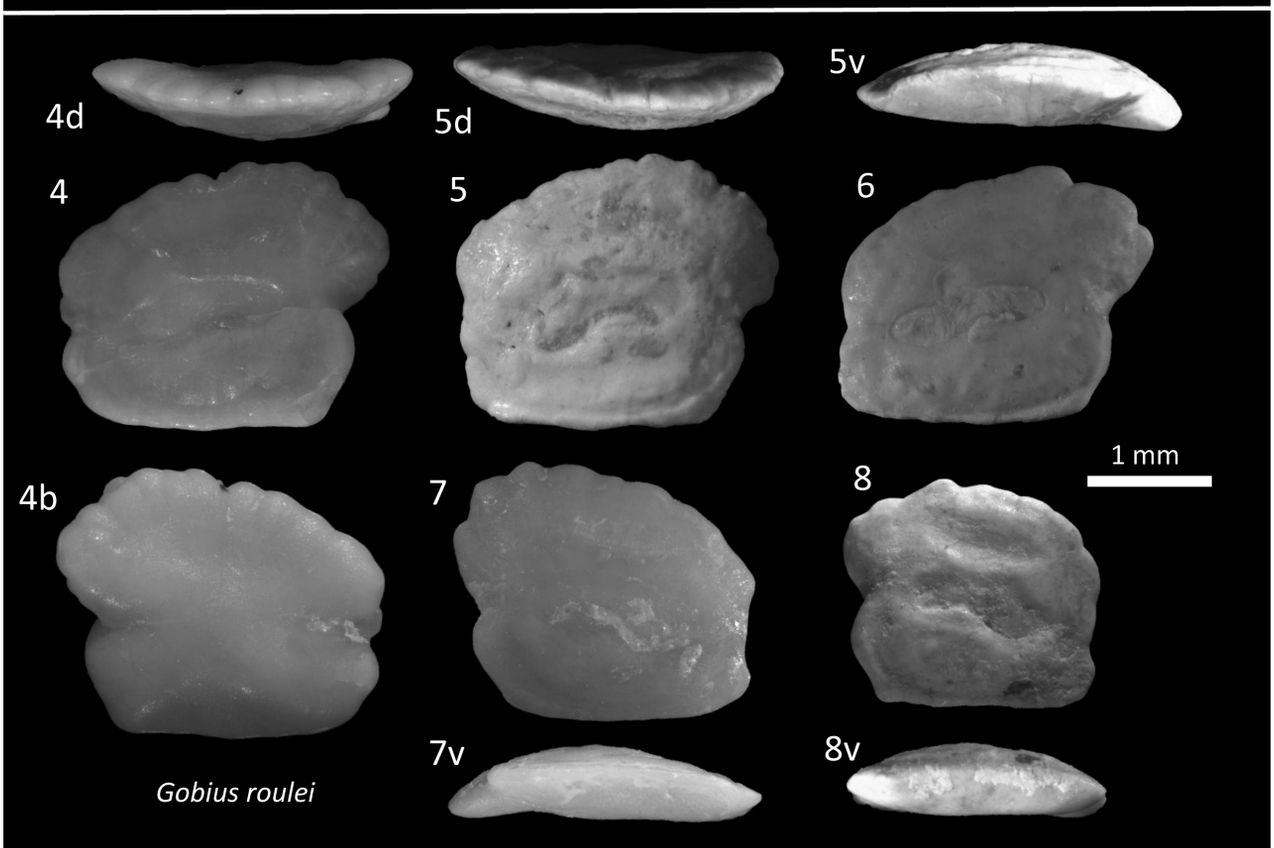
4d
5d
5v
4
5
6
1 mm
4b
7
8
7v
8v
*Gobius roulei*

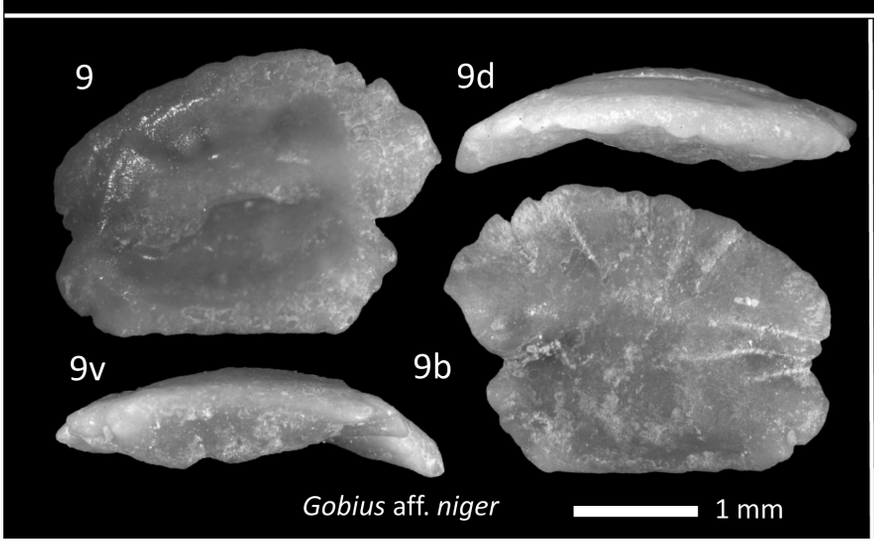
9
9d
9v
9b
*Gobius* aff. *niger*
1 mm

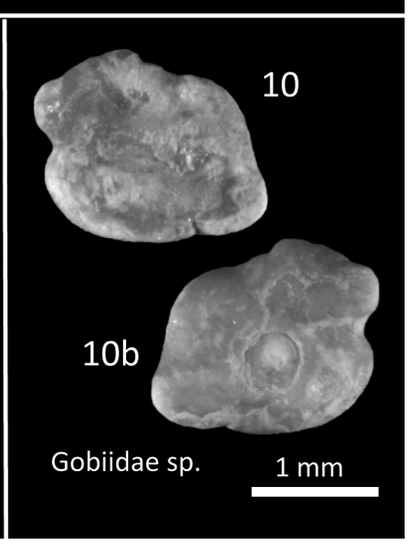
10
10b
Gobiidae sp.
1 mm

**Plate 23**

postero-ventral angle, lacks the predorsal extension, and has a markedly wide ostium.

***Gobius lombartei* nov. sp.**
Plate 24, figs 1-5

*Holotype* – RGM.1390651, Velerín Conglomerates.

*Paratypes* – 2 sagittas: RGM.1390652, RGM.1390653. Río del Padrón 1; Velerín Conglomerates 1.

*Other material* – 24 sagittas. Río del Padrón 1; El Lobillo 1; Velerín Conglomerates 7; Velerín Sandy Lens 5; Velerín Antena Hilltop 10.

*Locus typicus* – Velerín Quarry, close to Velerín Antena, along Camina Nicolas, Velerín, Estepona, province of Málaga, Spain.

*Stratum typicum* – Middle Pliocene, Piacenzian, fossiliferous medium- to fine-grained sands.

*Etymology* – Named after Dr A. Lombarte for his contributions to the identification of extant otoliths of Mediterranean fishes.

*Diagnosis* – Thin, rhomboid otoliths with obtuse rounded post-ventral and predorsal angles (110-115°), up to 5.75 mm in size. The prominent postdorsal projection makes a distinct outward angle with the straight dorsal rim. The preventral projection is prominent and pointed; above it the anterior rim displays a small concavity. Rims are smooth, sometimes with shallow undulations. The colliculum is slender with a constant height and – in adult specimens – lies at the ventral side of a wide bi-lobed sulcus.

*Description* – The holotype is a rhomboid otolith with a distinctly pointed preventral projection and a postdorsal sheet-like projection that is prominently outwardly bent. When viewing the inner face, the postdorsal projection forms one straight line with the rest of the dorsal rim, while it forms a distinct outward angle in ventral view. The posterior and anterior rims make a 65-70° angle with the ventral rim. The anterior rim is straight except for a concavity above the pointed preventral extension. The posterior rim runs parallel with two undulations. In juvenile specimens the outline is still dominated by the marked post-dorsal and antero-ventral extensions, but the upper anterior and the lower posterior rims are more vertical.
The inner face is convex. It becomes puffy in older specimens because of swelling around the sulcus. In smaller specimens the sulcus is long and slender. With increasing age, the sulcus widens particularly in dorsal direction into a bi-lobed depression that is narrowed in the centre of both the superior and inferior sides at the transition between ostium and cauda. This is paralleled by a thickening of the surface around the sulcus. The original colliculum structure does not follow the overall widening of the sulcus but remains at the ventral side of the deepened sulcus. In contrast to otoliths of most other *Gobius* species the height of the colliculum is constant along the ostium and cauda with no significant ostial lobe. It is pointed at the anterior end of the ostium and rounded at the posterior end of the cauda. Along the anterior part of the cauda a small elongate-oval iugum lies along the crista inferior.
The outside of the otoliths displays several elevations which are caused by folds running from the postdorsal end and the preventral point towards the centre and in older specimens also by a thickening of the postventral outer part. The otoliths are thin and vulnerable for mechanical erosion, particular at their (pre)dorsal part (see Pl. 24, fig. 2), and polishing of the inner side as seen in Pl. 24, figs 3,5. The original shape of the specimen depicted on Pl. 24, fig. 2 can be deduced from the growth lines visible on the outside (Pl. 24, fig. 2b). A few very small rhomboid otoliths (one depicted on Pl. 24, fig. 4) probably belong to the same species.

*Remarks* – The slender nature of the sulcus colliculum and its ventral localisation within the sulcus of adult specimens matches best with otoliths of *G. paganellus* and *G. cobitis*, two *Gobius* species that branch off 'early' in a molecular phylogenetic study (Iglésias *et al*., 2021), but both have a firm rectangular body with no pointed or a cut preventral extension (Reichenbacher & Cappetta, 1999, pl. 6, figs 3B-C; Lombarte *et al*., 2018; Gut *et al*., 2020) rather than the rhomboid shape of *G. lombartei*. In addition, the maximum size of the latter is larger than presently known for the extant counterparts. Lombarte *et al*. (2006) figure an otolith (OL=4.0 mm) of a 13.7 cm sized extant *G. paganellus*, which meets the maximum length of this extant species. For a 19.5 cm sized *G. cobitis* (max. length 27 cm) the OL amounted to 4.3 mm (Lombarte *et al*., 2006). However, at adult size otoliths of *P. cobitis* have a very irregular dorsal outline (Bauzá Rullán, 1962, pl. 5, figs 48-50; Lombarte *et al*., 2006; Nolf, 2018) while they are only square in smaller specimens (Lombarte *et al*., 2006; Schwarzhans *et al*., 2020b; Gut *et al*., 2020). The largest otolith of *G. lombartei* (OL=5.75 mm) does neither fit with the maximum size of *G. paganellus*, nor does its regular shape fit with those of large *G. cobitis*. The younger specimens of *G. lombartei* differ from the two extant gobiids by their slender sulcus.

*Distribution* – *Gobius lombartei* is encountered in Pliocene deposits of Estepona (Río del Padrón) and the Velerín Conglomerates.

**Plate 24**

Figures 1. ***Gobius lombartei* nov. sp.,** holotype, Velerín Conglomerates.
Figures 2-3. ***Gobius lombartei* nov. sp.,** paratypes, Río del Padrón.
Figures 4-5. ***Gobius lombartei* nov. sp.,** Velerín Conglomerates.
Figure 6. ***Thorogobius mirbachae* nov. sp.,** holotype, Velerín Quarry.

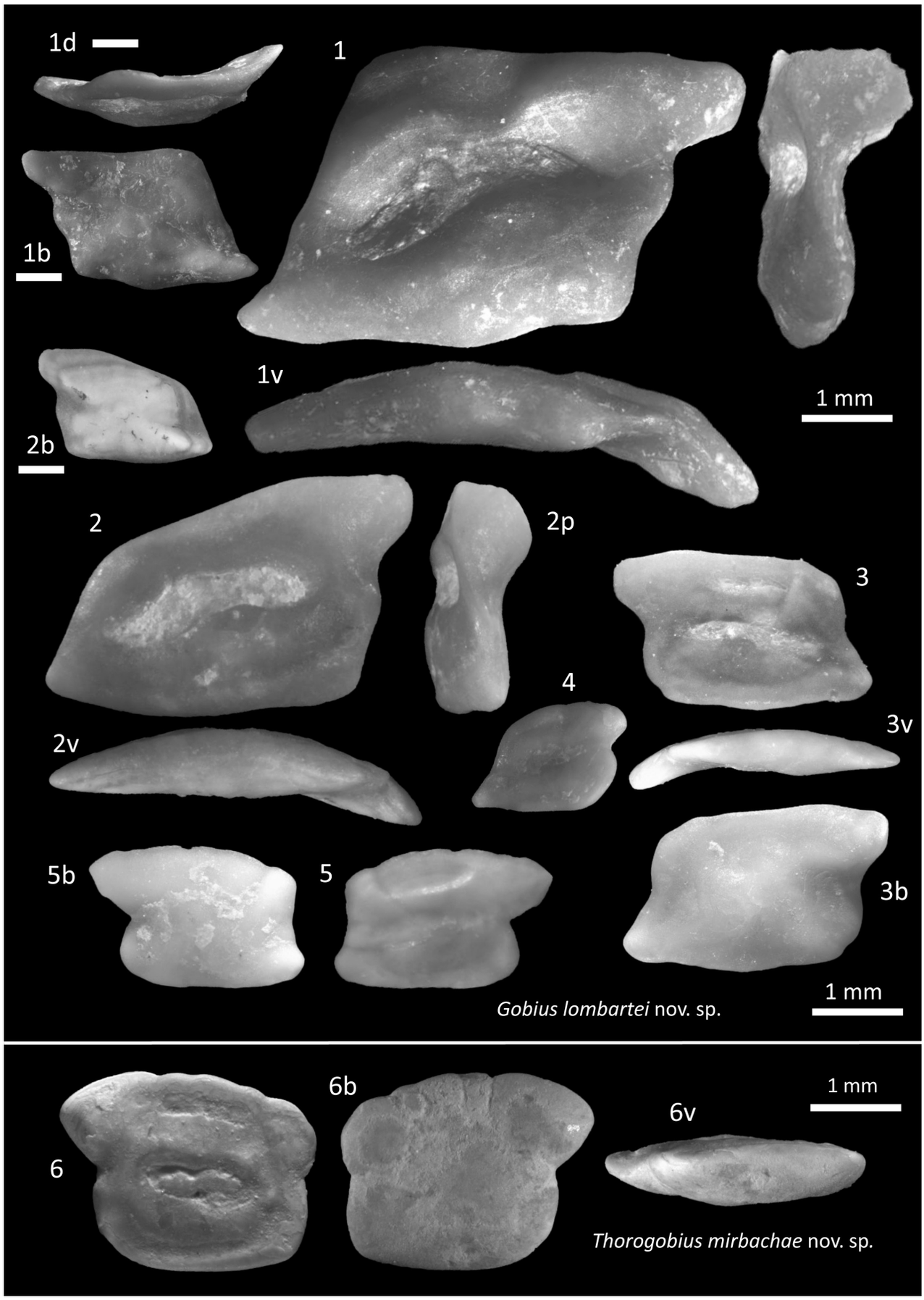
1d
1
1b
1v
1 mm
2b
2
2p
3
4
2v
3v
5b
5
3b
1 mm
*Gobius lombartei* nov. sp.
6b
1 mm
6v
6
*Thorogobius mirbachae* nov. sp.

**Plate 24**

***Gobius vittatus* Vinciguerra, 1883**
Plate 21, fig. 10

2020 *Gobius vittatus* – Gut *et al*., figs 4d-f (present-day otoliths).

*Material* – 2 sagittas. Velerín Antena Slope 1; Parque Antena 1.

Description – Small *Gobius* otolith with a somewhat rhomboid shape. Ventral and dorsal rims are regularly curved. Dorsal rim with a bluntly pointed postdorsal projection. The otoliths display a 'waist-line', formed by the concavities in the anterior and posterior rims. Mid-anterior rim is slightly concave and connected to a blunt antero-ventral projection, which is less prominent than the dorso-posterior one. The inner face is relatively flat, the outer face is ornamented with rounded knobs and markedly convex.

***'Gobius' pterois* nov. sp.**
Plate 25, figs 4-7

1994 ?*Mesogobius* sp. – Nolf & Cavallo, pl. 8 fig. 7.
2006 *Callogobius* sp. – Nolf & Girone, pl. 2, figs 4, 5.

*Holotype* – RGM.1390659, El Lobillo.

*Paratypes* – 3 sagittas RGM.1390660-RGM.1390662. Velerín Conglomerates 1; El Lobillo 2.

*Other material* – 19 sagittas. El Lobillo 5; Velerín Conglomerates 13.

*Locus typicus* – Zanclean material from a site called El Lobillo, which was exposed on the surface of a small, ploughed field.

*Stratum typicum* – Upper Zanclean sands.

*Etymology* – Named after its winged extension caused by the combined postdorsal angle and postdorsal projection.

*Diagnosis* – Rectangular *Gobius*-type otoliths (OL up to 3.2 mm; OL:OH=1.43-1.49) that are characterised by a small blunt preventral projection and significant postdorsal flap. The latter represents the bluntly pointed posterior projection joined with a high postdorsal angle. Some variability is observed in the extent of the postdorsal extension. The outer face is smooth, while the iugum along the central inferior part of the sulcus is indicative for the genus *Gobius*.

*Description* – Mainly from El Lobillo and Velerín Conglomerates a series of otoliths is present with variable properties, in particular with respect to their (post)dorsal extension. The otoliths are characterised by an elongate shape (OL:OH=1.43-1.49), a small blunt preventral projection, and a highly variable postdorsal projection. Above the pre-ventral projection the anterior rim runs vertically upward until it connects to the dorsal rim forming a blunt predorsal angle. The dorsal rim is straight (Pl. 25, figs 1, 3-5) or – as in Pl. 25, fig. 2 – interrupted by a marked concavity anterior of the postdorsal angle. The postdorsal angle projects to the middle of the cauda. From the postdorsal angle, the shape of the rim is defined by the variable postdorsal extension, that projects posteriorly without outward bending. The posterior rim is divided by a concavity that separates the dorso-posterior extension and a lower part that start perpendicular to the basis, but usually has been cut obliquely. The sulcus is sole-shaped with a distinct ostial lobe and a small iugum lining the antero-inferior side of the cauda. The shape of the iugum varies between granular, oval and small rod, but it is not clear whether this is related to ontogenetic factors or points to the existence of a multi-species complex. The inner side is slightly convex by a circum-sulcular thickening, which is bordered by a prominent ventral furrow and an elongate dorsal depression.

*Discussion* – A similar specimen has been reported by Nolf & Girone (2006, pl. 2, fig. 5) from the Zanclean of Montaldo Roero as *Callogobius* sp., the identification of which was based on a comparison with the extant *Callogobius maculipinnis* (Fowler, 1918) (see Nolf & Girone, 2006, pl. 10, figs 1-3). Although *Callogobius* is represented by *Callogobius weileri* (Bauzá Rullán, 1955) in the Mediterranean Pliocene, including at Estepona (Pl. 25, fig. 11), we place our specimens in the genus *Gobius* as the iugum along the sole-shaped sulcus and postdorsal extension matches better with this genus than with *Callogobius* otoliths with their central and hardly divided sulcus. We acknowledge that – in the light of a hypervariable postdorsal extension – there is also some resemblance with *Chromogobius zebratus* (Steindachner, 1863) specimens, particularly for the small specimen, but the former lack a iugum.

**Plate 25**

Figures 1-3. ***Thorogobius truncatus*** (Schwarzhans, 1978), Velerín Conglomerates (1, reversed), Río del Padrón (2), Velerín Quarry (3).
Figures 4, 6-7. ***'Gobius' pterois* nov. sp.,** paratypes**,** Velerín Conglomerates (4, reversed), El Lobillo (6, 7).
Figure 5. ***'Gobius' pterois* nov. sp.,** holotype**,** El Lobillo.
Figure 8. ***Chromogobius* cf. *zebratus*** (Kolombatović, 1891), El Lobillo.
Figures 9-10. ***Chromogobius britoi*** Van Tassel, 2001, Río del Padrón.
Figure 11. ***Callogobius weileri*** (Bauzá Rullán, 1955), Río del Padrón.

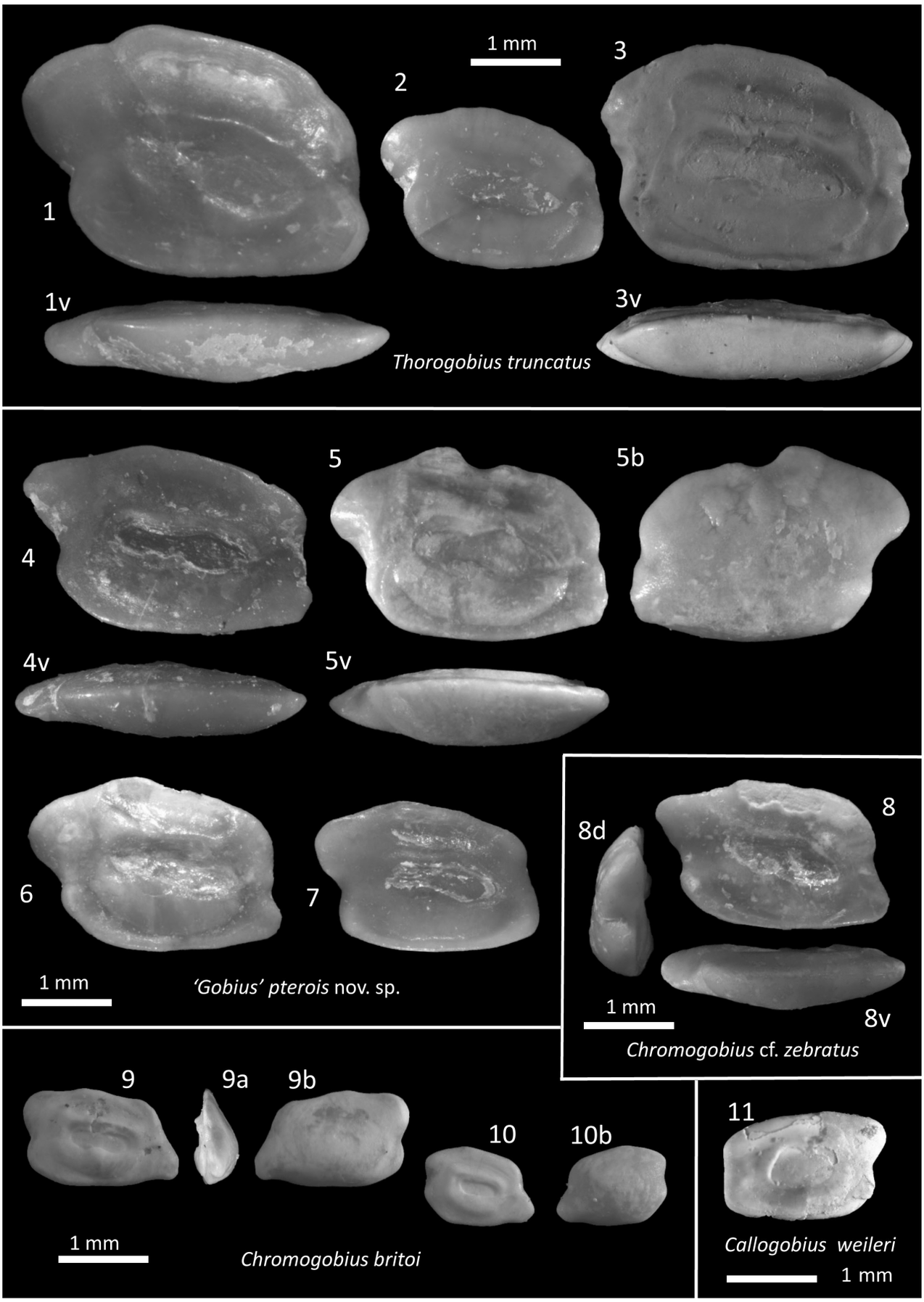
1 mm
1
2
3
1v
3v
Thorogobius truncatus
4
5
5b
4v
5v
6
7
1 mm
'Gobius' pterois nov. sp.
8
8d
1 mm
8v
Chromogobius cf. zebratus
9
9a
9b
10
10b
1 mm
Chromogobius britoi
11
Callogobius weileri
1 mm

**Plate 25**

Genus *Thorogobius* Miller, 1969

***Thorogobius mirbachae* nov. sp.**
Plate 24, fig. 6

*Holotype* – RGM.1390664, Velerín Quarry 1.

*Locus typicus* – Velerín Quarry, close to Velerín Antena, along Camina Nicolas, Velerín, Estepona, province of Málaga, Spain.

*Stratum typicum* – Middle Pliocene, Piacenzian, fossiliferous medium- to fine-grained sands.

*Etymology* – Named after Tanja Schulz-Mirbach (Systematic Zoology, Department of Biology II, LMU, Munich) for her contribution to the understanding of the physiological role of otoliths in fish.

*Diagnosis* – Compact otolith (OL=2.85 mm; OH=2.22; OT=0.85 mm; OL:OH=1.28) with an almost square body (without postdoral projection: 'OL':OH=1.10) and a straight and posteriorly pointed dorsal projection. Sulcus almost horizontal and divided in ostium and cauda with small, almost equal colliculi embedded in a broader sulcus and no ostial angle. Ostium with a minor ostial angle. No iugum.

*Description* – Medium-sized compact otolith with an almost square body and a slightly oblique (inclining in posterior direction) dorsal rim that continues as a dorsal lining of a prominent and bluntly pointed postdorsal projection. The OL:OH is 1.28 (without postdoral projection: 'OL':OH=1.10). The mid-dorsal rim has a few minor lobes, the other rims are smooth. The inner face is slightly convex and becomes flat at the dorsal depression. The compact sulcus is divided in ostium and cauda which are of similar length and comparable width. The sole-shaped sulcus has a small inclination (8°); the ostium has a minor ostial lobe. No iugum is present. The outer face is strongly convex along the rims and displays a slightly concave area in the middorsal part of the otolith. The thickness of the otolith is rather constant (OT=0.85 mm; OH:OT=2.6).

*Remarks* – No extinct or extant species of *Thorogobius* from the Mediterranean or central eastern Atlantic is known to us with otoliths of similar properties as those of *Thororogobius mirbachae.* Among extant *Thorogobius* species from SE Atlantic waters off Angola considerable variation is seen between between their otolith properties (see Schwarzhans *et al*., 2020a for iconography). Among them, *Thorogobius rofeni* Miller, 1988 has several characteristics in common with *T. mirbachae*, in particular the strongly square shape, the absence of outward bending as visible in dorsal or ventral view, the sulcus equally divided in ostium and cauda, and the absence of a iugum. *T. rofeni* also diplays important features that differ from *T. mirbachae*, in particular a more horizontal dorsal rim with the highest point in the blunt predorsal projection, a depressed middorsal part and an upwards orientated dorsal projection, while *T. mirbachae* has a rounded pre- and mid-dorsal rim with a posteriorly orientated dorsal projection The predorsal depression associated with the predorsal projection in *T. roheni* is also lacking in *T. mirbachae.*
*Thorogobius mirbachae* also differs from the Pliocene *T. truncatus* (Schwarzhans, 1978) (Pl. 25, figs 1-3), which has a lower predorsal angle, a more elongate shape and sulcus, and a round postdorsal extension that is inserted at a lower level of the posterior rim than in *Thorogobius mirbachae,* where it forms a continuation of the dorsal rim. These differences are not ontogentically related, because *Thorogobius truncatus* is present in our material in a range of sizes fully covering the size of the *T. mirbachae* specimen. None of the otoliths of a series of *Thorogobius* species that are figured by Schwarzhans (2020a) match with the specimen here described. It differs from the Late Miocene *T. petilus* Schwarzhans, Agiadi & Carnevale, 2020 in the dorsal rim, the higher situated notches on the anterior and posterior rims, being thicker, and the straighter ventral rim.

***Thorogobius truncatus* (Schwarzhans, 1978)**
Plate 25, figs 1-3

| | |
|---|---|
| 1978 | *Gobius truncatus* – Schwarzhans, figs 119, 120, 146. |
| 1998 | *Gobius truncatus* – Nolf, Mané & Lopez, pl. 7, fig. 11. |
| 2020b | *Thorogobius truncatus* – Schwarzhans, Agiadi & Carnevale, figs 11A-C. |

*Material* – 45 sagittas. Río del Padrón 3; El Lobillo 4; Velerín Carretera 8; Velerín Conglomerates 6; Velerín Quarry 6; Velerín Antena Sandy Lens 15; Velerín Antena Hilltop 3.

*Remarks* – The holo- and a paratype of *T. truncatus,* both 3.75 mm long, have length:height ratios of OL:OH=1.29-1.34 (Schwarzhans, 1978); a smaller specimen of 2.1 mm also has an OL:OH=1.30 (Schwarzhans *et al*., 2020a, figs 11A-C). The oblique sulcus has no ostial lobe and no iugum. The preventral rim projects at the level of the nearly straight preventral angle causing a blunt anterior rim. A wide postdorsal extension – that bends not or only slightly outward – covers more than half of the posterior rim. A notch marks its connection to the remainder of the dorsal rim.
Within our Pliocene population we find several specimens that meet the criteria of *Thorogobius truncatus* (Pl. 24, figs 1-3; OL:OH=1.34-1.41) as well as another group close to it but differing in important properties such as a larger OL:OH ratio and the presence a iugum and a pointed extended preventral extension. They are presented as *'Gobius' pterois.*

Genus *Chromogobius* de Buen, 1930

***Chromogobius britoi* Van Tassell, 2001**
Plate 25, figs 9-10

2020a *Chromogobius britoi* – Schwarzhans, Brzobohatý & Radwanska, pl. 6, figs 1a-c (present-day otolith).

*Material* – 4 specimens: Río del Padrón 4 (one with damaged inner side).

*Description* – Very small otoliths characterised by a rectangular shape with a spout-shaped antero-ventral extension and a largely straight ventral rim. The posterior rim has a shallow concavity in its middle adjacent to the round postdorsal extension. The dorsal rim has a pre- and a mid- to post-dorsal angle. The inner face is rather flat but with a swollen area around the sulcus. The short median sulcus is keyhole-shaped with a constant diameter and only slightly narrowed at the middle of the inferior crista. The sulcus is embedded in a ring-shaped perisulcular thickening, which is largest ventrally and narrow at the dorsal side where it also borders a dorsal field. The outside is very thick at the ventral side. This thickness tapers towards the dorsal rim, while it forms a round margin at the ventral rim, as visible in the anterior view (Pl. 25, fig. 9a).

*Remarks* – After comparing with the otoliths of the three *Chromogobius* species known from the Mediterranean Sea and eastern Atlantic Ocean today, we conclude that these small specimens match best those of present-day *Chromogobius britoi* (depicted in Schwarzhans *et al*., 2020a, pl. 3). They differ from the other *Chromogobius* species by the rounded postdorsal angle that hardly extends beyond the rectangular body of the otolith, and the thickset ventral outside. Extant *Gobius britoi* is known from Portuguese waters but presently not from the Mediterranean Sea.

***Chromogobius* cf. *zebratus* (Steindachner, 1863)**
Plate 25, figs 8

2020 *Chromogobius zebratus* – Agiadi *et al*., figs 3.b-c.
2020b *Chromogobius zebratus* – Schwarzhans, Agiadi Carnevale, figs 11I-K.

*Material* – 6 sagittas. El Lobillo 3, Velerín Conglomerates 2; Velerín Quarry 1.

*Description* – Elongate otoliths (OL:OH=1.51-1.59) which are about 1.5-2.0 times as large as the otoliths of *C. britoi*. They display a blunted or pointed pre-ventral projection and a prominent pointed postdoral extension. Furthermore, a thickening of the ventral outside exists, but it is less than in *C. britoi*. In posterior view (Pl. 25, fig. 8p) the thickness of the otolith is rather constant. The otoliths show a high resemblance with various *C. zebratus* specimens on the AFORO site (Lombarte *et al*., 2006), albeit they are larger. The maximum size of *C. zebratus* fish otoliths is almost double that of those of *C. britoi*, in line with a similar double size of the Pliocene otoliths, and its dorsal and anterior rims are straighter. An adequate ontogenetic series can further underpin the identification.

Family Pomacentridae Bonaparte, 1831
Genus *Chromis* Cuvier, 1814

***Chromis chromis* (Linnaeus, 1758)**
Plate 26, fig. 1-6

2008 *Chromis chromis* – Tuset *et al*., fig. 67:A1-A3.

*Material* – 24 sagittas. Río del Padrón 8; El Lobillo 15; Velerín Conglomerates 1.

*Remarks* – Small elliptical otoliths with a broad pointed rostrum, a lobate dorsal rim with – except in juvenile specimens – a prominent middorsal angle. The ventral rim is faintly crenulated; it is regularly curved without a midventral angle. The ostium widens anteriorly; the cauda bends at its posterior end towards the post-ventral rim. The specimens belong to the genus *Chromis* and – judging from a range of extant species from the Mediterranean and eastern Atlantic *Chromis* – they fit those of *Chromis chromis*. One specimen from Velerín Conglomerates (Piacenzian) has a reduced dorsal area as compared to the other specimens from Río del Padrón and El Lobillo (Zanclean). It is uncertain whether this reflects an ontogenetic or a specific difference. To the best of our knowledge this is the first report on the presence of the genus *Chromis* in the Pliocene.

Family Mugulidae Jarocki, 1822

**Mugilidae indet. 1 and 2**
Plate 26, figs 7-8

*Material* – Mugilidae indet. 1: 1 sagitta, Velerín Conglomerates (Pl. 25, fig. 7). Mugilidae indet. 2: 1 sagitta, Velerín Quarry (Pl. 25, fig. 8).

*Remarks* – Mugilidae indet. 1 is represented by the half (5 mm) of an adult otolith. It is related to the genera *Chelon* Artedi, 1793 and *Mugil* Linnaeus, 1758. Mugilidae indet. 2 is a small more intact otolith, with a characteristic ventral lining and thinning of the posterior part. Its inner side is convex. Its outside is concave and with a fold at the beginning of the postero-ventral tapering. Mugilidae indet. has been reported from the Zanclean of Monticello d'Alba, northern Italy (Nolf & Cavallo, 1994, pl. 7, fig. 8). Mugilidae usually live close to river mouths.

Family Atherinidae Risso, 1827
Genus *Atherina* Linnaeus, 1758

***Atherina presbyter* Cuvier, 1829**
Plate 26, figs 9-14

1994 *Atherina* sp. – Nolf & Cavallo, pl. 5 fig 8.
2009 *Atherina presbyter* – Nolf, pl. 41.

*Material* – 43 sagittas. Río del Padrón 3; El Lobillo 17; Velerín Carretera 9; Velerín Conglomerates 4; Velerín Quarry 5; Velerín Antena Slope 2; Velerín Antena Hilltop 3.

*Remarks* – Most of these *Atherina* specimens represent *A. presbyter*, but interspecific differences are small for this genus. One small *Atherina* specimen from Velerín Carretera (Pl. 26, fig. 14) has a narrow, slightly bent sulcus that reaches to the posterior rim. The length of the otolith is biggest at the dorsal part just above the sulcus and shortens from there to the ventral rim. *'Atherinidarum' bavayi* Steurbaut, 1984 was originally described from the Miocene of France and has been reported from Zanclean deposits in Italy (Nolf & Girone, 2006). However, this species differs from *Atherina* sp. by a more rounded oval shape and (often) the presence of a small middorsal denticle (Steurbaut, 1984).

Family Bothidae Schmitt, 1892
Genus *Arnoglossus* Bleeker, 1862

***Arnoglossus quadratus* Schwarzhans, 1999**
Plate 27, figs 4-6

1999 *Arnoglossus quadratus* – Schwarzhans, p. 174-175 figs 365-373.

*Material* – 4 sagittas. Río del Padrón 1; Velerín Conglomerates 1; Velerín Quarry 1; Velerín Antena Hilltop 1.

*Remarks* – Schwarzhans (1999) reported the presence of *Arnoglossus quadratus* in lower Pliocene sediments of NW Morocco. The otoliths that we attribute to this species (Pl. 29, figs 4-6) have a similar outline as those identified as *A. kokeni* Bassoli, 1906 (Pl. 29, figs 7-8), but they are more elongate (1.32-1.50 *vs*. 1.16-1.19), and differ by a lower ostium:cauda index (OsL:CaL=0.93-1.04 *vs.* OsL:CaL=2.00-2.45 in *A. kokeni*). Nolf (2013) considered *A. quadratus* identical to *A. kokeni* without further explanation, but the differences of *A. quadratus* with *A. kokeni* are larger than those between *A. kokeni* and *A. laterna* (Walbaum, 1792) (OL:OH=1.31 and OsL:CaL=1.69), which was also retrieved from the Velerín area (Pl. 29, fig. 9). We noticed that all our *A. quadratus* specimens are left sagittas (Pl. 29, figs 4-6). According to Schwarzhans (1999), *A. quadratus* does not show side-dimorphism. As two of the *Arnoglossus* species regard extinct species, final judgement of their nature will need larger populations of well-preserved sagittas.

Family Trichiuridae Rafinesque, 1810
Genus *Benthodesmus* Goode & Bean, 1882

***Benthodesmus elongatus* Clark, 1879**
Plate 28, figs 4-5

1998 *Benthodesmus elongatus* – Nolf, Mané & Lopez, pl. 6, figs 11-12.

*Material* – 2 sagittas. Velerín Quarry 2.

*Remarks* – *Benthodesmus elongatus* was reported from Zanclean deposits of Papiol (Catalunya, Spain) (see Nolf *et al*., 1998, pl. 6, figs 11-12, also for iconography of present-day *B. elongatus*). The otoliths from Velerín Conglomerates are very similar in characteristics and size to the specimen from Papiol. All three are very similar to the extant otolith.

Family Ammodytidae Bonaparte, 1835
Genus *Gymnammodytes* Duncker & Mohr, 1939

***Gymnammodytes cicerelus* (Rafinesque, 1810)**
Plate 28, fig. 3

2006 *Gymnammodytes cicerelus* – Lombarte *et al*., figs 7639, 6619, 10198 (present-day otoliths).

*Material* – 1 sagitta. Velerín Conglomerates.

*Description* – The otolith is characterised by its rectangular shape with an antirostrum and probably a rostrum that has been broken. Furthermore, it has a slightly convex dorsal rim that displays a postdorsal concavity with a blunt and vertical posterior rim. The ventral rim is almost

**Plate 26**
Figures 1-6. ***Chromis chromis*** (Linnaeus, 1758), Velerín Conglomerates (1), Río del Padrón (2), El Lobillo (3-6).
Figure 7. **Mugilidae indet**. **1**, Velerín Conglomerates.
Figure 8. **Mugilidae indet**. **2**, Velerín Quarry.
Figures 9-14. ***Atherina presbyter*** Cuvier, 1829, Velerín Conglomerates (9), Velerín Carretera (10, 13, 14), El Lobillo (11), Velerín Quarry (12).
Figure 15. ***Exocoetes volitans*** Linnaeus, 1758, Velerín Quarry.
Figures 16-17. ***Tylosaurus acus*** (Lacepède, 1803), El Lobillo (16), Velerín Conglomerates (17).
Figures 18-21. ***Trachurus* sp.,** Velerín Conglomerates (20,21), Velerín Quarry (18), Velerín Antena Slope (19).

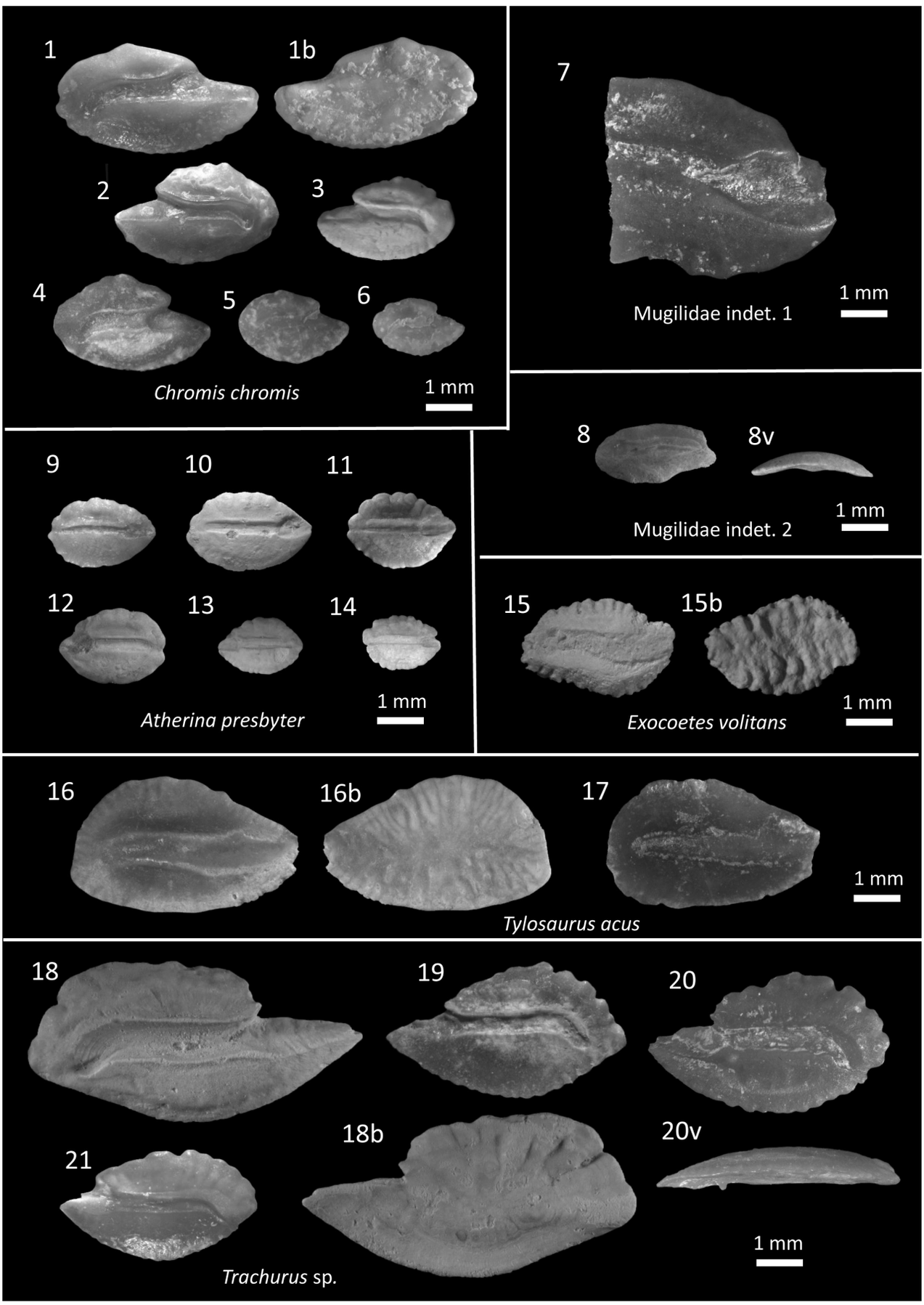
1
1b
2
3
4
5
6
Chromis chromis
1 mm
7
Mugilidae indet. 1
1 mm
8
8v
Mugilidae indet. 2
1 mm
9
10
11
12
13
14
Atherina presbyter
1 mm
15
15b
Exocoetes volitans
1 mm
16
16b
17
Tylosaurus acus
1 mm
18
19
20
18b
20v
21
Trachurus sp.
1 mm

**Plate 26**

straight along the middle but upward curved toward the rostrum and posterior rim.

*Remarks* – These features can be observed in part in otoliths of G*ymnammodytes cicerelis* and *G. semisquamatus* Jourdain, 1879. We are not aware of earlier fossil records of *Gymnammodytes* otoliths in the Mediterranean. Presently, three extant *Gymnammodytes* species are known. *Gymnammodytes cicerelus* is a subtropical Mediterranean and eastern Atlantic representative, *G. semisquamatus* lives in temperate waters around Great Britain and Ireland, including the North Sea, while *G. capensis* (Barnard, 1927) is confined to South Africa. Our specimen matches well with the general outline of part of the specimens of *G. cicerelus* (Lombarte *et al.*, 2006), but there is an overlapping interspecific variation with *G. semisquamatus* otoliths (Lombarte *et al*., 2006).

Family Trachinidae Rafinesque, 1815
Genus *Trachinus* Linnaeus, 1758

***Trachinus* sp.**
Plate 28, figs 7-8

*Material* – 5 sagittas. Velerín Conglomerates 5.

*Discussion* – Among the *Trachinus* otoliths of Velerín Conglomerates several strikingly thick specimens are present (Pl. 28, figs 7-8). They are characterised by a thick appearance, due to a high convexity of both the inner and outer surfaces, and by a strongly sigmoid sulcus that lies in the upper half of the otolith's inner face, but is still separated from the dorsal rim by an elongated dorsal depression. The posterior rim is obliquely and bluntly pointed at the connection to the ventral rim.
*Trachinus* sp. otoliths are more compressed, more thickset, and display a higher sigmoidity of the sulcus than those of *Trachinus draco* Linnaeus, 1758 or *T. radiatus* Cuvier, 1829 (see Lombarte *et al*., 2006 for iconography). The thick appearance is similar to otoliths of extant *Trachinus armatus* Bleeker, 1861 and *T. linoleatus* Fischer, 1885, which differ by a sulcus that is less sigmoidal, particularly the caudal part, and that lies closer to the dorsal rim (see Schwarzhans, 2019d for iconography). However, all specimens show signs of mechanical polishing. Therefore, although the specimens may represent another *Trachinus* species, better preserved material is needed for a final identification.

Family Uranoscopidae Bonaparte, 1831
Genus *Uranoscopus* Linnaeus, 1758

***Uranoscopus scaber* Linnaeus, 1758**
Plate 28, fig. 10

2006 *Uranoscopus scaber* – Nolf & Girone, pl. 2, fig. 13.
2010 *Uranoscopus scaber* – Nolf & Girone, figs 12.a1-a4.

*Material* – 2 sagittas. Velerín Conglomerates 2.

*Discussion* – Two specimens (one depicted on Pl. 28, fig. 10) match the shape of otoliths of the extant *Uranoscopus scaber*. Girone *et al*. (2010, figs 12a1-a4) provide an ontogenetic series of extant *Uranoscopus scaber* specimens. The oldest specimen is markedly higher than the younger ones (OL/OH=1.60 *vs*. OL/OH=1.8-2.2).

***Uranoscopus* sp.**
Plate 28, fig. 11

*Material* – 1 sagitta. Velerín Conglomerates 1.

*Description* – We retrieved another, but massive uranoscopid specimen from Velerín Conglomerates (Pl. 28, fig. 11; OL=8.2 mm; OL/OH=1.43; OT=2.5 mm), which is a high oval otolith that markedly surpasses the ontogenetic series of *Uranoscopus scaber* Linnaeus, 1758 reported by Girone *et al*. (2010) (see under *U. scaber*). Its median sulcus is divided in an ostium and a much smaller cauda. The preventral rim curls upward, to slightly above the level of the sulcus. A long sigmoid ostial channel connects the ostium to the anterior rim. Under the sulcus of the otolith a ventral thickening exists that is bordered by a ventral furrow. A dorsal field displays superficial furrows that are orientated parallelly in antero-dorsal direction.
The outer face is thicker at its ventral side than along the dorsal rim and displays a depression in the centre of the outer face. It is smooth with several furrows perpendicular to the dorsal rim.

*Discussion* – To the best of our knowledge, this specimen has no extant equivalent. Our specimen differs from otoliths of *U. scaber* by its size and height, the high ostium:cauda ratio and the ostial channel. Within a series

**Plate 27**

Figures 1-2. ***Lepidorhombus whiffiagonis*** (Walbaum, 1792), Velerín Conglomerates (1), Velerín Carretera (2).
Figure 3. ***Lepidorhombus boscii*** (Risso, 1810), Velerín Conglomerates.
Figures 4-6. ***Arnoglossus quadratus*** Schwarzhans, 1999, Velerín Antena Hilltop (4), Velerín Conglomerates (5), Río del Padrón (6).
Figures 7-8. ***Arnoglossus kokeni*** (Bassoli, 1906), Velerín Carretera (7), Velerín Quarry (8).
Figure 9. ***Arnoglossus laterna*** (Walbaum, 1792), Velerín Conglomerates.
Figures 10-11. ***Buglossidium luteum*** (Risso, 1810), Velerín Carretera.
Figure 12. ***Citharus* cf. *linguatula*** (Linnaeus, 1758), Velerín Conglomerates.
Figures 13-15. ***Microchirus variegatus*** (Donovan, 1802), El Lobillo (13, 15) Velerín Carretera (14).
Figure 16. ***Solea* sp.**, Río del Padrón.

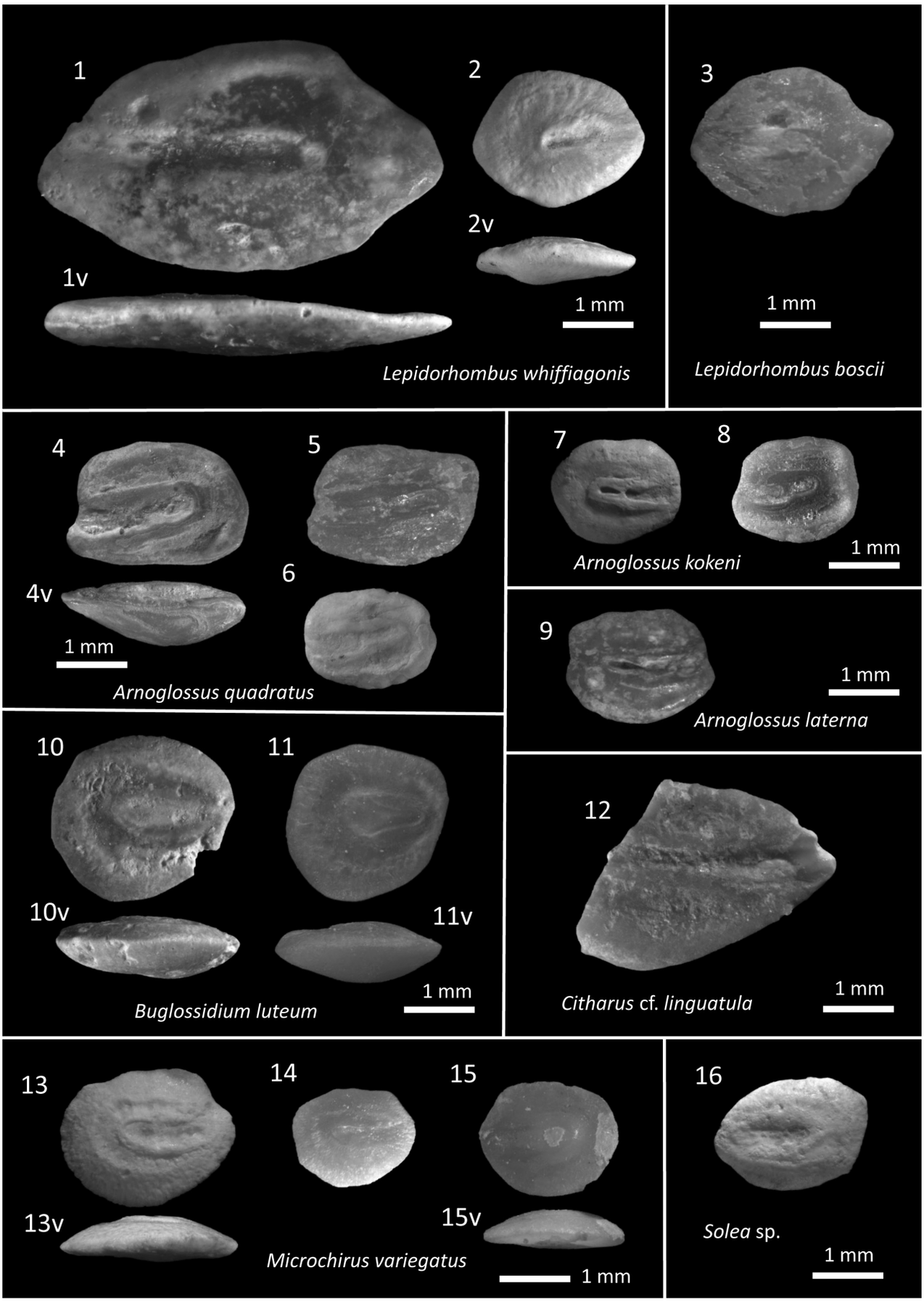
1
2
2v
1v
1 mm
Lepidorhombus whiffiagonis
3
1 mm
Lepidorhombus boscii
4
5
6
4v
1 mm
Arnoglossus quadratus
7
8
1 mm
Arnoglossus kokeni
9
1 mm
Arnoglossus laterna
10
11
10v
11v
1 mm
Buglossidium luteum
12
1 mm
Citharus cf. linguatula
13
14
15
13v
15v
Microchirus variegatus
1 mm
16
Solea sp.
1 mm

**Plate 27**

of otoliths of extant Uranoscopidae specimens reported by Schwarzhans (2019d, pl. 4, figs 17-31) we found no present-day equivalent. *Uranoscopus albesca* Regan, 1915 shows a similarity in outline and thickness, albeit that it is most thickset at its outer face, and differs by a closed non-divided sulcus. It is likely that *Uranoscopus* sp. represents another unknown species within the Uranoscopidae family.

Family Labridae Cuvier, 1816
Genus *Bodianus* Bloch, 1790

***Bodianus scrofa* (Valenciennes, 1839)**
Plate 28, fig. 12

*Material* – 1 sagitta. Velerín Antena Hilltop 1.

*Remarks* – This is the first report of the genus *Bodianus* in the Pliocene. The single specimen has many characteristics in common with published figures of otoliths of *Bodianus* species like *Bodianus bilunulatus* (Lacepède, 1801) from South Africa (Smale *et al*., 1995, pl. 114), but small differences in relative dimensions exist. Our specimen fits very well with an otolith of *Bodianus scrofa* (collection D. Nolf, RBINS, Brussels). *Bodianus scrofa* presently lives along islands in the eastern Atlantic Ocean from Madeira to Cape Verde Islands.

Family Acropomatidae Gill, 1893
Genus *Verilus* Poey, 1860

***Verilus mutinensis*** (Bassoli 1906).
Plate 29, figs 1-4

1906 Ot. (Sparidarum) *mutinensis* – Bassoli, pl II, fig. 36.
1971 *Neoscombrops praeannectens* – Weiler, pl. 9, figs 105-106.
1980 *Parascombrops* aff. *pseudomicrolepis* – Nolf & Martinell, pl. 4, figs 7-8.
1998 *Parascombrops mutinensis* – Nolf, Mané & Lopez, pl. 6, figs 6-8.
2017 *Verilus mutinensis* – Schwarzhans & Prokofiev, pl. 33, figs L,M.
2018 *Verilus mutinensis* – Agiadi *et al*., figs 5.50-52.

*Material* – 6012 sagittas. Río del Padrón 164; El Lobillo 180; Velerín Carretera 575; Velerín Conglomerates 1005; Velerín Sandy Lens 64; Velerín Quarry 3425; Velerín Antena Slope 324; Velerín Hilltop 265; Parque Antena 10.

*Remarks* – Otoliths of *Verilus mutinensis* are among the most frequently encountered in Estepona, particularly in the Piacenzian deposits around Velerín (see Table 1). In the past, several authors have proposed name changes to better define this species within a group of related Acropomatidae. In a review of the morphology of extant oceanic Acropomatidae including a comparison of otoliths of extant species with those of related fossil otoliths, Schwarzhans & Prokofiev (2017) concluded that the extinct species belongs to the genus *Verilus*, which applies here. The genus *Verilus* has disappeared from the Mediterranean and Eastern Atlantic nowadays, but several species are encountered in the Caribbean Sea and subtropical western Atlantic (Schwarzhans & Prokofiev, 2017; Schwarzhans *et al*., 2020c) or in Pacific waters (Froese & Pauli, 2022).

Family Polynemidae Rafinesque, 1815
Genus *Polynemus* Linnaeus, 1758

***Polynemus raffii* Nolf & Girone, 2006**
Plate 29, figs 10-12

1989 Polynemidae ind. – Nolf &Cappetta, pl. 16, figs 10-11.
2006 *Polynemus raffii* – Nolf & Girone, pl. 1, figs 11-12; pl. 9, figs 4-5.

*Material* – 5 sagittas. Velerín Quarry 2; Velerín Antena Hilltop 2; Parque Antena 1.

*Remarks* – Note the growth lines on the outside of the more mature *Polynemus raffii* (Pl. 28, fig. 10). They show the shape of the juvenile specimens (Pl. 29, figs 11-12) underpinning that they all belong to the same species.

**Plate 28**

Figure 1. ***Promethichthys prometeus*** (Cuvier, 1832), Velerín Carretera.
Figure 2. ***Ammodytes* sp.**, Parque Antena.
Figure 3. ***Gymnammodytes cicerelus*** (Rafinesque, 1810), Velerín Conglomerates.
Figures 4-5. ***Benthodesmus elongatus*** Clarke, 1879, Velerín Quarry.
Figure 6. ***Trachinus draco*** Linnaeus, 1758, Velerín Conglomerates.
Figures 7-8. ***Trachinus* sp.**, Velerín Conglomerates.
Figure 9. ***Trachinus radiatus*** Cuvier, 1829, Velerín Conglomerates.
Figure 10. ***Uranoscopus scaber*** Linnaeus, 1758, Velerín Conglomerates.
Figure 11. ***Uranoscopus* sp.**, Velerín Conglomerates.
Figure 12. ***Bodianus scrofa*** (Valenciennes, 1839), Velerín Sandy Lens.
Figure 13. **Labridae indet.**, El Lobillo.

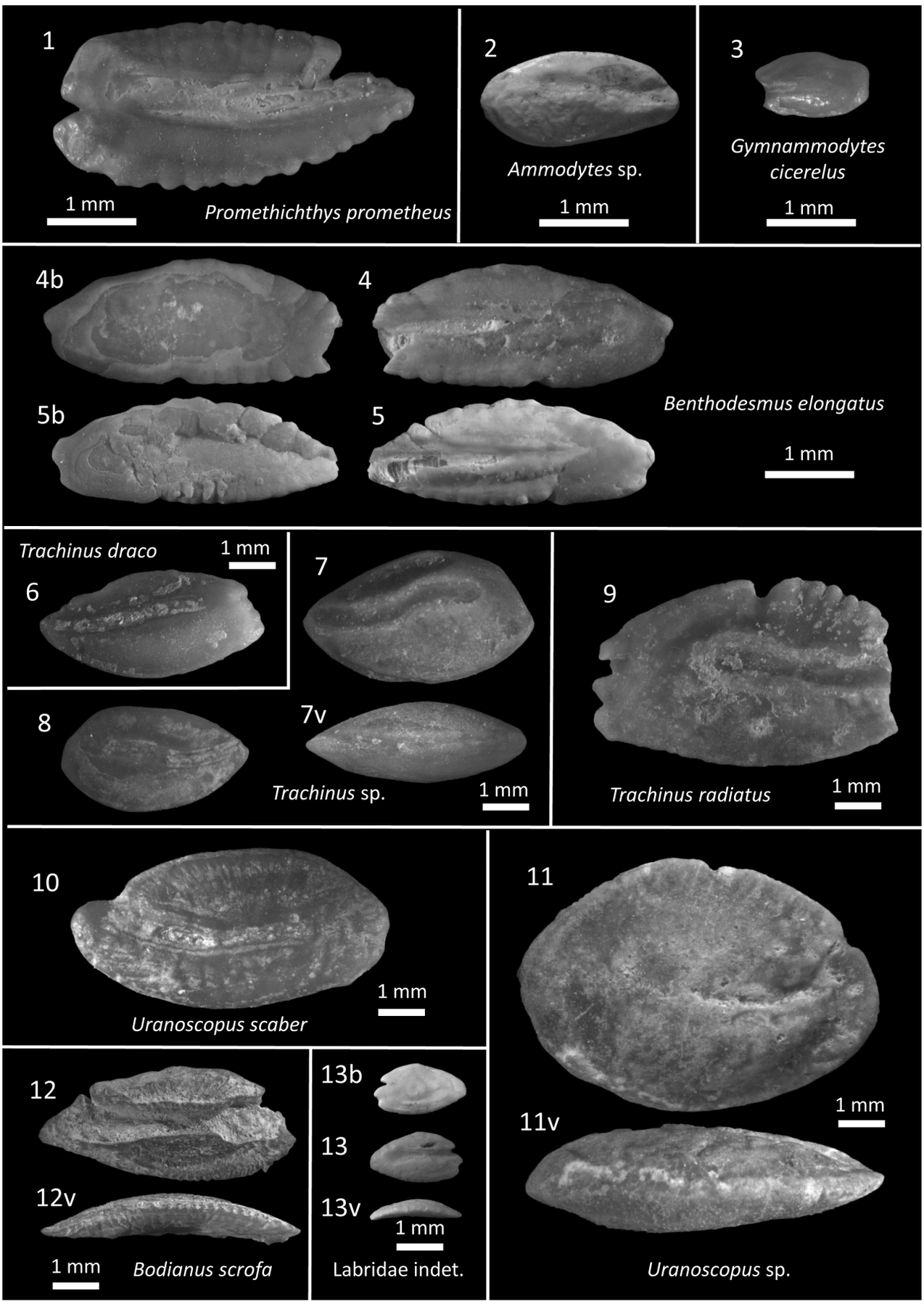
1
1 mm
Promethichthys prometheus
2
Ammodytes sp.
1 mm
3
Gymnammodytes cicerelus
1 mm
4b
4
5b
5
Benthodesmus elongatus
1 mm
Trachinus draco
1 mm
6
7
8
7v
Trachinus sp.
1 mm
9
Trachinus radiatus
1 mm
10
1 mm
Uranoscopus scaber
11
1 mm
11v
Uranoscopus sp.
12
12v
1 mm
Bodianus scrofa
13b
13
13v
1 mm
Labridae indet.

**Plate 28**

Family Bathyclupeidae Gill, 1896
Genus *Bathyclupea* Alcock, 1891

***Bathyclupea* sp.**
Plate 29, fig. 13

*Material* – 1 sagitta. Río del Padrón 1.

*Discussion* – The rhomboid shape and sulcus of these otoliths are very characteristic. At present, there are no members of the two bathyclupeid genera *Bathyclupea* and *Neobathyclupea* Prokofiev, 2014 living in the Mediterranean or eastern Atlantic. *Bathyclupea* sp. was reported from Mediterranean deposits from the lower Oligocene of northern Italy (Nolf & Steurbaut, 2004). Our find indicates that the genus was still present in the Mediterranean during the Early Pliocene.

Family Scombropidae Gill, 1862
Genus *Scombrops* Temminck & Schlegel, 1845

***Scombrops* cf. *boops* (Houttuyn, 1782)**
Plate 30, figs 6-9

1995 *Scombrops boops* – Smale *et al*., pl. 69 figs B2-B4 (present-day otoliths).

*Material* – 17 sagittas. El Lobillo 1; Velerín Carretera 1; Velerín Conglomerates 10; Velerín Sandy Lens 1; Velerín Quarry 4.

*Discussion* – The presence of *Scombrops* in Mediterranean deposits is unexpected. Three extant *Scombrops* species are known: *S. boops* in the South Atlantic (South Africa), Mozambique, Japan, and the East China Sea; *S. oculatus* (Poey, 1860) from the Caribbean; and *S. gilberti* (Jordan & Snyder, 1901) from Japan (Fricke *et al*., 2021). Our Pliocene otoliths match well with those of *Scombrops boops* (figured in Smale *et al*., 1995, pl. 69, fig. B2) and probably represent this species. However, we have not been able to compare them with *Scombrops oculatus* otoliths.

Family Priacanthidae Günther, 1842
Genus *Pristigenys* Agassiz, 1835

***Pristigenys adrianae* nov. sp.**
Plate 30, figs 10-11

*Holotype* – RGM.1390742, Velerín Quarry.

*Paratype* – 1 sagitta: RGM.1390743, Velerín Quarry.

*Locus typicus* – Velerín Quarry, close to Velerín Antena, along Camino Nicolas, Velerín, Estepona, province of Málaga, Spain.

*Stratum typicum* – Middle Pliocene, Piacenzian, fossiliferous medium- to fine-grained sands.

*Etymology* – Named after Adriana (Adrie) Kerkhof in honour of her life-long support of *Cainozoic Research* and the Work Group of Tertiary and Quaternary Research (WTKG).

*Diagnosis* – Large roundish to pentagonal otoliths that are slightly higher than long (estimated OL:OH=0.94-0.98). Strongly convex inner face, and concave outer face. Ventral rim with a midventral angle. The sulcus divides the otolith in two almost equal parts. It has a wide ostium and narrower cauda; the latter slightly longer than the ostium, and ending at a distance (20% of OL) of the posterior rim.

*Description* – Large roundish to pentagonal otoliths that are slightly higher than long (estimated OL=6.0-6.3 mm, OH=6.1-6.3). The predorsal rim is concave until a blunt predorsal angle, after which it forms a straight line with strong crenulations until the postdorsal angle, whereupon it runs straight and also crenulated downward to the posterior tip. The posterior tip varies between pointed to blunt in the two otoliths. A blunt rostrum exists, no excisura is present; the rostral part is damaged in the second otolith. The ventral rim is divided by a rounded midventral angle that lies beyond the ostium-cauda transition. The anterior part of the ventral rim is more coarsely ornamented than the anterior part.
The inner face is markedly convex. The slightly supramedian sulcus covers about 80% of the length of the otolith, still leaving the cauda at a significant distance to the posterior end. It is divided in a narrow cauda and a 2 to 3 times wider ostium that is widened along both the upper and lower rims. The cauda is about 1.1 times as long as the ostium. At the anterior-most part of the cauda the crista inferior forms an upward angle, thus narrowing the sulcus, while the crista superior remains straight. The outer face is concave in all directions; the coarse crenulation of the rim forms ridges toward the centre of the otolith.

*Discussion* – *Pristigenys adrianae* is similar to the Miocene *Pristiygenys rhombica* (Schubert, 1906). However,

**Plate 29**
Figures 1-4. ***Verilus mutinensis*** (Bassoli, 1906), Velerín Quarry (1, 2), Velerín Conglomerates (3), Velerín Carretera (4).
Figures 5-9. ***Epigonus constanciae*** (Giglioli, 1880), Velerín Sandy Lens (5, 8), Velerín Quarry (6), Velerín Carretera (7), Velerín Conglomerates (9).
Figures 10-12. ***Polynemus raffii*** Nolf & Girone, 2006, Velerín Quarry (10), Velerín Antena Hilltop (11, 12).
Figure 13. ***Bathyclupea* sp.,** Río del Padrón.
Figures 14-15. ***Anthias anthias*** (Linnaeus, 1758), Velerín Conglomerates (14), El Lobillo (15).

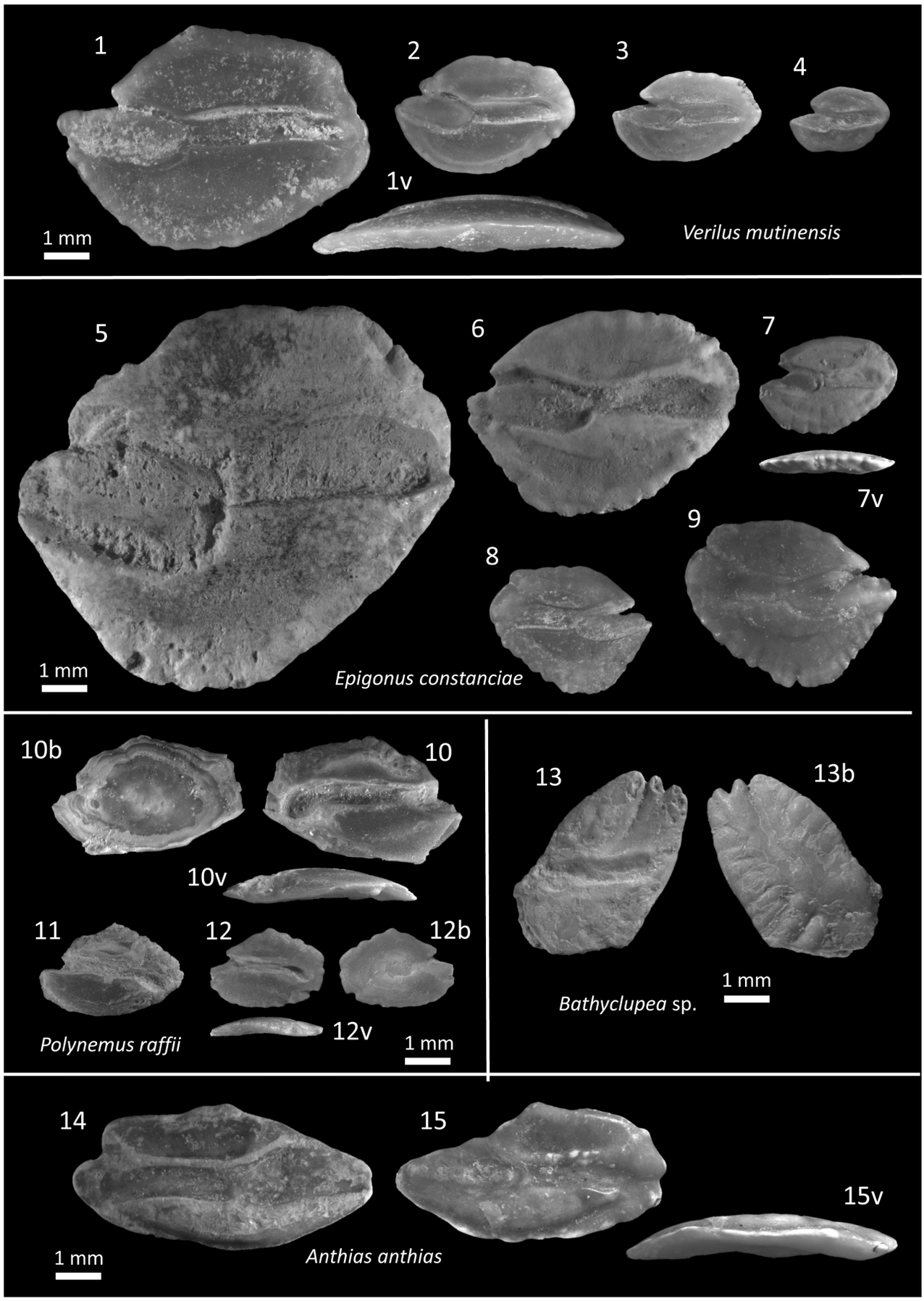
1
2
3
4
1v
1 mm
Verilus mutinensis
5
6
7
7v
8
9
1 mm
Epigonus constanciae
10b
10
10v
11
12
12b
12v
1 mm
Polynemus raffii
13
13b
1 mm
Bathyclupea sp.
14
15
15v
1 mm
Anthias anthias

**Plate 29**

it differs in several aspects. The upper part of the otolith is more extended than in *P. rhombica*. The cauda reaches close to the posterior rim in *P. rhombica*, while there is a significant distance in *P. adrianae*. Furthermore, *P. adrianae* has a concave predorsal rim, which is straight or convex in *P. rhombica*. There are 6 extant *Pristigenys* species, of which 5 are confined to the Pacific region, and one, *Pristigenys alta* (Gill, 1862), to the subtropical western Atlantic. The otoliths of *P. alta* have been depicted in Nolf (2013, pl. 225) and reveal that they also differ from those of *P. adrianae* by a sulcus that reaches close to the posterior rim and has an ostium:cauda ratio (OsL:CaL=2.5 to 3) that is much higher than in *P. adrianae*. Also, its dorsal area is lower and the dorsal rim is more rounded with middorsal irregularities in *P. alta* than in our specimens.

*Distribution*: *Pristigenys adrianae* is only known from the Piacenzian of Velerín, Estepona, Spain.

Family Haemulidae Gill, 1885
Subfamily *Haemulinae* (Forsskål, 1775)

**Haemulinae sp.**
Plate 31, fig. 2

*Material* – 1 sagitta: Velerín Antena Slope 1.

*Description* – Oval otolith with a blunt postdorsal projection and a vertical posterior rim. The dorsal rim is smooth and forms a broad plateau (Pl. 31, fig. 2d); the ventral rim is also smooth but has a sharp edge (Pl. 31, fig. 2v). The ventral rim bends regularly and delineates half of the otolith perimeter. At its anterior side it ends in a small rostrum. Ostium and cauda of the sulcus are clearly separated. The cauda is almost twice as long but narrower than the ostium. It is covered by a colliculum. At its posterior end the cauda bends to but does not completely reach the ventral rim. The ostium is covered by an oval colliculum and opens to the antero-dorsal rim. The excisura ostii is separated from a minor antirostrum by a small superficial notch. The excisura covers the anterior 24% of the dorsal otolith lining. The dorsal rim consists of a slightly bent blunt and thick rim with a small concavity before a rounded almost straight postdorsal angle after which the posterior rim runs straight downwards to join the ventral rim. The otolith is moderately thick across its entire body. The inner surface is convex in all directions. The outside is slightly concave in its central part.

*Remarks* – Our specimen matches properties of the Haemulinae subfamily that includes many genera, *e.g.*, *Orthopristis* Girard, 1858, *Isacia* Jordan & Fesler, 1893 and *Brachydeuterus* Gill, 1862. We refrain from further identification of our specimen within this large subfamily because of the availability of only a single otolith of probably a juvenile fish.

Family Cepolidae Rafinesque, 1815
Genus *Cepola* Linnaeus, 1764

***Cepola macrophthalma* (Linnaeus, 1758)**
Plate 30, figs 3-5

1906 *Ot*. (*Cepola*) *praerubescens* – Bassoli, pl. II, fig. 43.
1989 *Cepola rubescens* Linnaeus, 1766 – Nolf & Cappetta, pl. 16, fig. 4.
2006 *Cepola macrophthalma* – Lombarte *et al*., figs 6377-6379.
2010 *Cepola macrophthalma* – Schwarzhans, pl. 94, figs 4-7.

*Material* – 29 sagittas. Río del Padrón 2; El Lobillo 1; Velerín Carretera 7; Velerín Conglomerates 4; Velerín Quarry 5; Velerín Antena Slope 3; Velerín Antena Hilltop 7.

*Remarks* – Within the species *Cepola macrophthalma* two morphological forms are encountered. The variant *Cepola* otolith depicted in Pl. 30, fig. 4 has previously been attributed to *Cepola rubescens*, a name that is nowadays considered synonymous to *C. macrophthalma*. The specimen on Pl. 30, fig. 3 is representative for otoliths of an older fish. It has developed a pointed posterior end and parallel, almost horizontal middorsal and midventral rims, similar as in aged extant *C. macrophthalma* (based on a series of 40 pairs of extant otoliths of a range of sizes. A growth series of otoliths of present-day *C. macrophthalma* is available as a Supplementary figure 1 online, including data about the total length of the fish.

Family Scorpaenidae Risso, 1827
Subfamily Scorpaeninae Risso, 1827
Genus *Scorpaena* Linnaeus, 1758

***Scorpaena loppei* Cadenat, 1943**
Plate 31, fig. 6

2006 *Scorpaena loppei*– Lombarte *et al*., figs 10421, 10424, 10425 (present-day otoliths).

**Plate 30**
Figure 1. ***Chelidoperca*? sp.,** El Lobillo.
Figure 2. **Serranidae sp.**, El Lobillo.
Figures 3-5. ***Cepola macrophthalma*** Velerín Quarry (3, 5), Velerín Conglomerates (4).
Figures 6-9. ***Scombrops* cf. *boops*** Houttuyn, 1782, Velerín Carretera (6, 8), Velerín Conglomerates (7), Velerín Sandy Lens (9).
Figure 10. ***Pristigenys adrianae* nov. sp.**, paratype, Velerín Quarry.
Figure 11. ***Pristigenys adrianae* nov. sp.**, holotype, Velerín Quarry.

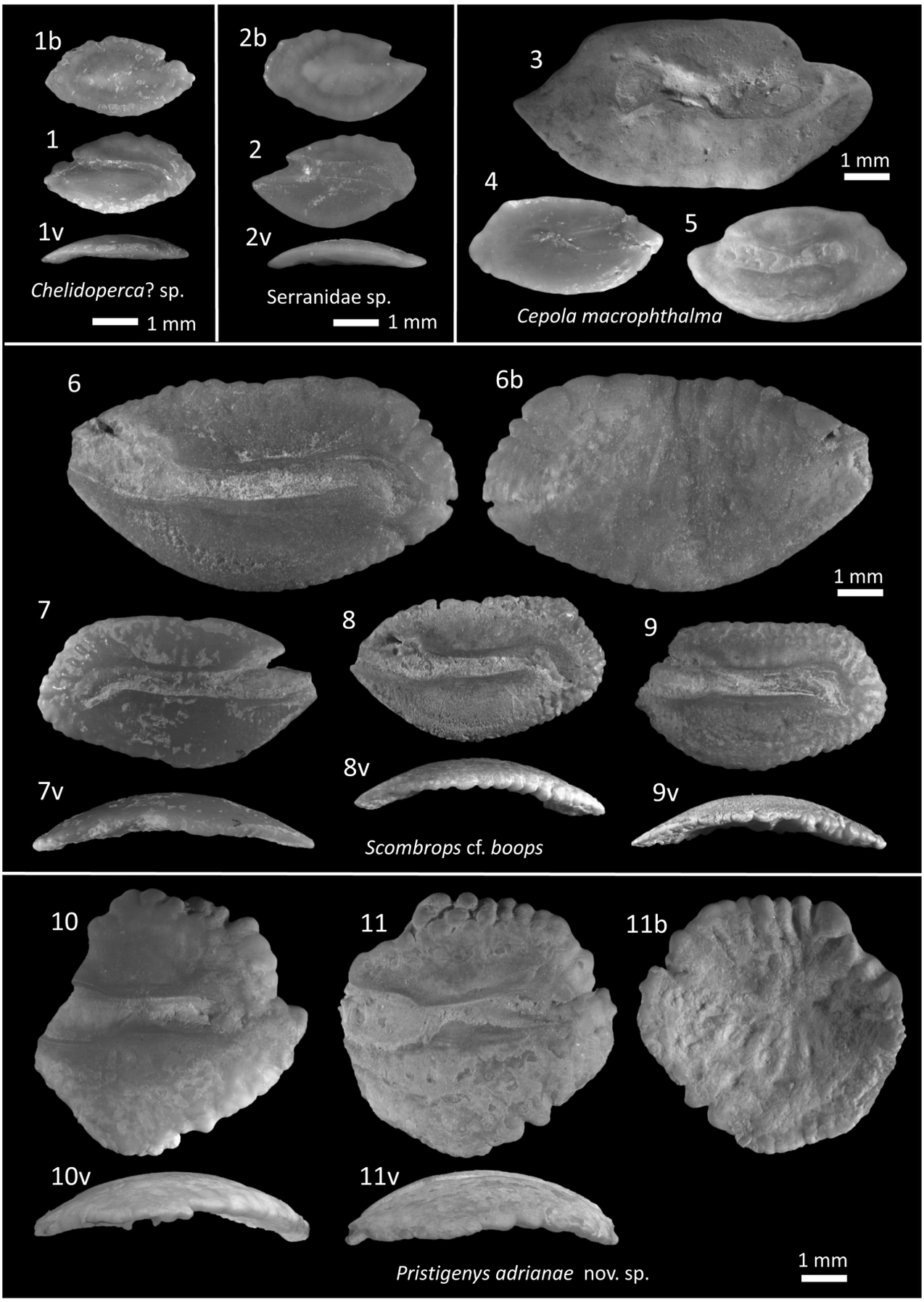
1b
1
1v
*Chelidoperca*? sp.
1 mm
2b
2
2v
Serranidae sp.
1 mm
3
4
5
1 mm
*Cepola macrophthalma*
6
6b
1 mm
7
7v
8
8v
9
9v
*Scombrops* cf. *boops*
10
10v
11
11v
11b
*Pristigenys adrianae* nov. sp.
1 mm

**Plate 30**

Material – 3 sagittas. El Lobillo 1; Velerín Conglomerates 1; Velerín Quarry 1.

*Remarks* – Small fusiform *Scorpaena* otolith that is recognised by its compressed shape (OL:OH=1.98) and relatively short rostrum. Extant Mediterranean *S. loppei* otoliths have been depicted in Tuset *et al*. (2008). To the best of our knowledge, *S. loppei* has not earlier been reported from the Mediterranean Pliocene.

***Scorpaena* cf. *notata* Rafinesque, 1810**
Plate 31, figs 7-9

2008 *Scorpaena notata* – Tuset *et al.,* figs 42.C1-C3 (present-day otoliths).

*Material* – 3 sagittas. El Lobillo 1; Velerín Conglomerates 2.

*Description* – One large otolith (OL=6.9 mm; OL:OH=2.15) and two small specimens of 3-4 mm (OL:OH=2.20-2.35) are available. Fusiform otoliths with roundly pointed posterior and anterior endings. Prominent, broadly pointed rostrum; short distinct antirostrum. Excisura ostii wide with 2-3 small lobes; small but distinct notch. Dorsal rim regular bent with shallow lobes at its posterior part. Ventral rim regularly bent and crenulated. Median sulcus with funnel-like ostium, slightly longer than cauda (OsL:CaL=1.15-1.25). The smaller cauda is ventrally curved. It is separated at a distance from the posterior rim by a prominent posterior area. Convex along the inner side; outer face concave in length direction.

*Discussion* – The small otoliths obtained probably represent juvenile specimens, which best fit with the extant *Scorpaena notata*. The rostrum and L/H ratio are longer than in otoliths of *S. loppei*. The otoliths of *S. elongata* Cadenat, 1943, *S. scofra* Linnaeus, 1758 and *S. porcus* Linnaeus, 1758 differ by their cauda shape and the posterior ventral rim.

Genus *Pontinus* Poey, 1860

***Pontinus* sp.**
Plate 31, fig. 10

2006 *Pontinus* sp. – Nolf & Girone, pl. 6, fig. 7.

*Material* – 1 sagitta. El Lobillo 1.

*Remarks* – Nolf & Girone (2006) reported this species from the Zanclean of Piemonte (Italy) and discussed its resemblance with the Western Atlantic *Pontinus longispinis* Goode & Bean, 1896.

Subfamily Tetraroginae Smith, 1949
Genus *Snyderina* Jordan & Starks, 1901

***Snyderina stillaformis* nov. sp.**
Plate 31, figs 3-5

*Holotype* – RGM.1390748, Velerín Quarry.

*Paratypes* – 2 sagittas: RGM.1390749, RGM.1390750. Velerín Quarry 1; Velerín Conglomerates 1.

*Locus typicus* – Velerín Quarry, close to Velerín Antena, along Camina Nicolas, Velerín, Estepona, province of Málaga, Spain.

*Stratum typicum* – Middle Pliocene, Piacenzian, fossiliferous medium- to fine-grained sands.

*Etymology* – From the Latin '*stilla*' and '*formis*', meaning 'droplet-shaped', referring to the prominent droplet shape of the sagittal otoliths.

*Diagnosis* – Spindle-shaped otoliths with an obtuse angular rostrum and a pointed to sharply pointed posterior end. The deepest point of the ventral rim is at 30%. The maximal height is at the middle of the dorsal rim. Inner face flat but with irregular elevations; outer face convex and smooth. Rather than a well-structured sulcus, the sulcus consists of two ellipse-shaped deepenings, which align obliquely on the otolith; the anterior one (ostium) close to but not connected to the anterior rim, the posterior one (cauda) with a furrow-like connection to the posterior rim. A dorsal depression lies above the cauda and the posterior end of the ostium, and is separated from them by a ridge of small thickenings.

*Description* – Droplet-shaped otoliths with convex outside, rather flat inner side, and gently curved dorsal and ventral rims. The otoliths have a prominently pointed posterior tip, while a weak angular rostrum is present

**Plate 31**
Figure 1. ***Pomadasys incisus*** (Bowdich, 1825), Velerín Conglomerates.
Figure 2. **Haemulinae sp.**, Velerín Antena Slope.
Figure 3. ***Snyderina stillaformis* nov. sp.**, holotype, Velerín Quarry.
Figure 4-5. ***Snyderina stillaformis* nov. sp.**, paratypes, Velerín Quarry (4), Velerín Conglomerates (5).
Figure 6. ***Scorpaena loppei*** Cadenat, 1943, Velerín Conglomerates.
Figures 7-9. ***Scorpaena* cf. *notata*** Rafinesque, 1810, Velerín Conglomerates (7, 8), El Lobillo (9).
Figure 10. ***Pontinus* sp.**, El Lobillo.
Figure 11. **Scorpaenidae sp.**, Velerín Sandy Lens.
Figure 12. ***Umbrina canariensis*** Valenciennes, 1843**,** Velerín Conglomerates.

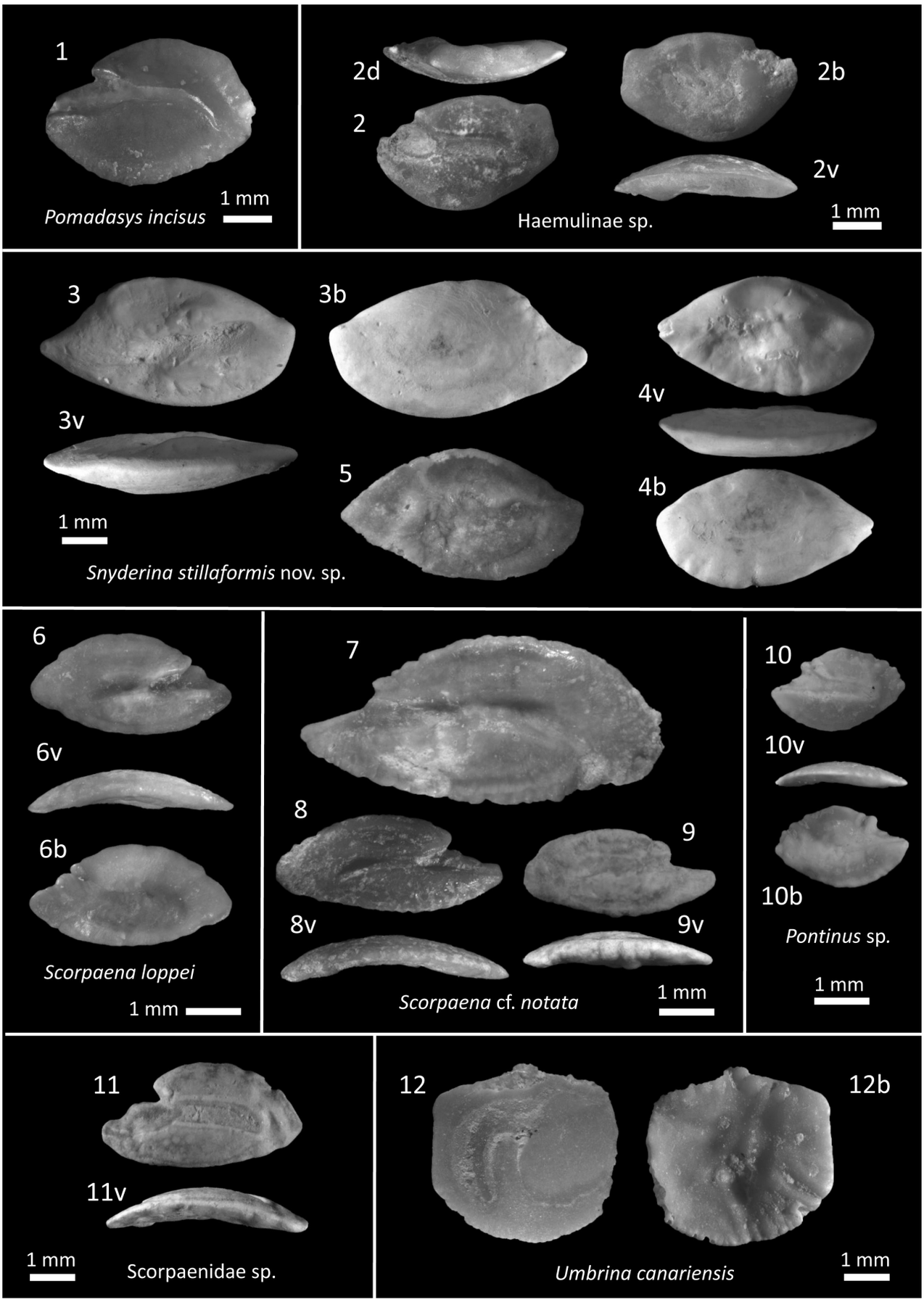
1
1 mm
Pomadasys incisus
2d
2
2b
2v
Haemulinae sp.
1 mm
3
3b
3v
4v
5
4b
1 mm
Snyderina stillaformis nov. sp.
6
6v
6b
Scorpaena loppei
1 mm
7
8
9
8v
9v
Scorpaena cf. notata
1 mm
10
10v
10b
Pontinus sp.
1 mm
11
11v
1 mm
Scorpaenidae sp.
12
12b
Umbrina canariensis
1 mm

**Plate 31**

in the middle of the convex anterior rim. The rims are smooth. In the middle-sized specimen the ventral rim displays a few shallow lobes. The sulcus consists of two pits of equal size, which are separated by a less deep collum. A shallow depression connects the caudal part with the ventral rim. A broad elevated ridge of thickenings is visible between a dorsal depression and the sulcus structures. Additional elevations are observed below the collum. The outer face is convex and smooth, with the thickest part at about ⅔ of the anterio-posterior axis (see ventral view, Pl. 31, fig. 3v).

*Discussion* – The shape of these otoliths is unprecedented. The only close species is the Pacific *Snyderina yamanokami* Jordan & Starks, 1901 (otolith iconography in Lin & Chang, 2012, pl. 90 on p. 315), which belongs to the Tetraroginae subfamily of the Scorpaenidae. However, its otoliths display a better structured and straighter sulcus. Another extant *Snyderina* species, *Snyderina guentheri* (Boulenger, 1889), has been encountered in the northern Indian Ocean, the Gulf of Aden and the Gulf of Oman (Naranji & Kandula, 2017), but otoliths of this rare species also differ in the more structured sulcus (unpublished data Werner Schwarzhans). There are no related species known in the eastern Atlantic or Mediterranean waters. A direct exchange of fishes from these eastern waters with the Mediterranean is unlikely during the Mio- and Pliocene. However, a faunal relic from the earlier Tethyan Sea cannot be excluded.

**Scorpaenidae sp.**
Plate 31, fig. 11

*Material* – 1 sagitta. Velerín Antena Sandy Lens 1.

*Description* – Semicircular otolith with weakly bent ventral rim, least in the mid-ventral part. Dorsal rim rounded with two small concavities in the postdorsal part. Strong blunt rostrum, clear antirostrum accentuated by a prominent notch. The excisura ostii almost reaches the rostral point. A colliculum-covered ostium strongly widens in antero-ventral direction. The cauda is slightly longer than the ostium; its width is constant. It slowly bends in postventral direction, but does not reach the postventral rim. The cauda is fully aligned by the crista superior and inferior. The inner side of the otolith is convex in antero-dorsal direction, while that of the dorsal rim is concave. A ventral furrow can be seen along the ventral rim, except for the most anterior and posterior parts. Outside without specific ornamentation. Overall, the otolith matches the characteristics of Scorpaenidae.

Family Triglidae Rafinesque, 1815
Genus *Prionotus* Lacepède, 1801

***Prionotus arenarius* nov. sp.**
Plate 32, figs 1-6

*Holotype* – RGM.1390756, Velerín Quarry.

*Paratypes* – 5 sagittas: RGM.1390757-RGM.1390761, Velerín Quarry 5.

*Other material* – 20 sagittas. Velerín Quarry 19; Velerín Antena Slope 1.

*Locus typicus* – Velerín Quarry, close to Velerín Antena, along the Camina Nicola, Velerín, Estepona, province of Málaga, Spain.

*Stratum typicum* – Middle Pliocene, Piacenzian, fossiliferous medium- to fine-grained sands.

*Etymology* – *Prionotus arenarius* is named after the sands ('arenas' in Spanish) of Velerín Quarry.

*Diagnosis* – Thickset, round to ellipsoid otoliths with a highly convex inner face and a flat outer face. Median or supramedian sulcus divided in ostium and cauda of about similar lengths. Small, pointed rostrum and in most cases an insignificant antirostrum. Maximum height at ⅓ of the dorsal rim. Ventral rim round or with a slight midventral angle. The ventral rim is decorated with small folds and furrows.

*Description* – Compact round-ellipsoid (OL:OH=1.21-1.37) (Pl. 32, figs 1-4) to ellipsoid otoliths (Pl. 32, figs 5-6) that can reach up to 5.8 mm. They display a small rostrum with a slightly crooked point. The antirostrum is insignificant. The dorsal rim is expanded, with its highest point somewhat anteriorly. The ventral rim is deep and regularly curved, incidentally with a slight midventral angle. In ventral view, it is thick and crenulated by folds and furrows. The posterior part is round, but can display a small, pointed end occasionally.
The sulcus is median to supramedian, divided in an equal ostium and cauda, somewhat narrowed around the distinct ostium-cauda transition. Ostium funnel-like, the anterior part upward oriented, the posterior part narrow. The cauda is longer than the ostium, widening into an oval posterior part and covered with a spoon-shaped colliculum. Due to differences in age and/or preservation, the sulcus is either broad with deeply sunken colliculi,

**Plate 32**
Figures 1, 3-6. ***Prionotus arenarius* nov. sp.**, paratypes, Velerín Quarry.
Figures 2. ***Prionotus arenarius* nov. sp.**, holotype, Velerín Quarry.
Figures 7-8. ***Chelidonichthys cuculus*** (Linnaeus, 1758), Velerín Carretera.
Figure 9. ***Chelidonichthys lastoviza*** (Bonnaterre, 1788), Velerín Quarry.
Figures 10-11. **Platycephalidae sp.**, Río del Padrón (10), El Lobillo (11).
Figures 12-13. ***Morone* sp.**, Velerín Conglomerates (12), El Lobillo (13).

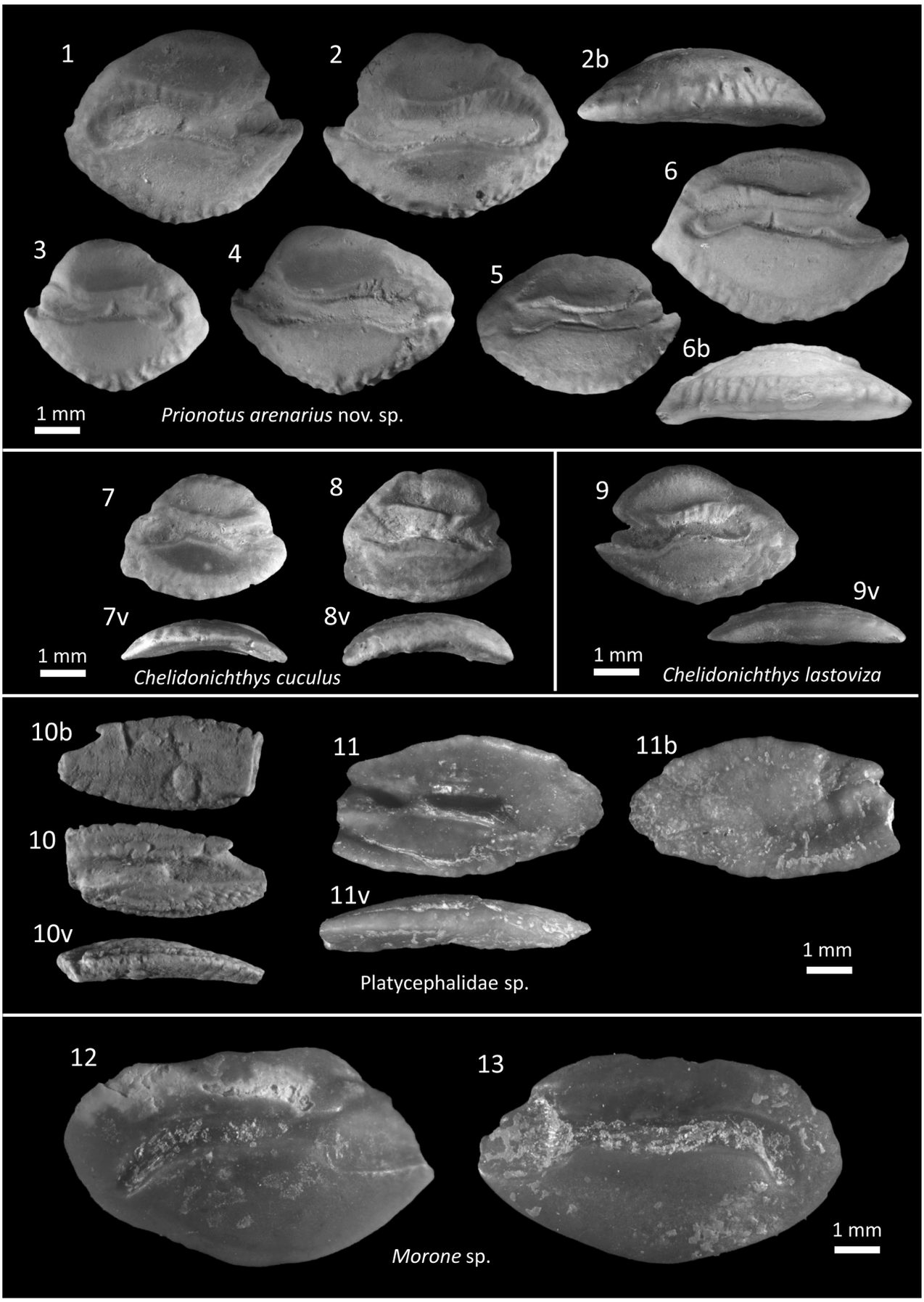
1
2
2b
6
3
4
5
6b
1 mm
*Prionotus arenarius* nov. sp.
7
8
7v
8v
1 mm
*Chelidonichthys cuculus*
9
9v
1 mm
*Chelidonichthys lastoviza*
10b
11
11b
10
11v
10v
1 mm
Platycephalidae sp.
12
13
1 mm
*Morone* sp.

**Plate 32**

or narrower with moderately uplifted colliculi. The crista superior above the cauda displays parallel furrows in adult specimens. Similar folds and furrows are present along the ventral rim reaching until the faint ventral furrow. The inner surface is strongly convex. The outer surface is smooth; it displays a straight elevation between the rostral point and the posterior point separating two depressed areas at its anterioventral part as well as at its postero-dorsal part.

*Remarks* – The rostral part, the sulcus shape and ventral view indicate that the species belongs to the genus *Prionotus*, which today is commonly encountered in Caribbean and western Atlantic waters, but not in the eastern Atlantic. The ornamentation of the dorsal and ventral rims, the wide sulcus and the upward pointed rostrum differ markedly from other triglid otoliths, such as *Chelidonichthys robustus* (Bloch & Schneider, 1801) and *Chelidonichthys gurnardus* (Linnaeus, 1758), which have been reported from the Zanclean of Italy (Nolf & Cavallo, 1994). Otoliths of *Prionotus europaeus* Schwarzhans, 2010 and *P. chamavensis* Schwarzhans, 2010 have been reported from the Early-Middle Miocene of the North Sea Basin (Schwarzhans, 2010a), but our specimens differ from those of *P. europaeus* by a more pronounced rostrum than antirostrum, while these are close to equal and positioned more ventrally in *P. europaeus*. Furthermore, the dorsal and ventral fields are more expanded and the outside is less concave in our otoliths than in those of *P. chamavensis*.
Four of the specimens are more elongate and display a narrower sulcus with the colliculi closer to the inner surface than in the other otoliths. They share characteristics comparable to the North and Central American *P. carolinus* (Linnaeus, 1771) and *P. punctatus* (Bloch, 1793), but probably are variant otoliths of *P. arenarius*.

Family Platycephalidae Swainson, 1839

**Platycephalidae sp.**
Plate 32, figs 10-11

*Material* – 2 sagittas. Río del Padrón 1; Velerín Conglomerates 1.

*Description* – Two fusiform but flat specimens are available of which one lacks the rostrum and the other the caudal part. One specimen (Pl. 32, fig. 10) has a prominent rostrum and a small but pointed antirostrum, the latter is still visible in the other specimen. The rims are irregularly rounded with an irregular crenulation, probably polished by erosion. The sulcus is divided in a nearly equal-sized deep ostium and cauda, which are separated by a shallow transition. The ostium widens at its anterior end; the cauda fades away at its posterior side, and remains far from the posterior rim (Pl. 32, fig. 11). Below the sulcus a convex ventral field is visible bordered by a prominent ventral furrow. In the smaller specimen only the antero-ventral part of the inner surface shows ridges of crenulations. Above the cauda there is a flat dorsal field that extends along the dorso-posterior part. The inner surface is slightly convex along the antero-posterior axis; the outside is irregularly shaped, almost flat, but slightly concave along the antero-posterior axis.

*Discussion* – The otoliths have characteristics of Platycephalidae such as an elongate flat shape and an elongate straight sulcus divided in an equal ostium and cauda. The curved posterior part is often more extruded and narrowed in genera such as *Sorsogona* Herre, 1934 and *Thysanophrys* Ogilby, 1898, but individual otoliths with a more rounded posterior part occur. However, the extended posterior portion is damaged in one specimen. The smaller specimen seems close to *Sunagocia arenicola* (Schulz, 1966), a species that nowadays is found in South African waters (otoliths see Smale *et al*., 1995, pl. 54, fig. G1 as *Thysanophrys arenicola*). However, the caudal ending is more distinct in this and related genera. The larger specimen shows affinities with otoliths of *Sorsogona portuguesa* (Smith, 1953) (see Smale *et al*., 1995, pl. 54D as *Grammoplites portuguesus*) from the southwestern Indian Ocean, but differs from it in the more convex ventral rim and less extended posterior portion.

Family Sparidae Rafinesque, 1818

Molecular phylogenetic data (De la Herrán *et al*., 2001; Chiba *et al*., 2009; Santini *et al*., 2014) indicate that the members of the Sparidae fan out into two clades (A and B) and that a few genera, in particular *Pagellus* Valenciennes, 1830 and *Spicara* Rafinesque, 1810, have members in each of these clades. While *Pagellus erythrinus* (Linnaeus, 1758) and *P. bellottii* Steindachner, 1882 are closely related within clade B, *P. acarne* (Risso, 1827) and *P. bogaraveo* (Brünnich, 1768) belong to clade A (De la Herrán *et al*., 2001; Santini *et al*., 2014). Similarly, *Spicara alta* (Osório, 1917) was placed in clade B, while *Spicara maena* (Linnaeus, 1758), *S. flexuosa* (Rafinesque, 1810) and *S. smaris* (Linnaeus, 1758) are related species in clade A (Chiba *et al*., 2009). This suggests that

**Plate 33**

Figures 1-4. ***Boops boops*** (Linnaeus, 1758)**,** Velerín Quarry (1,2), Río del Padrón (3), Velerín Conglomerates (4).
Figure 5. ***Diplodus vulgaris*** Geoffroy Saint-Hilaire, 1817, Conglomerates.
Figures 6-7. ***Diplodus annularis*** (Linnaeus, 1758), Velerín El Lobillo.
Figure 8. ***Diplodus puntazzo*** (Walbaum, 1792), Velerín Carretera.
Figures 9-11. ***Diplodus* cf. *puntazzo*** (Walbaum, 1792), Río del Padrón (9, 10), El Lobillo (11).
Figures 12-13. ***Oblada melanura*** (Linnaeus, 1758), Velerín Quarry (12), Velerín Sandy Lens (13).

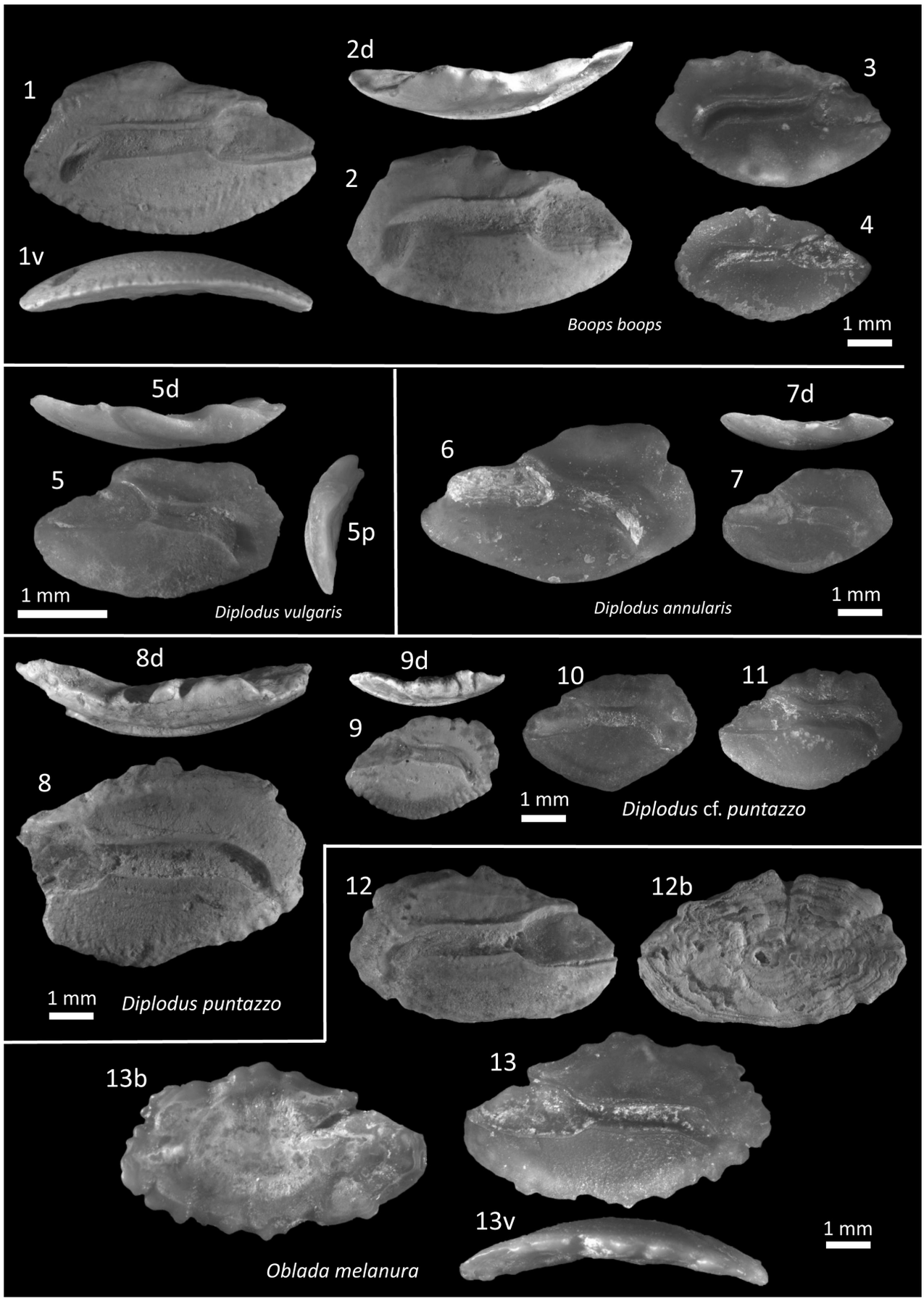
1
2d
3
2
1v
4
Boops boops
1 mm
5d
5
5p
1 mm
Diplodus vulgaris
7d
6
7
Diplodus annularis
1 mm
8d
9d
10
11
9
8
1 mm
Diplodus cf. puntazzo
12
12b
1 mm
Diplodus puntazzo
13b
13
13v
1 mm
Oblada melanura

**Plate 33**

their common genus name is not at par with the molecular phylogeny of Sparidae. Here, we have organised the Sparidae according to the clades (subfamilies) A and B of Santini *et al*. (2014). We use the original genus names because of their common use and because other studies with combined techniques and complete fish will be more appropriate to pinpoint the phylogeny and classification of extant Sparidae.
Otoliths reported from Pliocene deposits meet the characteristics of certain extant Sparidae (Nolf & Martinell, 1980; Nolf & Cavallo, 1995; Nolf & Girone, 2006). For the otoliths of major extant Mediterranean Sparidae descriptions are available, in particular in Tuset *et al*. (2008). Drawings of *Spicara alta* were kindly provided by D. Nolf (see below). Therefore, we have only made remarks on *Pagellus belottii*, *Rhabdosargus sarba* (Forsskål, 1775)*, Spondyliosoma cantharus* (Linnaeus, 1758), *Spicara maena/S. flexuosa* and *Spicara alta*.

**Sparidae, Clade A**
Genus *Rhabdosargus* Fowler, 1933

***Rhabdosargus sarba* (Forsskål, 1775)**
Plate 35, fig. 1

2017 *Rhabdosargus sarba* – Haleem *et al*., figs a, b (present-day otoliths).

*Material* – 1 sagitta. Velerín Conglomerates 1.

*Description* – The otolith has a prominent sulcus that consists of a short ostium that strongly widens in anteroventral direction and a long cauda that runs horizontally in its anterior part and subsequently bends strongly, ending on and perpendicularly to the ventral rim. The excisura ostia rim is long and ends in a notch, which may be enlarged by mechanical damage. The dorsal rim inclines obliquely up to the postdorsal angle (at ¾ of the otolith) from where the posterior rim bends steeply in ventral direction, finally ending at the ventral rim. The dorsal rim is irregularly shaped with lobes. Starting from the massive and rounded rostrum, the ventral rim is slightly bent, but its shape is affected by mechanical erosion. The outside of the otolith displays the original growth lines. In ventral view a torsion along the length axis is visible, which is a common characteristic in Sparidae.

*Remarks* – The otolith shows a striking resemblance with extant *Rhabdosargus sarba* (see Haleem *et al*., 2017, figs a-b), an Indo-West Pacific species that also lives in the Red Sea. It is presently not known from the Mediterranean Sea, except for one recent finding – probably as a migrant from the Red Sea – off the coast of Syria (Hanwi & Ali-Basha, 2021). The strongly bent cauda might also fit with otoliths of Plectorhinchinae Jordan & Thompson, 1912 subfamily of the Haemulidae and with some *Plectorhinchus mediterraneus* (Guichenot, 1850) specimens in particular (see Lombarte *et al*., 2006). However, the otolith displays in ventral view a torsion along its anteroposterior axis, a property that is characteristic for clade A Sparidae and not for Haemulidae.

Genus *Sarpa* Bonaparte, 1831

***Sarpa salpa* (Linnaeus, 1758)**
Plate 35, fig. 2

2008 *Sarpa salpa* (present-day otoliths) – Tuset *et al*., figs 61D1-3.
2009 *Sarpa salpa* (present-day otoliths) – Nolf, pl. 98.

*Material* – 1 sagitta. Velerín Carretera

*Description and Remarks* – Rectangular otolith with a short but massive rostrum and a smaller antirostrum. It has a deep excisura and a dorsal rim that inclines in an almost straight line toward the postdorsal angle followed by a concave posterior rim. The deepest point of the curved ventral rim lies in the anterior part of the inner face, after which the ventral rim continues posteriorly, parallel to the dorsal rim. It ends in a distinct postventral projection that is blunt and broadly rounded. The specimen shows signs of erosion but the growth lines on the outer surface show that the general pattern of the otolith remained intact. The inner face is convex in anterior-posterior direction, while its outer face is similarly concave. The features of this Sparid clade A otolith are very close to those of the extant *Sarpa salpa*. While this fish is common in the Mediterranean Sea today, it has not been recorded earlier from Pliocene or older sediments, possibly also because of the thin and fragile shape of its otoliths.

Genus *Spicara* Rafinesque, 1810

***Spicara* cf. *maena* (Linnaeus, 1758)**
Plate 35, figs 7-11

2020 *Spicara maena* – Agiadi *et al*., fig. 5r.

*Material* – 19 sagittas. Río del Padrón 3; El Lobillo 4; Velerín Carretera 1; Velerín Conglomerates 2; Velerín Quarry 3; Velerín Antena Hilltop 5; Parque Antena 1.

**Plate 34**
Figures 1-2. ***Lithognathus mormyrus*** (Linnaeus, 1758), Velerín Conglomerates (1), Velerín Carretera (2).
Figures 3-8. ***Pagellus acarne*** (Risso, 1826), Velerín Sandy Lens (3, 6), El Lobillo (4, 7), Velerín Quarry (5), Río del Padrón (8).
Figures 9-13. ***Pagellus bogaraveo*** (Brünnich, 1768), Velerín Quarry (9, 10, 12), Velerín Conglomerates (11), Velerín Antena Slope (13).

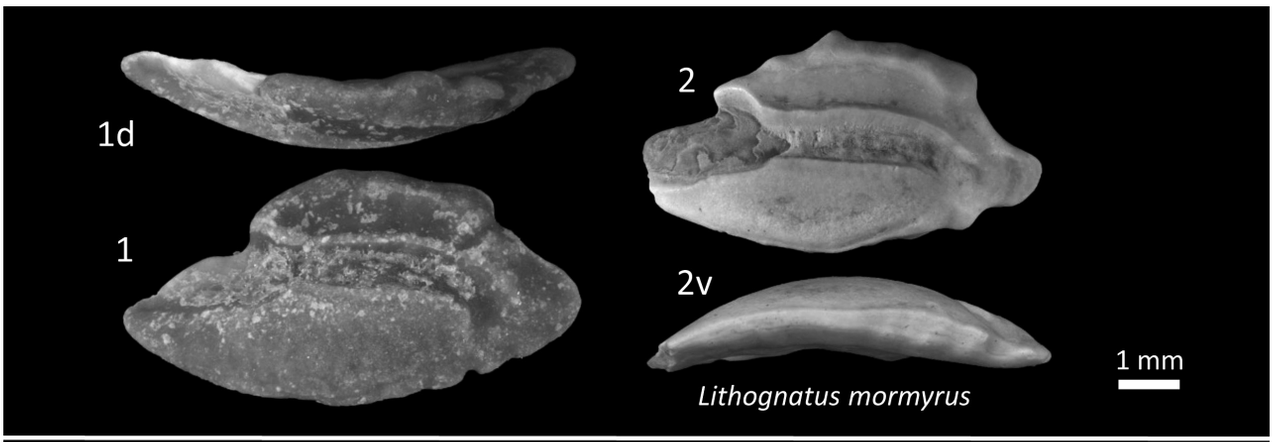
1d
1
2
2v
1 mm
Lithognatus mormyrus

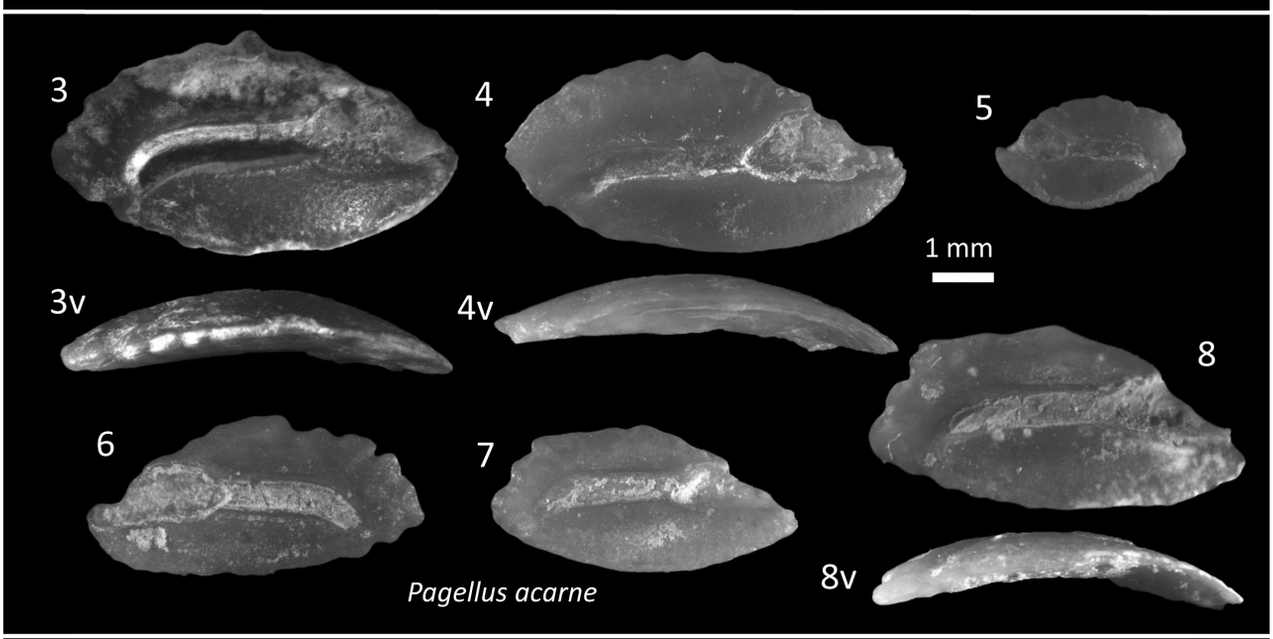
3
4
5
1 mm
3v
4v
8
6
7
8v
Pagellus acarne

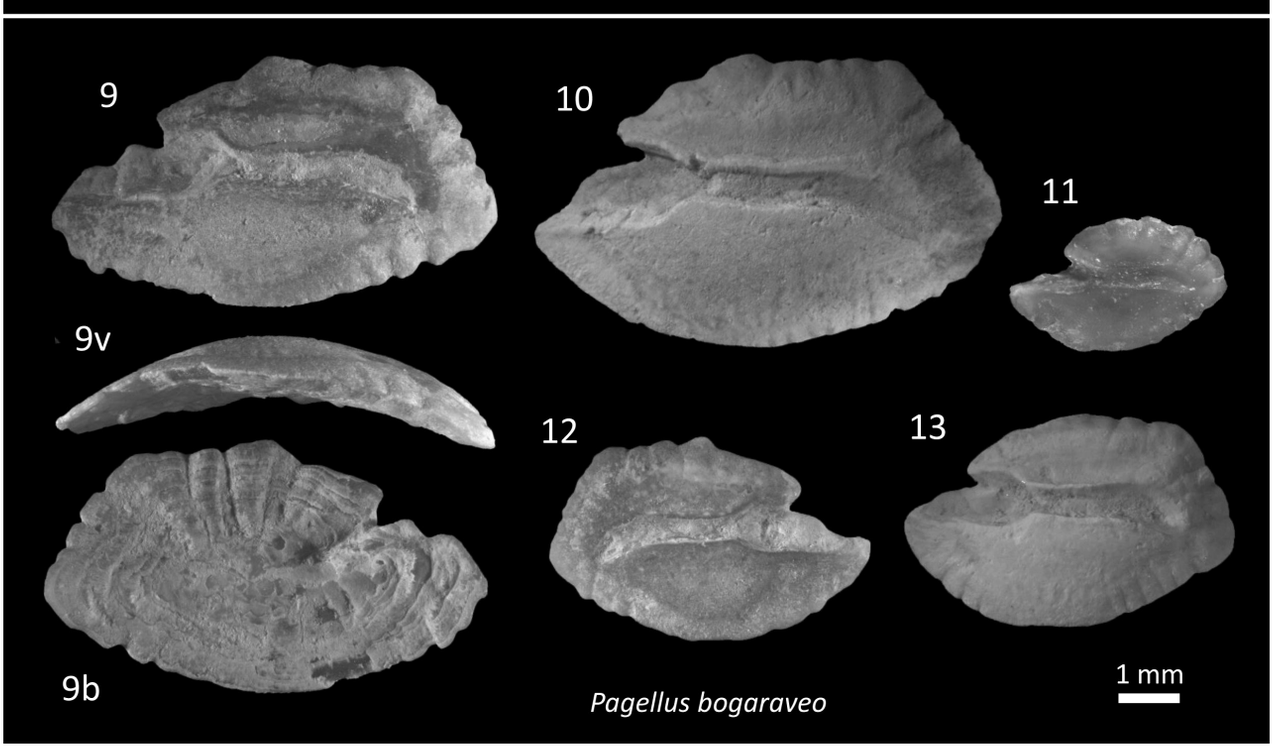
9
10
11
9v
12
13
9b
1 mm
Pagellus bogaraveo

**Plate 34**

*Discussion* – There is some overlap in the morphologies of the sagittas of *S. maena* and *S. flexuosa* in the present-day fishes (Tuset *et al*., 2008). The species separation of *S. maena* and *S. flexuosa* is estimated to have occurred within the Pliocene (Abbas *et al*., 2017). If so, a difference in the morphology of their sagittas may be even less prominent between the Zanclean and Piacenzian. In the light of these uncertainties, we have tentatively assigned the Pliocene otoliths to *Spicara* cf. *maena*.

**Sparidae sp. (clade A)**
Plate 35, figs 12-13

*Material* – 2 sagittas. Velerín Quarry 2.

*Description* – Elongate otoliths with a prominent and pointed rostrum and a small antirostrum. The rounded dorsal rim displays a marked postdorsal angle, connected to an oblique postdorsal rim that borders a characteristic posterior flap that extends posterior of the connection to the ventral rim. The posterior rim is straight and without concavity. The ventral rim is regularly rounded, with a slight midventral angle. All rims show an ornamentation of small lobes and furrows. The ostium of the sulcus is wide and fully opened to the anterior rim; the cauda is elongate, with parallel cristae slightly declining towards a small oblique bend at the end of the cauda. Inner face convex; outer face concave with folds and furrows perpendicular to the rims and disappearing in the centre of the outer face.

*Remarks* –The otoliths belong to clade A of the Sparidae, and probably represent juvenile specimens. However, otoliths of juvenile Sparidae show an overlapping variability. Hence, as long as no convincing adult specimens have been encountered an identification seems premature.

**Sparidae, Clade B**
Genus *Pagellus* Valenciennes, 1830

***Pagellus* cf. *bellottii* Steindacher, 1882**
Plate 36, fig. 7

2008 *Pagellus bellottii* – Tuset *et al.,* figs 58.B1-3 (present-day otoliths).

*Material* – 1 sagitta. Velerín Conglomerates 1.

*Discussion* – Overall, there is a high similarity between otoliths of *P. belottii* with those of *P. erythrinus* . Extant specimens of *P. bellottii* display a deep V-shaped bend in their ventral rim, but this can also occur in *P. erythrinus* (Lombarte *et al*., 2006). The cauda of large specimens of *P. belottii* seems longer than that of equal-sized *P. erythrinus*, but this feature becomes indistinct in younger specimens. Hence, we are uncertain whether otoliths of *Pagellus erythrinus* and *P. bellottii* can be sufficiently discriminated in Pliocene material as their morphologies may show a considerable overlap. A close relationship is also seen in a molecular phylogeny of these species (Santini *et al*., 2014).

***Spicara alta* (Osório, 1917)**
Plate 36, figs 8-9

*Material* – 5 sagittas. Velerín Conglomerates 4; Velerín Sandy Lens 1.

*Discussion* – These specimens (Pl. 36, figs 8-9) match the characteristics of otoliths of the extant *Spicara alta* as confirmed with extant material (see Pl. 36, figs 11-13, courtesy Dirk Nolf, Brussels). The specimens are close to those of juvenile *Dentex* Cuvier, 1814 and some specimens of *Spicara maena*. Molecular phylogenetic studies inferred from a mitochondrial gene analysis suggest that *Spicara alta* belongs to the clade that includes *Dentex* rather than that harbouring other *Spicara* species (Chiba *et al*., 2009). This needs further confirmation through an integrated study of molecular and morphological results.

## Discussion

This study on fish otoliths reveals the presence of 209 taxa in the Pliocene deposits of the community of Estepona (prov. Málaga, Spain), which comprises Estepona town (Zanclean outcrops) and adjacent village Velerín (Piacenzian deposits). From the combined Zanclean material 107 taxa were identified, 95 of which to the species level. From the combined material of the Piacenzian outcrops 185 taxa were retrieved of which 154 were identified to species level and the remainder at genus (22) or family (9) level.

Of the 209 taxa in total, 171 were identified as species, of which 17 are described as new species: *Pythonichthys gibbosus* nov. sp., *Saurenchelys silex* nov. sp., *Paraconger pinguis* nov. sp., *Gnathophis henkmulderi* nov. sp., *Diaphus postcavallonis*, nov. sp., *Diaphus mermuysi* nov. sp., *Kryptophanaron nolfi* nov. sp., *Bidenichthys mediter-*

**Plate 35**

Figure 1. ***Rhabdosargus sarba*** (Forsskål, 1775), Velerín Conglomerates.
Figure 2. ***Sarpa salpa*** (Linnaeus, 1758), Velerín Carretera.
Figures 3-6. ***Spicara smaris*** Linnaeus, 1758, Río del Padrón (3, 6), El Lobillo (4, 5).
Figures 7-11. ***Spicara* cf. *maena*** Linnaeus, 1758**,** Velerín Conglomerates (7, 9, 11), Río del Padrón (8), El Lobillo (10).
Figures 12-13. **Sparidae sp.**, juvenile otoliths, Velerín Conglomerates (12), Río del Padrón (13).

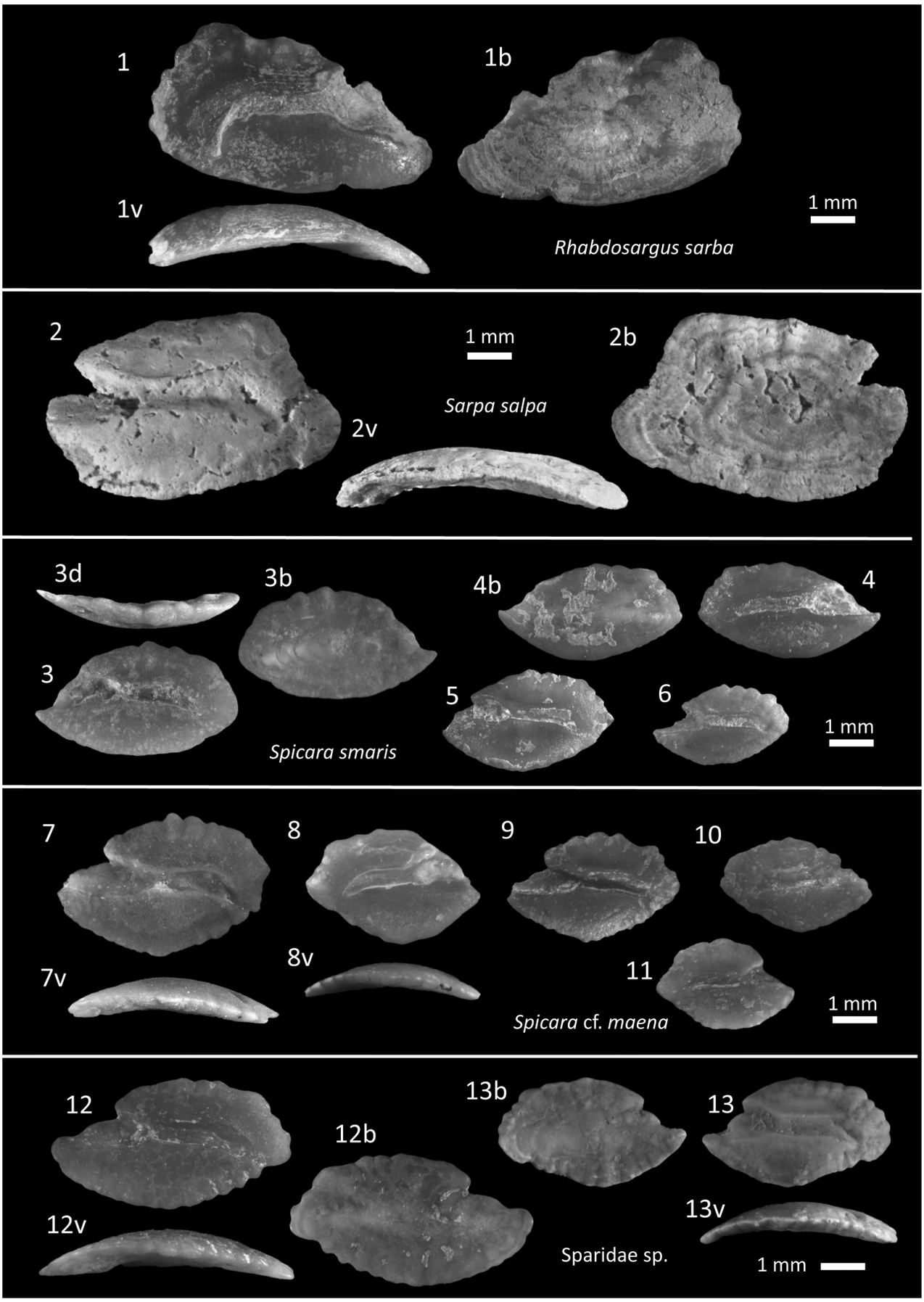
1
1b
1v
1 mm
Rhabdosargus sarba
2
1 mm
2b
Sarpa salpa
2v
3d
3b
4b
4
3
5
6
1 mm
Spicara smaris
7
8
9
10
8v
7v
11
1 mm
Spicara cf. maena
12
13b
13
12b
13v
12v
Sparidae sp.
1 mm

**Plate 35**

*raneus* nov. sp., *Fowleria velerinensis* nov. sp., *Buenia pulvinus* nov. sp., *Gobius alboranensis* nov. sp., *Gobius lombartei* nov. sp., *Thorogobius mirbachae* nov. sp., *'Gobius' pterois* nov. sp., *Snyderina stillaformis* nov.sp., *Prionotus arenarius* nov. sp. and *Pristigenys adrianae* nov. sp.. Thirty-eight taxa represent unknown species and could only be identified at genus or family level.

According to Guerra-Merchán *et al*. (2002, 2014) the outcrops near Estepona town belong to the Pliocene PL-2 unit unit (units according to Berggren, 1995). Those near Velerín to the PL-4. Their forminifers match with the MPl2 and MPl4b units (biozonation by Cita, 1975) reflecting late Early Zanclean and Middle Piacenzian, respectively. Landau *et al*. (2003) and Aguirre *et al*. (2005) consider the foraminifers and molluscs from outcrops near Velerín ranging from Late Zanclean to Early to Middle Piacenzian. The sediments on the Velerín Antena Hill, including their abundant mollusc fauna, are generally considered of Piacenzian origin. In our present study we see a marked difference in the otolith assemblages obtained from Río del Padrón and El Lobillo as compared to those from the outcrops of Velerín favouring a Zanclean origin of the deposits near Estepona town *vs*. the Piacenzian deposits of the Velerín sequence.

### *Close to Estepona town: a Zanclean otolith mixture of bathyal and shallow water fish*

An assemblage of 107 different taxa was identified from 3721 otoliths available from Río del Padrón and El Lobillo, *i.e.* 67 from Río del Padrón and 87 from El Lobillo. The section close to Río del Padrón was dated late part of Early Zanclean (MPl-2), based on pelagic foraminifers (Guerra-Mercán *et al*., 2002, 2014). Comparison of the mollusc faunas of both outcrops also pointed to a Zanclean origin of the sediments of Río del Padrón and El Lobillo (Landau *et al*., 2003). The fish faunas of Río del Padrón and El Lobillo are consistent with this interpretation. Both otolith assemblages largely agree with the Zanclean associations of Le Puget in France (Schwarzhans, 1986; Nolf & Cappetta, 1989), northern Italy (Nolf & Girone, 2006) and Sicily (Schwarzhans, 1978). They are characterised by the dominant presence of two species, namely *Diaphus cavallonis* and *Myctophum fitchi*. *Diaphus cavallonis* (≥3 mm) represent 46% and 19% of all otoliths from Río del Padrón and El Lobillo, respectively, and, including well preserved juvenile specimens, even over or close to 50% in both outcrops. Small specimens of *Myctophum fitchi* amount to 21-23% of the otolith associations.

In addition to the frequent appearance of *Diaphus cavallonis* in the northwestern Mediterranean Zanclean sediments, findings of the rarer *Diaphus befralai* Brzobohatý & Nolf, 2000 and *D.* sp. 2 are confined to the Zanclean. Other species that are regularly encountered in Río del Padrón and El Lobillo are *Anthias anthias* (Linnaeus, 1758), *Tylosaurus acus* Lacepède, 1803 and *Chromis chromis,* three extant species occurring in shallower waters (< 100 m) and often in the vicinity of rocky environments. Indeed, close to the El Lobillo outcrop, the Pliocene coast is visible in the contact between the marine Pliocene sediments and Jurassic rocks (Vera-Peláez *et al*., 2006). Mollusc faunas from Río del Padrón and El Lobillo also point to a shallow sea origin (Landau *et al*., 2003; Vera-Peláez *et al*., 2005). The variety of sparid and *Gobius*-type gobiid species present at these localities is in line with this conclusion. However, other frequent species from Río del Padrón and El Lobillo – also common in the Velerín area – are *Verilus mutinensis* (7.4-7.2%), *Hygophum hygomi* (6.7-5.8%), *Deltentosteus quadrimaculatus* (2.8-2.9%), *Nezumia ornata* Bassoli, 1906 (1.6-2.4%), *Spicara smaris* (1.0-2.3%) and *Micromesistius poutassou* (4.7% at El Lobillo *vs.* only 0.4% in Río del Padrón). Overall, the otolith assemblage is characterised by large numbers of otoliths of mesopelagic and benthic deep-water fishes, mixed with otoliths from shallower water, such as gobiids. Comparison with their present-day counterparts points to subtropical conditions.

Unexpectedly, *Ceratoscopelus maderensis* (Lowe, 1839) and *Gadiculus argenteus* are poorly represented at Río del Padrón and El Lobillo, although these species are well known from Zanclean deposits in Le Puget (France; Nolf & Cappetta, 1989) and Sicily (Schwarzhans, 1978). Their absence may be related to the local environmental conditions in Estepona being shallower and closer to rocks, probably in a bay. Overall, the otolith assemblages represent a mixture of bathyal and shallower marine origin and they have unique properties as well as many species in common with other Zanclean otolith assemblages in the western Mediterranean, which were interpreted as bathyal (200-1000 m). Only recently Agiadi *et al*. (2013a, 2020) and Schwarzhans *et al*. (2020b) described Zanclean otoliths that reflect fish communities that today live at depths of 100-150 m from Voutes in Crete and less than 100 m from Agia Triada (Peloponnesos, Greece).

**Plate 36**

Figures 1-2. ***Dentex macrophthalmus*** (Bloch, 1791), Velerín Carretera (1), Velerín Conglomerates (2).
Figure 3. ***Dentex maroccanus*** Valenciennes, 1830, Velerín Quarry.
Figures 4-6. ***Pagellus erythrinus*** (Linnaeus, 1758), Velerín Quarry.
Figure 7. ***Pagellus* cf. *bellottii*** (Steindachner, 1882), Velerín Conglomerates.
Figures 8-9. ***Spicara alta*** Osório, 1917, Velerín Conglomerates.
Figures 10-12. ***Spicara alta*** Osório, 1917, Present-day, left sagittas, Senegal, coll. Mor Sylla (drawings courtesy of Dirk Nolf, Brussels, scale bar = 1 mm).

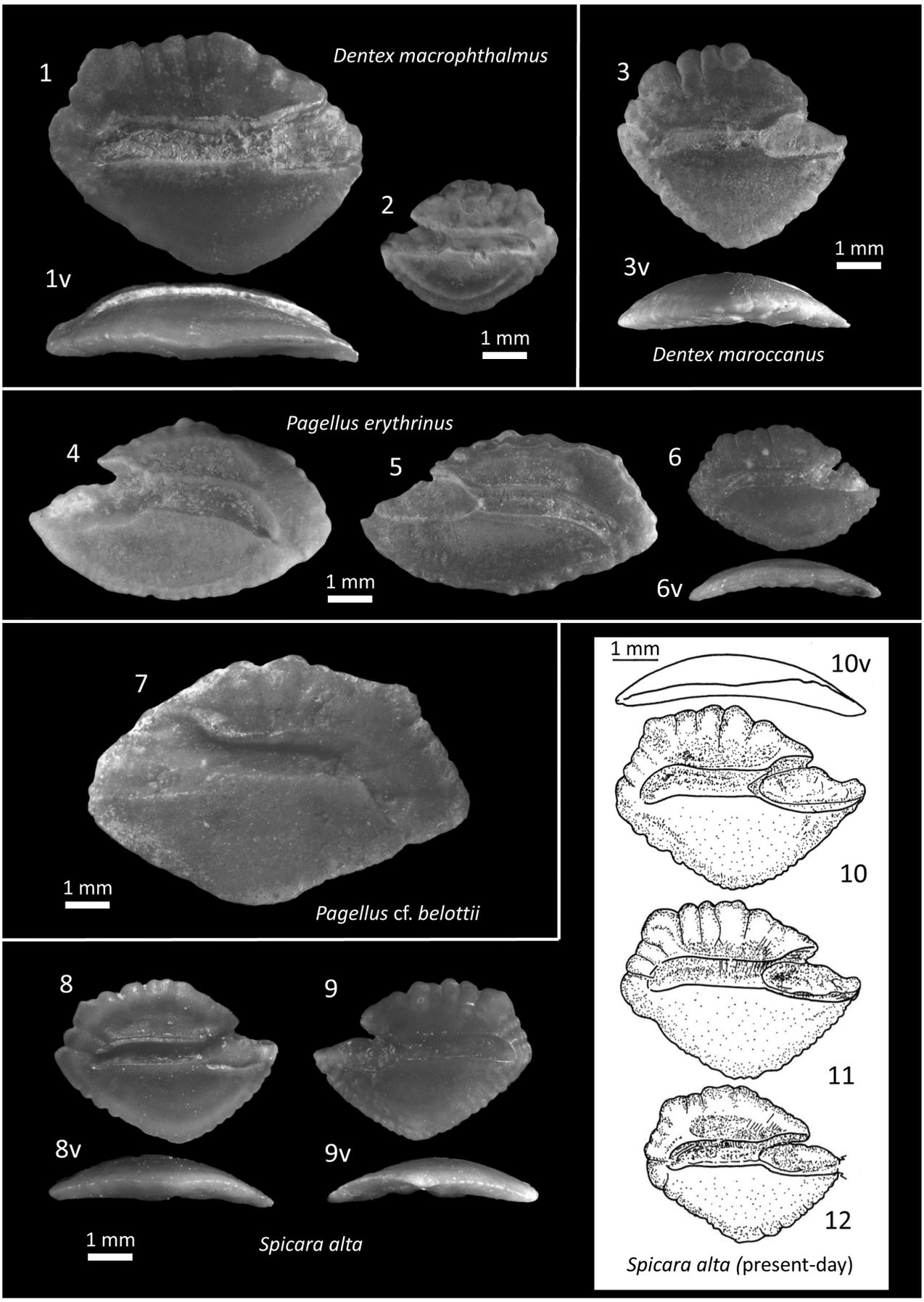
1
Dentex macrophthalmus
2
1v
1 mm
3
1 mm
3v
Dentex maroccanus
Pagellus erythrinus
4
5
6
1 mm
6v
7
1 mm
Pagellus cf. belottii
1 mm
10v
10
11
12
Spicara alta (present-day)
8
9
8v
9v
1 mm
Spicara alta

**Plate 36**

***Palaeobathymetric data: a mixture of otoliths from bathyal and bentho-neritic origins***

The 200 m isobath of the present-day Alborán Sea is at a distance of *ca* 12 km from the coast, from which point the shelf gently slopes down to 1000 m (see map in Braga & Comas, 1999). The 400 m isobath is at about 25 km from the coast, and has an invagination of 6-7 km coastwards suggestive of a submarine canyon near Estepona (see Sarhan *et al*., 2000, fig. 1). The 1000 m isobath is at > 50 km from Estepona and Málaga (see map in Braga & Comas, 1999; Janssen, 2004, p. 125). The Pliocene 1000 m isobath may have been located at roughly the same position, as a recent study showed that the Zanclean flood carved an erosion channel of several hundred metres deep at the bottom of the central Alborán Sea and further eastward (Garcia-Castellanos *et al*., 2020).

A bathymetric analysis of pelagic fish is complicated, in particular on meso- and bathypelagic species that show a daily vertical migration pattern to facilitate food access at night and protection against predators during daytime, a behaviour well known for myctophids (Schwarzhans & Carnevale, 2021). Therefore, knowledge of the thanatocoenosis of fish including their otoliths is important to be able to interpret bathyal data from fossil otolith assemblages. Dredges from the eastern Atlantic off Gabon and deep-water sediments from the Azores (Schwarzhans, 2013a) as well as Late Quaternary to present-day sediment samples from central Mediterranean Sea and NW Atlantic Ocean bottoms (Lin *et al*., 2018) have shown that large assemblages of myctophid otoliths occur at >200m, and that a smaller contribution of such otoliths is found in samples from 50-150 m.

More robust data can be obtained from the presence of otoliths of benthic and demersal fish, which remain close to the bottom and are also represented by large numbers of otoliths in the Estepona and Velerín outcrops. They regard in particular Macrouridae (depth for extant species 300- > 1500 m), the gadids *Gadiculus argenteus* and *Micromesistius poutassou* (200-300 m), the gobiid *Deltentosteus quadrimaculatus* (10-285 m) and the genus *Verilis* (data for extant western Atlantic species *V. pseudomicrolepis* Schultz, 1940 and *V. costai* Schwarzhans, Mincarone & Villarins, 2020 (180-576 m and 233-294 m, respectively) (Froese & Pauli, 2022). Besides Myctophidae, these fish represent the most frequently encountered species and suggest a sea depth of 200-300 m.

Nolf & Cappetta (1989, p. 223-224) developed a suitable method to estimate the bathymetry of otolith-bearing localities, based on a comparison with the bathymetric ranges of extant species and genera. To this end they plotted occurrence ranges of the individual extant fish (species or genus) versus a succession of depth intervals, and counted the number of interval bins that corresponded with each of the fish. We have used this method as well as a slightly modified method of calculating the bathymetry of deposits with mixed mesopelagic-neritic otolith assemblages.

In the original method of Nolf & Cappetta, a fish habitat ranging from 200 to 1000 m is counted 4 times (400%) when 200 m interval bins were used, while that of a laguna fish only once since they occur only in a single bin (100%). Fig. 4A shows the final outcome of such an analysis for 4 sites (Velerín Carretera, Velerín Conglomerates, Velerín Quarry and the Zanclean combination of Río del Padrón and El Lobillo). This approach favours mesopelagic and diurnally migrating fish in the analysis, because they are counted in more bins. To obtain a comparable 100% for each species in the evaluation, we have divided the contribution of the individual species by the number of interval bins covered. Fig. 4B shows the outcome of this analysis for all species that are represented by at least two specimens in a particular outcrop and that have a suitable extant counterpart. While the mesopelagic fishes are dominant, the data indicate that the Zanclean deposits of Estepona as well as the Velerín Conglomerates contain many otoliths of fishes with a shallow water habitat (0-50 m). In contrast, in Velerín Carretera the contribution of otoliths of fishes with a shallow water habitat is less, and a larger contribution of those of fishes living below 400 m is found (Fig. 4B).

To further understand the different signatures of the Estepona and Velerín/Velerín Antena Hill otolith assemblages we have analysed which common species displayed a preferential occurrence in one of the major sites. To that end, we have selected those species that (1) amount to at least 8 specimens in all outcrops together and (2) simultaneously are represented by ≥ 50% of all obtained otoliths of that species in one locality. Forty-five species meet both criteria and are presented in Table 2, together with three species that are close to the criteria. Together, they present 10 Zanclean (both outcrops combined) and 38 Piacenzian species, 17 from Velerín Carretera, 12 from Velerín Conglomerates; and 5 from Velerín Quarry and 4 from Velerin Antena-Slope and Hilltop combined.

In this 'preference' analysis, there is a striking difference in the bathyal properties of the studied groups. The otolith assemblage with a preferred presence in the combined Zanclean outcrops Río del Padrón and El Lobillo shows a shallow-sea habitat at depths varying between ≤ 10 m to ≤ 100 m for most of the species (Table 2). For Velerín Conglomerates these values range from ≤ 20 m to ≤ 200 m, also pointing to epipelagic-neritic marine conditions. The otoliths in majority found at Velerín Carretera reflect fish that preferred a mesopelagic habitat as deduced from their extant counterparts (Table 2), while those from Velerín Quarry and the upper sandy deposits of Velerín Antena hill corresponds to extant fish that live at intermediate or large depth. These data combined with the bathymetric data of Fig. 4B suggests an outer shelf to upper slope habitat for Velerin Carretera, an outer shelf platform habitat for Velerin Quarry and sandy deposits of the Velerín Antena Hill, and an inner or middle shelf shallow marine environment for the Estepona Zanclean deposits and Velerín Conglomerates. However, while there exists a clear hiatus between the Zanclean outcrops close to Estepona town and those of the Velerín area (*ca* 5

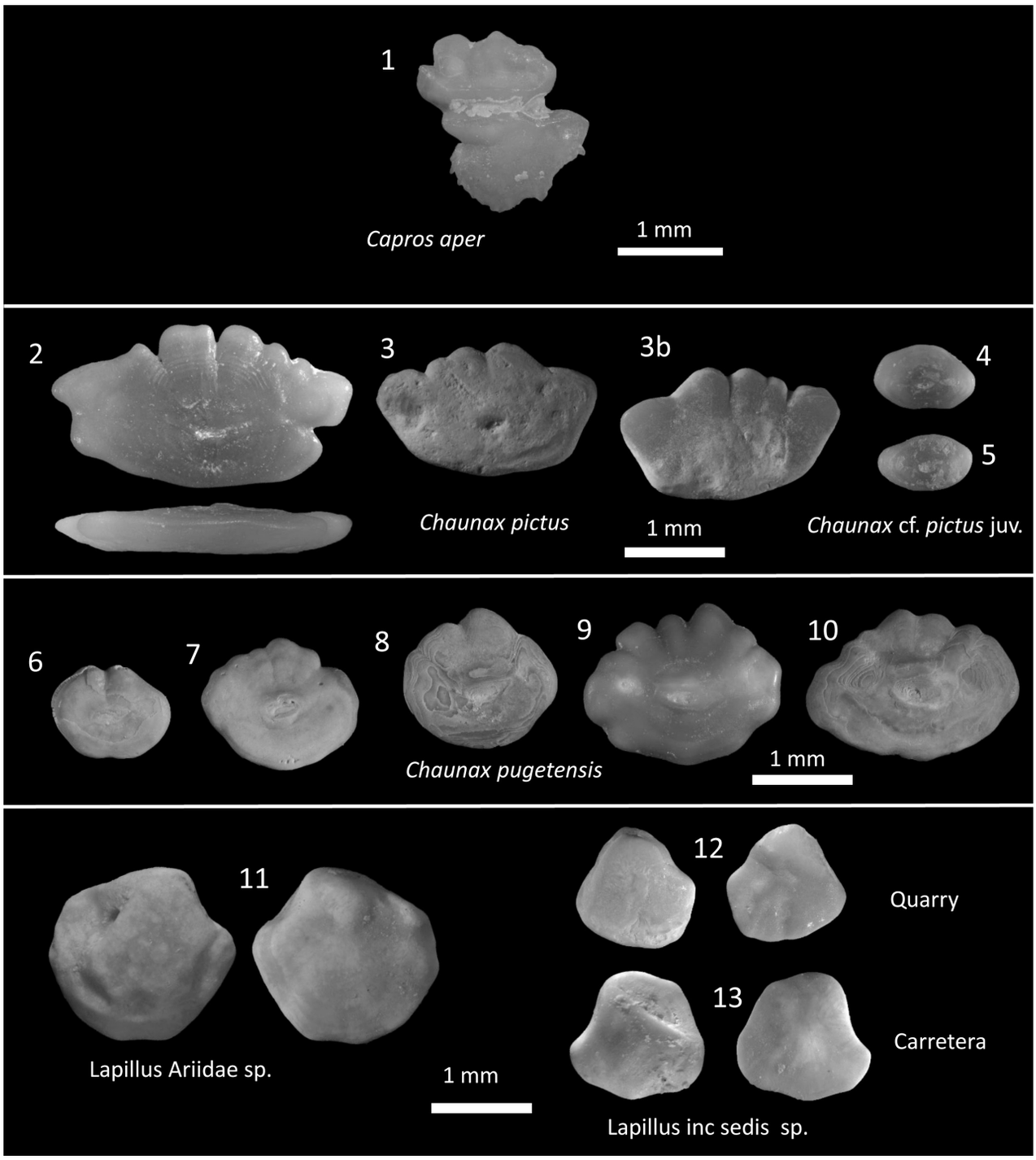


**Plate 37**

Figure 1. ***Capros aper*** (Linnaeus, 1758), El Lobillo.
Figures 2-5. ***Chaunax pictus*** Lowe, 1846,Velerín Conglomerates (2, 4, 5), Velerín Antena Slope (3).
Figures 6-10. ***Chaunax pugetensis*** Schwarzhans, 1986, Velerín Carretera.
Figure 11. **Ariidae sp.**, utricular otolith (lapillus), opposite views, Velerín Carretera.
Figures 12-13. ***inc. sedis*** **sp.**, utricular otoliths (lapilli), two opposite views per otolith, Velerín Quarry (12), Velerín Carretera (13).

km distance), the differences in the Velerín area itself are surprising given the short distances between the different localities, which reach about 700 m (between Velerín Carretera and Velerín Conglomerates).

This outcome is a bit surprising as we found an estimated habitat of 200-300 m when we compared the estimated depth habitats of the extant counterparts of the most frequent species in Estepona, myctophids, macrourids, *Gadiculus argenteus, Micromesistius poutassou, Veri-*

**Table 2.** Bathymetric data of species that are preferentially encountered in one locality at Estepona. A selection of species that are represented at one locality by ≥50% of all otoliths of that species that were obtained from all sites together, and simultaneously amount to at least 8 specimens in all outcrops together. Forty-five species met both criteria; 3 species that were close to the criteria were added. Grey tones indicate >75% and >50%. Bathymetric data from Whitehead *et al*. (1984) and Froese & Pauli (2022). For 6 extinct species bathymetric data (*) of an extant representative were used: *[1] *Gnatophis mystax*, *[2] *Chaunax pictus*, *[3] *Paraconger notialis*, *[4] *Apogon imberbis*, *[5] *Polyipnus polli*, *[6] *Verilus pseudomicrolepis*.

| Species | Total number of specimens in all outcrops | Specimens in a specific outcrop (Percentage of total number) | | | | | Benthic range (m) below sea level |
|---|---|---|---|---|---|---|---|
| | | Rio del Padrón & El Lobillo | Velerín Carretera | Velerín Conglom-erates | Velerín Quarry | Velerín Antena Slope & Hilltop | |
| *Diaphus befralai* Brzobohatý & Nolf, 2000 | 8 | 100.0 | 0.0 | 0.0 | 0.0 | 0.0 | – |
| *Diaphus cavallonis* Brzobohatý & Nolf, 2000 (≥ 2.9 mm) | 941 | 100.0 | 0.0 | 0.0 | 0.0 | 0.0 | – |
| *Chromis* cf. *chromis* (Linnaeus, 1758) | 24 | 95.8 | 0.0 | 4.2 | 0.0 | 0.0 | 3 – 35 |
| *Diplodus* cf. *puntazzo* (Walbaum, 1792) | 7 | 71.4 | 28.6 | 0.0 | 0.0 | 0.0 | 0 – 60 |
| *Spicara smaris* (Linnaeus, 1758) | 114 | 70.2 | 3.5 | 14.9 | 11.4 | 0.0 | 15 – 100 |
| *Myctophum fitchi* (Schwarzhans, 1979) | 1261 | 68.8 | 12.1 | 7.4 | 0.2 | 7.7 | – |
| *Pagellus acarne* (Risso, 1827) | 33 | 60.6 | 0.0 | 24.2 | 0.0 | 6.1 | 0 – 220 |
| *Tylosurus* cf. *acus* (Lacepède, 1803) | 7 | 57.1 | 0.0 | 28.6 | 14.3 | 0.0 | 0 – 20 |
| *Atherina presbyter* Cuvier, 1829 | 37 | 56.8 | 2.7 | 13.5 | 13.5 | 13.5 | 0 – 5 |
| *Gobius geniporus* Valenciennes, 1837 | 22 | 54.5 | 9.1 | 22.7 | 4.5 | 9.1 | 1 – 30 |
| *Nezumia* aff. *sclerorhynchus* (Risso, 1810) | 25 | 0.0 | 96.0 | 0.0 | 0.0 | 4.0 | 500 – 3200 |
| *Gnathophis henkmulderi* nov. sp. | 26 | 0.0 | 92.3 | 0.0 | 3.8 | 0.0 | 80 – 800 *[1] |
| *Japonoconger africanus* (Poll, 1953) | 21 | 4.8 | 90.5 | 0.0 | 4.8 | 0.0 | 25 – 6500 |
| *Chaunax pugetensis* (Schwarzhans, 1986) | 33 | 0.0 | 87.9 | 0.0 | 3.0 | 9.1 | 100 – 400 *[2] |
| *Lampanyctus crocodilus* (Risso, 1810) | 9 | 0.0 | 77.8 | 0.0 | 22.2 | 0.0 | 12 – 800 |
| *Scopelogadus* cf. *beanii* (Günther, 1887) | 13 | 15.4 | 76.9 | 0.0 | 7.7 | 0.0 | 800 – 2500 |
| *Lampanyctus photonotus* Parr, 1928 | 107 | 12.1 | 76.6 | 3.7 | 3.7 | 1.9 | 50 – 1000 |
| *Coelorinchus* cf. *mediterraneus* Iwamoto & Ungaro, 2002 | 44 | 2.3 | 72.7 | 13.6 | 2.3 | 2.3 | 800 – 1200 |
| *Lobianchia gemellarii* (Cocco, 1838) juv. | 22 | 13.6 | 68.2 | 9.1 | 0.0 | 0.0 | 25 – 500 |
| *Diaphus holti* Tåning, 1918 | 81 | 3.7 | 66.7 | 1.2 | 12.3 | 4.9 | 80 – 675 |
| *Diaphus splendidus* (Brauer, 1904) | 596 | 1.3 | 65.6 | 30.2 | 0.3 | 0.5 | 0 – 3000 |
| *Paratrisopterus glaber* Schwarzhans, 2010 | 83 | 2.4 | 62.7 | 2.4 | 31.3 | 1.2 | – |
| *Ceratoscopelus maderensis* (Lowe, 1839) | 629 | 0.3 | 61.8 | 5.1 | 17.6 | 7.3 | 12 – 800 |
| *Diaphus dirknolfi* Schwarzhans, 1986 | 216 | 0.5 | 54.6 | 0.0 | 44.0 | 0.9 | 50 – 500 |
| *Buglossidium luteum* (Risso, 1810) | 11 | 9.1 | 54.5 | 0.0 | 36.4 | 0.0 | 5 – 450 |
| *Coelorinchus caelorhincus* (Risso, 1810) | 290 | 14.8 | 51.4 | 18.3 | 2.8 | 7.9 | 200 – 500 |
| *Diaphus taaningi* Norman, 1930 | 14 | 28.6 | 50.0 | 0.0 | 0.0 | 21.4 | 40 – 472 |
| *Paraconger pinguis* nov. sp. | 47 | 4.3 | 0.0 | 91.5 | 2.1 | 2.1 | 25 – 50 *[3] |
| *Fowleria velerinensis* nov. sp. | 23 | 0.0 | 0.0 | 87.0 | 0.0 | 13.0 | – |
| *Lesueurigobius suerii* (Risso, 1810) | 52 | 1.9 | 3.8 | 82.7 | 7.7 | 0.0 | 1 – 230 |
| *Lithognathus mormyrus* (Linnaeus, 1758) | 45 | 11.1 | 8.9 | 75.6 | 0.0 | 4.4 | 0 – 50 |
| *Ophidion rochei* Müller, 1845 | 149 | 8.7 | 4.7 | 73.2 | 11.4 | 13.4 | 5 – 150 |
| *Gobius kolombatovici* Kovačić, & Miller, 2000 | 53 | 12.7 | 7.3 | 67.3 | 12.7 | 3.6 | 15 – 90 |
| '*Gobius*' *pterois* nov. sp. | 19 | 31.6 | 0.0 | 63.2 | 5.3 | 0.0 | – |
| *Scombrops* cf. *boops* (Houttuyn, 1782) | 17 | 5.9 | 5.9 | 58.8 | 23.5 | 0.0 | 20 – 400 |
| *Apogon lozanoi* Bauza, 1957 | 21 | 23.8 | 0.0 | 57.1 | 4.8 | 4.8 | 10 – 200 *[4] |
| *Dentex* aff. *maroccanus* Valenciennes 1830 | 23 | 26.1 | 0.0 | 56.5 | 13.0 | 4.3 | 20 – 250 |
| *Conger conger* (Linnaeus, 1758) | 27 | 25.9 | 7.4 | 55.6 | 11.1 | 0.0 | 0 – 100 |
| *Diplodus annularis* (Linnaeus, 1758) | 12 | 41.7 | 0.0 | 50.0 | 0.0 | 0.0 | 0 – 3 |

*table 2, continued*

| Species | Total number of specimens in all outcrops | Specimens in a specific outcrop (Percentage of total number) | | | | | Benthic range (m) below sea level |
|---|---|---|---|---|---|---|---|
| | | Rio del Padrón & El Lobillo | Velerín Carretera | Velerín Conglom-erates | Velerín Quarry | Velerín Antena Slope & Hilltop | |
| *Gephyroberyx darwinii* (Johnson, 1866) | 39 | 0.0 | 0.0 | 0.0 | 100.0 | 0.0 | 200 – 500 |
| *Prionotus arenasiensis* nov. sp. | 26 | 0.0 | 0.0 | 0.0 | 96.2 | 3.8 | – |
| *Polyipnus* sp. | 18 | 0.0 | 11.1 | 0.0 | 88.9 | 0.0 | 100 – 400 *[5] |
| *Bidentichthys mediterraneus* nov. sp. | 24 | 0.0 | 8.3 | 8.3 | 75.0 | 8.3 | – |
| *Verilus mutinensis* (Bassoli, 1906) | 6012 | 5.7 | 9.6 | 16.7 | 57.0 | 9.8 | 180 – 576 *[6] |
| *Ophidion barbatum* Linnaeus, 1758 | 26 | 0.0 | 0.0 | 19.2 | 7.7 | 73.1 | 5 – 150 |
| *Deltentosteus quadrimaculatus* Valenciennes, 1837 | 6181 | 2.7 | 15.5 | 10.9 | 17.0 | 53.5 | 10 – 285 |
| *Micromesistius poutassou* (Risso, 1826) | 2694 | 5.1 | 3.6 | 2.0 | 36.0 | 50.0 | 30 – 400 |
| *Echiodon dentatus* (Cuvier, 1829) | 328 | 0.9 | 25.3 | 9.5 | 15.2 | 47.9 | 120 – 3250 |

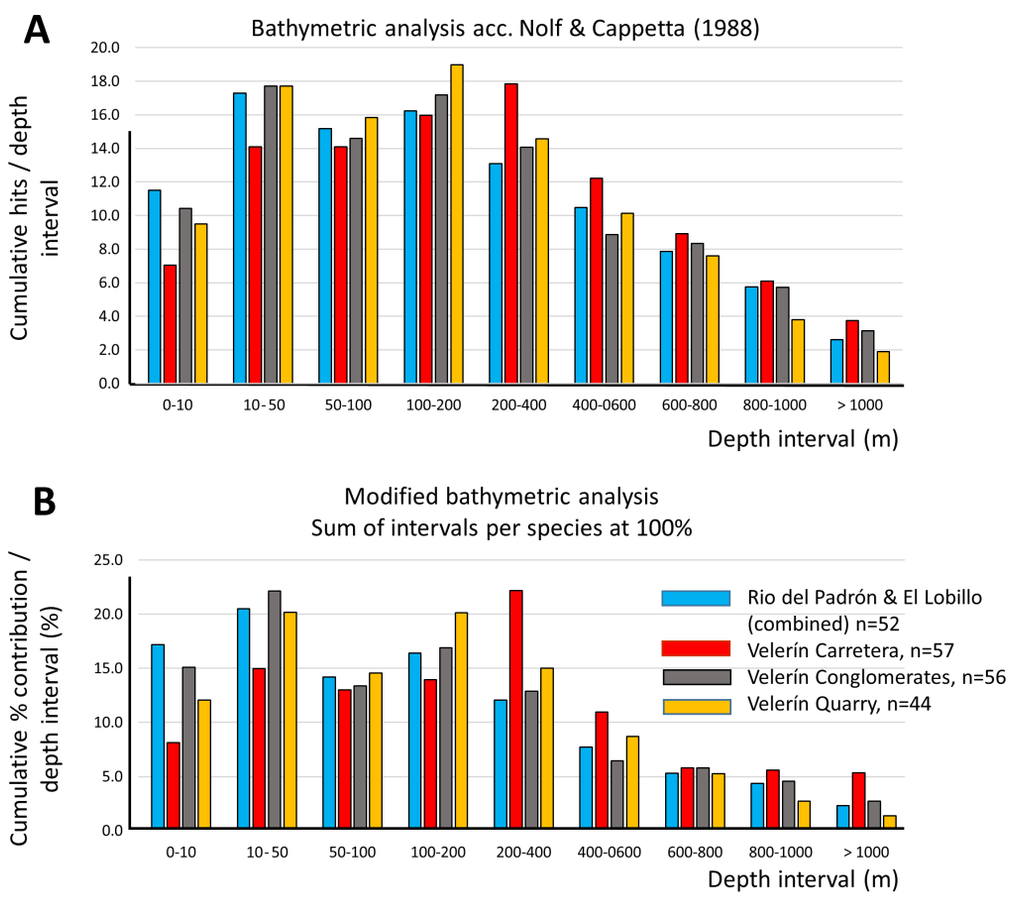


**Figure 4.** Bathymetric analyses of four otolith assemblages of Estepona. Otoliths were analysed of fish that had a present-day counterpart, and that were encountered at least twice in Estepona. **A.** Array according to Nolf & Cappetta (1989), which determines the number of depth intervals at which the (comparable) present-day fish species was reported. **B.** Modified array on the same data following the method introduced by us to reduce overestimation of species with a wide mesopelagic depth range. In the modified array each species contributes equally to the analysis results by dividing its presence in each of multiple intervals by the number of intervals resulting in a 100% overall contribution of each species. Bathymetric data from Whitehead *et al*. (1984) and Froese & Pauli (2022). N = number of species analysed.

*lus mutinensis* and *Deltentosteus quadrimaculatus* (see above). Two main reasons may explain this discrepancy. First, predators can forage in shallow water and carry ingested fish into deeper water, where their otoliths are excreted. Marine mammals also could leave numerous otoliths in the sediment from fish that passed their intestine tracts (Fitch & Brownell, 1986), but no remains of these animals have been documented at Estepona. A possible explanation for this fact is, that the sea was too narrow and shallow for them to permanently live there. Skeletons of toothed and baleen whales have been discovered more to the east (Italy), where the Mediterranean is wider and deeper. Moreover, remains of elasmobranchs are extremely scarce, only a few more or less complete teeth have been discovered, despite extensive collecting, belonging to at least 12 taxa (Table 3 by Frederik Mollen). There are, however, numerous fragments of crowns of teeth in the collection, perhaps pointing to bio-erosion which consumed the root of the teeth, leaving the crown to be fragmented through diagenesis.

An alternative explanation is needed, in particular for the conglomerates that represent the end stage of a delta fan. Such a delta fan contains a mixture of material derived from the local biotope and material that had been deposited initially at a higher level, but that subsequently migrated downwards during landslides from shallow into deep water, where the otoliths mixed with otoliths of mesopelagic fish into the final conglomerate. This suggestion explains the simultaneous presence of otoliths from shallow-water fishes with those of mesopelagic/bathyal ones, and is supported by the general polishing of many otoliths encountered in Velerín Conglomerates.

### *Velerín Carretera: a large mesopelagic contribution*

The otolith association of Velerín Carretera is interesting as it is very rich, particularly in species that normally live at advanced depth (> 400 m). They not only include large numbers and many species of meso- and bathypelagic Myctophidae (*Notoscopelus resplendens*, *Scopelopsis pliocenicus* (Anfossi & Mosna, 1976), *Ceratoscopelus*

**Table 3.** List of elasmobranch species present in the Pliocene of Estepona, 9 were identified to species level, systematics follow Cappetta (2006, 2012) and Stone & Shimada (2019) for the Carchariidae. (contribution by Frederik H. Mollen).

| Order | Family | Species | N° of specimens | |
|---|---|---|---|---|
| | | | Zanclean | Piacenzian |
| ?? HEXANCHIFORMES | ?? Hexanchidae | ?? *Hexanchus griseus* (Bonnaterre, 1788) | | 1 |
| SQUALIFORMES | Centrophoridae | *Centrophorus granulosus* (Bloch & Schneider, 1801) [1] | | 4 |
| | Dalatiidae | *Dalatias licha* (Bonnaterre, 1788) [2] | | 10 |
| SQUATINIFORMES | Squatinidae | *Squatina* sp. | | 6 |
| LAMNIFORMES | Carchariidae | *Carcharias* cf. *taurus* Rafinesque, 1810 [3] | | 3 |
| | Lamnidae | *Cosmopolitodus hastalis* (Agassiz, 1843) | | 1 |
| | | *Isurus oxyrinchus* Rafinesque, 1810 [4] | | 2 |
| CARCHARHINIFORMES | Carcharhinidae - Carcharhininae - Rhizoprionodontini | *Rhizoprionodon* sp. [5] | | 1 |
| | Carcharhinidae - Carcharhininae - Carcharhinini | *Carcharhinus* sp. [6] | | 29 |
| | Scyliorhinidae - Megascyliorhininae | *Megascyliorhinus miocaenicus* (Antunes & Jonet, 1970) [7] | | 1 |
| | Triakidae | *Galeorhinus galeus* (Linnaeus, 1758) | | 2 |
| SELACHII INDET. | | | 2 | 20 |
| RAJIFORMES | Rajidae | *Raja* cf. *clavata* Linnaeus, 1758 (teeth) [8] | | 2 |
| | | *Raja* sp. (denticle) [9] | | 1 |
| MYLIOBATIFORMES | Dasyatidae | *Dasyatis tortonesei* Capapé, 1975 [10] | | 1 |

Notes: [1]For a taxonomic discussion of present-day Mediterranean *Centrophorus* Müller & Henle, 1837 see Bellodi *et al*. (2022). [2]Mostly juveniles, but also adult; circumglobal species. [3] Typical 'heel' as in present-day *C. taurus* is lacking (see Hovestadt, 2020 – 'extension'). [4] Possible survivor from the Miocene. [5] Or lower anterior juv. *Sphyrna zygaena* (Linnaeus, 1758) or *lewini* (Griffith & Smith, 1834). [6] Perhaps mix with *Negaprion* sp. [7] ? Striae - Pliocene of Spain, Italy, Tunesia, etc. [8] Teeth are large (so not opted for *R.* cf. *asterias* Delaroche, 1809). [9] Claw-like prickle, possibly also *R.* cf. *clavata* or *asterias* (check Gravendeel *et al.,* 2002). [10] As *D. pastinaca* (Linnaeus, 1758) in Cappetta (2012), but see taxonomic discussion in Mollen (2019), see also Saadaoui *et al*. (2016).

*maderensis* (Lowe, 1839), *Lampanyctus photonotus* Parr, 1928, *Diaphus holti*, *D. splendidus*, *Hygophum hygomi* and *Mytophum fitchi*), but also an unusually large assemblage of different benthopelagic Macrouridae (*Coelorhinchus arthaberoides*, *C. caelorhincus*, *C. mediterraneus*, *Nezumia ornata* and *N. sclerorhynchus* (Risso, 1810)) and other deep living species, such as *Japonoconger africanus*, *Chaunax pugetensis* Schwarzhans, 1986 and *Scopelogadus beanii.* Deep-water fish are also best represented at Velerín Carretera when one evaluates the rarer species. The much higher numbers of deep-sea species at Velerín Carretera compared to the uphill Velerín Quarry (also a sediment of fine sands) or Velerín Conglomerates is challenging, because the transgression cycle during which the Piacenzian sands were deposited was estimated to result in a maximum sea level rise of about 50-100 m (Guerra-Merchan *et al*., 2014). Velerín Carretera is localised only 600-700 metres from Velerín Antena, Velerín Quarry and Velerín Conglomerates, which requires an explanation for the different otolith assemblages, but is not available yet. It may be due to a hidden fault or erosion of the 20-30 m thick Middle Piacenzian fossiliferous medium- to fine-grained sands at Velerín Carretera, by which an underlying earlier deposit of similar fossiliferous fine clayey sands became exposed.

### *Velerín Quarry*

The fossiliferous sandy sediments of Velerín Quarry not only show a dominant abundance of *Verilus mutinensis* and the gadids *Gadiculus argenteus* and *Micromesistius poutassou*, but also a rather selective occurrence of *Gephyroberyx darwini*, of which specimens were only obtained from Velerín Quarry (100%). For *Prionotus arenarius* this was 96%, for *Polyipnus* sp. 89% and for *Bidenichthys mediterraneus* 75%. It shows that *Gephyroberyx darwini* – which has only recently been caught alive in the eastern Mediterranean Sea (Andaloro *et al*., 2012) – has been pretty common during the Piacenzian in the environment of the sands deposited along the northwestern Alborán Sea coast. Large numbers of *Gephyroberyx darwini* are also known from the Miocene of the North Sea Basin (Hoedemakers, 1979; Schwarzhans, 2010a) and the palaeocanyon of of Saubrigues (Steurbaut, 1979), indicative of a deep neritic environment (Steurbaut, 1979). *Bidenichthys mediterraneus* is only known from the Pacific, except for *B. capensis*, which was found near the Cape, South Africa. The genus *Bidenichthys* is known from a few Pacific species and one from southern Africa (*B. capensis*). The regular presence of *Prionotus* was surprising as *Prionotus* is a genus that is presently known only from temperate waters of the north- and central western Atlantic Ocean, although it has also been identified from the Miocene of the North Sea Basin (Schwarzhans, 2010a). It is interesting that in the sands and clayey sands of Velerín Quarry a number of new fish taxa were found, such as *Kryptophanaron nolfi*, *Buenia pulvinus*, *Prionotus arenarius*, *Pristigenys adrianae*, *Snyderina stillaformis* and *Thorogobius mirbachae.* Whether this has any relation to changes in Atlantic currents (after the rise of the Panama isthmus, 3.5 My) (Coates *et al*., 1992; O'Dea *et al*., 2016), the climate changes of the western Mediterranean area including Andalusia (temperature dropping between 3.5 and 3.3 My) (Fauqette *et al*., 1999), or other changes in the Alborán Sea itself needs further integrated studies. However, it should be noticed that there is a striking difference between the Piacenzian populations in the Velerín area and that reported from the Atlantic Piacenzian of Vale do Freixo, Portugal (Nolf & Marques da Silva, 1997) and Morocco (Schwarzhans, 1981, 1986), which suggests environmental conditions as a driving factor rather than major changes in the contact with the Atlantic Ocean.

### *Velerin Conglomerates*

The analysis of (>50%) Conglomerates-selective species identified 12 species comprising Sparidae, *Gobius*-species (Gobiidae), Apogonidae and some Congridae. These species contrast with the association from Velerín Quarry and markedly with that from Velerín Carretera. They benefitted from the shallow sea and coarse substratum, which probably was covered with sea grass fields and algae as suggested from the rich mollusc fauna (Marques da Silva *et al*., 2006) .

Within the Congridae, *Paraconger pinguis* and *Conger conger* Linnaeus, 1758 are the most common species at Velerin Conglomerates contrasting to other congrids at Velerín Carretera (Table 2). Present-day Atlantic *Paraconger* species are encountered in shallow seas.

Within the commonly found otoliths of Apogonidae and Gobiidae six species are present in the Velerín Conglomerates sediment. Despite the lower number of otoliths available from Velerín Conglomerates, most specimens of *Apogon* and *Fowleria* were obtained from that site, probably related to the presence of pebblestones and/or shallow-water. Within the Gobiidae, two of the three *Gobius* lineage species with a high site selectivity, *Gobius kolombatovici* and *Lesueurigobius suerii,* are still present in the Mediterranean Sea at depths of 15-90 and up to 228 m, respectively.

The sparids display a large variety in all outcrops. They could be identified after comparison with otoliths of their present-day counterparts. *Boops boops* Linnaeus, 1758, *Lithognathus mormyrus* and *Dentex macrophthalmus* are common at Velerín Conglomerates. We also note the presence of four *Spicara alta* specimens in this outcrop. Interestingly, the morphology of these latter otoliths and their present-day counterparts (tropical; eastern central Atlantic; 50-200 m) are closer related to those of *Dentex* than to those of other *Spicara* species, in line with the molecular genetic data on extant fish (Chiba *et al*., 2019).

Altogether, otoliths from Velerín Conglomerates point

to the presence of a mixture of otoliths from neritic fish and large numbers of otoliths from mesopelagic/bathyal fish, such as Myctophidae and the macrourid *Nezumia* Jordan, 1904. This poses the question how the depositional environment of Velerín Conglomerates otoliths compares with that of Velerín Quarry, which represents an outer shelf - upper slope habitat. The sands at Velerín Quarry are located on top of the Conglomerates as well besides them, where they interdigitate. If Velerín Conglomerates and Velerín Quarry were contemporaneous deposits, as originally suggested by Guerra-Merchán *et al*. (2002), it seems justified to interpret the bathymetry of mixed mesopelagic - neritic otolith assemblages with caution and to accept a neritic to upper slope environment of deposition for most Velerín outcrops. However, a more plausible alternative might be that the otoliths representing a 'neritic' environment originated from the upper part of an extensive delta fan and subsequently were transported with the coarser sediments into deeper water, where they mixed with bathyal and mesopelagic elements. As such events are local, they may also contribute to the variation in otolith assemblages of the Velerín area.

### *Zanclean* vs. *Piacenzian* Diaphus *species*

The moderately large *Diaphus cavallonis* is a dominant species in the Zanclean of Estepona, but became replaced in the Velerín area by other *Diaphus* species, in particular *D. postcavallonis* and *D. splendidus*. Girone (2006, figs 8a, c) reported *Diaphus* aff. *cavallonis* from the Piacenzian Rio Merli section in northeastern Italy, that has similar characteristics as *D. postcavallonis* and we have assumed it to represent the same species. This suggests that the decrease of *Diaphus cavallonis* and increase of *D. postcavallonis* may have spread over the western Mediterranean Sea. It would be of interest to see whether this can be confirmed in other Piacenzian outcrops as a general Piacenzian phenomenon.

In a review on Miocene and Pliocene *Diaphus* otoliths, Brzobohatý & Nolf (2000) defined *Diaphus cavallonis* as a new species. They also reported *Diaphus* aff. *splendidus* as a species complex comprising all otoliths that showed 'a reasonable similarity to the present-day *D. splendidus* species'. On the basis of their flat and thin appearance and large size, Nolf & Girone (2006) identified a sub-assemblage – 71 specimens, all obtained from Rio Torsero (Ceriale, NW Italy; MPl3 foraminifer zonation) – as *Diaphus* aff. *adenomus*. We found accumulations of very similar and probably identical otoliths in the material from, in particular, Velerín Carretera and Velerín Conglomerates, but concluded that they better fit *D. splendidus*. From Velerín Carretera we also identified several specimens of *Diaphus adenomus*, which also have thin otoliths, but with a smaller OL:OH ratio, different properties of cauda and ostium and reach an even larger size (up to 7 mm in our small sample). It is remarkable that *D. splendidus* almost exclusively occurred in Velerín Carretera and Velerín Conglomerates, which have a contrasting bathymetric profile. This suggests either an unexpected geological age zone for both deposits, or a common factor in their environment independent of the difference in bathymetry.

### *Palaeobiogeography and -ecology*

The present-day Alborán Sea has a high coastal fertility thanks to upwelling in the northern part of the basin (Vergnaud-Grazzini & Pierre, 1991; Sarhan *et al*., 2000). Studies of molluscs also pointed to the possibility of upwelling along the coast of Málaga in the Pliocene (Landau *et al*., 2006; Marques da Silva *et al*., 2006). A great number of samples from Estepona contain a high number of well-preserved foraminifers and, to a lesser degree, ostracod valves (and carapaces) which points to a highly productive environment (Marques da Silva *et al*., 2006). The presence of charophytes in some of our samples (pers. obs. KH) indicates the presence of a river draining into the Alborán Sea, taking with it not only organic matter but also boulders, gravel and sand. The near-total absence of otoliths of Sciaenidae and Mugilidae, however, indicates that a river mouth, a typical environment for the occurrence of these fishes (Trewavas, 1977), was not in the immediate vicinity of the sampled localities.

We follow Briggs & Bowen (2012) for the classification of marine biogeographic provinces related to fish, which is slightly different from that for molluscs (see Landau *et al*., 2009 and references therein). In this model, the Lusitania Province runs from southern Great Britain to southern Morocco, including the Mediterranean and some NE Atlantic islands (Azores, Canary Islands and Madeira). Our analysis distinguishes between the Mediterranean part of the Lusitania Province and the remainder of the Lusitania Province, which is nearest to the Strait of Gibraltar and also belongs to the Atlantic Warm Region (Fig. 5). Our analysis shows, that the vast majority (93 species representing 79.5% of all species) occurs in the Lusitania Province (excl. Mediterranean). Of the 171 nominal species encountered at Estepona, 89 still occur in the Mediterranean today (Table 4; Fig. 5) of which at present 8 (mostly Gobiidae) are endemic to this realm (marked in dark grey in Table 4), an additional 10 do not occur in the Mediterranean anymore but exclusively in the tropical SE Atlantic (marked in light grey in Table 4), and 79 are shared with the Lusitania Province (of which 14 today have no records in the Mediterranean). *Grammonus ater* has one extant record in the Azores (Carneiro *et al*., 2014), but its main distribution is in the Mediterranean. *Ophidion rochei* has two extant records off Mauretania (https://www.gbif.org/species/5203044, accessed 13 February 2022), dating from 1972 and 1988, and later two other species were recognised from the area (*O. saldanhai* and *O. lozanoi*). Forty-two species (34.7% of all species) also occur more to the north in the cold temperate NE Atlantic, but all of them are also present in the Lusitania Province. The large concordance of tele-

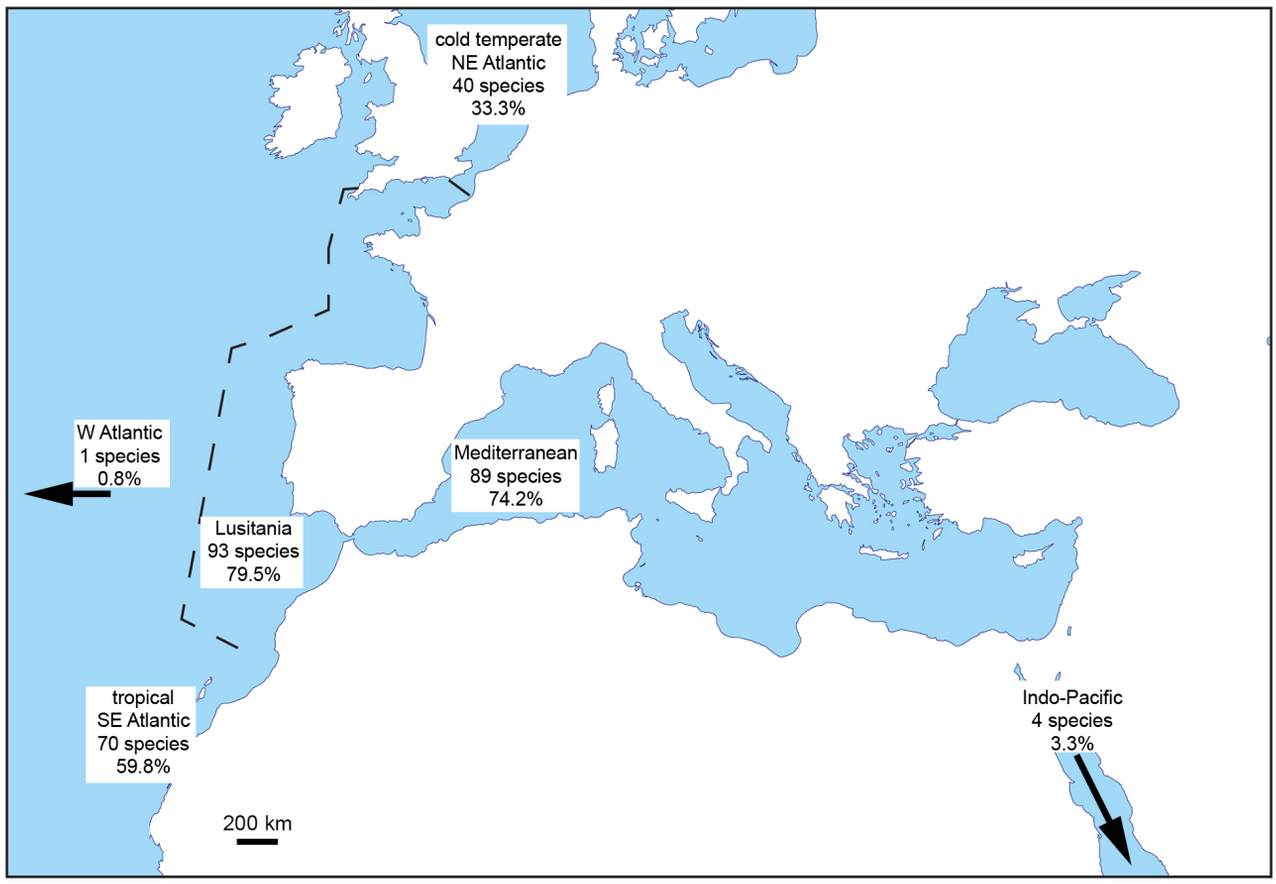


**Figure 5.** Map of Lusitania Province. Map showing the approximate boundaries of the Lusitania Province in the NE Atlantic, using the free software https://d-maps.com/carte.php?num_car=3134&lang=en. The number of extant species occurring at Estepona (n=117) is given as absolute and relative figures per province or region.

ost distributions between present-day and Pliocene indicates that the Lusitania Province was already evident during the Pliocene. A more in-depth ongoing study of the Pliocene assemblage of Dar Bel Hamri (NW Morocco) could shed light on this issue. Therefore, the conclusions given here are preliminary pending the publication of such a study.

From the aforementioned data it can be stated that the Mediterranean was populated with species from the adjacent Atlantic, which could easily penetrate the Alborán Sea through the Strait of Gibraltar. A similar conclusion was reached by Lin *et al*. (2017b, p. 38) and we agree that the "restoration of the Mediterranean fauna after the Messinian Salinity Crisis must have been rapid". There is only a limited number of species from the tropical SE Atlantic, indicating that the water temperature in the Mediterranean may have been slightly higher in the Pliocene than today. Such a conclusion is also corroborated by a study of microfossils which shows a *ca* 6°C higher summer temperature of the NE Atlantic for the Pliocene (Dowsett *et al*., 1996) and generally 2-3° higher for the Piacenzian with higher sea levels than today (Salzmann *et al*., 2011; De la Vega *et al*., 2020 and references therein) and a decreased sea-ice distribution in the Antarctic during the mid-Piacenzian warm period (Dowsett *et al*., 2012). We also identified four species which today have an exclusive Indo-Pacific distribution, but they are scarce in the collection. It is not clear how they may have entered the Mediterranean, given the fact that the connection between the eastern Mediterranean and the Indian Ocean had been closed since the Early Miocene (Rögl, 1998) and so far no otoliths of these species have been detected from the African Neogene.

One species, *Polymixia* cf. *lowei*, has been known in the Lusitania Province since the Miocene (Langhian), but today has an exclusive W Atlantic distribution, its northernmost distribution being around Newfoundland (https://www.gbif.org/species/2410398, accessed 13 February 2022). Several myctophid species recorded from Estepona, which today have a widespread distribution, have also been recognised from the Late Miocene or Pliocene onwards in the Caribbean: *Electrona rissoi*, *Lampadena dea* Fraser-Brunner, 1949*, Diaphus splendidus*, *Diaphus taaningi*, *Diaphus dirknolfi* and *Lobiancha dofleini* whereas two extinct European species have also been recorded from the Late Miocene (*Diaphus pedemontanus*) or Pliocene (*Diaphus cavallonis*) of the Caribbean (Schwarzhans & Aguilera, 2013).

The richness of the ichthyological record is mirrored by

**Table 4.** Actual distribution of extant species that also occurred in the Pliocene of Estepona. Light grey represents species from the Pliocene of Estepona, but today occurring in the tropical SE Atlantic only; dark grey represents species today endemic to the Mediterranean; ** represents those extant species known from the Miocene of the Mediterranean but not in the NE Atlantic Miocene.

| family group names | species | Present-day occurrences | | | | | |
|---|---|---|---|---|---|---|---|
| | | tropical SE Atlantic | Lusitania Province (excl. Medit.) | Medit. | cold temperate NE Atlantic | exclusive Indo-Pacific | exclusive W Atl |
| Ophichthidae | *Echelus myrus* (Linnaeus, 1758) | 1 | 1 | 1 | | | |
| Congridae | *Conger conger* (Linnaeus, 1758) | | 1 | 1 | 1 | | |
| | *Gnathophis mystax* (Delaroche, 1809) ** | | 1 | 1 | | | |
| | *Japonoconger africanus* (Poll, 1953) | 1 | | | | | |
| Alepocephalidae | *Xenodermichthys copei* (Gill, 1884) ** | 1 | 1 | | 1 | | |
| Argentinidae | *Argentina sphyraena* Linnaeus, 1758 | 1 | 1 | 1 | 1 | | |
| Microstomatidae | *Microstoma microstoma* (Risso, 1810) | 1 | 1 | 1 | 1 | | |
| Sternopthychidae | *Maurolicus muelleri* (Gmelin, 1789) | 1 | 1 | 1 | 1 | | |
| Phosichthyidae | *Vinciguerria poweriae* (Cocco, 1838) | 1 | 1 | 1 | | | |
| | *Phosichthys* cf. *argenteus* Hutton, 1872 ** | 1 | | | | | |
| Synodontidae | *Synodus saurus* (Linnaeus, 1758) | | 1 | 1 | | | |
| Chlorophthalmidae | *Chlorophthalmus agassizi* Bonaparte, 1840 | 1 | | | | | |
| Scopelarchidae | *Scopelarchus analis* (Brauer, 1902) ** | 1 | 1 | | | | |
| Myctophidae, Gymnoscopelinae | *Notoscopelus resplendens* (Richardson, 1845) ** | 1 | 1 | 1 | | | |
| | *Notoscopelus elongatus* (Costa, 1844) | | | 1 | | | |
| | *Ceratoscopelus maderensis* (Lowe, 1839) ** | | 1 | 1 | | | |
| | *Lampadena dea* Fraser-Brunner, 1949** | 1 | | | | | |
| | *Lampanyctus crocodilus* (Risso, 1810) | 1 | 1 | 1 | 1 | | |
| | *Lampanyctus photonotus* Parr, 1928 | 1 | 1 | | | | |
| Myctophidae, Diaphinae | *Diaphus adenomus* Gilbert, 1905 | 1 | 1 | | | | |
| | *Diaphus anderseni* Tåning, 1932 | 1 | | | | | |
| | *Diaphus* aff. *arabicus* Nafpaktitis, 1978 | | | | | 1 | |
| | *Diaphus holti* Tåning, 1918 ** | 1 | 1 | 1 | 1 | | |
| | *Diaphus rafinesquii* (Cocco, 1838) ** | 1 | 1 | 1 | 1 | | |
| | *Diaphus splendidus* (Brauer, 1904) ** | 1 | | | | | |
| | *Diaphus taaningi* Norman, 1930 | 1 | | | | | |
| | *Diaphus termophilus* Tåning, 1928 | 1 | 1 | | | | |
| | *Lobianchia dofleini* (Zugmayer, 1911) | 1 | 1 | 1 | 1 | | |
| | *Lobianchia gemellarii* (Cocco, 1838) ** | 1 | 1 | 1 | 1 | | |
| Myctophidae, Myctophinae | *Benthosema* aff. *glaciale* (Reinhardt, 1837) ** | 1 | 1 | 1 | 1 | | |
| | *Electrona rissoi* (Cocco, 1829) | 1 | 1 | 1 | 1 | | |
| | *Hygophum* aff. *benoiti* (Cocco, 1838) | 1 | 1 | 1 | | | |
| | *Hygophum hygomi* (Lütken, 1892) | 1 | 1 | 1 | | | |
| | *Myctophum punctatum* Rafinesque, 1810 ** | 1 | 1 | 1 | 1 | | |
| Polymixiidae | *Polymixia* cf. *lowei* Günther, 1859 | | | | | | 1 |
| Zeniontidae | *Zenion* cf. *hololepis* Goode & Bean, 1896 ** | 1 | 1 | | | | |
| Macrouridae | *Coelorinchus caelorhincus* (Risso, 1810) | 1 | 1 | 1 | 1 | | |
| | *Coelorinchus mediterraneus* Iwamoto & Ungaro, 2002 | | | 1 | | | |
| | *Nezumia* aff. *sclerorhynchus* (Risso, 1810) ** | 1 | 1 | 1 | | | |
| Trachyrincidae | *Trachyrincus scabrus* (Rafinesque, 1910) ** | 1 | 1 | 1 | 1 | | |
| Moridae | *Physiculus huloti* Poll, 1953 | 1 | | | | | |
| Gadidae | *Phycis blennoides* (Brünnich, 1768) | | 1 | 1 | 1 | | |

*Table 4, continued*

| family group names | species | Present-day occurrences | | | | | |
|---|---|---|---|---|---|---|---|
| | | tropical SE Atlantic | Lusitania Province (excl. Medit.) | Medit. | cold temperate NE Atlantic | exclusive Indo-Pacific | exclusive W Atl |
| | *Phycis phycis* (Linnaeus, 1766) | 1 | 1 | 1 | | | |
| | *Gaidropsarus mediterraneus* (Linnaeus, 1758) | | 1 | 1 | 1 | | |
| | *Gadiculus argenteus* Guichenot, 1850 | | 1 | 1 | 1 | | |
| | *Micromesistius poutassou* (Risso, 1826) | | 1 | 1 | 1 | | |
| | *Trisopterus minutus* (Linnaeus, 1758) | | 1 | 1 | 1 | | |
| Trachichthyidae | *Gephyroberyx darwinii* (Johnson, 1866) | 1 | 1 | | | | |
| Melamphaidae | *Melamphaes typhlops* Lowe, 1843 | 1 | 1 | | | | |
| | *Scopelogadus beanii* (Günther, 1887) | 1 | 1 | | 1 | | |
| Carapidae | *Echiodon dentatus* (Cuvier, 1829) | | 1 | 1 | | | |
| Ophidiidae | *Brotula* cf. *multibarbata* Temminck & Schlegel, 1846 | | | | | 1 | |
| | *Ophidion barbatum* Linnaeus, 1758 | | 1 | 1 | | | |
| | *Ophidion rochei* Müller, 1845 | | | 1 | | | |
| | *Ophidion* cf. *saldanhai* Matallanus & Brito, 1999 | 1 | | | | | |
| Bythitidae | *Grammonus ater* (Risso, 1810) | | | 1 | | | |
| | *Cataetyx alleni* (Byrne, 1906) | | 1 | 1 | | | |
| Apogonidae | *Apogon imberbis* (Linnaeus, 1758) | 1 | 1 | 1 | | | |
| Gobiidae, *Pomatoschistus* lineage | *Buenia massutii* Kovačić, Ordines & Schliewen, 2017 | | 1 | 1 | | | |
| | *Deltentosteus quadrimaculatus* Valenciennes, 1837 ** | | 1 | 1 | | | |
| Gobiidae, *Aphia* lineage | *Lesueurigobius suerii* (Risso, 1810) ** | | 1 | 1 | | | |
| Gobiidae, *Gobius* lineage | *Gobius bucchichi* Steindachner, 1870 | | 1 | 1 | | | |
| | *Gobius fallax* Sarrato, 1889 ** | | | 1 | | | |
| | *Gobius geniporus* Valenciennes, 1837 | | | 1 | | | |
| | *Gobius cobitis* Pallas, 1814 | | 1 | 1 | | | |
| | *Gobius kolombatovici* Kovačić, & Miller, 2000 | | | 1 | | | |
| | *Gobius* aff. *niger* Linnaeus, 1758 | | 1 | 1 | 1 | | |
| | *Gobius roulei* de Buen, 1928 | | 1 | 1 | | | |
| | *Gobius vittatus* Vinciguerra, 1883 | | | 1 | | | |
| | *Chromogobius* aff. *britoi* Van Tassell, 2001 | | 1 | | | | |
| | *Chromogobius* cf. *zebratus* (Kolombatović, 1891) | | | 1 | | | |
| Pomacentridae | *Chromis* cf. *chromis* (Linnaeus, 1758) | 1 | 1 | 1 | | | |
| Atherinidae | *Atherina presbyter* Cuvier, 1829 | | 1 | 1 | 1 | | |
| Exocoetidae | *Exocoetus volitans* Linnaeus, 1758 | 1 | 1 | 1 | | | |
| Belonidae | *Tylosurus* cf. *acus* (Lacepède, 1803) | 1 | 1 | 1 | | | |
| Citharidae | *Citharus linguatula* (Linnaeus, 1758) | 1 | 1 | 1 | | | |
| Scophthalmidae | *Lepidorhombus boscii* (Risso, 1810) | 1 | 1 | 1 | 1 | | |
| | *Lepidorhombus whiffiagonis* (Walbaum, 1792) | | 1 | 1 | 1 | | |
| Bothidae | *Arnoglossus laterna* (Walbaum, 1792) | 1 | 1 | 1 | 1 | | |

*continued on next page*

*Table 4, continued*

| family group names | species | Present-day occurrences | | | | | |
|---|---|---|---|---|---|---|---|
| | | tropical SE Atlantic | Lusitania Province (excl. Medit.) | Medit. | cold temperate NE Atlantic | exclusive Indo-Pacific | exclusive W Atl |
| Soleidae | *Buglossidium luteum* (Risso, 1810) | | 1 | 1 | 1 | | |
| | *Microchirus variegatus* (Donovan, 1802) ** | | 1 | 1 | 1 | | |
| Gempylidae | *Promethichthys prometheus* (Cuvier, 1832) ** | 1 | 1 | | | | |
| Trichiuridae | *Benthodesmus elongatus* Clarke, 1879 | 1 | 1 | | 1 | | |
| Ammodytidae | *Gymnammodytes cicerelus* (Rafinesque, 1810) | | 1 | 1 | 1 | | |
| Trachinidae | *Trachinus draco* Linnaeus, 1758 | | 1 | 1 | 1 | | |
| | *Trachinus radiatus* Cuvier, 1829 | 1 | 1 | 1 | | | |
| Uranoscopidae | *Uranoscopus scaber* Linnaeus, 1758 | 1 | 1 | 1 | | | |
| Labridae | *Bodianus scrofa* (Valenciennes, 1839) | 1 | 1 | | | | |
| Epigonidae | *Epigonus constanciae* (Giglioli, 1880) ** | 1 | 1 | 1 | | | |
| Serranidae | *Anthias anthias* (Linnaeus, 1758) | 1 | 1 | 1 | | | |
| Scombropidae | *Scombrops* cf. *boops* (Houttuyn, 1782) | | | | | 1 | |
| Haemulidae | *Pomadasys incisus* (Bowdich, 1825) | 1 | 1 | 1 | | | |
| Cepolidae | *Cepola macrophthalma* (Linnaeus, 1766) | 1 | 1 | 1 | 1 | | |
| Scorpaenidae | *Scorpaena loppei* Cadenat, 1943 | 1 | 1 | 1 | | | |
| | *Scorpaena* cf. *notata* Rafinesque, 1810 | 1 | 1 | 1 | | | |
| Triglidae | *Chelidonichthys lastoviza* (Bonnaterre, 1788) | 1 | 1 | 1 | 1 | | |
| | *Chelidonichthys cuculus* (Linnaeus, 1758) | | 1 | 1 | 1 | | |
| Sciaenidae | *Umbrina canariensis* Valenciennes, 1843 | | 1 | 1 | | | |
| Sparidae, clade A | *Boop boops* (Linnaeus, 1758) | 1 | 1 | 1 | 1 | | |
| | *Diplodus annularis* (Linnaeus, 1758) | | 1 | 1 | | | |
| | *Diplodus vulgaris* (Geoffroy St Hilaire, 1817) ** | 1 | 1 | 1 | | | |
| | *Diplodus* cf. *puntazzo* (Walbaum, 1792) | 1 | 1 | 1 | | | |
| | *Lithognathus mormyrus* (Linnaeus, 1758) | 1 | 1 | 1 | | | |
| | *Oblada melanura* (Linnaeus, 1758) | 1 | 1 | 1 | | | |
| | *Pagellus acarne* (Risso, 1827) | 1 | 1 | 1 | 1 | | |
| | *Pagellus bogaraveo* (Brünnich, 1768) | | 1 | 1 | 1 | | |
| | *Rhabdosargus sarba* (Gmelin, 1789) | | | | | 1 | |
| | *Sarpa salpa* (Linnaeus, 1758) | 1 | 1 | 1 | | | |
| | *Spicara* cf. *maena* (Linnaeus, 1758) | | 1 | 1 | | | |
| | *Spicara smaris* (Linnaeus, 1758) | | 1 | 1 | | | |
| Sparidae, clade B | *Dentex macrophthalmus* (Bloch, 1791) | 1 | 1 | 1 | | | |
| | *Dentex maroccanus* Valenciennes 1830 | 1 | 1 | 1 | | | |
| | *Pagellus* cf. *bellottii* Steindachner, 1882 | | 1 | 1 | | | |
| | *Pagellus erythrinus* (Linnaeus, 1758) | 1 | 1 | 1 | 1 | | |
| | *Spicara alta* (Osório, 1917) | 1 | | | | | |
| Caproidae | *Capros aper* (Linnaeus, 1758) | 1 | 1 | 1 | 1 | | |
| Chaunacidae | *Chaunax pictus* Lowe, 1846 ** | 1 | 1 | | | | |
| | | **70** | **93** | **89** | **40** | **4** | **1** |
| **total number** | **117 species** | **59.80%** | **79.50%** | **74.20%** | **33.30%** | **3.30%** | **0.80%** |

that of the gastropod fauna, for which close to an estimated 1000 species may occur (Landau & Micali, 2021). Landau *et al*. (2004b, and references therein) observed a mixed shallow-water/bathyal environment for their associations. The gastropod fauna too is described as being thermophilic, with many species still occurring along the W African coast, which is seen as the primary area of origin for the repopulation of the Mediterranean after the Messinian Salinity Crisis (Landau & Micali, 2021 and references therein). The proximity to the Atlantic Ocean

(Landau *et al*., 2004a) and the phenomenon of upwelling (Landau *et al*., 2006) probably played a key role in the abundance of gastropod species. Moreover, the presence of laminarian algae, indicative for upwelling, was inferred from the occurrence of the gastropod *Patella pellucida* Linnaeus, 1758 (Landau *et al*., 2004a; Marques da Silva *et al*., 2006).

Landau *et al*. (2003) postulated the presence of a small Miocene relict fauna of gastropods. The existence of a refuge basin in the western Alborán Sea has recently been reiterated by Booth-Rea *et al*. (2018), who hypothesised a volcanic arc archipelago in the eastern Alborán Sea, allowing land animals to cross over from Africa to Europe or vice versa. In this hypothesis, the connection between the western Alborán Sea and the NE Atlantic remained open and accessible for any ichthyological exchange between both. Table 4 lists those species present at Estepona that still occur in the present-day fauna. Many extinct species or even taxa described in open nomenclature belong to genera still occurring today, but some of these genera are so widespread that no secure data can be obtained to assess their potential area of origin for reintroduction into the Mediterranean after the MSC. The caption of Table 1 indicates the nearest geographic relatives; the marine biogeographic regions follow Briggs & Bowen (2012). Of the Pliocene species recorded at Estepona, 64 already occurred in the Miocene of the Mediterranean and of these, 24 were also encountered in the NE Atlantic Miocene, whereas 39 have not been found there and 1 occurrence is doubtful (*Coelorinchus caelorhincus*, see Table 1). It has to be emphasised, however, that otoliths from the Miocene Lusitania Province are known only from Portugal (see the revision by Steurbaut & Jonet, 1982) and the Aquitaine Basin in the northern part of that province. Of those 38 species, 27 still occur outside the Mediterranean in the NE Atlantic today (see Table 4, records marked with **) and might just as well have survived the MSC thanks to their occurrence outside the Mediterranean. The 11 remaining taxa (*Scopelopsis pliocenicus*, *Diaphus befralai*, *Diaphus cavallonis*, *Diaphus pedemontanus*, *Myctophum fitchi*, *Hoplostethus praemediterraneus* Schubert, 1905, *Grammonus* aff. *bassoli*, *Hoeseichthys brioche*, *Lesueurigobius stazzanensis*, *Callogobius weileri* and *Arnoglossus kokeni*) are exclusively known as fossils from the Mediterranean Miocene and Pliocene and may have survived in a sanctuary such as proposed by Booth-Rea *et al*. (2018). A preliminary list of otolith-based taxa from Dar Bel Hamri (Schwarzhans, 1986) mentions *Myctophum fitchi* in the Pliocene of NW Africa, just outside the Strait of Gibraltar, indicating that this species has either been present in the Miocene of that area or has entered the NE Atlantic from the Mediterranean in the Pliocene. A further 18 species (*Echelus myrus* (Linnaeus, 1758), *Polymixia* cf. *lowei*, *Phycis blennoides*, *Paratrisopterus glaber*, *Micromesistius poutassou*, *Trisopterus minutus* (Linnaeus, 1758), *Gephyroberyx darwini*, *Bellotia* aff. *obliqua*, *Gobius geniporus*, *Arnoglossus laterna*, *Trachinus radiatus*, *Scorpaena* cf. *notata*, *Chelidonichthys lastoviza*, *Chelidonichthys cuculus*, *Lithognathus mormyrus* (Linnaeus, 1758), *Spicara smaris*, *Pagellus* cf. *bellottii* and *Capros aper* (Linnaeus, 1758)) are known exclusively from the Miocene of the NE Atlantic and were absent in the Mediterranean during that time, they may have entered the Mediterranean during the Zanclean flooding or later. Moreover, one species, *Notoscopelus elongatus*, which occurred in the Mediterranean during the Tortonian (Lin *et al*., 2017b), is now for the first time recorded from the Pliocene. Today it is endemic to the western Mediterranean. The fact that it was encountered in small numbers in the Zanclean of Estepona might be seen as a relic from the Miocene in the sense of Booth-Rea *et al.* (2018) or could just as well as reflect a new entry during the Zanclean reflooding into the Mediterranean.

Taken together, the vast majority of the species still occurring today in the Mediterranean also occur in the warm Lusitania Province, which probably was the origin of the repopulation of Mediterranean after the MSC, although a few, now extinct, species might very well have survived in a refugium in the western Alborán Sea during the MSC.

### *Comparison with Neogene faunas from the Mediterranean and adjacent NE Atlantic*

Overviews of the evolution of the Neogene to present-day otolith-based teleost fish faunas in the Mediterranean and adjacent Atlantic were presented by Landini & Sorbini (2005, also including skeleton-based taxa) and Lin *et al*. (2017b). We will here add own observations in relation to the taxa discovered at Estepona, based on nominal species only (Table 1).

Of the 171 nominally valid species known from Estepona, 81 already occurred in the Miocene, of which 64 within and 17 exclusively outside the Mediterranean, 24 species are common to both realms. Above, a more detailed discussion is provided regarding the possible existence of a sanctuary in the western Mediterranean during the Messinian Salinity Crisis (MSC).

Zanclean assemblages from the NE Atlantic have rarely been reported: one from Brittany (France, Lanckneus & Nolf, 1979) and a preliminary list from Dar Bel Hamri (NW Morocco by Schwarzhans, 1986) with three new species added later (Schwarzhans, 1993, 1999). These assemblages have only 9 species in common with Estepona, whereas the latter has 65 species in common with the Mediterranean. This discrepancy seems unnatural and is no doubt due to the local environment and scarcity of studied Zanclean assemblages from the Lusitania Province. Our study adds 25 species to the Zanclean otolith-based teleost fauna of the Mediterranean.

Otolith assemblages published from the Atlantic Piacenzian are even scarcer and comprise only 13 nominal species (from Vale de Freixo, see Nolf & Marques da Silva,

1997) in common with Estepona, all of them also known from other sites in the Mediterranean. The Piacenzian of the Mediterranean was poorly known prior to our study, with only 58 species identified thus far (see Table 1). *Pterothrissus compactus* was recorded from the site of Pichegu in SE France, which was dated as Piacenzian in Nolf & Cappetta (1989), but later re-dated to Zanclean in Brzobohatý & Nolf (1996), an age that we maintain in our Table 1 Our study adds 95 nominal species to the otolith-based teleostean fauna of the Mediterranean Piacenzian. These figures also point to a striking discrepancy in our current knowledge between Mediterranean and NE Atlantic Piacenzian.

## Acknowledgements

The authors would like to thank Dirk Nolf (Brugge/RBINS, Brussels) and Werner Schwarzhans (Hamburg/Copenhagen University) for their open discussions, valuable advice and the courtesy to permit the use of some of their drawings in this manuscript. Laetitia Despontin (RBINS, Brussels) is thanked for the SEM images of *Cepola macrophthalma*. Frederik H. Mollen (Bonheiden, Belgium) identified the elasmobranch species. Tanja Schultz-Mirbach is thanked for her interest in the Estepona fauna and for giving us access to material of several sites. We are indebted to Stef Mermuys, Henk Mulder, Bernie Landau and André Jansen for providing sieved concentrate and dedicatedly collected otoliths, without which our study would not have been possible. A word of thanks also to Frank Wesselingh and colleagues from Naturalis Biodiversity Center (Leiden) for providing facilities and supportive discussions and to Annelise Folie and Julien Lalange for allowing us access and for photographing otoliths from the collection in their care (RBINS, Brussels).

## References

Abbas, E.M., Soliman, T., El-Magd, M.A., Farrag, M.M.S., Ismail, R.F. & Kato, M. 2017. Phylogeny and DNA barcoding of the family Sparidae inferred from mitochondrial DNA of the Egyptian waters. *Journal of Fisheries and Aquatic Science* 12: 73-81. https://doi.org/10.3923/jfas.2017.73.81

Agiadi, K., Antonarakou, A., Kontakiotis, G., Kafousia, N., Moissette, P., Cornée, J.-J., Manoutsoglou, E. & Karakitsios, V. 2016. Connectivity controls on the late Miocene eastern Mediterranean fish fauna. *International Journal of Earth Sciences* 106: 1147-1159. https://doi.org/10.1007/s00531-016-1355-7

Agiadi, K., Girone, A., Koskeridou, E., Moissette, P., Cornée, J.-J. & Quillévéré, F. 2018. Pleistocene marine fish invasions and paleoenvironmental reconstructions in the eastern Mediterranean. *Quaternary Science Reviews* 196: 80-99. https://doi.org/10.1016/j.quascirev.2018.07.037

Agiadi, K., Giamali, C., Girone, A., Moissette, P., Koskeridou, E. & Karakitsios, V. 2020. The Zanclean marine fish fauna and palaeoenvironmental reconstruction of a coastal marine setting in the eastern Mediterranean. *Palaeobiodiversity and Palaeoenvironments* 100(3): 773-792. https://doi.org/10.1007/s12549-019-00404-4

Agiadi, K., Koskeridou, E., Triantaphyllou, M., Girone, A. & Karakitsios, V. 2013a. Fish otoliths from the Pliocene Heraklion Basin (Crete Island, Eastern Mediterranean). *Geobios* 46: 461-472. https://doi.org/10.1016/j.geobios.2013.07.004

Agiadi, K., Koskeridou, E., Triantaphyllou, M. & Karakitsios, V. 2013b. Paleobathymetry of a Pliocene Voutes coast (Heraklion, Crete). *Bulletin of the Geological Society of Greece* XLVII: 10 pages.

Agiadi, K., Triantaphyllou, M., Girone, A. & Karakitsios, V. 2011. The Early Quaternary palaeobiogeography of the eastern Ionian deep-sea Teleost fauna: A novel paleocirculation approach. *Palaeogeography, Palaeoclimatoloy, Palaeoecology* 306(3-4): 228-242. https://doi.org/10.1016.j.palaeo.2011.04.029

Agiadi, K., Vasileiou, G., Koskeridou, E., Moissette, P. & Cornée, J.-J. 2019. Coastal fish otoliths from the Early Pleistocene of Rhodes (eastern Mediterranean). *Geobios* 55: 1-15. https://doi.org/10.1016/j.geobios.2019.06.006

Agorreta, A., San Mauro, D., Schliewen, U., Van Tassell, J.L., Kovačić, M., Zardoya, R. & Rüber, L. 2013. Molecular phylogenetics of Gobioidei and phylogenetic placement of European gobies. *Molecular Phylogenetics and Evolution* 69: 619-633.

Aguirre, J., Cachao, M., Domènech, R., Lozano-Francisco, M. C., Martinell, J., Mayoral, E., Santos, A., VeraPeláez, J. L. & Da Silva, C. M. 2005. Integrated biochronology of the pliocene deposits of the Estepona basin (Málaga, S Spain). Palaeobiogeographic and palaeoceanographic implications. *Revista Española de Paleontología*, 20 (2), 225-244. ISSN 0213-6937.

Andaloro, F., Falautano, M., Finoia, M.G. & Castriota, L. 2012. Second record of *Gephyroberyx darwinii* in the Mediterranean Sea. *Marine Biodiversity Records* 5(3): e101.

Bassoli, G.G. 1906. Otoliti fossili terziari dell'Emilia. *Rivista Italiana di Paleontologia* 12: 36–61.

Bauzá-Rullán, J. 1957. Nueva contribución al estudio de los otolitos de peces actuales y fosiles de España. *Memorias y Comunicaciones del Instituto Geológico Provincial* 16: 33-44.

Bauzá-Rullán, J. 1962. Contribución al estudio de los otolitos de peces. *Boletin de la Real Sociedad Española de Historia Natural (B)* 60: 5-26.

Bellodi, A., Benvenuto, A., Melis, R., Mulas, A., Barone, M., Barría, C., Cariani, A., Carugati, L., Chatzispyrou, A., Desrochers, M., Ferrari, A., Guallart, J., Hemida, F., Mancusi, C., Mazzoldi, C., Ramírez-Amaro, S., Rey, J., Scannella, D., Serena, F., Tinti, F., Vella, A., Follesa, M.C. & Cannas, R. 2022. Call me by my name: unravelling the taxonomy of the gulper shark genus *Centrophorus* in the Mediterranean Sea through an integrated taxonomic approach. *Zoological Journal of the Linnean Society* 195(3): 815-840. zlab110. https://doi.org/10.1093/zoolinnean/zlab110

Bitner, M.A. & Martinell, J. 2001. Pliocene Brachiopods from the Estepona areas (Málaga, South Spain). *Revista Española de Paleontología* 16(2): 177-185. https://doi.org/10.7203/sjp.16.2.21597

Booth-Rea, G., Ranero, C.R. & Grevemeyer, G. 2018. The

Alboran volcanic-arc modulated the Messinian faunal exchange and salinity crisis. *Scientific Reports* 8: 13015. https://doi.org/10.1038/s41598-018-31307-7

Braga, J.C. & Comas, M.C. 1999. Environmental significance of an uppermost Pliocene carbonate debris flow at site 978. *Proceedings of the Ocean Drilling Program, Scientific Results* 161: 77-81.

Briggs, J.C. & Bowen, B.W. 2012. A realignment of marine biogeographic provinces with particular reference to fish distributions. *Journal of Biogeography* 39: 12-30. https://doi.org/10.1111/j.1365-2699.2011.02613.x

Brzobohatý, R. & Nolf, D. 1996. Otolithes de myctophidés (poissons téléostéens) des terrains tertiaries d'Europe: révision des genres *Benthosema*, *Hygophum*, *Lampadena*, *Notoscopelus* et *Symbolophorus*. *Bulletin de l'Institut royal des Sciences naturelles de Belgique, Sciences de la Terre* 66: 151-176.

Brzobohatý, R. & Nolf, D. 2000. *Diaphus* otoliths from the European Neogene (Myctophidae, Teleostei). *Bulletin de l'Institut royal des Sciences naturelles de Belgique, Sciences de la Terre* 70: 185-206.

Campana, S.E. 2004. *Photographic Atlas of Fish Otoliths of the Northwest Atlantic Ocean*. NRC Research Press, Ottawa, Ontario. 284 pp.

Cappetta, H. 2006. Elsmobranchii post-Triadici (index specierum et generum). *In*: Riegraf, W. (ed.) *Fossilium Catalogus, I. Animalia, Pars 142*, pp. 1-472. Backhuys Publishers, Leiden.

Cappetta, H. 2012. Chondrichthyes. Mesozoic and Cenozoic Elasmobranchii: Teeth. *In*: Schultze, H.-P. & Kuhn, O. (eds) *Handbook of Paleoichthyology, Volume 3E*. Verlag Dr F. Pefiel, Munich. 512 pp.

Carneiro, M., Martins, R., Landi, M. & Costa, F.O. 2014. Updated checklist of marine fishes (Chordata: Craniata) from Portugal and the proposed extension of the Portuguese continental shelf. *European Journal of Taxonomy* 73: 1-73. https://doi.org/10.58582/ejt.2014.73

Carnevale, G., Gennari, R., Lozar, F., Natalicchio, M., Pellegrino, L. & Dela Pierre, F. 2019. Living in a deep desiccated Mediterranean Sea: An overview of the Italian fossil record of the Messinian salinity crisis. *Bollettino della Società Paleontologica Italiana* 58: 109-140.

Carnevale, G. & Schwarzhans, W. 2022. Marine life in the Mediterranean during the Messinian Salinity Crisis. A paleoichthyological perspective. *Rivista Italiana di Paleontologie e Stratigrafia* 128: 283-324.

Chaine J. & Duvergier J. 1931. Sur des otolithes fossiles de la Catalogne. *Publicacions de l'Institut de Ciències, Institució Catalana d'Historia Natural*, *Memoria* 3: 9-38.

Chiba, S.N., Iwatsuki, Y., Yoshino, T. & Hanzawa, N. 2009. Comprehensive phylogeny of the family Sparidae (Perciformes: Teleostei) inferred from mitochondrial gene analyses. *Genes and Genetic Systems* 84: 153–170. https://doi.org/10.1266/ggs.84.153

Cita, M.B. 1975. Studi sul Pliocene e sugli strati di passaggio dal Miocene al Pliocene. VIII. Planktonic foraminiferal biozonation of the Mediterranean Pliocene deepsea record. A revision. *Rivista Italiana di Paleontologie e Stratigrafia* 81 527–544.

Coates, A.G., Jackson, J.B.C., Collins, L.S., Cronin, T.M., Dowsett, H.J., Bybell, L.M., Jung, P. & Obando, J.A. 1992. Closure of the Isthmus of Panama: The near-shore marine record of Costa Rica and western Panama. *Geological Society of America Bulletin* 104 (7): 814–828. https://doi.org/10.1130/0016-7606(1992)104<0814:COTIOP>2.3.CO;2

De la Herrán, R., Ruiz Rejón, C., Ruiz Rejón, M. & Garrido-Ramos, M.A. 2001. The molecular phylogeny of the Sparidae (Pisces, Perciformes) based on two satellite DNA families. *Heredity* 87: 691-697. https://doi.org/10.1046/j.1365-2540.2001.00967.x

De la Vega, E., Chalk, T.B., Wilson, P.A., Bysani, R.P. & Foster, G.L. 2020. Atmospheric $CO_2$ during the Mid-Piacenzian Warm Period and the M2 glaciation. *Scientific Reports* 10: 11002. https://doi.org/10.1038/s41598-020-67154-8

Dell'Angelo, B., Landau, B. & Marquet, R. 2004. Polyplacomorpha from the Early Pliocene of Estepona (Málaga, southwest Spain). *Bollettino Malacologico, Supplemento* 5: 25-44.

Denton, J.S.S. 2018. Diversification patterns of lanternfishes reveal multiple rate shifts in a critical mesopelagic clade targeted for human exploitation. *Current Biology* 28: 933–940. https://doi.org/10.1016/j.cub.2018.01.082

DiBattista, J.D., Randall, J.E. & Bowen, B.W. 2012. Review of the round herrings of the genus *Etrumeus* (Clupeidae: Dussumieriinae) of Africa, with description of two new species. *Cybium* 36(3): 447-460. https://doi.org/10.26028/cybium/2012-363-004

Dowsett, H., Barron, J. & Poore, R. 1996. Middle Pliocene sea surface temperatures: a global reconstruction. *Marine Micropaleontology* 27: 13-25. https://doi.org/10.1016/0377-8398(95)00050-X

Dowsett, H.J., Robinson, M.M., Haywood, A.M., Hill, D.J., Dolan, A.M., Stoll, D.K., Chan, W.-L., Abe-Ouchi, A., Chandler, M.A., Rosenbloom, N.A., Otto-Bliesner, B.L., Bragg, F.J., Lunt, D.J., Foley, K.M. & Riesselman, C.R. 2012. Assessing confidence in Pliocene sea surface temperatures to evaluate predictive models. *Nature Climate Change* 2: 365-371. https://doi.org/10.1038/NCLIMATE1455

Fauquette, S., Suc, J.P., Guiot, J., Diniz, F., Feddi, N., Zheng, Z., Bdessais, E. & Drivaliari, A. 1999. Climate and biomes in the West Mediterranean area during the Pliocene. *Palaeogeography, Palaeoclimatology, Palaeoecology* 152: 15–36. https://doi.org/10.1016/S0031-0182(99)00031-0

Fitch, J.E. & Brownwell, R.L. 1986. Fish otoliths in cetacean stomachs and their importance in interpreting feeding habits. *Journal of the Fisheries Research Board of Canada* 25: 2561-2574.

Fricke, R., Eschmeyer, W.N. & Van der Laan, R. (eds) 2021. *Eschmeyer's Catalog of Fishes: Genera, Species, References*. Available from https://researcharchive.calacademy.org/research/ichthyology/catalog/fishcatmain.asp [accessed 15 January 2022].

Froese, R. & Pauli, D. (eds). 2022. FishBase. Available from www.fishbase.org version 02/2022 [accessed 8 August 2022].

Gaemers, P.A.M. 1976. New gadiform otoliths from the Tertiary of the North Sea Basin and a revision of some fossil and Recent species. *Leidse Geologische Mededelingen* 49: 507-537.

Gaemers, P.A.M. & Poulsen, J.Y. 2017. Recognition and distri-

bution of two North Atlantic *Gadiculus* species, *G. argenteus* and *G. thori* (Gadidae), based on otolith morphology, larval pigmentation, molecular evidence, morphometrics and meristics. *Fishes* 2(3): 15. https://doi.org/10.3390/fishes2030015

Garcia-Castellanos, D., Micallef, A., Estrada, F., Camerlenghi, A., Ercilla, G., Periáñez, R. & Abril, J.M., 2020. The Zanclean megaflood of the Mediterranean – Searching for independent evidence. *Earth-Science Reviews* 201: 103061. https://doi.org/10.1016/j.earscirev.2019.103061

Gierl, C.G. 2019. *A Fresh Look on Fossil Gobioids and Gobioid Phylogeny.* Thesis Ludwig-Maximilians-Universität München, Germany. 159 pp.

Girone, A., 2000. The use of fish otoliths for paleobathymetric evaluation of the Lower to Middle Pleistocene deposits in Southern Italy. *Bollettino della Società Paleontologica Italiana* 39(2): 235-242.

Girone, A., 2003. The Pleistocene bathyal teleostean fauna of Archi (southern Italy): palaeoecological and palaeobiogeographic implications. *Rivista Italiana di Paleontologia e Stratigrafia* 109(1): 99-110.

Girone, A. 2005. Response of otolith assemblages to sea-level fluctuations at the Lower Pleistocene Montalbano Jonico Section (southern Italy). *Bollettino della Società Paleontologica Italiana* 44(1): 35-45.

Girone, A. 2006. Piacenzian otolith assemblages from northern Italy (Rio Merli section, Emilia Romagna). *Bollettino della Società Paleontologica Italiana* 45(2-3): 159-170.

Girone, A., Nolf, D. & Cappetta, H. 2006. Pleistocene fish otoliths from the Mediterranean Basin: a synthesis. *Geobios* 39: 651-671. https://doi.org/10.10126.j.geobios.2005.05.004

Girone, A., Nolf, D. & Cavallo, O. 2010. Fish otoliths from the pre-evaporitic (Early Messinian) sediments of northern Italy: their stratigraphic and palaeobiogeographic significance. *Facies* 56: 399-432.

Girone, A. & Varola, A. 2001. Fish otoliths from the Middle Pleistocene deposits of Montalbano Jonico (Southern Italy). *Bollettino della Società Paleontologica Italiana* 40(3): 431-443.

Gravendeel, R., Van Neer, W. & Brinkhuizen, D. 2002. An identification key for dermal denticles of Rajidae from the North Sea. *International Journal of Osteoarchaeology* 12: 420-441. https://doi.org/10.1002/oa.645

Guerra-Merchán, A., Palmqvist, P., Lozano-Franscisco, M.C., Vera-Peláez, J. L. & Triviño Rodríguez, A. 1996. Análysis sedimentológico y paleoecológico del yacimiento plioceno de Parque Antena (Estepona, Málaga). *Revista Española de Paleontología* 11: 226-234.

Guerra-Merchán, A., Serrano, F., Hlila, R., El Kadiri, K., Sanz de Galdeano, C. & Garcés, M. 2014. Tectono-sedimentary evolution of the peripheral basins of the Alboran Sea in the arc of Gibraltar during the latest Messinian-Pliocene. *Journal of Geodynamics* 77:158-170.

Guerra-Merchán, A., Serrano, F. & Ramallo, D. 2002. Evolución sedimentaria y paleo-geográfica pliocena del borde septentrional de la cuenca de Alborán en el área de Estepona (provincia de Málaga, Cordillera Bética). *Pliocénica* 2: 31–43.

Gut, C., Vukić, J., Šanda, R., Moritz, T. & Reichenbacher, B. 2020. Identification of past and present gobies: distinguishing *Gobius* and *Pomatoschistus* (Teleostei: Gobioidei) species using characters of otoliths, meristics and body morphology. *Contributions to Zoology* 89: 282-323. https://doi.org/10.1163/18759866-bja10002

Haleem, S.Z.A.A., Al-Kahrusi, L.H. & Al-Marzouq, A.S. 2017. *Fish Otolith Atlas for Arabian Sea of Oman*. Marine Science and Fisheries Centre Al Bustan Muscat, Sultanate of Oman. pp. 108-109. ISBN 978-99969-0-989-4

Hanwi, N. & Ali-Basha, N. 2021. First record of Goldlined seabream *Rhabdosargus sarba* (Forsskål 1775), Sparidae, in the Mediterranean Sea (Syrian waters). *Marine Biodiversity Records* 14: 12. https://doi.org/10.1186/s41200-021-00207-7

Hidaka, K., Tsukamoto, Y. & Iwatsuki, Y. 2017. *Nemoossis*, a new genus for the eastern Atlantic long-fin bonefish *Pterothrissus belloci* Cadenat 1937 and a redescription of *P. gissu* Hilgendorf 1877 from the northwestern Pacific. *Ichthyological Research* 64(1): 45-53. https://doi.org/10.1007/s10228-016-0536-5

Hoedemakers, K. 1997. Fish otoliths from the Langenfeldian (Miocene) of Gross Pampau (northern Germany). *Tertiary Research* 18(1-2): 51-65.

Hoedemakers, K. & Battlori, J. 2005. Fish otoliths from the Early and Middle Miocene of the Penedès (Catalunya, Spain). *Batalleria* 12: 105-134.

Hovestadt, D.C. 2020. Taxonomic adjustments of the Oligocene and Miocene Odontaspididae and Carchariidae based on extant specimens. *Cainozoic Research* 20(2): 229-255.

Huyghebaert, B. & Nolf, D. 1979. Otolithes de Téléostéens et biostratigraphie des Sables de Zonderschot (Miocène moyen de la Belgique. *Mededelingen van de Werkgroep voor Tertiaire en Kwartaire Geologie* 16: 59-100.

Iglésias, P., Vukič J., Sellos, D.Y., Soukupová, T. & Šanda, R. 2021. *Gobius xoriguer*, a new offshore Mediterranean goby (Gobiidae), and plylogenetic relationships within the genus *Gobius*. *Ichthyological Research* 68: 445-459. https://doi.org/10.1007/s10228-020-00797-9

Iwamoto, T. & Ungaro, N. 2002. A new grenadier (Gadiformes, Macrouridae) from the Mediterranean. *Cybium* 26(1): 27-32.

Janssen, A.W. 2004. Holoplanktonic molluscan assemblages (Gastropoda, Heteropoda, Thecosomata) from the Pliocene of Estepona (Spain, Málaga). *Palaeontos* 5: 103-131.

Klausewitz, W. & Zajonz, U. 2000. *Saurenchelys meteori* n. sp. from the deep Red Sea and redescriptions of the type specimens of *Saurenchelys cancrivora* Peters, 1865, *Chlopsis fierasfer* Jordan & Snyder, 1901 and *Nettastoma elongatum* Kotthaus, 1968 (Pisces: Nettastomatidae). *Fauna of Arabia* 18: 337-355.

Koken, E. 1884. Über Fisch-Otolithen, insbesondere über diejenige der norddeutschen Oligocän Ablagerungen. *Zeitschrift der Deutschen Geologischen Gesellschaft* 36: 500-565.

Koken, E. 1891. Neue Untersuchungen an tertiäiren Fisch-Otolithen. II. *Zeitschrift der Deutschen Geologischen Gesellschaft* 43: 77-170.

Lanckneus, J. & Nolf, D. 1979. Les otolithes des Téléostéens redoniens de Bretagne (Néogène de l'Ouest de la France). *Bulletin de l'Institut de Géologie du Bassin d'Aquitaine* 25: 83-109.

Landau, B., Beu, A. & Marquet, R. 2004b. The Early Pliocene

Gastropoda (Mollusca) of Estepona, southern Spain. Part 5: Tonnoidea, Ficoidea. *Palaeontos* 5: 35-102.

Landau, B. & Marques da Silva, C., 2006. The Early Pliocene Gastropoda (Mollusca) of Estepona, southern Spain. Part 9: Olividae. *Palaeontos* 9: 1-21.

Landau, B., Marques da Silva, C. & Gill, C. 2009. The Early Pliocene Gastropoda (Mollusca) of Estepona, southern Spain. Part 8: Nassariidae. *Palaeontos* 17: 1-101.

Landau, B., Marquet, R. & Grigis, M. 2003. The Early Pliocene Gastropoda (Mollusca) of Estepona, Southern Spain. Part 1: Vetigastropoda. *Palaeontos* 3: 1-87, pls 1-19.

Landau, B., Marquet, R. & Grigis, M. 2004a. The Early Pliocene Gastropoda (Mollusca) of Estepona, southern Spain. Part 2: Orthogastropoda, Neotaenioglossa. *Palaeontos* 4: 1-108.

Landau, B.M. & Micali, P. 2021. The Early Pliocene Gastropoda (Mollusca) of Estepona, Southern Spain. Part 13: Murchisonelloidea and Pyramidelloidea. *Caenozoic Research* 21(2): 201-393.

Landini, W. & Sorbini, C. 2005. Evolutionary dynamics in the fish faunas of the Mediterranean basin during the Plio-Pleistocene. *Quaternary International* 140-141: 64-89. https://doi.org/10.1016/j.quaint.2005.05.019

Lin, C.-H., Taviani, M., Angeletti, L., Girone, A. & Nolf, D. 2017a. Fish otoliths in superficial sediments of the Mediterrean Sea. *Palaeogeography, Palaeoclimatology, Palaeoecology* 471: 134-143. https://doi.org/10.1016/j.palaeo.2016.12.050

Lin, C.-H., Brzobohatý, R., Nolf, D. & Girone, A. 2017b. Tortonian teleost otoliths from northern Italy: taxonomic synthesis and stratigraphic significance. *European Journal of Taxonomy* 322: 1-44. https://doi.org/10.5852/ejt.2017.322

Lin, C.-H. & Chang, Y.P. 2012. *Otolith Atlas of Taiwan Fishes*. Available from https://oto.biodiv [accessed 15 January 2022].

Lin, C.H., Chiang, Y.P., Tuset, V.M., Lombarte, A. & Girone, A. 2018. Late Quaternary to recent diversity of fish otoliths from the Red Sea, central Mediterranean, and NE Atlantic sea bottoms. *Geobios* 51: 335–358.

Lin, C.-H., Girone, A. & Nolf, D. 2015. Tortonian fish otoliths from turbiditic deposits in Northern Italy: Taxonomic and stratigraphic significance. *Geobios* 48: 249-261. https://doi.org/10.1016/j.geobios.2015.03.003

Lombarte, A., Chic, Ò., Parisi-Baradad, V., Olivella, R., Piera, J. & García-Ladona, E. 2006. A web-based environment from shape analysis of fish otoliths. The AFORO database. *Scientia Marina* 70: 147-152. http://isis.cmima.csic.es/aforo/index.jsp [accessed 28 February 2022].

Lombarte, A., Miletić, M., Kovačić, M., Otero-Ferrer, J.L. & Tuset, V.M. 2018. Identifying sagittal otoliths of Mediterranean Sea gobies: variability among phylogenetic lineages *Journal of Fish Biology* 92: 1768–1787. https://doi.org/10.1111/jfb.13615

López-Fuerte, F.O., González-Acosta, A.F., Fernández-Rivera, F.J., Flores-Ramírez, S., Palacios-Salgado, D.S. 2018. Biological notes, taxonomy and distribution of *Phthanophaneron harveyi* (Rosenblatt & Montgomery, 1976) (Trachichthyiformes: Anomalopidae) in the mid-gulf of California, Mexico. *Cahiers de Biologie Marine* 59: 1–7.

Lozano-Franscisco, M.C., Vera-Peláez, J.L. & Guerra-Merchán, A. 1993. Arcoida (Mollusca, Bivalvia) del Plioceno de la provincia de Málaga, España. *Treballs del Museu de Geologia de Barcelona* 3: 157-188.

Marques da Silva, C., Landau, B.M., Domènech, R. & Martinell, J. 2006. Pliocene Atlanto-Mediterranean biogeography of *Patella pellucida* (Gastropoda, Patellidae): Palaeoceanographic implications. *Palaeogeography, Palaeoclimatology, Palaeoecology* 233: 225-234. https://doi.org/10.1016/j.palaeo.2005.10.002

Martin, R.P., Olson, E.E., Girard, M.G., Smith, L. & Davis, M.P. 2018. Light in the darkness: New perspective on lanternfish relationships and classification using genomic and morphological data. *Molecular Phylogenetics and Evolution* 121: 71-85. https://doi.org/10.1016/j.ympev.2017.12.029

Mollen, F. 2019. Making Louis Agassiz's wish come true: combining forces and a new protocol for collecting comparative skeletal material of sharks, skates and rays, as a comment and an addition to '*The need of providing tooth morphology in descriptions of extant elasmobranch species*' by Guinot *et al*. (2018). *Zootaxa* 4571(2): 295-300. https://doi.org/10.11646/zootaxa.4571.2.13

Møller, P.R., Schwarzhans, W., Lauridsen, H. & Nielsen, J.G. 2021. *Bidenichthys okamotoi*, a new species of the Bythitidae (Ophidiiformes, Teleostei) from the Koko Seamount, Central Pacific. *Journal of Marine Science and Engineering* 9: 1-14.

Müller, A. 1994. Pliozäne Ichthyofaunen (Pisces: Neoselachii, Teleostei) aus Griechenland (NW-Peloponnes). *Münstersche Forschungen zur Geologie und Paläontologie* 76: 201-241.

Naranji, M.K. & Kandula, S. 2017. A new record of Gunther's waspfish *Snyderina guentheri* (Boulenger, 1889) (Scorpaeniformes: Tetrarogidae) from Visakhapatnam, India. *Journal of Threatened Taxa* 9 (4): 10130-10132. https://doi.org/10.11609/jott.2879.9.4.10130-10132

Nelson, J., Grande, T.C. & Wilson, M.V.H. 2016. *Fishes of the World. 5th Edition*. Wiley, v-xli + 707 p.

Nielsen, J.G. & Cohen, D.M. 1986. *Melodichthys*, a new genus with two new species of upper bathyal bythitids (Pisces, Ophidiiformes). *Cybium* 10(4): 381-387.

Nolf, D. 1978. Les otolithes des Téléostéens de l'Oligo-Miocène belge. *Annales de la Société royale zoologique de Belgique* 106: 3-119.

Nolf, D. 1980. Étude monographique des otolithes des Ophidiiformes actuels et révision des espèces fossiles (Pisces, Teleostei). *Mededelingen van de Werkgroep voor Kwartaire en Tertiaire Geologie* 17(2): 71-195.

Nolf, D. 1985. Otolithi Piscium. *In*: Schultze, H.P. (ed.) *Handbook of Paleoichthyology* 10. 145 pp. Fisher, Stuttgart & New York.

Nolf, D. 2013. *The Diversity of Fish Otoliths, Past and Present*. Operational Directorate "Earth and History of Life" of the Royal Belgian Institute of Natural Sciences, Brussels, Belgium, 581 pp.

Nolf, D. 2018. *Otolith Atlas of Fishes from the North Sea and the English Channel*. Fauna of Belgium, Royal Belgian Institute of Natural Sciences. 276 pp.

Nolf, D. & Brzobohatý, R. 2002. Otolithes de poissons du paléocanyon de Saubrigues (Chattien à Langhien), Aquitaine méridionale, France. *Revue de Micropaléontologie* 45(4): 261-296. https://doi.org/10.1016/S0035-1598(02)90049-8

Nolf, D. & Brzobohatý, R. 2004. Otolithes de poissons du Mio-

cène inférieur piémontais. *Rivista Piemontese di Storia naturale* 25: 69-118.

Nolf, D. & Cappetta, H., 1980. Les otolithes de téléostéens du Miocène de Montpeyroux (Hérault, France). *Palaeovertebrata* 10(1): 1-28.

Nolf, D. & Cappetta, H. 1989. Otolithes de poissons pliocènes du Sud-Est de la France. *Bulletin de l'Institut royal des Sciences naturelles de Belgique, Sciences de la Terre*, 58: 209-271.

Nolf, D. & Cavallo, O. 1994. Otolithes de poissons du Pliocène Inférieur de Monticello de Alba (Piémont, Italie). *Rivista Piemontese di Storia Naturale* 15: 11-40.

Nolf, D., De Potter, H. & Lafond-Grellety, J. 2009. *Hommage à Joseph Chaine et Jean Duvergier. Diversité et variabilité des otolithes des poissons*. Palaeo Publishing and Library, Mortsel, Belgium, 59 pp., 149 plates.

Nolf, D. & Girone, A. 2000. Otolithes de poissons du Pleistocène inférieur (Santernien) de Morrona (sud-est de Pisa). *Rivista Piemontese di Storia Naturale* 20: 3-18.

Nolf, D. & Girone, A. 2006. Otolithes de poissons du Pliocène inférieur (Zancléen) des environs d'Alba (Piémont) et de la côte ligure. *Rivista Piemontese di Storia Naturale* 27: 77-114.

Nolf, D., Mañé, R. & Lopez, A. 1998. Otolithes de poissons du Pliocène inférieur de Papiol, près de Barcelone. *Palaeovertebrata* 27: 1-17.

Nolf, D. & Marques da Silva, C. 1997. Otolithes de poissons pliocènes (Plaisancien) de Vale de Freixo, Portugal. *Revue de Micropaléontologie* 40(3): 273-282.

Nolf, D. & Martinell, J. 1980. Otolithes de Téléostéens du Pliocène des environs de Figureas (Catalogne). *Geologica et Palaeontologica* 14: 209-234.

Nolf, D. & Steurbaut, E. 1983. Révision des otolithes de téléostéens du Tortonian stratotype et de Montegibbio (Miocène supérieur d'Italie septentrionale). *Mededelingen van de Werkgroep voor Tertiaire en Kwartaire Geologie* 20: 143-197.

Nolf, D. & Steurbaut, E. 2004. Otolithes de poissons de l 'Oligocène inférieur du bassin Liguro-Piémontais oriental, Italie. *Rivista Piemontese di Storia Naturale* 25: 21-68.

Nolf, D. & Stringer, G.L. 1992. Neogene paleontology in the northern Dominican Republic. 14. Otoliths of teleostean fishes. *Bulletins of American Paleontology* 102(340): 45-81.

O'Dea, A., Lessios, H.A., Coates, A.G., Eytan, R.I., Restrepo-Moreno, S.A., Cione, A.L., Collins, L.S., de Queiroz, A., Farris, D.W., Norris, R.D., Stallard, R.F., Woodburne, M.O., Aguilera, O., Aubry, M.-P., Berggren, W.A., Budd, A.F., Cozzuol, M.A., Coppard, S.E., Duque-Caro, H., Finnegan, S., Gasparini, G.M., Grossman, E.L., Johnson, K.G., Keigwin, L.D., Knowlton, N., Leigh, E.G., Leonard-Pingel, J.S., Marko, P.B., Pyenson, N.D., Rachello-Dolmen, P.G., Soibelzon, E., Soibelzon, L., Todd, J.A., Vermeij, G.J. & Jackson, J.B.C. 2016. Formation of the Isthmus of Panama. *Science Advances* 2(8): e1600883. https://doi.org/10.1126/sciadv.1600883

Ordines, F., Ramírez-Amaro, S., Burgos, C., Baro, J., Kovačić, M. & Sobrino, I. 2019. First record of *Buenia massutii* Kovačić, Ordines & Schliewen, 2017 in the Atlantic Ocean based on molecular and morphological evidences. *Journal of Applied Ichthyology* 36 (1): 85-89. https://doi.org/10.1111/jai.13985

Paxton, J.R. 1972. Osteology and relationships of the lanternfishes (family Myctophidae). *Bulletin of the Los Angeles County Museum of Natural History* 13: 1-78.

Paxton, J.R. 1979. Nominal genera and species of lanternfishes (family Myctophidae). *Contributions in Science* 322: 1-28. https://doi.org/10.5962/p.226854

Prokofiev, A.M. 2004. On the attribution of *Paratrisopterus avus* to the genus *Gadiculus* (Gadiformes: Gadidae). *Journal of Ichthyology* 44: 412-417.

Psomadakis, P.N., Giustino, S. & Vacchi, M. 2012. Mediterranean fish biodiversity: an updated inventory with focus on the Ligurian and Tyrrhenian seas. *Zootaxa* 3263: 1-46.

Quéro, J.-C., Hureau, J.-C., Karrer, C., Post, A. & Saldanha, L. 1990. *Check-List of the Fishes of the Eastern Tropical Atlantic*. 3 volumes. JNICT, Lisbon.

Raffi, S. & Monegatti, P. 1993. Bivalve taxonomy diversity throughout the Italian Pliocene as a tool for climate - oceanographic and stratigraphic inferences. *Ciências da Terra* 12: 45-50.

Reichenbacher, B. & Cappetta, H. 1999. First evidence of an early Miocene marine teleostean fauna (otoliths) from La Paillade (Montpellier, France). *Palaeovertebrata* 28: 1-46.

Rivaton, J. & Bourret, P. 1999. Les otolithes des poissons de l'Indo-Pacifique. *Documents scientifiques et techniques II* 2: 378 pp.

Robba, E. 1970. Otoliti del Tortoniano-tipo (Piemonte). *Rivista Italiana di Paleontologia* 76(1): 89-172.

Rögl, F. 1998. Palaeogeographic considerations for Mediterranean and Paratethys seaways (Oligocene to Miocene). *Annalen des Naturhistorischen Museums Wien* 99A: 279-310.

Ruiz, F., Abad, M. & García, E.X.M. 2004. Análisis tafonómico preliminar de la icitiofauna pliocénica del S.O. de España. *Geogaceta* 35: 127-130.

Saadaoui, A., Saida, B., Elglid, A., Séret, B. & Bradai, M.N. 2016. Taxonomic observations on stingrays of the genus *Dasyatis* (Chondrichthyes: Dasyatidae) in the Gulf of Gabès (Southeastern Mediterranean Sea). *Zootaxa* 4173(2): 101-113. https://doi.org/10.11646/zootaxa.4173.2.1

Salzmann, U., Williams, M., Haywood, A.M., Johnson, A.L.A., Kender, S. & Zalasiewicz, J. 2011. Climate and environment of a Pliocene warm world. *Palaeogeography, Palaeoclimatology, Palaeoecology* 309: 1-8. https://doi.org/10.1016/j.palaeo.2011.05.044

Santini, F., Carnevale, G. & Sorenson, L. 2014. First multilocus timetree of seabreams and porgies (Percomorpha: Sparidae), *Italian Journal of Zoology* 81(1): 55-71. https://doi.org/10.1080/11250003.2013.878960

Santos, A. & Mayoral, E. 2006. Bioerosive structures of sclerozoan foraminifera from the lower pliocene of southern Spain: a contribution to the palaeoecology of marine hard substrate communities. *Palaeontology*, 49 (4) pp. 719–732.

Sarhan, T., García Lafuente, J., Vargas, M., Vargas, J.M. & Plaza, F. 2000. Upwelling mechanisms in the northwestern Alboran Sea. *Journal of Marine Systems* 23 (4): 317-331.

Schubert, R.J. 1906. Die Fischotolithen des österreichisch-ungarischen Tertiärs. III. *Jahrbuch der kaiserlich-königlichen geologischen Reichsanstalt* 56: 623-706.

Schulz-Mirbach, T., Ladich, F., Plath, M. & Heß, M. 2019. Enigmatic ear stones: what we know about the functional role and evolution of fish otoliths. *Biological Reviews* 94:457-

482. https://doi.org/10.1111/brv.12463

Schwarzhans, W. 1978. Otolithen aus dem Unter-Pliozän von Süd-Sizilien und aus der Toscana. *Berliner Geowissenschaftliche Abhandlungen (A)* 8: 1-52.

Schwarzhans, W. 1980. Die tertiäire Teleosteer-Fauna Neuseelands, rekonstruiert anhand von Otolithen. *Berliner Geowissenschaftliche Abhandlungen (A)* 26: 1-211.

Schwarzhans, W. 1981. Die Entwicklung der Familie Pterothrissidae (Elopomorpha; Pisces), rekonstruiert nach Otolithen. *Senckenbergiana lethaea* 62: 77-91.

Schwarzhans, W. 1986. Die Otolithen des Unter-Pliozäns von Le Puget, S-Frankreich. *Senckenbergiana lethaea* 67(1-4): 219-273.

Schwarzhans, W. 1993. A comparative morphological treatise of recent and fossil otoliths of the family Sciaenidae. *Piscium Catalogus. Part Otolithi Piscium* Vol. 1: 1-245.

Schwarzhans, W. 1999. A comparative morphological treatise of recent and fossil otoliths of the order Pleuronectiformes. *Piscium Catalogus. Part Otolithi Piscium* Vol. 2: 1-391.

Schwarzhans, W. 2010a. *The Otoliths from the Miocene of the North Sea Basin*. Backhuys Publishers, Leiden & Margraf Publishers, Weikersheim, Germany, 352 pp.

Schwarzhans, W. 2010b. Otolithen aus den Gerhartsreiter Schichten (Oberkreide: Maastricht) des Gerhartsreiter Grabens (Oberbayern). *Palaeo Ichthyologica* 4: 1-100.

Schwarzhans, W. 2013a. Otoliths from dredges in the Gulf of Guinea and off the Azores – an actuo-paleontological case study. *Palaeo Ichthyologica* 13: 7-40.

Schwarzhans, W. 2013b. A comparative morphological study of the Recent otoliths of the genera *Diaphus*, *Idiolychnus* and *Lobianchia* (Myctophidae). *Palaeo Ichthyologica* 13: 41-82.

Schwarzhans, W. 2014. Otoliths from the middle Miocene (Serravallian) of the Karaman Basin, Turkey. *Cainozoic Research*, 14: 35-69.

Schwarzhans W. 2019a. Reconstruction of the fossil marine bony fish fauna (Teleostei) from the Eocene to Pleistocene of New Zealand by means of otoliths. *Memorie della Società Italiana di Scienze Naturali e del Museo di Storia Naturale di Milano* 46: 3-326.

Schwarzhans, W. 2019b. A comparative morphological study of otoliths of the Congridae, Muraenosocidae, Nettastomidae and Colocongridae (Anguilliformes). *Memorie della Società Italiana di Scienze Naturali e del Museo di Storia Naturale di Milano* 46: 327-354.

Schwarzhans, W. 2019c. A comparative morphological study of otoliths of the Moridae (Gadiformes). *Memorie della Società Italiana di Scienze Naturali e del Museo di Storia Naturale di Milano* 46: 355-370.

Schwarzhans, W. 2019d. A comparative morphological study of otoliths of Recent otoliths of the so-called Trachinoidei. *Memorie della Società Italiana di Scienze Naturali e del Museo di Storia Naturale di Milano* 46: 371-388.

Schwarzhans, W., Agiadi, K. & Carnevale, G. 2020b. Late Miocene - early Pliocene evolution of Mediterranean gobies and their environmental and biogeographic significance. *Rivista Italiana di Paleontologia e Stratigrafia* 126(3): 657-724.

Schwarzhans, W. & Aguilera, O. 2013. Otoliths of the Myctophidae from the Neogene of tropical America. *Palaeo Ichthyologica* 13: 83-150.

Schwarzhans, W., Brzobohatý, R. & Radwańska, U. 2020a. Goby otoliths from the Badenian (middle Miocene) of the Central Paratethys from the Czech Republic, Slovakia and Poland: A baseline for the evolution of the European Gobiidae (Gobiiformes; Teleostei). *Bollettino della Società Paleontologica Italiana* 59: 125-173.

Schwarzhans, W., Carnevale, G., Bratishko, A., Japundžić, S. & Bradić, K. 2017 Otoliths in situ from Sarmatanian (Middle Miocene) fishes of the Paratethys. Part II: Gadidae and Lothidae. *Swiss Journal of Palaeontology* 136: 19-43.

Schwarzhans, W.W. & Prokofiev, A.M. 2017. Reappraisal of *Synagrops* Günther, 1887 with rehabilitation and revision of *Parascombrops* Alcock, 1889 including description of seven new species and two new genera (Perciformes: Acropomatidae). *Zootaxa* 4260(1): 1-74. https://doi.org/10.11646/zootaxa.4260.1.1

Smale, M.J., Watson, G. & Hecht, T. 1995. Otolith atlas of Southern Africa marine fishes. *Ichthyological Monographs of the J.L.B. Smith Institute of Ichthyology* 1: xiv + 253 pp, 149 plates.

Spadini, V. 2019. Pliocene Scleractinians from Estepona (Malaga, Spain). *Atti della Societa Toscana di Scienze Naturali, Memorie, Serie A*, 126: 75-94. doi 10.2424/ASTSN.M.2019.14

Steurbaut, E. 1979. Les otolithes de Téléostéens des Marnes de Saubrigues (Miocène d'Aquitaine méridionale, France). *Palaeontographica A* 166: 50-91.

Steurbaut, E. 1982. Les otolithes de téléostéens du gisement de Peyrère à Peyrehorade (couches de passage de l'Oligocène au Miocène d'Aquitaine méridionale, France). *Mededelingen van de Werkgroep voor Tertiaire en Kwartaire Geologie* 19(2): 35-57.

Steurbaut, E. 1983. Les otolithes de Téléostéens de la Formation de Tanaro (Langhien inférieur du Piémont, Italie septentrionale). *Geologica et Palaeontologica* 17: 255-263.

Steurbaut, E. 1984. Les otolithes de Téléostéens de l'Oligo-Miocène d'Aquitaine (Sud-Ouest de la France). *Palaeontographica A* 186(1-6): 1-162.

Steurbaut, E. & Jonet, S. 1982. Révision des otolithes de Téléostéens du Miocène portugais. *Bulletin van de Belgische Vereniging voor Geologie* 90(3): 191-229.

Stone, N.R. & Shimada, K. 2019. Skeletal anatomy of the bigeye sand tiger shark, *Odontaspis noronhai* (Lamniformes: Odontaspididae), and its implications for lamniform phylogeny, taxonomy, and conservation biology. *Copeia* 107(4): 632-652. https://doi.org/10.1643/CG-18-160

Trewavas, E. 1977. The sciaenid fishes (croakers or drums) of the Indo-West Pacific. *Transactions of the Zoological Society of London* 33: 529–541.

Tuset, V.M., Azzurro, E. & Lombarte, A. 2012. Identification of Lessepsian fish species using the sagittal otolith. *Scientia Marina* 76(2): 289-299. https://doi.org/10.3989/scimar.03420.18E

Tuset, V.M., Lombarte, A. & Assis, C.A. 2008. Otolith atlas for the Western Mediterranean, North and Central Eastern Atlantic. *Scientia Marina* 72, Supplement 1: 7-198.

Van der Laan, R., Eschmeyer, W.N. & Fricke, R. 2014. Family-group names of Recent fishes. *Zootaxa* 3882(1): 3-230. https://doi.org/10.11646/zootaxa.3882.1.1

Veen, J. & Hoedemakers, K. 2005. *Synopsis iconographique des otolithes de quelques espèces de poissons des côtes ouest africaines*. Wetlands International, 40 pp.

Vera-Peláez, J.L. & Lozano-Francisco, M.C. 2004. La colección de escafópodos pliocénicos (Mollusca, Scaphopoda) del Museo Municipal Paleontológico de Estepona (Málaga, España) con la descripción de tres nuevas especies. *Pliocénica* 4: 51-95.

Vera-Peláez, J.L., Lozano-Fancisco, M.C., Muñiz Solís, R., Gili, C., Martinell, J., Domènech, R., Guerra-Merchán, A. & Palmqvist, P. 1995. Estudio preliminar de la malacofauna del Plioceno de Estepona (Málaga, España). *Iberus* 13(2): 93-117.

Vera-Peláez, J.L., Martinell, J. & Lozano-Francisco, M.C. 1999. Turridae (Gastropoda, Prosobranchia) del Plioceno inferior de Málaga (España). *lberus* 17(1 ), 1-19.

Vera-Peláez, J.L. Navarro Luengo, I. & Lozano-Fancisco, M.C. 2006. El patrimonio paleontológico en el término municipal de Estepona (Málaga, España). *Pliocenica* 5: 26-44.

Vergnaud-Grazzini, C. & Pierre, C., 1991. High fertility in the Alboran Sea since the last glacial maximum. *Paleoceanography* 6(4): 5119-536.

Weiler, W. 1942. Die Otolithen des rheinischen und nordwestdeutschen Tertiärs. *Abhandlungen des Reichsamts für Bodenforschung, Neu Folge* 206: 9-140.

Weiler, W. 1971. Fisch Otolithen aus dem Jungtertiär Süd-Siziliens. *Senckenbergiana lethaea* 52: 5-37.

Whitehead, P.J.P., Bauchot, M.-L., Hureau, J.-C., Nielsen, J. & Tortonese, E. (eds) 1984. *Fishes of the North-eastern Atlantic and the Mediterranean*. 3 volumes. UNESCO, Paris.

Supplementary Online Materials available at
www.wtkg.org/tijdschriften/cainozoic-research